A molecular analysis of the relation between TDP-43 and tau pathology

Niblock, Michael

Awarding institution:
King's College London

Title: A molecular analysis of the relation between TDP-43 and tau pathology

Author: Michael Niblock

A molecular analysis of the relation between TDP-43 and tau pathology

A thesis submitted to King's College London in fulfilment of the degree of doctor of philosophy (Biochemistry)

By

Michael Niblock BSc MSc

Kings College London

Department of Clinical Neuroscience

Institute of Psychiatry

Jan 2013

Declaration

I hereby declare that with the exception of the scoring of the brain sections which was carried out by Dr Tibor Hortobágyi, all of the work presented in this thesis is my own work

Michael Niblock

January 2013

Acknowledgements

Firstly I would like to thank my supervisors, Dr Jean-Marc Gallo and Dr Tibor Hortobágyi for all the support they have given me. I would also like to thank past and present members of Jean-Marc's lab including Dr Teresa Rodriguez-Martin, Dr Carl Spickett and Dr Karen Anthony for developing the technique and showing me the basics of molecular biology. Lastly, a big thank you Rebecca Jones for support throughout my PhD and for help with statistics.

Table of contents

List of tables

List of Figures

Abbreviations

3R	Three repeat
4R	Four repeat
AD	Alzheimer's disease
aFTLD-U	Atypical frontotemporal lobar degeneration with ubiquitinated inclusion
AGD	Argyrophilic grain disease
ALS	Amyotrophic lateral sclerosis
APP	Amyloid Precursor Protein
bp	Base pair
BIBD	Basophilic inclusion body disease
C9ORF72	Chromosome 9 open reading frame 72
CBD	Cortical basal degeneration
cDNA	Complementary DNA
CHMP2B	Charged multivescicular body protein 2B
CNS	Central nervous system
CUG-BP	CUG binding protein
dATP	2'-deoxyadenosine 5'-triphosphate
dCTP	2'cytidine 5'-triphosphate
dGTP	2'guanosine 5'-triphosphate
dNTP	2'-deoxynucleotides 5'-triphosphate
DM	Myotonic dystrophy
DNase	Deoxyribonuclease
E10	Tau exon 10
ESE	Exonic splicing enhancer
ESS	Exonic splicing silencer

FTD-3 Frontotemporal dementia linked to chromosome 3

FTDP-17 Frontotemporal degeneration with parkinsonism linked to chromosome 17

FTDP-U Frontotemporal degeneration with parkinsonism with ubiquitin positive inclusions

FUS Fused in sarcoma

GAPDH Glyceraldehyde-3-phosphate dehydrogenase

GRN Progranulin

GSK-3β Glycogen synthase kinase 3 beta

HBSS Hank's buffered salt solution

hnRNP Heterogenous ribonucleoproteins

ISE Intronic splicing enhancer

ISS Intronic splicing silencer

kb Kilobases

kDa Kilodaltons

MAP Microtubule associated protein

MAPT Microtubule-associated protein tau

MND Motor neuron disease

MSTD Multiple system tauopathy with dementia

MBNL Muscleblind-like proteins

mRNA Messenger RNA

NFT Neurofibrillary tangles

NIFID Neuronal intermediate filament inclusion disease

NES Nuclear export signal

NLS Nuclear localisation signal

NMD	Nonsense mediated decay
PBS	Phosphate buffered saline
PHF	Paired helical filaments
PiD	Pick's disease
Pre-mRNA	Pre-messenger RNA
Pre-miRNA	Pre-micro RNA
PSP	Progressive supranuclear palsy
PTB	Polypyrimidine tract-binding protein
rpm	Revolutions per minute
RNase	Ribonuclease
RNP	Ribonucleoprotein
RRM	RNA recognition motif
RS	Serine- and arginine-rich domain
RT	Reverse transcription
SDS	Sodium dodecyl sulphate
SDS-PAGE	SDS-polyacrylamide gel elctrophoresis
SNP	Single nucleotide polymorphism
SR proteins	Serine- and arginine-containing proteins
TAR	Trans-active response
TARDBP	Tar DNA binding protein
Tra2beta	Transformer 2beta
UPS	Ubiquitin proteasome system
UTR	Untranslated region
VCP	Valosin-containing protein
v/v	Volume/volume

WMT-GGI	white matter tauopathy with globular glial inclusions
w/v	weight/volume

Publications arising from this thesis

Niblock, M. S., and Gallo, J-M., (2012) Tau alternative splicing in familial and sporadic tauopathies. *Biochemical Society Transactions* **40**, 677-680

Abstract

Tau is a microtubule associated protein found in inclusions in tauopathies including Alzheimer's disease. One known cause of neurodegeneration is an excess of exon 10 inclusion in tau mRNA which is caused by several mutations in the *MAPT* gene, encoding tau. Processing of the Amyloid Precursor Protein (APP) generates β-amyloid (Aβ) peptides which are deposited as amyloid plaques in AD brain. APP transcripts containing alternatively spliced exon 7 are increased in AD brain and processing of APP exon 7 containing protein isoforms may result in increased Aβ production.

Recently, the DNA and RNA- binding protein, Tar DNA binding protein of 43 kDa (TDP-43) inclusions have been found in 20-35% of AD cases as well as other tauopathies. TDP-43 has roles RNA processing regulation including pre-mRNA splicing. Cytoplasmic inclusions of TDP-43 result in a loss of nuclear TDP-43 and suggest a loss of TDP-43 function that may impair its role in multiple RNA processing events. Our hypothesis is that TDP-43 dysfunction affects tau and APP RNA processing either directly or indirectly.

We analysed post-mortem from human brain tissue and found an increase in severity of tau pathology associated with the presence of TDP-43 inclusions suggesting that TDP-43 dysfunction may modify tau pathology in AD brain. We found increased expression of tau exon 10 that correlated with increased expression of APP exon 7 in a subset of AD cases however there was no association between presence of TDP-43 inclusions and altered tau or APP splicing.

Our results define a subset of AD cases with high levels of tau exon 10 inclusion. These finding suggest that therapeutic interventions based on equilibrating splicing imbalances in tau exon 10 may be relevant for a sub-group of AD cases.

Chapter one: Introduction

Alzheimer's disease (AD) is characterised neuropathologically by the accumulation of neurofibrilliary tangles (NFT) composed of abnormally phosphorylated microtubule associated protein tau and extracellular Aβ plaques composed of proteolytic fragments of APP. Protein deposits are the defining feature of the majority of neurodegenerative diseases and the identification of different proteins found in neuronal deposits has enabled a system of categorisation based on the immunoreactivity of nuclear, cytoplasmic or extra-cellular inclusions.

1.1. Frontotemporal Lobar Degeneration

Frontotemporal lobar degeneration (FTLD) is the second commonest form of cortical dementia of early-onset (< 65 years of age) after AD. FTLD comprises a clinically, genetically and neuropathologically heterogeneous collection of disorders. The most common clinical manifestation is behavioural variant FTD (bvFTD) where patients present with changes in personality and interpersonal conduct (Piguet et al., 2011b). Language disorders such as progressive non-fluent aphasia and semantic dementia collectively known as primary progressive aphasia (PPA) are also common clinical phenotypes in FTLD (Snowden et al., 2007a).

Major progress has been made in identifying the molecular basis of FTLD. There are now four known subtypes based on neuropathological inclusion type and these represent the most common protein inclusions found in FTLD (Table 1.1). Clinical

phenotype correlates better with specific patterns of brain atrophy rather than the particular molecular neuropathology underlying it.

Molecular classification	Pathological subtype	Associated genes
FTLD-tau		*MAPT*
3R	PiD	
4R	CBD PSP AGD MSTD WMT-GGI	
3R and 4R	NFT-dementia	
3R, 4R or 3R and 4R depending on type of mutation	FTDP-17	
FTLD-TDP		*TARDBP* *GRN* *C9orf72*
	Type A Type B Type C Type D	*VCP*
FTLD-FUS		*FUS*
	aFTLD-U NIFID BIBD	
FTLD-UPS		
	FTD-3	*CHMP2B*

Table 1.1 Genetic correlates of the molecular subtypes of FTLD. Table adapted from Rademakers et al. (2012).
aFTLD-U: atypical frontotemporal lobar degeneration with ubiquitinated inclusion *AGD:* argyrophilic grain disease, *BIBD:* basophilic inclusion body disease, *C9ORF72:* chromosome 9 open reading frame 72, *CBD:* cortical basal degeneration, *CHMP2B:* charged multivescicular body protein 2B, *FTD-3:* frontotemporal dementia linked to chromosome 3, *FTDP-17:* frontotemporal degeneration with parkinsonism linked to chromosome 17, *FUS:* fused in sarcoma, *GRN* progranulin gene, *MAPT:* microtubule-associated protein tau, *MND:* motor neuron disease, *MSTD:* multiple system tauopathy with dementia, *NFT:* neurofibrillary-predominant, *NIFID:* neuronal intermediate filament inclusion disease, *PiD:* Pick's disease, *PSP:* progressive supranuclear palsy, *TARDBP:* tar DNA binding protein gene, *UPS:* ubiquitin proteasome system, *VCP:* valosin-containing protein, *WMT-GGI:* white matter tauopathy with globular glial inclusions, *3R:* tau pathology containing predominantly three-repeat tau, *4R:* tau pathology containing predominantly four-repeat tau.

1.1.2. FTLD-Tau

FTLD-Tau has tau pathology and account for around 40% of all FTLD cases. These include frontotemporal dementia with parkinsonism linked to chromosome 17 (FTDP-17) caused by hereditary mutations in the *MAPT* gene and sporadic tauopathies such as Cortical Basal Degeneration (CBD) Progressive Supranuclear Palsy (PSP) and Pick's disease (PiD).

Both PSP and CBD are primarily movement disorders but dementia may be a prominent symptom in both diseases. PSP patients have postural instability, parkinsonism (rigidity and bradykinesia) and difficulty in moving eyes particularly in the vertical direction (Litvan et al., 1996). The core clinical features of CBD are progressive asymmetrical rigidity, apraxia and progressive aphasia (Kertesz et al., 2000).

Microscopic examination of PSP brain typically shows rounded or globose neurofibrilliary tangles (NFT) often in the globus pallidus while in CBD, ballooned neurons are often found in the superior frontal gyrus (Dickson, 1999). Another distinguishing feature of the two diseases is the presence of distinctive tufted astrocytes in frontal areas in PSP whereas CBD has tau positive processes radially arranged around a central astrocyte. These lesions are referred to as astrocytic plaques because they have a similar structural pattern to neuritic plaques found in AD (Dickson, 1999). PiD is characterised by Pick bodies containing tau and are found in frontal and temporal cortices (Piguet et al., 2011a). There is considerable overlap in both pathological and clinical symptoms in PSP and CBD (Boeve et al., 2003).

1.1.3. FTLD-TDP

Tau-negative FTLD cases where the major ubiquitinated protein was unknown until recently were labelled as FTLD with ubiquitinated inclusions (FTLD-U). TDP-43 is the major component of ubiquitinated cytoplasmic and intranuclear inclusions found in both FTLD-U (now called FTD-TDP and accounting for around 50% of cases) and in the majority of non-mutant SOD-1 Amyotrophic Lateral Sclerosis (ALS) cases (Neumann et al., 2006). TDP-43 inclusions were initially thought to be a specific marker for FTLD-U and ALS however the presence of TDP-43 inclusions has been found in other tauopathies which now defines a class of neurological diseases collectively known as TDP-proteinopathies. The molecular link between FTLD-U and ALS confirmed observations of significant overlap of clinical and pathological features in ALS and FTLD-TDP and it has been suggested that these two diseases form a continuum and have a common mechanism of neurodegeneration (Geser et al., 2010; Geser et al., 2009a). Examination of TDP-43 distribution in FTLD-TDP, ALS and mixed FTLD/ALS brains showed that in FTLD brains, TDP-43 pathology accompanied by neuronal loss and gliosis was found in all brain regions including sub-cortical structures such as the basal ganglia and amygdala. ALS brains also showed widespread TDP-43 pathology but ALS was associated with a higher burden of inclusions in lower motor neuron nuclei (Geser et al., 2009b). Mutated genes which give rise phenotypically to FTLD and result in neuronal and glial TDP-43 inclusions have been the identified and include progranulin (*PGRN*) and Valosin containing protein (*VCP*).

Mutations in *TARDBP* produce TDP-43 inclusions and predominately give rise to ALS. However the number of familial cases of ALS (FALS) is small, accounting for

10% of all ALS cases and mutations in TDP-43 account for 4-6% of FALS cases (Andersen and Al-Chalabi, 2011).The recently discovered hexanucleotide repeat expansion in the *C9ORF72* gene produces TDP-43 inclusions and causes FTLD, ALS or mixed FTLD-ALS phenotype (DeJesus-Hernandez et al., 2011; Renton et al., 2011). The different mutated genes that give rise to TDP-43 inclusions also result in different inclusion morphologies and inclusion types in FTLD-TDP-43 and have been categorised (Table 1.2) (Mackenzie et al., 2006; Mackenzie et al., 2011; Sampathu et al., 2006). However it is not known if these different morphologies are indicative of different disease mechanisms.

TDP-43 type	Cortical pathology	Common phenotype
Type A	Many NCI Many short DN Predominantly layer 2	bvFTD PNFA
Type B	Moderate NCI Few DN All layers	bvFTD MND with FTD
Type C	Few NCI Many long DN Predominantly layer 2	SD bvFTD
Type D	Few NCI Many short DN Many lentiform NII All layers	Familial IBMPFD

Table 1.2 Classification system for TDP-43 pathology
(Taken from Mackenzie et al., (2011)).
bvFTD: behavioural variant frontotemporal dementia, *DN:* dystrophic neurites, *FTD*: Frontotemporal dementia, *IBMPFD:* inclusion body myopathy with Paget's disease of bone and frontotemporal dementia, *NCI:* neuronal cytoplasmic inclusions, *NII:* neuronal intranuclear inclusions, *PNFA:* progressive non-fluent aphasia, *SD*: semantic dementia

1.1.4 FTLD-FUS

A group of FTLD-U cases that were tau- and TDP-43-negative and previously characterised by immunoreactivity of neuronal inclusions for ubiquitin have recently been identified as having protein inclusions containing Fused in Sarcoma (FUS; also known as Translated in Liposarcoma (TLS) (Mackenzie et al., 2011; Neumann et al., 2009a; Neumann et al., 2009b). Cases included a set of brains with a very homogenous clinical and neuropathological phenotype, very early onset (35 years), negative family history for dementia and characteristic neuronal intranuclear inclusions (NII) (Mackenzie et al., 2008; Roeber et al., 2008). These brains had ubiquitin and p62 immunoreactivity a protein involved in the ubiquitin-proteasome system, and were termed atypical FTLD-U (aFTLD-U). Other tau- and TDP-43-negative cases included neuronal intermediate filament and α-internexin-positive inclusions (NIFID) and basophilic inclusion body disease (BIBD) (Munoz et al., 2009; Neumann et al., 2009b) and these conditions are now considered subtypes of FTLD-FUS (Mackenzie et al., 2010) and account for approx 10% of cases in FTLD-FUS (Urwin et al., 2010). FUS is a DNA and RNA binding protein with similarities to TDP-43 (Lagier-Tourenne and Cleveland, 2009). FUS plays a role in alternative splicing and transcription and is predominately nuclear, but also shuttles between the nucleus and the cytoplasm. FTLD-FUS brains have large cytoplasmic inclusions and a small number of nuclear inclusions.

1.1.5 FTLD-UPS

The fourth category is FTLD- ubiquitin proteasome system (UPS).These cases are tau-, TDP-43- and FUS- negative and inclusions can be demonstrated with immunohistochemistry against proteins of the UPS such as p62 (Mackenzie et al., 2009, 2010). Cases are rare and include a large Danish family and an unrelated

Belgian patient with frontotemporal dementia linked to chromosome 3 (FTD-3). A mutation in the *CHMP2B* gene has been identified in FTD-3 cases and is most likely to cause disease by altering the endosome-lysosome pathway and autophagy (Isaacs et al., 2011; Skibinski et al., 2005; van der Zee et al., 2008b) although *CHMP2B* mutations do not account for all FTLD-UPS cases (Urwin et al., 2010).

In a subset of FTLD-TDP brains, immunoreactivity for p62 has been found at a higher intensity than TDP-43, particularly in the cerebellum (Pikkarainen et al., 2008). The recently discovered hexanucleotide repeat *C9ORF72* gene mutation predominantly gives rise to TDP-43 inclusions however TDP-43-negative, p62-positive staining was found in the cerebellum of FTLD brains with *C9ORF72* mutations (Al-Sarraj et al., 2011; King et al., 2011; Murray et al., 2011a). Semi quantitative scoring of p62 immunoreactivity and TDP-43 in a subset of these cases showed higher p62 immunoreactivity compared to TDP-43 immunoreactivity in the frontal and temporal cortices and sub- cortical structures including the hippocampus (Troakes et al., 2012). At present the mechanism of neurodegeneration caused by *C9ORF72* mutations is not known. These findings suggest that components of the UPS and lysosomal autophagy pathways are involved, however there may be other inclusion proteins yet to be discovered in *C9ORF72* mutants.

1.2. RNA processing and alternative splicing

RNA binding proteins (RBP) including TDP-43 and FUS are found in cytoplasmic and nuclear inclusions in neurodegenerative disease. The mechanism of neurodegeneration is not known however protein sequestration into inclusions may result in either a loss of function or potential gain of function of the protein. RBP play a role in many levels of RNA regulation and thus has directed attention to the role of RNA processing misregulation in the pathogenesis of neurodegenerative disease.

RNA is the essential intermediary used to convert specific DNA sequences in the nucleus into functional proteins in the cytoplasm. RNA processing is highly complex and involves multiple proteins and processes to translate proteins from RNA transcripts. Eukaryotic pre-mRNA undergoes multiple post-transcriptional processing events including capping, splicing and polyadenylation which occur co-transcriptionally within the nucleus.

Splicing describes an essential RNA processing event which removes non-coding sequences (introns) from pre-mRNA and joins together neighbouring coding sequences (exons) to form a mature mRNA. The spliceosome, a multiprotein-multiRNA complex, performs pre-mRNA splicing in eukaryotic cells. Splicing occurs either constitutively where exons of a pre-mRNA are joined together as they are ordered on the DNA sequence or alternatively where one or more exons may or may not be included in RNA transcripts. A key stage in splicing is exon definition where short exon sequences are located amongst vast stretches of intronic RNA. For the spliceosome to locate splice sites, splicing regulatory elements (SRE) are used

which consist of short cis-sequences on pre-mRNA exons or introns that bind trans-acting splicing factors. SREs can act to either stimulate (enhancers) or repress (silencers) splicing of exons. Splice site selection is hugely complex and still not completely specified, however combinatorial control of many influences including *cis* silencer and enhancer elements and local context all play a role (for a recent review see (De Conti et al., 2012)).

Alternative Splicing (AS) is a process where particular exons may be included or excluded from the final mRNA and is a crucial mechanism for gene regulation and for generating proteomic diversity. Recent estimates suggest that around 95% of human multi-exon genes are alternatively spliced (Wahl et al., 2009). Determination of levels of alternative splicing utilises cis-acting splicing silencers and enhancers at the RNA level and the same spliceosomal machinery as constitutive splicing. In addition, alternatively spliced variants can be produced according to different sequence elements at the DNA level such as promoters and transcriptional enhancers (Kornblihtt, 2005). On the trans-acting side, the abundance, cell localisation and phosphorylation state of various splicing factors play a major role in expression of alternatively spliced transcripts (Park et al., 2004; Zhang et al., 2008b).

Global changes in alternative splicing have been demonstrated in AD brains by RNA sequencing and microarrays (Tollervey et al., 2011b; Twine et al., 2011). Tollervey et al.,(2011) show that levels of many RBP proteins are altered in neurodegenerative disease and that particular splicing factors such as Neuro-oncological ventral antigen-1 (Nova 1) can alter alternative splicing of multiple target RNAs in human brain. Nova1 and Nova 2 are splicing factors specific to the central nervous system

and both regulate alternative splicing by binding specific intronic sequences of transcripts containing a YCAY tetramer, where Y indicates a pyrimidine (Ule et al., 2003). Nova1 and Nova 2 knock-out mice show altered splicing levels in transcripts containing the intronic Nova binding sequence (Ule et al., 2003). In Nova 2 knockout mice a microarray analysis found 591 exons that were differentially spliced (Ule et al., 2005). Analysis of the function of the Nova-regulated transcripts showed Nova preferentially regulates transcripts encoding proteins that function in the synapse and many of these proteins interact with each other (Ule et al., 2005). Fox1 (also known as A2BP1) and Fox 2 (also known as RBM9) are RBP expressed in human brain, heart and skeletal muscle and have a consensus RNA binding (U)GCAUG motif (Zhang et al., 2008a). The Fox binding motif is enriched proximal to a set of brain specific exons that are alternatively spliced (Sugnet et al., 2006; Yeo et al., 2007). Computational analysis of the splicing pattern of exons flanked by the Fox 1 and 2 binding motif in human tissue showed that the targets of Fox 1 and 2 splicing factors play important roles in neuromuscular functions (Zhang et al., 2008a).

These findings show that many RBP have specific RNA targets containing binding motifs. A single splicing factor can coordinate splicing events of very specific groups of proteins involved in a functional network. In neurodegenerative disease, levels of trans-factors are altered and result in misregulation of RNA processing of its gene targets and may alter major functional networks. Many different RNA processing steps in a network can be misregulated to cause disease (Anthony and Gallo, 2010).

1.3. Tar DNA Binding Protein-43

1.3.1. Functional domains of TDP-43

TDP-43 protein has similar structural properties to the heterogeneous ribonucleoprotein (hnRNP) A/B family and TDP-43 had been found to be a RBP involved in alternative splicing and transcription (Buratti and Baralle, 2001; Ou et al., 1995). It also has multiple roles in RNA processing such as DNA transcription, DNA replication and repair, pre-mRNA splicing and stability, mRNA export/retention processes and protein translation (Dreyfuss et al., 2002; He and Smith, 2009; Prasanth et al., 2005). TDP-43 exerts skipping of exon 9 of cystic fibrosis transmembrane conductance regulator (CFTR) by binding to UG repeats on the CFTR gene and recruiting an hnRNP A/B inhibitory complex which blocks spliceosome assembly (Buratti and Baralle, 2008). The two highly conserved RNA recognition motifs (RRM1 and RRM2) allow the protein to bind double stranded DNA and single stranded RNA and are required for TDP-43 to regulate alternative splicing of target RNAs including CTFR exon 9 skipping (Buratti and Baralle, 2001; Ou et al., 1995). TDP-43 has two nuclear localisation signals (NLS) situated between the N-terminus and RRM1 (Figure 1.1). The second RNA binding region also contains a nuclear export signal (NES). The C-terminal of TDP-43 is predicted to be unstructured and has regions rich in glycine/serine and glycine/asparagine (Figure 1.2). The function of glycine-rich regions (GRR) are not well defined however the general properties include protein-protein and protein-DNA interactions (Babu et al., 2011; Gsponer and Babu, 2009). As they are unstructured, different folding conformations may be adopted when interacting with different partners such as

proteins, DNA or RNA and this may allow TDP-43 to bind to dispersed UG repeats (Rogelj, 2011).

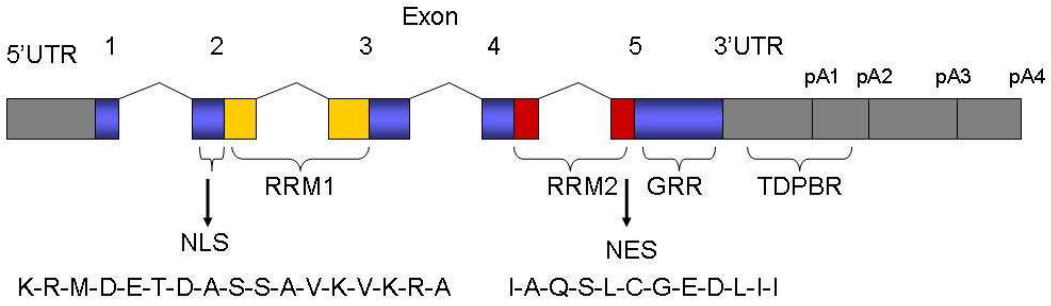

Figure 1.1. Exon structure and structural domains of TDP-43
5'UTR, 5' untranslated region; GRR, Glycine rich region; RRM RNA recognition motif; NES nuclear export signal; NLS nuclear localisation signal; TDPBR TDP-43 binding region; pA1 polyadenylation site 1.

1.3.2 TDP-43 mutations

Multiple mutations in the *TARDBP* gene have been found and provide evidence of a direct link between TDP-43 dysfunction and neurodegeneration. The majority of ALS-linked pathogenic mutations in TDP-43 are found in the GRR (Sreedharan et al., 2008). Some TDP-43 mutations result in increased levels of TDP-43 cleavage fragments in the presence of a proteasomal inhibitor in lymphoblastoid cell lines derived from mutation carriers compared to non-carriers (Kabashi et al., 2008; Rutherford et al., 2008). Insoluble C-terminal fragments of 25 kDa and 35 kDa are found in homogenates of all brains harbouring TDP-43 inclusions (Neumann et al., 2006). TDP-43 mutations may promote cleavage of the full length protein into fragments that do not function in RNA processing (Buratti and Baralle, 2001) and as a consequence result in a loss of TDP-43 function. Some of TDP-43 mutations accelerate TDP-43 aggregation in vitro and enhance TDP-43 toxicity in yeast

(Johnson et al., 2009) and suggest that gain of toxic function as a mechanism for the role of TDP-43 misregulation in neuronal cell death.

1.3.3. Alternative splicing and transcription role for TDP-43 in brain

Recent functional analyses of TDP-43 role in mice and human cells confirm roles in alternative splicing and transcription and show that TDP-43 has multiple targets (Polymenidou et al., 2011; Sephton et al., 2011; Tollervey et al., 2011a; Xiao et al., 2011). Polymenidou et al. (2011) show that TDP-43 downregulation in mice, decreases levels of 601 genes and some of these target genes were other RBP including Fused in Sarcoma (Fus; also known as Translated in Liposarcoma (Tls) and Double-stranded RNA-specific editase 1 (Adarb 1) (Polymenidou et al., 2011). This suggests that TDP-43 misregulation in disease has the potential to alter levels and splicing of other splicing factors and alter multiple pathways. These authors found that genes most altered by TDP-43 downregulation were those involved in synaptic activity. Whether these findings are applicable to the human brain is arguable because most TDP-43 binding sites are in unconserved intronic regions and so TDP-43 targets in mice may be different to those in humans.

RNA targets of TDP-43 binding and regulation have also been studied in more physiological relevant tissues including human brain, human embryonic stem cells and SH-SY5Y cells by analysis of UV-cross-linking and immunoprecipitation (UV-CLIP) (Tollervey et al., 2011a; Xiao et al., 2011). These authors found TDP-43 binds predominantly to intronic UG repeat RNA sequences as previously reported (Buratti and Baralle, 2001). Although TDP-43 has specificity for UG repeats Tollervey et al., (2011a) show that TDP-43 binds to UG motifs that has other RNA

nucleotide sequence interspersed between the UG sequences over a ~200 nucleotide region. The majority of TDP-43 binding is to intronic sequences and indicates that TDP-43 binds to pre-mRNA in the nucleus. The UV-CLIP technique also confirmed previous human targets of TDP-43 binding including FUS, CDK6 and NEFL (Ayala et al., 2008; Strong et al., 2007). Knock down of TDP-43 in SH-SY5Y cells showed altered splicing in 158 genes measured by microarray. Many of the validated alternatively spliced genes that TDP-43 regulates are involved in neuronal development (Tollervey et al., 2011a).

1.3.4. TDP-43 role in post-transcriptional regulation

TDP-43 associates with the Drosha complex which is a large multi-protein complex involved in microRNA (miRNA) biogenesis (Buratti et al., 2010; Ling et al., 2010). Primary miRNA transcripts are transcribed by RNA polymerase II and can be thousands of base pairs in length (Lee et al., 2004). The Drosha complex processes these transcripts in the nucleus producing precursor miRNAs (pre-miRNA) which are approximately 70 nucleotides in length and characterised by a stem loop structure. After nuclear export, pre-miRNAs are cleaved in the cytoplasm by Dicer to generate mature miRNA. Generally miRNAs regulate RNA stability by base pairing to target mRNAs, usually in the 3'UTR, and repress translation by deadenylation of transcripts and subsequent degradation of mRNA targets (Fabian et al., 2010; Filipowicz et al., 2008). The 3' untranslated region (3'UTR) is important for the regulation of mRNA stability, and localisation due to the presence of specific sequences that govern the spatial and temporal expression of a specific RNA (Kuersten and Goodwin, 2003; Xie et al., 2005).

Knockdown of TDP-43 in Hep-3B cells down and up- regulated 11 specific miRNAs (Buratti et al., 2010). The two most significantly altered miRNAs (let-7b and miR-663) both contain a UG repeat sequence which is the canonical RNA binding sequence for TDP-43 (Buratti and Baralle, 2001). Cyclin-dependent kinase 6 (CDK6) is one of the targets of let-7b regulation and has previously been found to be upregulated following TDP-43 down-regulation (Ayala et al., 2008).

In human spinal cord, TDP-43 binds to and stabilises the 3'UTR of neurofilament light (NEFL) possibly for transport of NEFL transcripts into an RNA/ protein complex (RNP particle) and translocation to a site of translation (Strong et al., 2007).

Taken together these results show that TDP-43 plays a major role in splicing and transcription in the nucleus of neurons. It binds to DNA and regulates transcription of many target genes and potentially other splicing factors. TDP-43 binding targets are predominantly intronic and usually contain UG repeats however UG repeats may be dispersed over many nucleotides. TDP-43 also has a role in post-transcriptional events including regulation of microRNA. This suggests that in TDP-43 inclusion bearing neurons, the mislocalisation of TDP-43 into cytoplasmic inclusions and subsequent loss of nuclear TDP-43 may result in misregulation not only of splicing and transcription but also translation into protein of target genes.

1.3.5. TDP-43 aggregation: stress granules

Protein aggregation in cells is generally thought to have negative consequences however in certain circumstances such as heat stress where cellular damage has occurred, particular proteins reversibly aggregate into stress granules (SG) which temporarily stop all but the most essential cellular processes. SG are cytoplasmic ribonucleoprotein foci which transiently assemble and contain mRNAs, RNA binding proteins and stalled translation initiation complexes to slow down growth, translation and conserve ATP for the repair of stress-induced damage (Anderson and Kedersha, 2002). The translational arrest that accompanies environmental stress is selective, while housekeeping transcripts are turned off, translation of heat shock proteins is enhanced (Anderson and Kedersha, 2008). T-cell intracellular antigen-1 (TIA-1) and TIA 1 related protein (TIAR) are markers of SG (Kedersha et al., 1999). These RBP shuttle between the nucleus and cytoplasm, however, in response to environmental stress they rapidly aggregate in the cytoplasm to form SG (for a review see (Anderson and Kedersha, 2008; Thomas et al., 2011)). Nucleation of SGs occurs via a reversible protein aggregation mechanism which is dependent on prion-related domains present in TIA-1, TIAR and (Gilks et al., 2004). TDP-43 is also sequestered into SG after oxidative and environmental stress *in vitro*. *In vitro*, TDP-43 does not play a role in initiating stress granule formation (Colombrita et al., 2009) but may modulate stress granule assembly (McDonald et al., 2011). SG composition is different according to different environmental stressors and TDP-43 is recruited to SGs, *in vitro*, only in certain stressor conditions (Dewey et al., 2012). For example, treatment of HeLa cells with arsenite, an inducer of oxidative stress, causes TDP-43 recruitment to SGs however arsenite treatment of HEK 293 cells does not recruit TDP-43 into SG (Dewey et al., 2011; McDonald et al., 2011) showing that TDP-43

is not a core component of SGs. The prion-related domain within TDP-43 C-terminus most likely mediates interactions with SG (Fuentealba et al., 2010; Liu-Yesucevitz et al., 2010).

1.3.6 Prion domains of TDP-43

Prions cause the transmissible spongiform encephalopathies which include scrapie in sheep and Creutzfeldt-Jakob disease in humans. The infectious prion particle is a misfolded prion protein (PrPsc) which are able to convert natively folded prion protein (PrPc) into a misfolded version through the direct interaction with the misfolded copy (Alberti et al., 2009; Chien et al., 2004; Prusiner, 1982; Toombs et al., 2010). Prion formation follows a crystallisation-like model in which the PrPsc aggregate acts as a nucleus or seed to recruit monomeric PrPc into a growing PrPsc polymer (Lansbury Jr and Caughey, 1995). Infection occurs as prionoids break off the self-aggregating PrPsc polymer and become seeds in their own right. Prions are an infectious agent capable of transference across species, “prionoid” describes a prion-like process where infection occurs within a single tissue or organism and does not transfer to other organisms (Aguzzi, 2009; Aguzzi and Rajendran, 2009).

Around 1% of all proteins have a prion domain and there is a 12 fold enrichment for proteins that have a RRM, for example FUS and many hnRNP proteins have prion-like domains (Doi et al., 2010; Haider et al., 2009; Kenan et al., 1991; King et al., 2012).

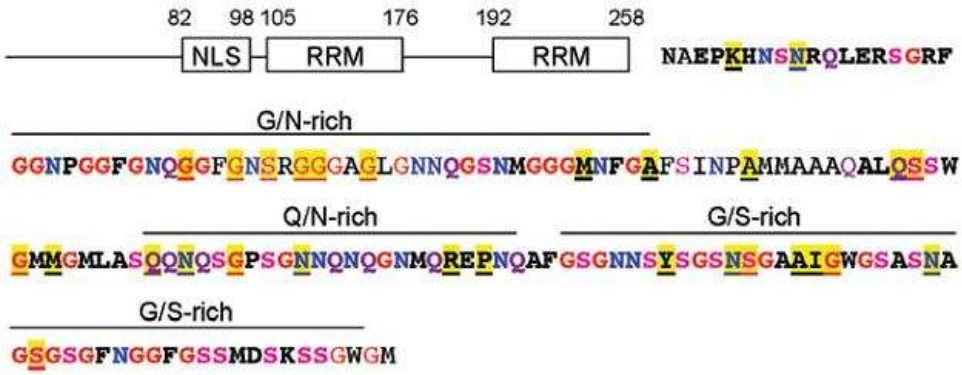

Figure 1.2. The glycine rich and prion domain of TDP-43; taken from Rogelj et al., (2011).
Asparagines are labelled in blue, glutamines in purple, serines in pink, glycines in red and arginines in green. The amino acids in TDP-43 affected by mutations are underlined and shaded in yellow

The C-terminal domain of TDP-43 containing the prion-like domain plays a critical role in TDP-43 proteinopathies, with detergent insoluble C-terminal fragments of 25-35kDa found in homogenates of all brains harbouring TDP-43 inclusions (Neumann et al., 2007b; Neumann et al., 2006). Overexpression of C-terminal TDP-43 constructs designed to mimic the 25 and 35kDa TDP-43 fragments in disease cause cytoplasmic inclusion formation that co-stain with SG markers in human neuroblastoma cells (Liu-Yesucevitz et al., 2010). Expression of peptides containing 12 repeated sequences of the TDP-43 prion domain (residues 331-369) result in aggregates in US02 cells, HEK 293 cells and rat primary neurons (Budini et al., 2012). The aggregates contain endogenous TDP-43 and these results suggest that the prion domain of TDP-43 is critical for aggregation.

In other studies, nuclear TDP-43 CTFs generated with an inducible tobacco etch virus which cleaves TDP-43 at the second RRM were transported to the cytoplasm, however these fragments were degraded and showed no aggregation (Pesiridis et al.,

2011). These authors show that TDP-43 CTF inclusion formation *in vitro* requires "two hits", TDP-43 cleavage and an additional stressor such as depletion or inhibition of RNA transport for TDP-43 aggregates to form (Pesiridis et al., 2011).

The majority of ALS-linked pathogenic mutations found in TDP-43 are in the GGR and the effects of these mutations are diverse (Gendron et al., 2012). *In vitro,* transfection of four different TDP-43 mutations increased the number of cells with TDP-43 inclusions compared to cells transfected with wild type TDP-43 in cells treated with arsenite. Mutant TDP-43 colocalised with TIA-1 showing that TDP-43 inclusions were associated with SGs *in vitro* (Liu-Yesucevitz et al., 2010). Colocalisation of TDP-43 inclusions and SG markers was also demonstrated in human brain tissue from ALS and FTLD cases (Liu-Yesucevitz et al., 2010), however no colocalisation between TDP-43 inclusions and components of SG has been found in ALS brain in other studies (Colombrita et al., 2009; Neumann et al., 2007a; Nijholt et al., 2012).

These findings suggest possible mechanisms for TDP-43 inclusion formation. TDP-43 inclusions colocalise with some SG markers and this shows that an altered stress response could cause cytoplasmic accumulation of TDP-43 (Dewey et al., 2012). In brains from patients harbouring TDP-43 mutations, the increased aggregation properties of particular TDP-43 mutations could result in defects in SG assembly or disassembly. The "two hit" hypothesis suggests that TDP-43 cleavage and chronic cellular stress such as that brought about by aging and environmental stressors could increase SG formation and seed TDP-43 aggregation (Dewey et al., 2012; Polymenidou and Cleveland, 2011).

Evidence for a prion-like propagation of many aggregated proteins has been found in neurodegenerative disease linked proteins including tau and TDP-43, (for reviews see (Aguzzi and Rajendran, 2009; Hardy, 2005; Polymenidou and Cleveland, 2011; Soto, 2012)). The prionoid hypothesis for TDP-43 inclusion propagation is controversial, however it remains a compelling hypothesis for the clinically observed spread of pathology in FTLD, ALS and TDP-43 inclusions in AD (Furukawa et al., 2011; Udan and Baloh, 2011).

1.4. TDP-43 Autoregulation Mechanisms

mRNAs primarily function as templates for protein synthesis and therefore cells have evolved translation-dependent quality control mechanisms to dispose of defective mRNAs that would synthesize abnormal proteins. Nonsense mediated decay (NMD) eliminates mRNAs that prematurely terminate translation and thus reduce the potentially toxic effects of defective transcripts that are routinely generated during gene expression and pre-mRNA splicing (Maquat et al., 2010; Schoenberg and Maquat, 2012). The NMD pathway is also utilised to regulate levels of many splicing factors by coupling alternative splicing with NMD (AS-NMD) (McGlincy and Smith, 2008). It is now known that all members of the human and mouse heterogenous ribonuclear proteins (hnRNPs), of which TDP-43 is a member, and serine-arginine (SR) proteins are maintained by autoregulatory and cross-regulatory pathways using AS-NMD. An example of AS-NMD that has been demonstrated for SRP55 involves the protein binding to the nascent SRP55 RNA transcript and splicing a cryptic exon containing a termination codon (TC; also known as a nonsense codon) into the transcript. For SRP55 the “poison exon” is

spliced into the transcript between exon 2 and 3, the normal SRP55 transcript contains 6 exons (Lareau et al., 2007). The spliceosome leaves an exon junction complex (EJC) marker at each exon-exon junction of the spliced mRNA (Le Hir et al., 2001; Le Hir et al., 2000). During the pioneer round of translation the ribosome removes the EJCs. In the SRP55 example, the ribosome will terminate translation at the first TC encountered, which is the TC contained in the poison exon. The TC in the poison exon is regarded as a premature termination codon (PTC) since there are EJCs remaining on the transcript marking exon-exon boundaries and therefore proteins within the EJC including Upf3 and Upf2 recruit Upf1 which triggers NMD degradation of the transcript (for reviews and references see (Maquat and Gong, 2009; Saltzman et al., 2008)).

Many variations on this basic autoregulatory mechanism are used by the different hnRNP and SR proteins and all result in an autoregulatory feedback loop to maintain constant levels of RBP. What is striking is the level of conservation of these mechanisms used for AS-NMD. Exons and flanking intronic regions involved in AS-NMD coincide with extreme sequence conservation regions called ultraconserved elements (Lareau et al., 2007; Ni et al., 2007; Saltzman et al., 2008) and show that AS-NMD is a ubiquitous mechanism shared by organisms from flies to man.

Analysis of TDP-43 autoregulation in HEK 293 cells is presented in depth in two papers by the Baralle group, Ayala et al., (2011) and Avendaño-Vázquez et al., (2012) and their notation is used for the following summary (see also Figure 1.3). Binding activity of TDP-43 protein to copies of its RNA transcript is mediated by RRM1, the C-terminal domain and regions within the 3’UTR TDPBR.

Downregulation of TDP-43 transcript is dependent on binding sites located in the TDP-43 3'UTR known as the TDP-43 binding region (TDPBR). Using cross linking immunoprecipitation (CLIP), (Ayala et al., 2011) show that most TDP-43 protein binding to the TDP-43 transcript occurs within a 34 nucleotide sequence within the 3'UTR TDPBR. TDP-43 protein specifically binds the TDPBR but with less efficiency than the canonical RNA TDP-43 binding sequence (UG repeats), however this is in line with a less efficient binding region for autoregulatory purposes (Ayala et al., 2011).

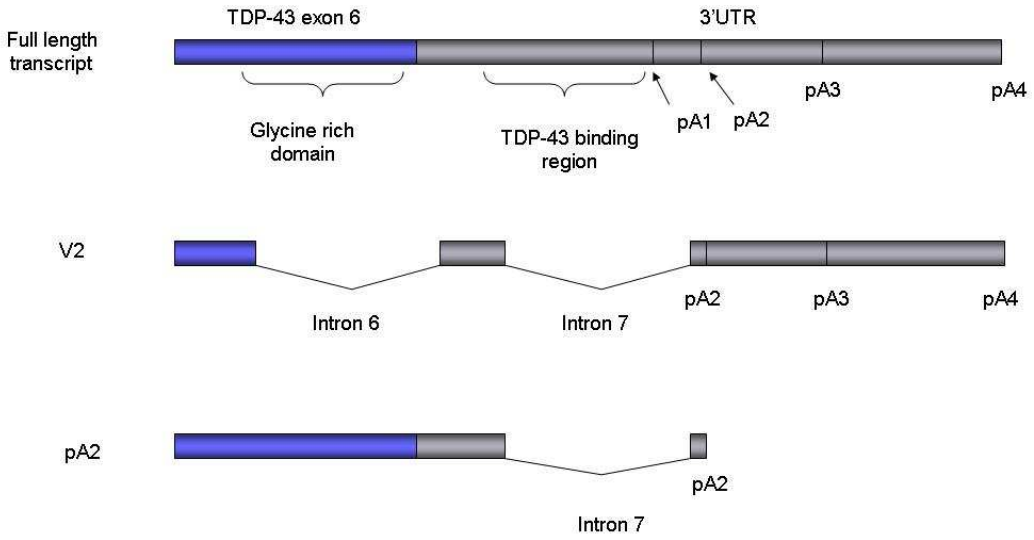

Figure 1.3. 3'UTR splicing of TDP-43.
The 3'UTR of TDP-43 has four polyadenylation sites and in HEK cells there is a preference for the first (pA1) and fourth (pA4) to be used (Ayala et al., 2011).

The Baralle group identified two TDP-43 transcripts that are potentially the products of autoregulatory splicing. The TDP-43 V2 isoform has two cryptic introns 6 and 7 spliced in the 3'UTR. The 5'splice site in intron 6 starts around 118 base pairs from the beginning of exon 6 and removes the TDP-43 glycine rich domain, the Q/N rich "prion domain", the termination codon and around 540 bp of 3'UTR. The intron 7

splice site starts in 3'UTR and splices out the TDPBR and the first poly-adenylation site (pA1) and since pA1 is spliced, the V2 transcript utilises either pA2 or pA4.

A number of mechanisms for detection and degradation of PTC containing transcripts that are targeted to the NMD pathway have been proposed (Bhuvanagiri et al., 2010; Brogna and Wen, 2009). Transcripts that have introns spliced in the 3'UTR usually trigger degradation via the NMD pathway and this may be due to the presence of an EJC beyond the authentic canonical stop codon which is interpreted as premature because splicing junctions are not normally present beyond a stop codon (Giorgi et al., 2007; Lareau et al., 2007). Ayala et al. (2011) found that the V2 transcript was subject to NMD, transcript levels were increased when the NMD pathway was inhibited by cycloheximide or by knockdown of the crucial NMD pathway component, Upf1, in HEK293 cells. Splicing of intron 6 also removes the authentic stop codon and therefore the V2 transcript may also be subject to degradation via the non-stop decay pathway however this is unlikely because there are downstream stop codons that would substitute for the authentic stop codon. Non-stop decay is a translation-dependent degradation pathway for transcripts that lack stop codons which may arise due to mutations, premature polyadenylation or transcriptional arrest (Klauer and van Hoof, 2012).

In HEK 293 cells with tetracyline inducible TDP-43 expression, the V2 transcript is not detected when overexpression of TDP-43 is induced in their system suggesting that the V2 transcript is not the major form of autoregulation for TDP-43. Instead the authors demonstrate that a novel mechanism of autoregulation occurs in TDP-43

where intron 7 is spliced out of the 3'UTR and the transcript (pA2) is retained in the nucleus and thus is not available for translation.

NMD coupled with AS regulates gene expression and provides an additional layer of post-transcriptional regulation in many RBP. TDP-43 transcripts shows complex 3'UTR splicing which results in autoregulation of TDP-43 transcript levels. Levels of TDP-43 proteins are tightly regulated and loss of TDP-43 in mice is lethal, whereas overexpression of human TDP-43 in mice is toxic (Cannon et al., 2012; Wils et al., 2010; Wu et al., 2010). These findings suggest that the nuclear clearance of TDP-43 protein in TDP-43 proteinopathies could feedback to alter levels of its own transcript. The consequences of the reduction of nuclear TDP-43 protein has on autoregulation of TDP-43 transcript levels are not known but misregulation of TDP-43 may contribute to neurodegeneration.

1.5. The microtubule-associated protein tau

Microtubule (MT) stability and mechanical properties are regulated by interactions with accessory proteins such as the microtubule-associated proteins (MAPs). Microtubules are an important component of the cytoskeleton and play a role in cell shape organisation, mitosis, intracellular transport amongst other functions. *MAPT*, the gene name for tau protein, was first co-purified with microtubules and linked to the discovery of microtubule self-assembly. The stabilisation and polymerisation of MTs along axons is a well characterised function of tau.

1.5.1. Tau expression and alternative splicing

The *MAPT* gene consists of 16 exons, with exons -1 and 16 transcribed but not translated (Andreadis et al., 1992). Eight of the 16 exons are potentially alternatively spliced (2, 3, 4a, 6, 8, 10, 13, and 14) which results in protein isoforms ranging in size from 58 kDa to 110 kDa. The 110 kDa "big tau" isoform contains exon 4a and is expressed exclusively in the retina and the PNS (Andreadis, 2005). Tau exons 2, 3 and 10 are alternatively spliced in the human adult CNS.

Tau isoforms expressed in the CNS have either three or four MT binding repeats (3R or 4R tau respectively) and the isoforms containing four repeats has a higher affinity for MTs compared to the 3R isoform (Butner and Kirschner, 1991; Goode et al., 2000; Trinczek et al., 1995). Exons 2 and 3 code for acidic inserts in the N-terminal projection domain. Exon 3 is never expressed without exon 2 and, on the basis of how many N-terminal domains present (2-3-, 2+3- and 2+3+), are termed 0N, 1N and 2N respectively and appear in the brain with prevalence 1N > 0N > 2N (Andreadis, 2005).

Foetal expression of tau is exclusively 0N3R in humans (Takuma et al., 2003) while in human adults six isoforms are expressed by different combinations of exon 10 and the two N-terminal exons. 3R and 4R transcripts are distributed and expressed at similar levels in the adult brain as measured by *in situ* hybridisation, except for the granule cells of the dentate gyrus which had almost exclusive 3R expression (Goedert et al., 1989). Total levels of tau RNA and protein are differentially expressed in different brain regions with a 1.5 fold increase in RNA expression in the frontal cortex, the brain area with the highest expression, compared to white

matter which had the lowest expression, measured by exon arrays (Trabzuni et al., 2012).

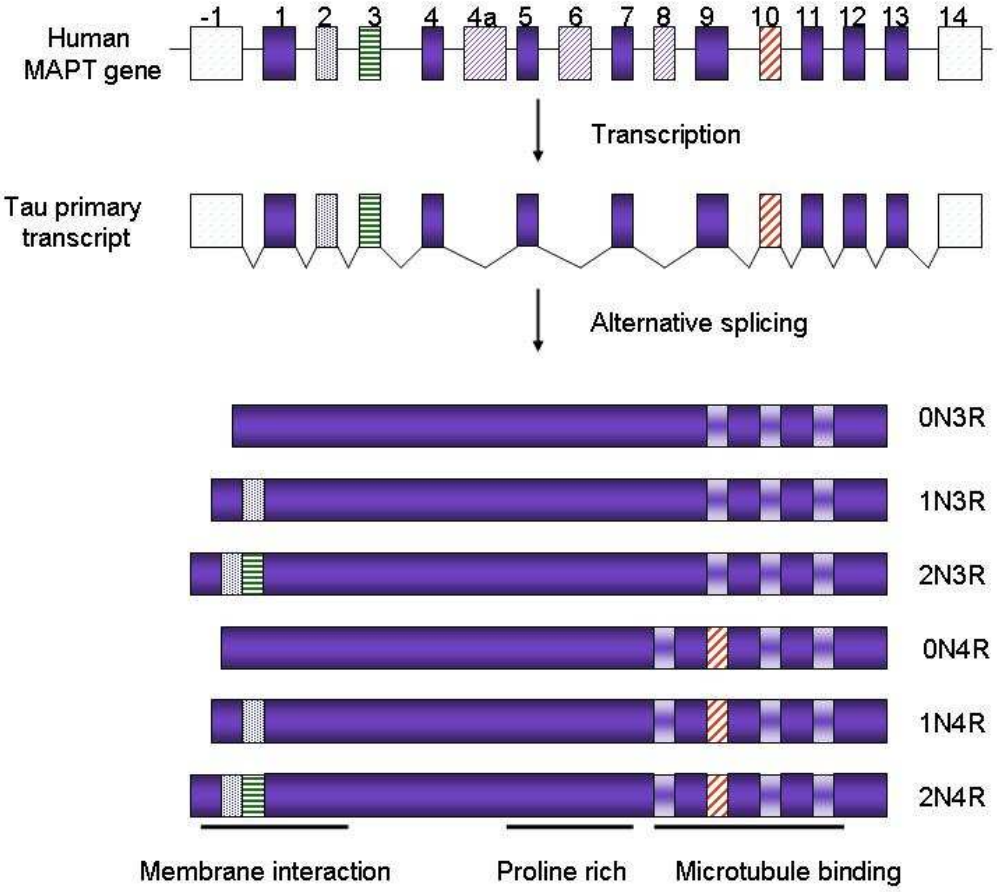

Figure 1.4. Exon structure and alternative splicing of the *MAPT* gene
Alternative splicing of exons 2, 3, and 10 generates six tau isoforms in the human CNS. Isoforms differ by the presence of exons 2 and 3 in the N- terminus, and exon 10 in the C-terminus containing either three (3R) or four (4R) microtubule-binding repeats. 0N3R, the shortest form is the only isoform found in foetal brain

1.5.2. Tau function

Tau exon 10 (E10) codes for one of four imperfect MT repeat binding domains, all of which are highly conserved in vertebrates. The repeats bind to MTs and tau isoforms affect this function to different degrees (Drechsel et al., 1992; Trinczek et al., 1995). Affinity for MT is altered by the number of MT binding repeat domains present on the protein. 4R tau binds to MT more efficiently than 3R tau (Butner and Kirschner, 1991; Goode et al., 2000; Trinczek et al., 1995). Tau has multiple phosphorylation sites and MT binding is regulated by phosphorylation (Bramblett et al., 1993; Hanger et al., 1998; Lindwall and Cole, 1984). Generally higher phosphorylation equates to less MT binding.

MAPs, including tau, regulate axonal transport of mitochondria, via motor proteins such as kinesin. Tau competes with motor proteins for binding to the microtubule surface (Dixit et al., 2008) and MAPs may even block the path of motor proteins (Mandelkow et al., 2004). Expression of 4R tau isoforms in vitro causes more mitochondrial clustering than 3R tau expression in primary neurons (Stoothoff et al., 2009) suggesting that the stronger affinity 4R tau has for MT causes more motor protein pausing compared to 3R tau.

The N-terminal projection domain, which contains alternatively spliced exons 2 and 3, mediates interactions with the plasma membrane (Brandt et al., 1995) and the length of the projection domain also determines spacing between MTs for tau as well as other MAPs (Chen et al., 1992).

1.5.3. *MAPT* mutations in FTDP-17

Mutations in *MAPT* cause FTDP-17 and the functional consequences of FTDP-17 mutations fall into two categories: those with a primary effect at the protein level and those influencing the alternative splicing of tau pre-mRNA. The majority of mutations acting at the protein level alter the MT binding properties and reduce tau protein binding and affinity for MT (Hong et al., 1998), suggesting that the interaction of tau with MT is crucial for preventing the self-assembly of tau (Hasegawa et al., 1998). Mutations acting at the RNA level alter the ratio of 4R/3R tau isoforms (Hutton et al., 1998). Around half of the known tau mutations have their primary effect at the RNA level altering splicing usually by increasing tau transcripts containing exon 10 although others have the opposite effect and increase 3R transcripts (Goedert, 2005). Tau splicing mutations cause FTDP-17 possibly by destabilising a predicted stem-loop structure at the exon 10- intron 10 boundary which alters exon 10 splicing (Hutton et al., 1998; Spillantini et al., 1998b; Varani et al., 1999). Most of the work that supports formation of the stem loop has been done *in vitro* and these structures may not form *in vivo* because multiple splicing proteins bind to pre-mRNA and prevent the formation of secondary structures (Caffrey and Wade-Martins, 2007). An alternative theory is that intron 10 contains cis-sequences that bind trans-acting factors and these ssites are altered by mutations (Andreadis, 2006; D'Souza et al., 1999; D'Souza and Schellenberg, 2000).

Mutations that occur in intron 10 are labelled according to the number of nucleotide they are from the 3’ end of exon 10. The intronic 10+16 mutation and the intronic 10+14 mutation result in a 4R/3R ratio of ~2-6 compared to control of ~1 measured

by RT-PCR in the frontal cortex and cerebellum (Hong et al., 1998; Hutton et al., 1998). Splicing regulation of tau exon 10 is multilayered and weak splice sites flank tau exon 10 and may allow the subtle spatial and temporal regulation of 3R and 4R isoforms. Known splicing regulatory elements within exon 10 include three ESEs at the 5' end and one centrally located ESS and these bind splicing factors including Tra2beta and SF2/ASF (Caffrey and Wade-Martins, 2007; Glatz et al., 2006; Kondo et al., 2004).

Volumetric analysis by MRI imaging of brains with different *MAPT* mutations show that generally FTDP-17 mutations result in atrophy in the temporal cortex however the different types of *MAPT* mutations result in different patterns of atrophy (Whitwell et al., 2009). For mutations that alter tau splicing, the medial temporal lobe is the main area of atrophy while brains with mutations causing reduced MT binding show more widespread atrophy including the frontal lobe and the lateral temporal lobe (Whitwell et al., 2009).

The severity of tau pathology and the morphology of inclusions is heterogenous even within brains harbouring the same mutation. The neuronal pathology of 12 brains all with the 10+16 tau mutation, which increases 4R tau transcripts, was assessed and the authors found that the frontal pole, temporal pole and the medial temporal lobe were severely affected with tau positive neuronal and glial inclusions, with a selective preservation of the posterior part of the superior temporal gyrus in four cases (Lantos et al., 2002). These authors note that the brain samples examined showed considerable differences in severity of the tau inclusions suggesting that

even for a dominant mutation other factors such as epigenetic factors and environment can alter pathology to a considerable degree.

1.5.4. Tau aggregation

Neuropathological examination of FTDP-17 cases shows abundant phosphorylated filamentous tau pathology, however the morphology of the tau filaments is determined, to a significant degree, as to whether the mutation alters splicing of exon 10 or MT binding of tau (Goedert, 2005; Goedert and Jakes, 2005).

For mutations that cause splicing mutations, twisted ribbon structures have been found (Crowther and Goedert, 2000) whereas mutations that result in loss of MT binding (P301L) irregularly twisted ribbons and straight filaments have been reported (Spillantini et al., 1998a) (Spillantini et al., 1998b).

Tau aggregation is dependent on the assembly of a nucleus or seed onto which tau monomers can grow (Friedhoff et al., 1998; Guo and Lee, 2011). The assembly of tau monomers into filaments, results in the formation of a cross-β sheet structure which is a feature of all fibrils belonging to the amyloid class (Barghorn and Mandelkow, 2002). The seeds act as a template, recruiting more tau however the fibrillar structure of the aggregates is dependent on the whether the seed is composed of exclusive 3R exclusive 4R or a mixture of 3 and 4R tau (Dinkel et al., 2011; Yu et al., 2012).

The association between splicing imbalances at the RNA level and deposition of 4R insoluble protein in FTDP-17 cases (Connell et al., 2005; Umeda et al., 2004) suggests that an excess of a particular translated tau isoform can seed tau

aggregation. In AD both 4R and 3R tau is found in tau aggregates and suggests that a different pathways toward tau aggregation are involved in different tauopathies.

1.5.5. Exon 10 expression in tauopathies

Imbalances in tau 4R/3R RNA splicing ratio have been demonstrated in post-mortem brain samples of patients with neurodegenerative tauopathies such as corticobasal degeneration (CBD), progressive supra-nuclear palsy (PSP) and Pick's disease (PiD) (Chambers et al., 1999; Takanashi et al., 2002; Umeda et al., 2004). The altered 4R/3R tau ratio is also found in insoluble protein deposits in tauopathy brains (Buée and Delacourte, 1999; Gibb et al., 2004; Hanger et al., 2002). In PSP and CBD a predominance of 4Rtau isoforms are found and in PiD there is a predominance of 3R isoforms although 4R isoforms are also present in some cases (Arai et al., 2001; King et al., 2001). Arai et al., (2001) report that in their PiD brains they found thorn shaped astrocytes that stain for 4R tau similar to those found in dementia pugilistica, AD and PSP and they suggest that these inclusions may be the source of 4R tau isoforms in PiD.

In AD, conflicting results have been reported regarding tau alternative splice isoform expression, with some studies reporting an equal tau 4R to 3R RNA ratio (Boutajangout et al., 2004; Chambers et al., 1999; Connell et al., 2005; Ingelsson et al., 2006; Umeda et al., 2004) and other reports where increases in 4R tau transcripts have been found (Glatz et al., 2006; Yasojima et al., 1999). The conflicting results may be due to small differences in tau splicing ratios in AD that conventional RT-PCR methods are not sensitive enough to detect (Conrad et al., 2007). With more targeted techniques, tau splicing imbalances have been found in a subset of neurons

harbouring tau pathology. For example, Ginsberg et al. (2006) micro-aspirated single cells from the nucleus basalis which are cholinergic neurons previously shown to contain tau aggregates in AD and mildly cognitively impaired (MCI) cases. Levels of 4R and 3R tau isoforms were measured by microarray analysis and they found 3R tau transcripts reduced in both AD and MCI patients. Conrad et al. (2007) use single molecule profiling to detect levels of all six tau transcripts expressed in control and AD brains. Patient cDNA was PCR-amplified in a gel matrix containing PCR primers and reagents which give rise to a polymerasation colony (polony) containing all six tau isoforms. Polonies were probed with exon specific coloured fluorophores and tau isoform expression were quantified in 250-2500 polonies (Conrad et al., 2007; Zhu et al., 2003). A 1.3 fold increase in 4R tau was found in AD samples compared controls with 4R0N isoforms contributing to the increase. They also found a 1.6 fold decrease in exon 2 containing transcripts with 2N3R and 1N3R isoforms being significantly reduced in AD brains. These results suggest that AD tangle bearing neurons show increases in 4R tau transcripts. RNA extracted from a brain sample will typically contain both tangle bearing and non-tangle bearing neurons and when quantified with conventional RT-PCR based methods, small differences in RNA transcript levels may be averaged out.

These findings show an association between tau splicing imbalances, particularly increases in 4R transcripts, and post-mortem confirmed tauopathy and suggests that tau splicing ratio imbalances are a risk factor for tauopathy. In AD contradictory finding regarding levels of tau exon 10 have been reported, however using sensitive techniques, increases in exon 10 transcripts have been found in tangle bearing neurons (Conrad et al., 2007; Ginsberg et al., 2006).

1.5.6. Tau haplotypes

Genetic variation in the *MAPT* gene contributes to the risk of developing neurodegenerative disease. H1 and H2 SNPs that define the *MAPT* haplotype extend over 2 million bases (2Mb) and include many genes other than *MAPT* (Pittman et al., 2005). A 900kb inversion in the 17q21 region of chromosome 17 which includes the *MAPT* gene results in two major tau haplotypes H1 and H2. Tau H1 and H2 haplotypes differ only in their intronic sequence and are defined by SNPs spanning the whole *MAPT* gene and include a 238bp intronic deletion in H2. In addition to the H1 and H2 haplotype defining SNPs there exist SNPs that vary only on the H1 background, the H2 haplotype is largely invariant (Pittman et al., 2004). Three H1-specific SNPs, that define the H1c subhaplotype, and span a 56.3kb region upstream of *MAPT* exon 1 to the 3' region of intron 9 were found to be highly associated with PSP and CBD (Pittman et al., 2005; Rademakers et al., 2005). In addition, multiple *MAPT* loci spanning 20kb either side of the *MAPT* gene were found to be associated with AD in a gene-wide analysis of data from a genome-wide association study (GWAS) (Gerrish et al., 2012). Taken together these results suggest that *MAPT* risk-causing SNPs span regions that are potentially involved in both transcription and/or splicing regulation of tau (Pittman et al., 2005). To test if tau transcription was altered in the H1c haplotype, Myers et al. (2007) used qRT- PCR to measure total tau levels and found that the presence of at least one H1c allele increased total MAPT expression by 11-13% in frontal and temporal cortex in AD and control brains. Additionally, the authors found that the H1c allele increased 4R tau isoform expression in the same sample set by approximately 25% (Myers et al., 2007).

Another study determining exon 10 splicing and transcriptional differences in H1 and H2 tau haplotypes used a method where cDNA from H1/H2 heterozygotes in control human frontal cortex and the globus pallidus were PCR amplified with primers that span exonic SNPs that distinguish H1 and H2 tau haplotypes in either exon 1 or exon 9 (Caffrey et al., 2006). The PCR products were used as templates for primer extension and these products were quantified by matrix-assisted laser desorption/ionisation-time of flight mass spectrometry (MALDI-ToF). No differences were found in total tau expression between H1 and H2 in both brain regions. However Caffrey et al., (2006) found 1.43 fold increases in 4R tau in the H1 haplotype compared to H2 in the globus pallidus and 1.29 fold increases in 4R transcripts in the frontal cortex (Caffrey et al., 2006). In a further study, the authors used the same method to measure tau haplotype expression differences in tau exons 2 and 3 with sets of PCR primers for each of the three tau N-terminal transcripts (0N, 1N and 2N). Caffrey et al. (2008) found two-fold increases in the 2N transcripts in H2 haplotypes in the frontal cortex and the globus pallidus. The H2 haplotype is negatively associated with PSP and CBD and therefore considered protective.

Using exon arrays, Trabzuni et al. (2012) found increases in tau exon 3 expression in H2 haplotypes and neither 4R nor total *MAPT* expression was increased in H1 or H1c haplotypes in human brain samples from various regions including frontal, temporal and occipital cortex, hippocampus, thalamus and cerebellum. At present these findings consistently point to a protective effect of the H2 allele conferred by increases in tau exon three. There are no consistent findings regarding the mechanism of how SNPs on the H1 tau haplotype increase risk for tauopathy.

1.6. APP

The two major neuropathological hallmarks in the AD brain are the presence of senile plaques and neurofibrillary tangles. Senile plaques are composed mainly of insoluble Aβ peptides derived from proteolytic cleavage of Amyloid Precursor Protein (APP). There are two different routes for APP proteolysis. The non-amyloidogenic pathway involves α-secretase cleavage within the Aβ region resulting in a secreted N-terminal APP fragment (sAPPα) and a membrane bound C-terminal fragment (C83 or CTFα). Alternatively the amyloidogenic route occurs through intramembranous cleavage by β-secretase producing a β C-terminal fragment (C99 or CTFβ) and a secreted N-terminal fragment (sAPPβ). The CTFβ is cleaved by γ-secretase to produce Aβ.

APP was initially identified as a cell surface receptor (Kang et al., 1987) and it may play a role in other functions such as cell adhesion (Ghiso et al., 1992) and neurite outgrowth (Small et al., 1999) however it is not clear, at present, what the major roles are of the full length protein or the secreted fragments in the CNS.

Three major APP isoforms are produced from the alternative splicing of exon seven and eight (APP770) exon seven (APP751) and neither seven or eight (APP695). Exon seven codes for a Kunitz family of protease inhibitors domain (KPI) domain and the presence or absence of this domain is the main difference between the APP isoforms. Exon eight codes for a chondroitin sulphate glycosaminoglycan (CS GAG) attachment site (Jacobsen and Iverfeldt, 2009). Very low quantities of an APP transcript APP714 are produced in the human CNS, which is the result of alternative splicing of exon eight alone (Golde et al., 1990).

Although there has been conflicting evidence regarding differential expression of APP isoforms in AD (for review see Panegyres et al. (2000)), more recently a number of studies have found consistent increases in expression of APPKPI, APP770 and APP751, isoforms in AD brains compared to controls (Matsui et al., 2007; Preece et al., 2004) or diminished APP695 expression in AD (Tharp et al., 2012).

Matsui et al., (2007) found that NSE, a marker for neurons, decreased in AD brains while GFAP, an astrocyte marker, increased. There were no differences in total APP expression in controls and AD measured by qRT-PCR although there was a significant increase in APPKPI containing isoforms in AD brains at the RNA and protein level, and the increased APPKPI expression correlated with increased GFAP. The authors conclude that the increase in APPKPI (APP770 and APP751) and decrease in APP695 reflects the loss of neurons and subsequent gliosis found in AD brains. In view of the findings that astrocyte expression of APP is extremely low (Guo et al., 2012), the origin of the increases in KPI-containing APP transcripts found in AD is, at present, not clear. Altered levels of splicing factors in disease may play a role in changing APP isoform ratios (Donev et al., 2007).

The different processing pathways for APP containing the KPI domain, may impact on the disease process. In transfected cells, KPI-containing APP proteins are processed differently with APP751 expressing cells producing less sAPPα compared to APP695 expressing cells (Ho et al., 1996). Cells transfected with APP770 secreted more Aβ than cells transfected with either APP751 or APP695 (Donev et al., 2007),

these findings suggest that the APP KPI domain diminishes α-cleavage and results in more Aβ production.

The KPI-containing APP isoforms have previously been reported to be predominately expressed in astrocytes (Chauvet et al., 1997; LeBlanc et al., 1997; Tran, 2011; Yasuoka et al., 2004), however, it has recently been demonstrated by immunohistochemistry that in fact astrocyte APP expression is extremely low, at least in mice (Guo et al., 2012).

1.7. Alzheimer's Disease

Alzheimer's disease (AD) is a neurodegenerative disorder that is characterised clinically by progressive impairments in memory and cognition. AD is the most common cause of dementia accounting for between 60-80% of dementia cases. The two hallmark characteristic pathologies in AD are:
1) Alzheimer-type plaques composed predominately of extracellular amyloid- beta (Aβ), also containing hyperphosphorylated tau-positive dystrophic neurites.
2) intraneuronal neurofibrilliary tangles (NFT) made up of paired helical filaments of abnormally hyperphosphorylated microtubule associated protein tau (MAPT).

On the basis of studies that measure quantity and location of neurofibrillary pathologies (NFT and NT) (Braak and Braak, 1991; Braak et al., 2011) and amyloid plaques (Alafuzoff et al., 2009; Thal et al., 2002; Thal et al., 2000) in AD, staging systems have been developed that differentiate initial, intermediate and advanced stages of AD. The insoluble fibrous protein deposits in AD progressively accumulate and are distributed in a characteristic pattern. Initially Aβ deposits and

neurofibrillary lesions develop concomitantly although at different locations in the brain with Aβ plaques starting in cortical regions and NFT initiating in the noradrenergic projection neurons of the locus coeruleus (Braak et al., 2011). The severity of the amyloid pathology correlates with neurofibrillary lesions in AD brain (Thal et al., 2002).

Tau pathology is a useful marker for AD progression because NFT density is correlated with disruption of specific neuronal circuits and cognitive decline (Giannakopoulos et al., 2007; Nelson et al., 2012; Nelson et al., 2009). Although this correlation suggests that tau deposition may mediate AD-associated toxicity the links between tau aggregation, clinical symptoms and toxicity is at present not clear.

Ultrastructural analysis of mature tau filaments isolated from AD brain show that the tau protein deposits appear as two protofilaments wound around each other and these fibrillar structures are called paired helical filaments (PHF). PHF-tau may be preceded by pretangles (Bancher et al., 1989; Braak et al., 1994) or granular oligomeric tau (Maeda et al., 2007) both of which differ morphologically from fibrillar tau but all tau aggregates share a β-sheet structure as with other amyloidogenic proteins (Sahara et al., 2008). The bulk of tau protein inclusions in AD are made up of neuro-fibrillary tangles (NFT) in cell bodies and neuropil threads (NT) in dendrites (Mitchell et al., 2000). Neuritic plaques display clusters of radially orientated neuronal processes, which are tau immunoreactive, often surrounding an amyloid core.

Mutations in Presenilin (*PSEN*) and *APP* genes cause AD however the frequency of these mutations is very uncommon. The vast majority of AD cases are sporadic and in a recent GWA study, common SNPs at *PSEN1*, *PSEN2* and APP did not show any association with AD, showing that common genetic variation at these loci are not a risk factor for sporadic AD while SNPs across the whole *MAPT* locus confer a small amount of risk for sporadic AD (Gerrish et al., 2012). The most highly associated gene for sporadic AD is Apolipoprotein E4 (ApoE). Three common isoforms apoE2, apoE3 and apoE4, determined at the DNA level by the ε2,ε3, and ε4 alleles of the *APOE* gene. The ε4 isoform is the strongest predisposing allele while the ε2 allele is protective (Corder et al., 1994; Corder et al., 1993). Compared to individuals with no ε4 alleles, the increased risk for AD is 2-3 fold in people with a single APOE ε4 allele and ~12 fold in ε4 homozygotes (Bertram et al., 2007; Roses, 1996). Other genetic risk factors for sporadic AD include clusterin (*CLU*) and bridging integrator 1 (*BIN1*) (Harold et al., 2009) amongst others, see http://www.alzforum.org/ for the latest GWAS results. The contribution of each of these individual genes to risk of AD is very small however their combined effect, possibly converging in a single pathway, may play a larger role in AD pathogenesis.

1.7.1. TDP 43 in AD

Around 20-35% of AD cases, in addition to tau neurofibrilliary tangles (NFT) and Aß plaques, also have TDP-43 inclusions (Amador-Ortiz et al., 2007; Arai et al., 2009; Higashi et al., 2007; Hu et al., 2008; Kadokura et al., 2009; Uryu et al., 2008). Amador- Ortiz et al., (2007) found all AD brains that were TDP-43 positive had TDP-43 inclusions in the entorhinal cortex with variable pathology outside the limbic regions. Two AD-TDP subtypes were identified, “limbic” type with

inclusions only in the limbic structures such as the amygdala, hippocampus and entorhinal cortex and “diffuse” with additional frontal and temporal cortical TDP-43 inclusions, subsequently an “amygdala only” type has also been identified (Hu et al., 2008). Diffuse type AD TDP-43 positive brains had significantly more TDP-43 immunoreactivity in the cingulate gyrus and nucleus accumbens than limbic type suggesting that the severity of TDP-43 pathology was greater in the diffuse type compared to the limbic type (Amador-Ortiz et al., 2007). These authors also noted that a small number of NFTs had TDP-43 positive immunoreactivity and with double labelling for phospho-tau (CP-13) and TDP-43 immunoreactivity they found two different patterns of colocalisation, in some neurons there was double labelling of the inclusion with overlap of the two epitopes however more commonly the two epitopes were only partially overlapping.

The significance of TDP-43 inclusions in AD is not known however there is evidence to suggest that the presence of TDP-43 inclusions may alter both pathology and clinical symptoms of AD patients.

1.7.2. TDP-43 may alter tau pathology in AD

Tau pathology has a well established topographical progression and a number of researchers report a very similar progression of TDP-43 pathology in AD spreading from limbic structures to association cortices (Higashi et al., 2007; Hu et al., 2008; King et al., 2010) and suggests possible additive effects between tau and TDP-43 pathologies.

Many studies find that high proportions of AD brains with TDP-43 also have hippocampal sclerosis (HS) and may be due to the combination of tau and TDP-43

pathologies (Probst et al., 2007). HS refers to extensive neuronal loss in the subiculum and CA1 region of the hippocampus and in young patients is often associated with temporal lobe epilepsy (Probst et al., 2007; Zarow et al., 2008). In older patients, HS is often associated with other neurodegenerative diseases including AD, vascular dementia and FTLD-TDP. HS in the context of AD, where extensive NFT pathology in the hippocampus is observed, is regarded as neuronal cell loss disproportionate with the degree of NFT tau pathology present (Amador-Ortiz et al., 2007; Pao et al., 2011) although some investigators do not recognise HS in the setting of other neurodegenerative diseases such as AD (Lippa and Dickson, 2004).

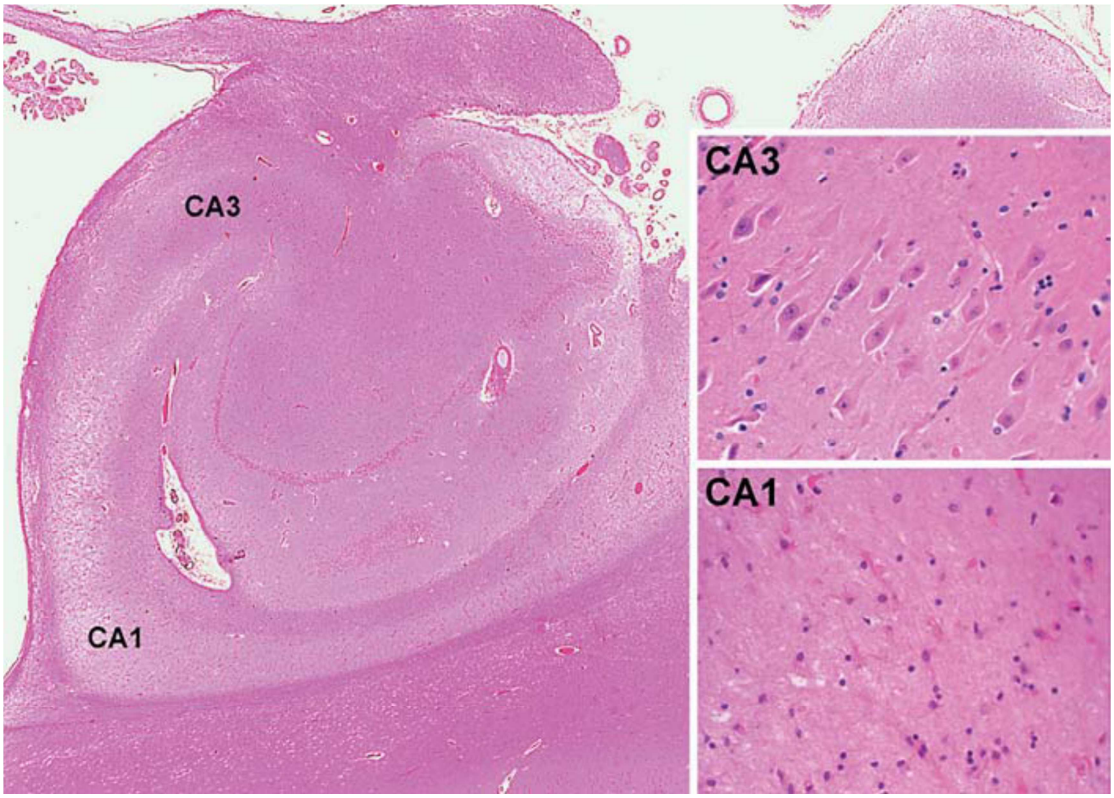

Figure 1.5. Hippocampal Sclerosis is characterised by selective neuronal loss in CA1 with relative preservation of neurons in CA3. From Dickson et al. (2010).

A range of 29% to 100% of AD brains with TDP-43 pathology are reported to also have HS and, where reported, is significantly more common in TDP-43 pathologically immunoreactive brains than in TDP-43-negative brains (Amador-Ortiz et al., 2007; Bigio et al., 2010; Davidson et al., 2011; Dickson et al., 2010; Josephs et al., 2008).

Although high rates of HS may be observed in FTLD-TDP (Blass et al., 2004; Josephs and Dickson, 2007; Pao et al., 2011), HS is more often associated with TDP-43 inclusions in AD (Probst et al., 2007) and has been found in other tauopathies such as PSP (Yokota et al., 2010).

On the basis that tight correlations exist between HS and TDP-43 pathology in AD, some researchers consider that AD with HS and TDP-43 inclusions is a distinct subtype of AD (Robinson et al., 2011). Other researchers note that the correlation between HS and TDP-43 is not absolute and that many cases of HS do not have any TDP-43 pathology and suggest that HS in AD is a coincidence of two common pathologies (Davidson et al., 2011). However the prevalence of TDP-43 pathological immunoreactivity in HS-positive brains may be underestimated in some studies that assess HS only from one brain hemisphere because, in some cases, HS is only present unilaterally (Nelson et al., 2011; Probst et al., 2007; Zarow et al., 2012).

It is unclear why TDP-43 inclusions occur in sporadic tauopathies however it may be accounted for by genetic risk factors. Mutations in the progranulin gene (*PGRN*) result in haploinsufficiency of progranulin expression and cause FTLD-TDP (Baker et al., 2006). A 3’ untranslated region (UTR) single nucleotide polymorphism (SNP),

which is predicted to block a microRNA binding site in the progranulin gene, has been associated with FTLD-TDP and may increase risk of developing disease (Rademakers et al., 2008) although this finding has not been replicated (Simón-Sánchez et al., 2009). The *PGRN* 3'UTR SNP was also associated with HS in AD cases with TDP-43 inclusions (Dickson et al., 2010). Genetic variation in genes in which mutations have previously shown to cause TDP-43 pathology may increase the risk for developing TDP-43 pathology.

1.7.2. TDP-43 may alter clinical symptoms in AD

A major question that arises is whether TDP-43 pathology contributes to AD pathology and/or clinical symptoms. Most AD patients have an amnestic presentation where memory loss is the most dominant presenting symptom and is severe before other deficits emerge. However, AD is clinically heterogenous (Snowden et al., 2007b; Stopford et al., 2008) and at autopsy, some patients that present with language or behavioural problems more typical of FTLD- tau or FTLD-TDP, show AD pathology (Bigio et al., 2010). AD patients with a language phenotype (primary progressive aphasia; PPA) have previously shown no correlation between distribution of AD pathology (tau and Aβ) and clinical symptoms (Galton et al., 2000; Mesulam et al., 2008; Munoz et al., 2007). Bigio et al., (2010) tested if the atypical PPA phenotype found in a subset of AD patients could be accounted for by concomitant TDP-43. No correlation was found between distribution of TDP-43 pathology and atypical AD clinical symptoms for PPA however TDP-43 pathology was associated neuronal loss in the hippocampal region and suggests that TDP-43 pathology contributes to clinical deficits associated with hippocampal cell loss such as memory.

MRI scanning of AD brains showed that those with TDP-43 inclusions had a lower hippocampal volume than AD brains without TDP-43 inclusions (Josephs et al., 2008). HS was significantly more prevalent in the TDP-43 positive group than the TDP-43 negative group. The authors report that within the group of subjects with TDP-43 pathology there were no differences in hippocampal loss in those with and without HS which suggests that TDP-43 pathology, independent of HS, is associated with hippocampal atrophy. The presence of TDP-43 also impacts memory and cognition. TDP-43 immunoreactive brains had clinically worse dementia with lower Mini-Mental State Examination and Boston Naming test scores than those without TDP-43 pathology (Josephs et al., 2008). In this study the AD TDP-43 positive cases were older at disease onset and at death however the lower memory and cognitive scores were significantly lower when adjusted for age at death and therefore suggests that disease duration was not impacting on clinical measures.

A consistent finding across MRI and neuropathology studies is that TDP-43 in AD results in neuronal loss in the hippocampus and correlates with loss of memory. The mechanism of how TDP-43 may interact with or exacerbate tau pathology in the hippocampus in AD is not known

1.8. Aims of this thesis

Intracellular neurofibrillary tangles composed of hyperphosphorylated tau and extracellular plaques composed of Aβ derived from proteolytic processing of APP are the two hallmark pathologies of AD. TDP-43 inclusions are also found in a subset of AD cases. TDP-43 has a role in multiple RNA processing events including splicing. In brain with TDP-43 inclusions dysfunction of TDP-43 may result in altered RNA processing. Altered splicing ratios of both tau and APP have been associated with AD however these results have been inconsistently found.

Our hypothesis is that TDP-43 dysfunction affects tau and APP RNA processing either directly or indirectly and increases disease severity.

The aim of this thesis is to correlate AD molecular pathology with the presence of TDP-43 pathology.

The specific objectives are:

To measure isoform ratios of tau exon 10 from control and AD brains with and without TDP-43 inclusions.

To measure isoform ratios of APP exon 7 and 8 from control and AD brains with and without TDP-43 inclusions.

To characterise TDP-43 3'UTR isoform ratios involved in TDP-43 autoregulation, from control, FTLD and AD brains with and without TDP-43 inclusions.

Chapter two: Material and Methods

2.1. Materials

Molecular biology, microbiology and cell culture reagents were purchased from Invitrogen Ltd (Paisley, UK) unless otherwise stated. All other chemicals were purchased from Sigma-Aldrich Ltd (Dorset, UK) except where indicated. Ultrapure water from an Elga Maxima water purification system was used to prepare stock and buffer solutions.

2.1.1. General reagents and stock solutions

Agarose

Ammonium persulphate , 10% (w/v) (National Diagnostics Ltd., Yorkshire, UK)

Ampicillin, 100mg/ml in ultra-pure water

Ammonium persulphate (APS)

Beta-mercaptoethanol (Merck Biosciences, Hertfordshire, UK)

Bromophenol blue, 0.5% (w/v)

Bovine albumin (Thermo Scientific)

Chloroform

Dithiothreitol (DTT)

Ethanol , 99% (v/v) (Merck Biosciences, Hertfordshire, UK)

Ethidium Bromide (10mg/ml)

Foetal bovine serum (FBS) (Sera Laboratories International, West Sussex, UK)

Isopropyl-beta-D-thiogalactopyranoside (IPTG)

L-glutamine

Glycerol

Guanidine

Isopropanol (Merck Biosciences, Hertfordshire, UK)

Methanol, 100% (v/v) (Merck Biosciences, Hertfordshire, UK)

N,N,N',N'-tetra-methylethylenediamine (TEMED) (National Diagnostics Ltd.)

N-Lauroylsarcosine solution (sarkosyl)

Pencillin/Streptomycin

Phenol-chloroform

Phenylmethanesulfonylfluoride (PMSF)

Polyoxethelene sorbitan monolaurate (Tween 20)

Sodium dodecyl sulphate (SDS) (National Diagnostics Ltd.)

Sodium lauroyl sarcosinate (sarkosyl)

SYBR Green (Roche Diagnostics)

Tetramethylethylenediamine (TEMED) (National Diagnostics Ltd.)

TRIS (hydroxymethyl) aminomethane hydrochloride

Trizol ® reagent (Invitrogen)

Trypsin-EDTA

X-gal (Promega, Southampton, UK)

2.1.2. Bacterial strains

Escherichia coli (E.coli) host strain, JM109 (Promega, Southampton, UK) was used to amplify plasmids.

2.1.3. Bacterial culture media and reagents

Luria- Bertani (LB) broth base

A pre-mixed powder consisting of (per one litre): 1% (w/v) SELECT Peptone 140, 0.5% (w/v) NaCl and 0.5% SELECT yeast extract, pH 7.0 was purchased. A 2%

(w/V) solution was prepared in 1 litre culture flasks and autoclaved at 121ºC for 15 mins.

LB ampicillin (LB-amp) medium

A Nalgene syringe filter, 0.2 µm pore size was used to prepare filter-sterilised stock of ampicillin, 100mg/ml in ultra-pure water. A final concentration of 100µg/ml was added to autoclaved LB.

LB-agar

A pre-mixed powder consisting of 1.2% (w/v) SELECT-agar in LB was purchased. A 3.2 % (w/v) solution of LB-agar was prepared in ultra-pure water and autoclaved at 121ºC for 15 mins.

LB-amp agar

Ampicillin stock solution was added to cooled, autoclaved LB-agar to give a final concentration of 100µg/ml. 20ml of LB-amp agar was poured into 10cm diameter sterile Petri dishes and allowed to cool.

2.1.4. Solutions for the preparation of plasmid DNA

Miniprep

All solutions were purchased as part of a QIAprep® Spin Miniprep Kit (Qiagen, West Sussex, UK).

2.1.5. DNA analysis solutions

Tris-acetate-EDTA (TAE) 50x

2M Tris-acetate-EDTA (pH 8.0)

50mM EDTA

Agarose gel loading solution 6x

0.25% (w/v) orange G

40% (w/v) sucrose

DNA size markers

Quick-load™ 1kb DNA ladder (New England Biolabs, Hertfordshire, UK): 10002, 8001, 6001, 5001, 4001, 3001, 2000, 1500, 1000, 500 bp fragments. The 3001 bp fragment is of a higher concentration for easy identification.

Quick-load™ 100 bp DNA ladder (New England Biolabs, Hertfordshire, UK): 1517, 1200, 1000, 900, 800, 700, 600, 500, 400, 300, 200, 100 bp fragments. The 1000 and 500bp fragments are of a higher concentration for easy identification.

QIAquick gel extraction/reaction cleanup kit

QIAquick kit (Qiagen) was used to extract and purify DNA from agarose gels.

2.1.6. DNA analysis solutions

DNA extraction

DNA was extracted from cells with proteinase K (Qiagen). RNA was degraded with RNase A/T1 (New England Biolabs, Hertfordshire, UK). DNA was purified with phenol-chloroform.

2.1.7. RNA analysis solutions

RNA extraction

RNA was extracted from cells using Trizol® reagent, a solution of phenol and guanidine. RNA was extracted from human brain with the RNeasy lipid tissue kit (Qiagen).

DNAse treatment

DNA was degraded by with Turbo DNAse kits (Ambion, UK).

2.1.8. Reverse transcription solutions

Reverse transcription (RT) was perforemed using a kit (Applied Biosystems, Cheshire, UK). The reagents are listed as final concentrations with stock concentrations in brackets. Non-DEPC treated, nuclease free water was purchased from Ambion Ltd. (Cheshire, UK).

-1x RT buffer (10x RT buffer: 500 mM KCl, 100mM Tris-HCl, pH 8.3)

-55mM magnesium chloride (25mM)

-500 µM of each deoxyNTPs (dNTPs) (dNTP mixture containing 2.5 mM of aATP, dCTP, dGTP and dDTP)

- 25µM oligo-dT (dT16) (50 µM in 10mM Tris-HCl pH 8.3)

- 0.4 U/µl RNase inhibitor (20 U/µl in 20 mM HEPES-KOH, pH 7.6, 50 mM KCl, 8mM DTT, 50 % (v/v) glycerol)

- 1.25 U/µl Multiscribe Reverse Transcriptase (50 U/µl)

2.1.9. PCR solutions

Taq polymerase in storage buffer B

PCR was carried out using Taq DNA polymerase in storage buffer B (Promega). Taq DNA polymerase is a thermostable enzyme that replicates DNA at 74ºC and exhibits

a half-life of 40 mins at 95 ºC. Taq catalyses the polymerisation of nucleotides into duplex DNA in the 5' to 3' direction in the presence of magnesium.

Taq DNA polymerase 5x buffer

Containing (working concentration 1:10)

50mM KCl

10 mM Tris-HCl pH 9.0

1.5 $MgCl_2$

1% (v/v) Triton X-100

2'-Deoxynucleoside 5'-triphosphates (dNTPs)

Each nucleotide (Amersham Pharmacia Biotech UK Ltd., Buckinghamshire, UK) was supplied as a 100mM solution in sterile ultra-pure water (pH 7.5). A 12.5x stock solution containing 2.5 mM of each dNTP was prepared by mixing 5µl of dATP, dCTP, dGTP and dTTP with 180ul of sterile H_2O

Primers

Primers were synthesised by MWG-Biotech and diluted to a working stock solution of 2 µM for end point RT-PC or 10µM for qRT-PCR. Primers for target genes (*MAPT* and APP) were designed to span exon-exon boundaries to avoid amplification from genomic DNA. qRT-PCR cDNA products were all ~100 bp. qRT-PCR Primers for housekeeping genes were purchased from Primerdesign, UK.

DY682 labelled primers.

The technique used in our analysis of tau exons 2,3and 10, APP exons 7 and 8 and TDP-43 3'UTR expression was to label the forward primer with a DY682 fluorophore which incorporates into PCR products during RT-PCR. Analysis by quantifying the fluorophore signal is more accurate than using DNA intercalators such as ethidium bromide because one transcript contains one fluorophore and therefore the fluorophore signal measured is proportional to transcript number not transcript size.

Quantitative reverse transcription polymerase chain reaction

FastStart SYBR Green 2x Master Mix containing 2mM ROX (Roche, UK) was used to bind cDNA.

NAME	LOCATION	SEQUENCE	PRODUCT SIZE (BP)
GAPDH	Exon 4	5'-GCCCAATACGACCAAATCC-3'	166
	Exon 6	5'-AGCCACATCGCTCAGACAC-3'	
Tau 9-13	Exon 9	5'-DY682- CTGAAGCACCAGCCAGGAGG-3'	E10+ 368
	Exon 13	5'-AGCCACATCGCTCAGACAC-3'	E10- 275
Tau N-terminal	Exon 1	5'-DY682-TACGGGTTGGGGGACAGGAAAGAT -3'	2N 284 1N 197
	Exon 4	5'-GGGGTGTCTCCAATGCCTGCTTCT-3'	0N 110
Total tau	Exon 11/12	5'-CCATCATAAACCAGGAGGTGGCC-3'	148
	Exon 12/13	5'-GGTCAGCTTGTGGGTTTCAATCTT-3'	
APP exon 7 & 8	Exon 6	5'-DY682-CACCACAGAGTCTGTGGAAG-3'	APP770 313
	Exon 9	5'-AGGTGTCTCGAGATACTTGTC-3'	APP751 256 APP695 88
Total APP	Exon 3/4	5'-CGCTGCTTAGTTGGTGAGTTTG-3'	140
	Exon 4/5	5'-CTCTTCTCACTGCATGTCTCTTTGG-3'	
TDP 3'UTR	3'UTR	5'-GAACTGCTGTTTGCCTGATTGG-3'	3'UTR 1176
	3'UTR	5'-CTGCTATGAATTCTTTGCATTCAGG-3'	pA2 472

Table 2.1. Primers used in RT-PCR splicing analyses and qRT-PCR

2.1.10. SDS-polyacrylamide gel electrophoresis (SDS-PAGE) solutions

Tris-HCl SDS stock buffers

The Tris-HCl SDS stock buffers used for the preparation of the resolving and stacking gels were purchased from National Diagnostics Ltd. ProtoGel™ Resolving Buffer solution consisted of 1.5 M Tris-HCl (pH 8.8) and 0.1% (w/v) SDS, whereas

ProtoGel™ Stacking Buffer consisted of 0.5 M Tris-HCl (pH 6.8) and 0.1% (w/v) SDS.

Acrylamide working stock

Acrylamide stock was purchased as ProtoGel™ solution (National Diagnostics Ltd.) and consists of

- 30% (w/v) acrylamide
- 0.8% (w/v) bis-acrylamide

Laemmli sample buffer 6x

1.5 M Tris 0.5M pH 6.8

30% (w/v) SDS

10% (w/v) bromophenol blue

5% (v/v) glycerol

5% (v/v) DTT

Resolving gel, pH 8.8

- 10% (w/v) bis-acrylamide
- 25% (v/v) resolving buffer
- 0.01% (w/v) APS
- 0.1% (v/v) TEMED

Running buffer (10x), pH 8.3

- 0.25 M Tris-HCl
-1.92 M Glycine

- 1% (w/v) SDS

Stacking gel, pH 6.8

- 4% (w/v) bis-acrylamide
- 25% (v/v) stacking buffer
- 0.075% (w/v) APS
- 0.15% (v/v) TEMED

2.1.11. Protein molecular weight markers

Precision Plus Protein Stadards (all blue) were purchased from Bio-Rad Laboratories Ltd. and contained ten proteins of 10 kDa, 15 kDa, 20 kDa, 25 kDa, 37 kDa, 50 kDa, 75 kDa, 100 kDa, 150 kDa, and 250 kDa. The 25 kDa, 50 kDa, and 75 kDa proteins serve as a reference bands because they are three times as intense as the other bands.

2.1.12. Western blotting and immuno-detection solutions

Electro-blotting transfer buffer

- 25 mM Tris-HCl (pH 8.3)
- 192 mM Glycine
- 20% (v/v) methanol

Blocking solution

5% (w/v) skimmed milk powder in PBS- Tween-20 [0.1 % (w/v)]

Primary antibody incubation solution

5% (w/v) skimmed milk powder in PBS- Tween-20 [0.1 % (w/v)]

Secondary antibody incubation solution

PBS- Tween-20 [0.1 % (w/v)]

2.1.13. Antibodies

PRIMARY ANTIBODIES				
Antibodies	**Species**	**Epitope**	**Origin**	**Dilution**
Total tau	Rabbit polyclonal	C-terminus aa 243-441	DAKO	1:10,000
GAPDH	Mouse monoclonal	Not stated	Sigma	1:5000
AT8	Mouse monoclonal	serine 202/ threonine 205	Autogen biosciences	1:1000
TDP-43	Rabbit polyclonal	serines 409/410	cosmobio	1:4000
SECONDARY ANTIBODIES				
Name	**Antibody**	**Origin**	**Dilution**	
IRDye™ 800	Rabbit polyclonal	Rockland	1:10,000	
Alexa Fluor® 680	Mouse monoclonal	Molecular probes	1:10,000	

Table 2.2. Antibodies used in this study.

2.1.14. Cell culture

All medium used for the culture of cell lines supplemented with:

- 2mM L-glutamine

- Penicillin (100 units/ml)

- Streptomycin (100 µg/ml)

Medium for SH-SY5Y cells

DMEM/ F12

15% (v/v) FBS

Hank's balanced salt solution (HBSS)

HBSS was purchased from Invitrogen Ltd. as a 1x solution without calcium chloride, magnesium chloride, or magnesium sulphate. This solution was used for washing cells before trypsinisation.

Trypsin solution

Trypsin-EDTA (TE) was purchased from Invitrogen Ltd. as a solution containing 0.05% (w/v) TE in PBS.

2.1.15. Miscellaneous stock solutions

Phosphate Balanced Solution (PBS)

PBS tablets were purchased from Sigma Aldrich Co. Ltd. One tablet was dissolved in 200 ml of H_2O to give a final concentration of:

0.01 M phosphate buffer pH 7.4

0.0027 M potassium chloride

0.137 M sodium chloride

2.1.16. Human brain tissue

Human brain tissue was obtained from neurologically normal (control) and individuals with AD (Braak stages V- VI) from the London Neurodegenerative Disease MRC Brain Bank, Institute of Psychiatry, King's College London, (Ethical Committee Protocol 174/02). Staging of AD cases and definitive diagnosis for AD cases with and without TDP-43 inclusions were made according to established neuropathological criteria by neuropathologists at Kings College Hospital. Dissection was carried out by Dr Tibor Hortobágyi and Claire Troakes.

Tissue was collected and stored in tubes at -70ºC until analysis. 200 and 100mg of tissue was dissected. 100mg was put directly into matrix lysing-D tubes (Qbiogene) and used for RNA extraction using the FastPrep sample preparation system. Brain regions selected include Frontal lobe BA 8/9, Temporal lobe BA 21, Amygdala, Hippocampus and Cerebellum.

BB case No.	PM diagnosis	Age	Sex	PMD hours	pH	Braak stage
A239/03	Control	78	M	9.5	6.63	
A359/08	Control	80	F	3	6.4	
A308/09	Control	66	M	52	6.66	
A292/09	Control	38	F	43	6.85	
A123/09	Control	78	M	24	6.28	
A113/09	Control	18	M	24.5	6.44	
A048/09	Control	81	M	18	6.72	
A063/10	Control	90	F	50	5.94	
A057/10	Control	92	F	48	6.08	
A310/09	Control	84	F	35	6.11	
A303/09	Control	80	M	60	5.19	
A065/11	Control	97	M	44	6.26	
A346/10	Control	84	F	34	5.74	
A136/10	Control	89	F	41	6.43	
A144/10	Control	92	F	23	6.57	
A249/07	ADTDP+	74	M	69	6.77	6
A205/07	ADTDP+	73	M	24.5	6.37	6
A349/08	ADTDP+	86	F	14	6.56	6
A348/07	ADTDP+	85	M	16	6.4	4
A063/09	ADTDP+	89	M	62	6.82	5
A076/09	ADTDP+	97	M	16.5	6.18	5
A169/10	ADTDP+	85	F	10	6.85	5
A114/10	ADTDP+	86	M	45	7.1	6
A283/09	ADTDP+	77	M	9.5	7.12	5
A188/10	ADTDP+	69	M	120	6.61	6
A168/10	ADTDP+	88	F	33	6.74	6
A267/09	ADTDP+	90	F	70	5.98	5
A122/09	ADTDP+	68	F	10.5	6.84	6
A308/07	ADTDP+	83	F	76	6.56	6
A037/04	ADTDP-	96	F	39	6.62	N/A
A039/02	ADTDP-	92	F	4	6.63	N/A
A331/07	ADTDP-	80	F	12.5	6.48	5
A098/04	ADTDP-	84	M	73	6.86	6
A191/07	ADTDP-	69	F	16.3	7.43	6
A192/07	ADTDP-	96	F	19	6.57	5

A210/05	ADTDP-	84	F	24	6.57	5
A240/06	ADTDP-	97	F	12	6.9	5
A141/07	ADTDP-	80	M	41	6.33	6
A050/04	ADTDP-	91	F	28.5	6.64	N/A
A058/07	ADTDP-	81	M	74	6.76	6
A160/06	ADTDP-	71	M	32	6.42	6
A187/07	ADTDP-	82	F	69	6.67	5
A122/04	ADTDP-	86	M	25.5	6.72	5
A065/04	ADTDP-	91	F	28.5	6.19	6
A123/99	FTDP-17	60	M	3	5.96	
A174/99	FTDP-17	63	F	22	6.82	
A074/00	FTDP-17	67	M	35	6.01	
A171/02	FTDP-17	71	M	5	6.68	
A070/99	FTDP-17	52	F	72	6.61	
A388/94	DM1	58	M	12	7	

Table 2.3. Brain samples dissected and collected from the IOP brain bank

2.2. Methodology

2.2.1. RNA extraction from human post-mortem brain tissue

All RNA methods were carried out with RNase free plasticware and RNase free non-DEPC treated water (Ambion).

Total RNA was isolated from frozen blocks of human brain. Samples were homogenised in matrix lysing-D tubes in conjunction with the Fastprep sample preparation system. Total RNA was extracted with Qiagen RNeasy lipid tissue kit as follows.

1 ml of 4°C Qiazol lysis solution (containing phenol and guanidine thiocyanate) was added to lysing matrix-d tubes (qbiogene) containing approximately 100 mg of brain tissue. Matrix d tubes contain ceramic beads that homogenize the sample when used in conjunction with Fastprep 24 machine. Total RNA was extracted from the

homogenised samples using the Qiagen RNeasy lipid tissue kit according to the manufacturer's protocol. RNA was eluted in 40 µl of RNase free water and contaminant DNA removed using DNA free kit (Ambion) according to the manufacturer's instructions. RNase-free tubes (for storage of RNA), lysis solution, buffers and RNase free water (for elution) are provided with the Qiagen RNeasy lipid tissue kit.

2.2.2. RNA isolation from rat and mouse brain tissue

Total RNA was isolated from frozen blocks of mouse brain and rat brain (snap frozen in liquid nitrogen) using the Qiagen RNeasy lipid tissue kit using the same protocol as for the human brain samples except we used a mortar and pestle instead of the matrix lysing-D tubes for homogenisation of these samples. Approximately 100 mg of brain tissue (kept on dry ice before use) was homogenised in 1 ml of 4ºC Qiazol lysis solution. The brain tissue was homogenised immediately, approximately 20 strokes, on ice and RNA extracted as for the human samples.

2.2.3. Total RNA isolation from SH-SY5Y cells

SH-SY5Y cells were grown in a monolayer in 6-well plates and lysed with 1ml of Trizol® reagent (Invitrogen Ltd.) added directly onto each well. Cells were lysed by passin the cells through a pipette several times. Homogenised cells were incubated at room temperature for 5 mins to break nucleic acid-protein complexes in the cells. 200µl chloroform was added to the homogenate and vortexed for 15 secs. Centrifugation of the homogenate was carried out at 12,500 rpm for 15 mins at 4°C. The clear layer containing RNA was pipetted into new tubes. RNA was precipitated with 500µl isopropanol by incubating for 15 mins at room temperature. The resultant

RNA pellet was obtained after centrifugation at 12,500 rpm for 15 mins at room temperature and was washed three times with 1 ml of 75% (v/v) ethanol before resuspension with 50 µl of RNase free water. DNA was removed using DNA free kit (Ambion) according to the manufacturer's instructions. The isolated RNA was stored at -70ºC.

2.2.4. Quantification and DNase treatment of RNA

DNase treatment of isolated RNA removes contaminant genomic DNA from the RNA sample. A DNA-free kit (Applied Biosystems) was used to treat RNA according to the manufacturer's instructions. 5µl of 10 × DNase buffer and 1µl of rDNase were added to the RNA and incubated for 30 mins at 37ºC. To stop the reaction, 5µl of DNase inactivation reagent was added and incubated for ~2mins at room temperature. DNAase inactivation Reagent was pelleted by centrifugation and the supernatant containing RNA was transferred to a new tube. RNA concentration was determined by using a Nanodrop spectrophotometer (Thermo Scientific) using the manufacturer's software. 1.5µl of each undiluted RNA samples was analysed, recording the concentration in ng/µl and the A260/A280 ratio and 260/230 ratio recorded (a ratio of A260/A280 > 1.8 indicates that there is little protein contamination in a RNA sample).

2.2.5. RNA integrity

RNA integrity number (RIN) was measured with the Agilent RNA 6000 Pico kit using the Agilent Bioanalyser. Chips were prepared for all human brain RNA according to the manufacturer's instructions. 550 µl of the RNA 6000 Pico gel matrix was placed in a centrifuge tube with a filter and centrifuged at 1500 ×g for 10 mins at room temperature and was divided into 65µl aliquots. After the addition of 1µl of the RNA 6000 pico dye concentrate to the 65µl aliquot of filtered gel, the gel-

dye mix was vortexed and centrifuged at 13,000 ×g for 10 mins. 1µl (3 ng/µl) RNA from each sample was added in the wells of one chip followed by the addition 1 µl of diluted RNA 6000 ladder in the ladder well. The chips consist of interconnected microchannels that separate RNA fragments based on their size. The dye intercalates directly with RNA and pass detectors at different speeds. The software compares the unknown samples with to the ladder to determine the concentration of the unknown samples and to identify ribosomal RNA peaks (18S and 28S for eukaryotic RNA). In perfectly extracted RNA the 28S peak is twice as high as the 18S and the Agilent software measures the area under these peaks to calculate a RIN where 1 is most degraded and 10 being most intact. We tested our AD and control samples for RIN. RT-PCR was found to reliable at a RIN above 3.5 and only these samples were used in the splicing analysis.

2.2.6. Reverse transcription of RNA

Reverse transcription (RT) was performed using reagents from Taqman RT Kit (GE Healthcare). 0.5 µg of total RNA was reverse transcribed in a total volume of 10µl. Master mixes for each reaction are as follows:

Reagent	Volume (µl)	Final Concentration
10 × Buffer	1	1/10 dilution
$MgCl_2$ (25mM)	2.2	5.5mM
dNTP mix	2.0	500µM of each dNTP
Oligo-dT	0.5	2.5µM
RNase inhibitor	0.2	0.4 U/µl
Reverse transcriptase (50 U/µl)	0.25	1.25 U/µl

A G-storm thermal cycler was used to perform the RT reaction with conditions as follows:

25ºC for 10 minutes – oligo dT hybridisation

48ºC for 30 minutes – reverse transcription

95ºC for 5 minutes – denature reverse transcriptase

4ºC for storage

2.2.7. Polymerase chain reaction (PCR)

PCR was performed with GoTaq polymerase reagents (Promega) using primers listed in Table 2.1. Master mixes for multiple reactions were prepared to avoid variability. For one reaction, the PCR mix was as follows:

Reagent	Volume (µl)	Final Concentration
5 × Buffer	10	1/5 dilution
dNTP mix	4	200µM
Forward primer	5	5.5mM
Reverse primer	5	2.5µM
H_2O	15.5	0.4 U/µl
Taq polymerase	0.5	1.25 U/µl

40 µl of the PCR mix was mixed with 10 µl of the RT reaction. PCR controls without RNA (no template condition) and no reverse transcriptase (no RT condition) were routinely carried out to detect DNA contamination in the RT-PCR reaction.

Products from completed PCR reactions were separated on 2% agarose gels containing ethidium bromide (a DNA intercalator) and were visualised under UV light.

Quantifying of PCR products with DNA intercalators such as ethidium bromide is problematic when more than one PCR product arises due to alternative splicing because the signal intensity under UV light is proportional to the length of DNA as well as the amount present.

To quantify ratios of alternatively spliced isoforms more accurately, our laboratory has developed a method where alternatively spliced variants can be visualised and measured on the Odyssey infrared imaging system. Primers were modified by attaching a fluorophore (DY682) at the 5' end of the forward primer and manufactured by MWG Eurofins. The proportion of labelled to unlabelled forward primer has been optimised. The resulting PCR products were separated on 2% agarose gels and quantified with the Odyssey imaging system. Only one molecule of fluorophore incorporated into an individual molecule of the PCR product, independently of the length of the PCR product and therefore the ratio of intensities between PRC products reflects the molar ration of alternatively spliced isoforms. Amplification was performed according to the cycling parameters below.

GAPDH primers

1 cycle	Denaturation	95ºC for 5 mins
28 cycles	Denaturation	94ºC for 30 sec
	Annealing	62ºC for 30 sec

	Extension	72ºC for 1 min
1 cycle	Extension	72ºC for 10 mins
1 cycle	Storage	4ºC

APP

1 cycle	Denaturation	95ºC for 5 mins
30 cycles	Denaturation	94ºC for 30 sec
	Annealing	55ºC for 1 min
	Extension	72ºC for 2 min
1 cycle	Extension	72ºC for 10 mins
1 cycle	Storage	4ºC

Tau 9- 13

1 cycle	Denaturation	95ºC for 5 mins
28 cycles	Denaturation	94ºC for 2 mins
	Annealing	60ºC for 30 sec
	Extension	72ºC for 20 sec
1 cycle	Extension	72ºC for 10 mins
1 cycle	Storage	4ºC

Tau N term

1 cycle	Denaturation	95ºC for 5 mins
30 cycles	Denaturation	94ºC for 1 min

	Annealing	65ºC for 1 min
	Extension	72ºC for 45 sec
1 cycle	Extension	72ºC for 10 mins
1 cycle	Storage	4ºC

TDP 3'UTR

1 cycle	Denaturation	95ºC for 5 mins
31 cycles	Denaturation	94ºC for 1 min
	Annealing	60ºC for 1min
	Extension	72ºC for 1½min
1 cycle	Extension	72ºC for 10 mins
1 cycle	Storage	4ºC

Table 2.4. PCR primer cycling parameters

2.2.8. Quantitative RT-PCR

Taqman RT Kit (GE Healthcare) was used to synthesize the first strand cDNA as described 2.2.6. Amplification and detection steps are performed concurrently for each cyle. qRT-PCR was performed with the Applied Biosystems 7900HT instrument. The fluorophore used in this study was SYBR Green (Roche Diagnostics). SYBR green does not fluoresce when free in solution and will bind to all double stranded DNA (dsDNA) molecules independent of sequence. Fluorescence emission occurs after binding to dsDNA due to conformational changes in the dye. The increase in SYBR green signal (measured at 530 nm)

correlates with the amount of PCR product amplified during the reaction and the number of cycles to reach a preset threshold is recorded (CT).qRT-PCR was performed in 384 well plates with 20 ng template cDNA. Dissociation curves were determined for each of the target genes (MAPT and APP) to show that only a single product was amplified from the primer pairs. Master mixes for multiple reactions were prepared to avoid variability. For one reaction the qRT-PCR mix was as follows:

Reagent	Volume (µl)	Final Concentration
SYBR Green	5	1 ×
Forward primer	0.5	10µM
Reverse primer	0.5	10µM
H_2O	2	
cDNA	2	10 ng/µl

8 µl of the PCR master mix was added to 2 µl of the cDNA and all samples were measured in duplicates.

1 cycle	Denaturation	95ºC for 10 mins
40 cycles	Denaturation	94ºC for 15 sec
	Annealing	60ºC for 30 sec
	Extension	72ºC for 15 sec

Table 2.5. qRT-PCR cycling parameters

2.2.9..Determination of housekeeping genes

Primers and software for determining the optimal housekeeping genes for each brain area was analysed using a geNorm kit (Primerdesign, UK). geNorm enables the selection of the optimal set of reference genes from a series of tested candidate reference genes. A set of six genes were tested for each brain region. cDNA from 6 samples of control and AD brains were tested for each region with primers for all six candidate genes.

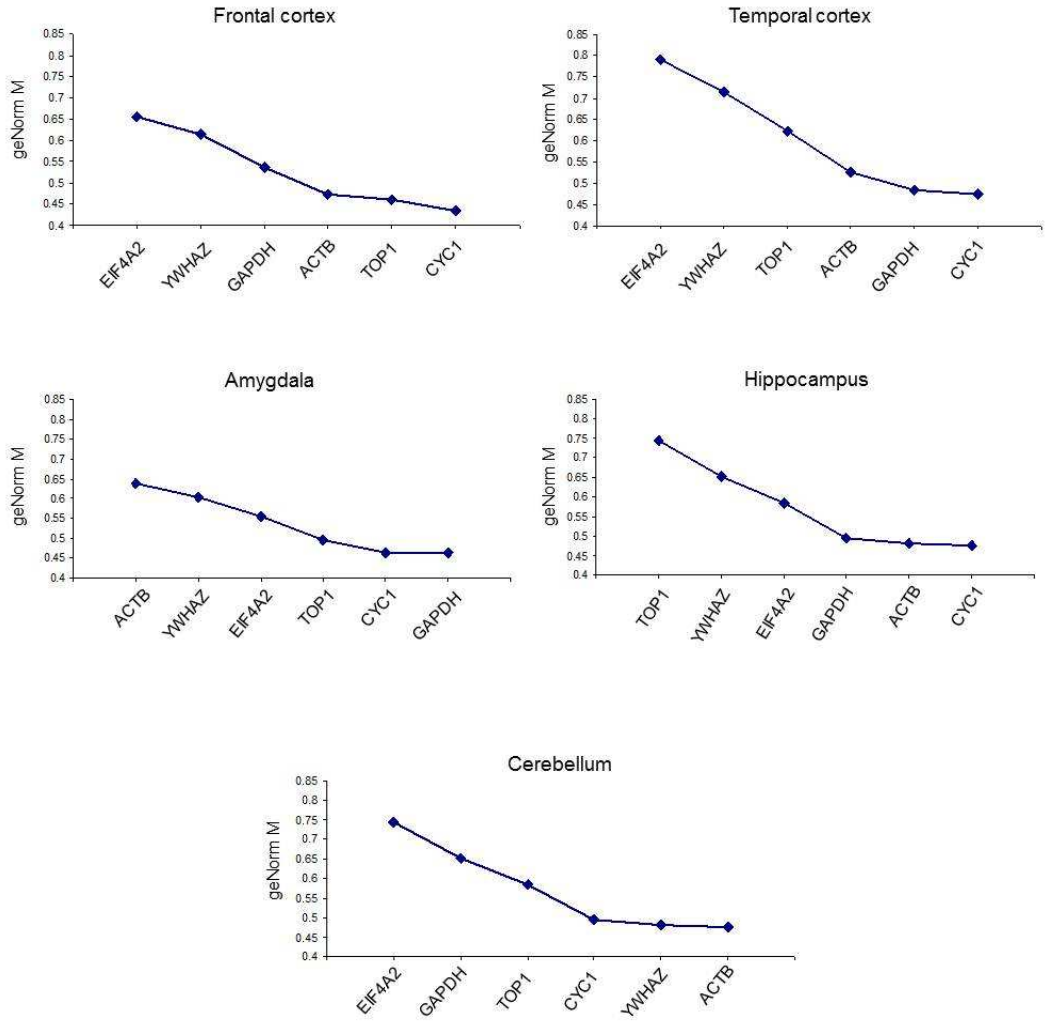

Figure 2.1. Ranking of candidate genes according to their stability for each brain region.

Genorm^{PLUS} software was used to rank candidate genes for stability across six brains with data from a qRT-PCR analysis according to the manufacturer's protocol. The stability of each candidate gene was ranked with the least stable genes for the six brains on the left and most stable on the right (Figure 2.1). For each target gene, two of the most stable reference genes were used for a relative CT analysis.

2.2.10. Validation of PCR primers

The primers used for genes of interest for both qRT-PCR and RT-PCR were designed on the basis of the GenBank cDNA sequence using the primer designing tool Primer3. Each primer was tested for specificity using the NCBI Blast program. The primers were then tested using end point PCR, were cut out of agarose gels and sequenced. All sequenced PCR products were aligned to published sequence from ensemble. Primers used for qRT-PCR were also tested for amplification of a single product with the Applied Biosystem 7900HT machine.

2.2.11. Cloning

PCR products resulting from primer sets Tau N-term (0N, 1N and 2N), APP (APP770, APP 751 and APP695) and TDP-43 3'UTR alternative isoform PCR products were validated (Tau 9-13 and GAPDH primers have previously been validated). PCR products were cut out of 2% agarose gels; DNA was extracted from agarose and purified using the QIAquick gel extraction kit (Qiagen).

Ligation

The DNA was ligated into pGEM-T easy vectors (Promega). Ligation of cDNA insert (extracted PCR product) and vector was performed overnight on slush ice with 1 µl T4 ligase and 1 µl ligase buffer (Promega) in a total volume of 10 µl. 100 ng of

vector DNA was used and the amount of insert DNA calculated according to the manufacturer's instructions:

$$\frac{\text{ng of vector} \times \text{kb size of insert}}{\text{Kb size of vector}} \times \frac{\text{molar ratio of insert}}{\text{vector}}$$

Transformation of E.coli cells

20 ng of plasmid DNA was transformed into 50 µl of competent JM109 *Escherichia coli (E. coli)* cells (Promega), and incubated on ice for 20 mins. The *E. coli* cells were subsequently heat shocked at exactly 42ºC for 45 secs and returned to ice for 2 mins. 950 µl of sterile LB medium without antibiotic was added to the bacterial suspension and incubated for at least 1 hour at 37ºC to allow for expansion of the bacteria containing the DNA insert. Bacteria were centrifuged for 5 mins at 8000 rpm and re-suspended in 50 µ of LB broth. Cells were streaked out onto LB agar plates (LB/ampicillin/IPTG/X-Gal) and placed in incubator overnight at 37°C.

IPTG/X-Gal allows colonies containing the DNA insert to be selected by blue/white selection. White colonies containing the PCR insert were selected and grown in 5 ml LB broth/ampicillin in a Unitron Infors AG shaker, overnight shaking 225 rpm at 37°C.

Plasmid DNA digestion by restriction endonucleases

The presence of the cDNA insert was confirmed with small scale restriction enzyme analytical digest and agarose gel electrophoresis before sequencing. 1 µl of 1 unit/µl restriction enzyme (Promega), was used to digest cDNA inserts from 1 µg of plasmid DNA. With 2 µl 10 × buffer and ultra-pure water to produce a final volume

of 20 µl. Reactions were performed at 37ºC for 2 hours to allow for complete digestion of plasmid DNA followed by a denaturation step at 65ºC for 10 mins. Digest products were visualised on 2% agarose gels to confirm the presence and size of the cDNA insert. Samples were sent for sequencing (MWG ecofins) and the insert DNA sequence was compared and validated with cDNA sequences downloaded from ensembl. (http://www.ensembl.org/index.html)

2.2.12.. Cell culture

All materials used for cell culture were purchased sterile or sterilised by autoclaving at 121ºC for 15 mins. Regular tests for mycoplasma contamination were performed. All procedures were performed in class II microbiological safety cabinets.

In this study translation was inhibited in SH-SY5Y cells by cycloheximide (CHO) treatment. SH-SY5Y cells are a third generation human neuroblastoma cell line that originated from the SK-N-SH line derived from a bone marrow biopsy in 1970 (Biedler et al., 1973; Ross et al., 1983).

Culture of cell lines

Cells were cultured in DMEM/F-12 and supplemented with 15% (v/v) FBS. In addition, all media contained 100 units/ml penicillin, 100 mg/ml streptomycin and 2 mM L-glutamine. Cells were maintained at 37°C in a humidified atmosphere of 5% CO_2/ 95% air in a Heraeus Hera cell incubator. Cells were passaged at a sub-confluent stage and disposed of after passage ~35.

Passaging of SH-SY5Y cells

Cells were maintained by passaging when approximately 80% confluent. Culture medium was aspirated and the cells washed with HBSS. Cells were then trypsinised by the addition of Trypsin-EDTA solution and incubating at 37ºC until cells were fully detached. Cells were then re0suspended in culture medium to inactivate the trypsin. Cells were recovered by centrifugation at room temperature at 1000 rpm for 5 mins using a Sorvall® Legend T centrifuge, re-suspended in 10 ml of fresh medium and resseded at ~1/10 dilution.

Plating of cells

For plating cells in six well plates, cells were washed in HBSS and detached from the flask surface by incubation with 1-2 ml of trypsin (0.05% (v/v) trypsin/EDTA) at 37°C for 5 min. When the cells were detached, 9ml of medium was added. The cell suspension was centrifuged at 500 × g for 5 min at room temperature and the supernatant removed. The cell pellets were then resuspended in the appropriate volume of medium and plated according to protocol approximately one million cells per well of a 6 well plate. Cells were allowed to attach overnight and were used for experimental procedures after at least 12 hours from plating.

Cycloheximide treatment of SH-SY5Y cells

SH-SY5Y were plated in 6 well plates ~ 1 million per well. Once the cells had attached to the plate surface, the media was aspirated and new media was added, in the cycloheximide (CHX) condition, the media contained CHX at 10 µg/ml, control had new media. Cells were treated for 12 hours and the RNA was extracted.

2.2.13. Preparation of human brain homogenate

Brain tissue was obtained from the London Neurodegenerative Diseases Brain Bank, Institute of Psychiatry, Kings College London. Ethical approval was obtained from the local Ethics Committee.

0.2g of human brain samples from the amygdala was homogenised on ice with a mechanical homogeniser (Ultra Turrax® T8, Werke GmbH & Co., Germany) in autoclaved 1ml Tris buffer containing 50mM Tris/HCl pH 7.4, 150mM NaCl, 1mM PMSF and EDTA free Protease inhibitor tablets (Roche). The homogenate was centrifuged at 12,000 ×g for 20 mins at 4°C. Transfer 800µl of the supernatant into high speed centrifuge tubes for extraction of sarkosyl insoluble tau. Transfer the remainder of the supernatant to new tubes and 1x volume of the Tris buffer was added to these samples. This samples is the low centrifuge material and was used for western blotting at ~1µg/µl.

Isolation of insoluble tau

Sarkosyl was added to the 800µl high speed centrifugation sample for a final concentration of 1% (from 20% stock) and the solution was shaken for 30mins at room temperature. The samples were centrifuged at 47,000 rpm for 1 hour at 21ºC on a Beckman Coulter ultra-centrifuge. The pellet containing sarkosyl insoluble tau was collected and washed with 200µl of 1% sarkosyl and re-centrifuged at 47,000 rpm for 10 mins. The wash step was repeated. The resulting insoluble tau pellet was dissolved in 40µl of 8M guanidine and 2% ß-mercaptoethanol and allowed to mix for 1hour rocking at room temperature.

Protein quantification assay

A pierce BCA assay was used to measure the concentration of protein in the samples from the low speed centrifugation. BSE standards of known concentration were made in 96 well plates and the unknown samples were added to wells at a 1 in 10 concentration. The 96 well plate was incubated at 37°C for 30 mins and read on a spectrophotometer at 562nm.

Dialysis and concentration of the sarkosyl insoluble samples

Insoluble tau extracted from human brain is hyperphosphorylated. In order to determine the tau species present in these samples, phosphorylation is removed with lambda phosphatase. Lambda phosphatase enzymes are inhibited in the presence of strong denaturing agents such as guanidine. 10-12 of the insoluble tau samples were dialysed in 1 litre autoclaved dialysis buffer for ~4 hours. Dialysis buffer consisted of 50mM Tris/HCl pH 8.0 and 0.1mM EDTA. Novagen D-Tube dialysis tubes were used and we followed the manufacturer's instructions. 250µl of autoclaved H_2O was pipetted into tubes and left for >5mins to re-hydrate the dialysis tube membranes. H_2O was removed and the sarkysol insoluble samples were added and dialysed in dialysis buffer for 4 hours with stirring. Samples containing ~50µl of sarkosyl insoluble tau were recovered from the dialysis tubes. For analysis by western blotting, the whole sample from 0.2 g of tissue must be run in one lane and a total volume of 50µl is too much volume for this and needs to be reduced. Amicon ultra (molecular weight cut off 30 kDa) centrifugal concentrators were used to decrease volume according to the manufacturer's instructions. 50µl samples were added to the centrifuge concentrator tubes and topped up with fresh dialysis buffer to 450µl total volume. Samples were spun at 14000 ×g for 15mins and result in a volume of ~15-

20µl of sample. To release sample the tubes were placed in the centrifuge upside down and spun at 1000 ×g for 2 mins.

Dephosphorylation of samples with lambda phosphatase

Both samples of insoluble tau and samples from the low speed centrifugation samples were dephosphorylated with lambda phosphatase (New England Biolabs).

Buffer for lambda phosphatase 10×

50mM HEPES pH 7.5

100mM NaCl

2mM DTT

0.01% Brij 35

The insoluble tau samples had a volume of ~ 15 µl, the low speed centrifugation samples had a variable volume and used at 1µg/µl. A master mix of 10 × buffer and 10 × $MgCl_2$ was made and 0.2µl of lambda phosphatase was added to the master mix per sample. For the insoluble tau samples 3 µl of the master mix and lambda phosphatase was added to each sample. Tubes were placed in a heat block for 2.5 – 3 hours at 30°C.

2.2.14. Western blotting

2.5 µl of the 6 × sample buffer was added to each sample before western blotting. Proteins were separated by SDS-PAGE on 10% polyacrylamide gels (Protogel, National Diagnostics) using the Mini Protean III gel system (Biorad) and were transferred to a 0.45 µm pore size nitrocellulose membrane (Schleicher and Schuel) using the wet transfer method (Bio-rad). The nitrocellulose membrane and gel were

sandwiched between sponges and filter papers soaked in transfer buffer. Transfer was performed at 100V for 1 hour. Non-specific protein binding sites were blocked by incubation with 5% (w/v) skimmed milk in PBS + 0.1% (v/v) Tween-20 (PBST). The membrane was washed 3 × in PBST and incubated in DAKO/ GAPDH primary antibody (in PBS-T) overnight at 4 °C. Membranes were then washed (3 × 10 min) in PBST. Incubation with an appropriate species specific secondary antibody conjugated to a fluorescent label was performed at room temperature for one hour in 5% (w/v) milk/ PBST. After three more washes in PBST and a final wash in PBS, proteins were detected using the LI-COR Odyssey® infrared imaging system (Li-cor Biotechnology).

Chapter Three: Tau expression and splicing in brain regions affected in Alzheimer's disease.

Splicing mutations in a subset of FTDP-17 brains show that increases in 4R tau are pathological. Post-mortem brain samples from disease-affected areas of PSP and CBD brains show increases in 4R tau at the RNA level (Chambers et al., 1999; Takanashi et al., 2002; Umeda et al., 2004) and at the protein level (Buée and Delacourte, 1999; Luk et al., 2010). PiD can show increases in 3R tau isoforms (de Silva et al., 2006; Delacourte et al., 1996) although both 3R and 4R tau has been found in PiD (Arai et al., 2001; Taniguchi et al., 2004; Zhukareva et al., 2002) and this may be due to astrocytic inclusions (see Introduction). (Arai et al., 2001) These findings suggest that 4R/3R tau isoform imbalances may constitute a pathogenic pathway for tau pathology. In AD, it has been generally assumed that the 4R/3R ratio is in balance however there are a number of papers providing evidence that an increase in 4R isoforms occurs in a subset of neurons harbouring tau inclusions (see Introduction). The lack of consensus on the AD tau 4R/3R ratio may be, in part, due to the multiplicity of pathways operating in AD which results in heterogenous sets of AD samples.

3.1. TDP-43 role in tau exon 10 alternative splicing

Around 20-35% of AD cases have TDP-43 cytoplasmic inclusions and, to a much lesser extent, nuclear inclusions (Amador-Ortiz et al., 2007). Concomitant TDP-43 pathology in AD cases is of particular interest because of its known role in regulation of RNA processing such as alternative splicing. TDP-43 clearance from the nucleus may result in a loss of function and impair splicing and transcription of target RNAs. Whether secondary pathologies such as TDP-43 contribute to changes

in *MAPT* splicing or expression in disease is an issue of considerable research interest.

Many AD brains show co-existence of insoluble tau and TDP-43 however inclusions most likely represent an end stage of a molecular cascade and earlier steps in that cascade may be more directly linked to pathogenesis. It is therefore important to understand the mechanisms underlying all aspects of TDP-43 and tau processing and functioning.

In this chapter the main research question was to investigate a possible association between TDP-43 dysfunction in disease brain and altered tau splicing, transcription and post-transcriptional processing.

Tau splicing ratios of exons 2,3 and 10 were quantified at the RNA level in human control, Myotonic Dystrophy1 (DM), FTDP-17 and AD brains with and without TDP-43 inclusions in five different brain regions. Control status was confirmed by histolopathology examination carried out at Kings College Hospital on sections prepared from paraffin embedded brain samples. Diagnosis was performed by a neuropathologist and all controls did not have plaques or tangles or AD-type changes that were not consistent with normal aging. A single DM1 case that was available to us was included in our sample set because tau exon 10 (4R) transcript expression has been reported to be decreased in DM1 (Jiang et al., 2000). DM1 is caused by an expansion mutation of CUG repeats in the 3'UTR of dystrophia myotonica protein kinase (*DMPK*) mRNA (Brook et al., (1992) and DM1 patients may carry several kilobases of CUG repeats. The nuclear retention of these transcripts results in *DMPK*

haploinsufficiency, however reduced *DMPK* protein does not cause the major symptoms of the disease (Fu et al., 1993; Jansen et al., 1996). CUG repeats form a double stranded hairpin structure which acts as a sink for CUG binding RBP such as muscleblind-like (*MBNL*) family and results in a loss of function of these splicing factors and may result in altered splicing of MAPT amongst other transcripts. Expression of expanded CUG repeats in the 3'UTR of *DMPK* activates protein kinase C (PKC) of which CUGBP1 is a target. Hyperphosphorylation of CUGBP1 stabilises the protein and effectively results in up-regulation of CUGBP1 (Kuyumcu-Martinez et al., 2007).

4R/3R tau ratios in control and AD brains were correlated across the five different brain regions to test for consistency over the different brain regions. Total tau mRNA levels were quantified in affected and non-affected brains and relative *MAPT* expression was compared between control, FTDP-17 and AD group brains in five brain regions. Relative *MAPT* expression and splicing ratios were correlated with tau haplotype. Tau isoform ratios of soluble and insoluble protein were quantified in control and AD brain samples from the amygdala. Tau protein 4R/3R ratios were correlated with RNA 4R/3R ratios from the amygdala in control and AD brains. Finally, semi-quantitative measures of tau pathology were analysed in brain sections for differences between AD brains with TDP-43 inclusions and AD brains without TDP-43 inclusions in four brain regions (frontal and temporal cortex, amygdala and hippocampus).

3.2. Determination of PCR conditions for detection of tau exon 10 RNA

When using RT-PCR to quantify and calculate a ratio of multiple splicing products it is important to accurately measure the point at which the primers plateau for all PCR

products because each product may have a different plateau due to different cycling efficiencies and this will alter the splice ratio calculation. The RT-PCR reaction starts with an exponential increase and eventually plateaus due to decreasing reaction components and declining enzyme activity. In the exponential phase of the reaction, if the primer efficiency is 100%, then for every cycle there is a doubling of PCR product. Factors that impact efficiency include contaminants in the sample, PCR product length and RNA integrity (Fleige and Pfaffl, 2006; Tichopad et al., 2004; Tichopad et al., 2002).

Another confounding factor in quantifying small differences in alternatively spliced products using DNA intercalators such as ethidium bromide is that the signal intensity under UV light is proportional to the length of DNA as well as the amount of DNA present. Since PCR products from alternatively spliced isoforms will differ in length, the amount of ethidium bromide intercalated in the larger PCR product will increase signal but will not accurately reflect the quantity relative to a smaller alternatively spliced product. In order to address this problem we designed and optimised a PCR protocol with modified PCR primers that allow the determination of molar ratios of PCR product.

The presence or absence of tau exon 10 can be detected with a forward primer annealing to exon 9 and reverse primer annealing to tau exon 13 (tau 9-13 primer pair). A DY682 label was attached to the 5’ end of the forward primer (DY682 is a substitute for infra-red dye IRD700). PCR products containing the labelled forward primer can be quantified with an infra-red scanner (Figure 3.1A). The IR labelled primer modification gives an accurate access to the molar ratio of spliced isoforms as

the intensity of the fluorescence signal is independent of the length of the PCR product. The advantages of this technique are that RT-PCR is a standard technique which is easy to perform and the DY682 tag modification of the PCR forward primer is easy to get manufactured. Quantification of PCR products from alternatively spliced isoformsby other methodologies such as qRT-PCR requires at least two sets of primers and exon 10 in *MAPT* is particularly difficult to accurately quantify by qRT-PCR because of the inherent repeated nature of the microtubule domains, cross reactivity of tau4R specific primer for tau3R has been reported in previous publications using qRT-PCR (Connell et al., 2005; Takanashi et al., 2002). qRT-PCR also requires determination of stable housekeeping genes and similar reaction efficiencies between primer pairs for accurate quantification. Using RT-PCR with a modified forward primer and primers that span alternative exons at least two PCR products are produced from a single primer pair. A molar ratio can be calculated from the two products and therefore there is no need for housekeeping genes.

cDNA from human brain, adult mouse and rat brain and cultured SHSY-5Y cells were PCR amplified with the modified forward 9-13 primer pair and visualised with a IR scanner as well as with a UV trans-illuminator (compare above and below Figure 3.1A) In the human samples, two PCR products were found and these products were sequenced. The longer 368 base pair (bp) product contains tau exon 10 and represents 4R tau, the shorter 275 bp product has no exon 10 and represents tau 3R. PCR products from adult mouse and rat brain show expression of tau E10 inclusion (4R) only. The smaller sized bands (approx 182bp) visualised in the rat brain lanes are PCR products derived from mis-priming on the forward primer. Tau 9-13 primers were designed primarily for use with human cDNA, and rat cDNA

varies from the human sequence in this region. cDNA from quadruplicate samples were analysed with the tau 9-13 primer pair at different numbers of cycles. Quantification of 3R and 4R in arbitrary fluorescent units was determined with Odyssey software and fluorescent unit vs cycle number was plotted. The linear range of the amplification curve was determined for the primer pair (Fig. 3.1B) which was between 25-30 cycles for both 4R and 3R transcripts. The number of cycles finally used for quantification was 29 cycles.

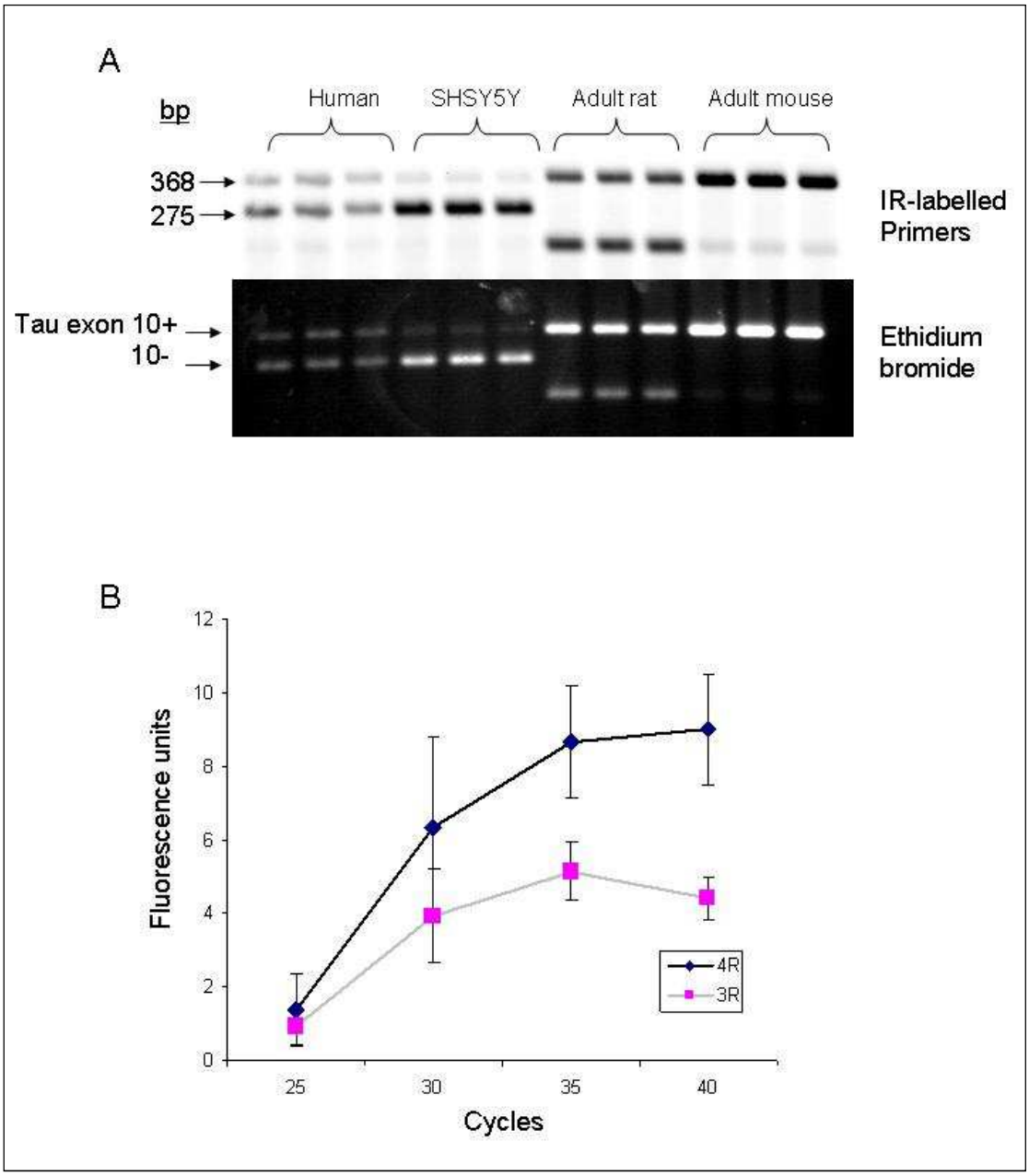

Figure 3.1. PCR products from modified DY682 forward primer 9-13 pair.
1A. IR- labelled forward 9-13 primers were PCR amplified with cDNA from various sources. PCR products of 368bp correspond to tau transcripts that include exon 10 (4R tau), products of 275bp correspond to transcripts excluding exon 10 (3R tau). 1B. cDNA from quadruplicate samples were PCR-amplified at different numbers of cycles (25, 30, 35, and 40) and PCR products were quantified and plotted to determine linear and plateau stages.

3.3. Tau exon 10 expression in frontal cortex

Tau mRNA and protein in the human frontal cortex has been found to be very highly expressed compared to all other brain regions tested including occipital cortex, putamen, cerebellum and white matter (Trabzuni et al., 2012). Tau pathological inclusions are present in the frontal cortex at later stages of AD corresponding to Braak stages V and VI (Braak and Braak, 1991; Braak et al., 2011). In FTLD-TDP, the frontal and temporal cortices have extensive TDP-43 pathology. TDP-43 inclusions in AD brains are predominant in the hippocampus and amygdala and usually only sparsely found in the frontal and temporal cortex (Arai et al., 2009; Hu et al., 2008).

Human brain samples from AD cases with TDP-43 inclusions (AD TDP+), AD cases without TDP-43 inclusions (AD TDP-), DM1, FTDP-17 cases and controls were identified from neuropathology reports. Brain samples were dissected from five brain areas, frontal and temporal cortices, amygdala, hippocampus and cerebellum at the IOP brain bank. All AD cases had been neuropathologically examined and confirmed AD cases and the presence or absence of pathological TDP-43 immunoreactivity was also confirmed in these cases. The six FTDP-17 brains dissected, had been identified at the Institute of Neurology at Queens Square, London (Janssen et al., 2002; Lantos et al., 2002), all had the 10+16 mutation which increases expression of 4R tau isoforms (Hutton et al., 1998). Samples were stored at -80°C until analysis.

RNA was extracted from all samples in all brain regions and RNA integrity (RIN) was measured for each sample. A RIN of 3.6 was an arbitrary cut-off that was

experimentally determined and RT-PCR with samples below this threshold were not reliable and therefore not included. Of the six FTDP-17, 10+16 brains sampled from the frontal cortex, only three had RIN above 3.6. RNA was reverse transcribed and the resulting cDNA was analysed by PCR with the modified DY682 forward primer 9-13 pair. Throughout these experiments RNA corresponding to the housekeeping protein glyceraldehyde-3-phosphate dehydrogenase (GAPDH) was used as an endogenous RT-PCR loading control. PCR products were run on 2% agarose gels and scanned into an Odyssey IR reader (Figure 3.2 A). The 4R and 3R tau bands were quantified and a 4R/3R ratio was calculated for each sample and plotted on a scatter graph (Figure 3.2 C). In addition, sample group 4R/3R means were calculated (Figure 3.2 B). All group comparisons were tested by t-test.

The three FTDP-17 samples had a 4R/3R tau ratio average of 2.8 (S.D. 0.28) compared to control average of 0.71 (S.D. 0.19) which was a highly significant increase in 4R/3R tau ratio compared to controls ($p \leq 0.0001$). The FTDP-17 samples used in this study were expected to show increases in 4R tau due to the mutation and were included as a positive control for the RT-PCR method. For example, Hutton et al. (1998) measured the 4R/3R ratio by RT-PCR in frontal cortex in two different 10+16 mutation brains and found one had a 4R/3R ratio of ~4 and the other ~2.

The AD TDP- samples had a 4R/3R ratio average of 0.87 (S.D. 0.18; control 4R/3R ratio average 0.71) and was significantly increased compared to control ($p = 0.035$). The AD TDP+ samples had a 4R/3R ratio average of 1.0 (S.D. 0.29) and 4R tau isoforms were significantly different compared to controls ($p = 0.005$). There were

no differences found in 4R/3R ratio averages between the AD groups. The single DM1 sample we sampled showed a mean 4R/3R tau ratio of 0.73 and this was identical to the mean of the control samples (average ratio control = 0.71). No statistical analysis can be done with a single sample and therefore this sample was not included in graphs and we will report the results only.

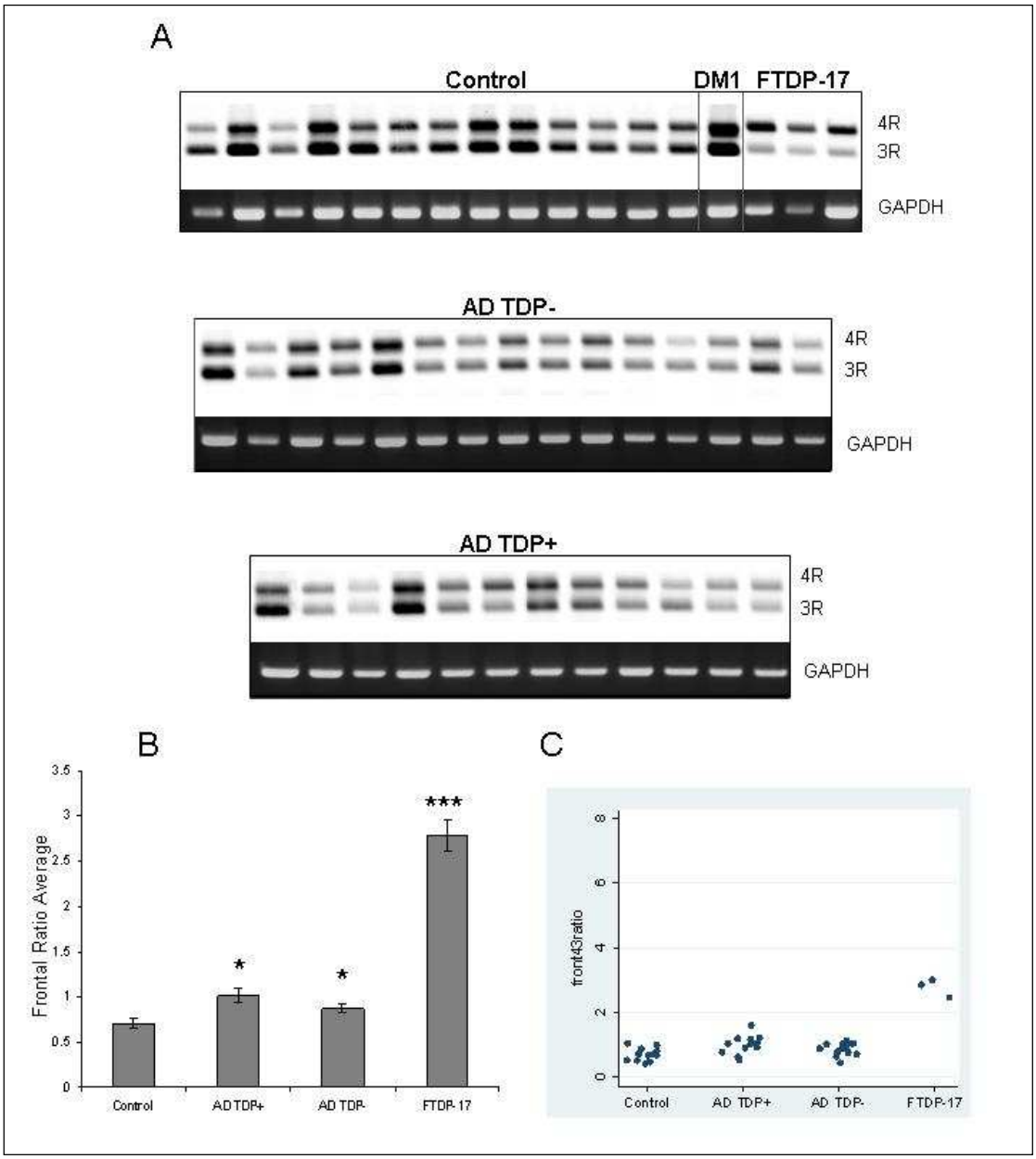

Figure 3.2. Tau exon 10 splicing in frontal cortex of control, DM1, FTDP-17 and Alzheimer's disease brain.

(A) Exon 10 inclusion was assayed by RT-PCR with IR-labelled forward 9-13 primer pair.

(B) Mean 4R/3R ratios were calculated for each group ± SEM. Significance was set at $p \leq 0.05$, *** = $p \leq 0.0005$. Significant differences shown in this graph are all case vs control.

(C) Scatter plots showing 4R/3R ratios for each brain sampled

3.4. Tau exon 10 expression in the temporal cortex

In AD, tau temporal cortex neuropathology is associated with Braak stages III-IV (Braak and Braak, 1991; Braak et al., 2011).

For the temporal cortex, three FTDP-17 brains had a RIN above 3.6. RNA from the temporal cortex samples was reverse transcribed and amplified with the DY682 labelled forward 9-13 primers. The PCR products were run on agarose gels (Figure 3.3 A), the 4R and 3R bands were quantified and 4R/3R ratios were calculated and plotted (Figure 3.3 B and C).

Similar to the frontal cortex, FTDP-17 brains have a 4R/3R ratio average of 3.2 (S.D. 0.38) compared to control average ratio of 0.9 (S.D. 0.24) indicating a highly significant increase in 4R containing tau transcripts in the FTDP-17 brains compared to controls ($p \leq 0.001$). For the AD groups ADTDP- 4R/3R ratio average was 1.1 (S.D. 0.44) and the AD TDP+ 4R/3R average was 1.1 (S.D. 0.38) compared to the control 4R/3R average of 0.9 and these differences were not significant. There were no differences in 4R/3R ratio averages between AD groups. The DM1 brain showed a large decrease in 4R containing PCR products (ratio = 0.69; control average = 0.9).

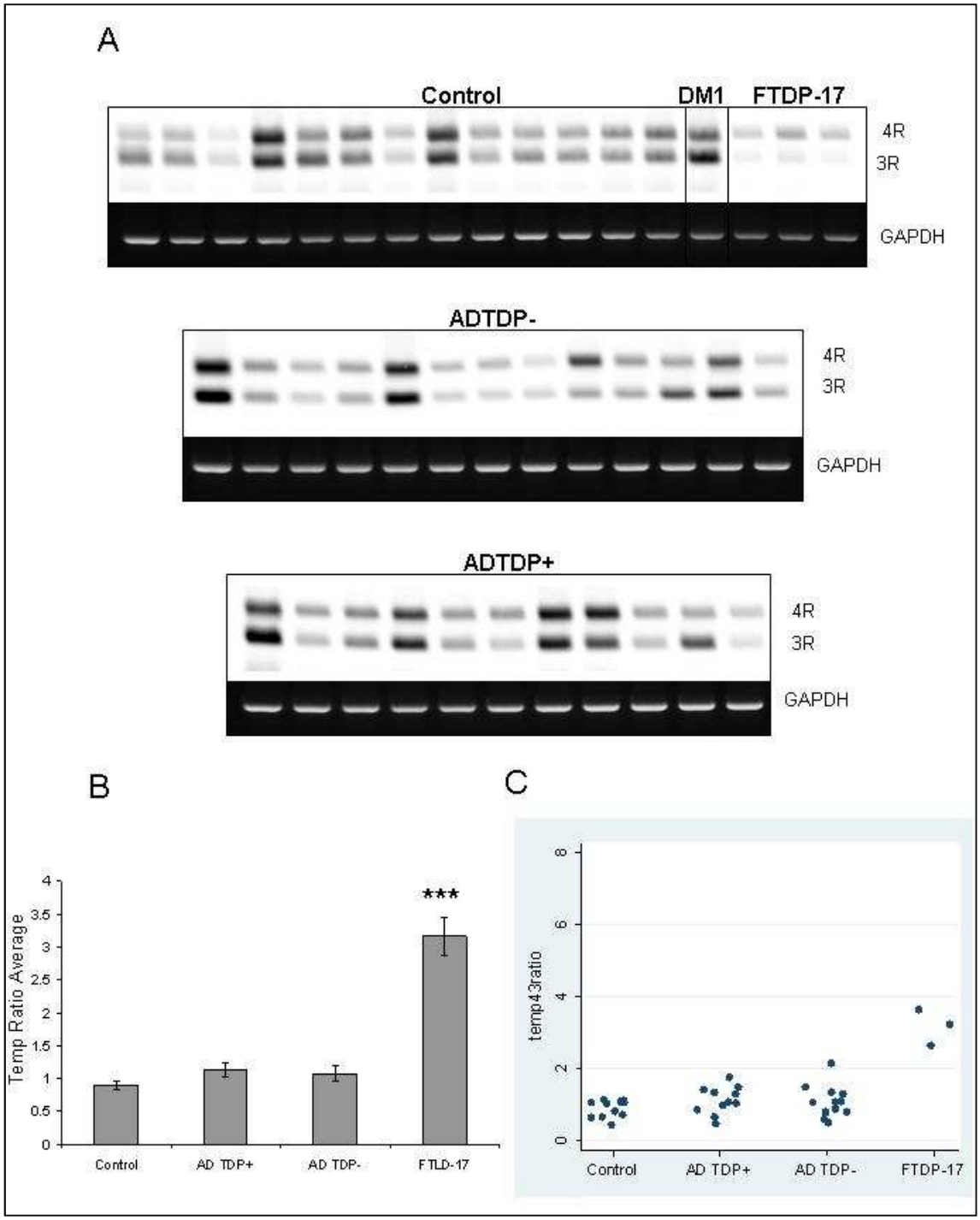

Figure 3.3. Tau exon 10 splicing in temporal cortex of control, DM1, FTDP-17 and Alzheimer's disease brain.
(A) Exon 10 inclusion was assayed by RT-PCR with IR-labelled forward primer pair.
(B) Mean 4R/3R ratios were calculated for each group ± SEM. Significance was set at $p \leq 0.05$, *** = $p \leq 0.0005$. Significant differences shown in this graph are all case vs control.
(C) Scatter plots showing 4R/3R ratios for each brain sampled

3.5. Tau exon 10 expression in the amygdala

The amygdala is consistently affected by tau pathology in AD and this may be due to its afferent connections to the entorhinal cortex (Vogt et al., 1990), which also shows extensive tau pathology and is considered one of the brain areas that is affected early in AD (van Hoesen et al., 1991). In AD brains with TDP-43 inclusions the amygdala is consistently affected (Amador-Ortiz et al., 2007; Arai et al., 2009). The amygdala may be highly susceptible to TDP-43 pathology because some brains have amygdala only TDP-43 pathology and it has been suggested that TDP-43 pathology starts in limbic regions and spreads into temporal and frontal regions at later stages in the disease course somewhat like tau Braak stages in AD (Hu et al., 2008).

We checked for the presence or absence of TDP-43 pathology in brain sections (Section 3.19). In our samples amygdala brain sections were not available for all cases however all of the ADTDP+ cases sampled had TDP-43 inclusions in the amygdala. There was one case with “amygdala only” TDP-43 inclusions (sample A249/07).

Splicing analysis showed two of the FTDP-17 cases have very high tau 4R/3R ratios compared to controls and one score is at normal 4R/3R ratio (sample A171/02; Figure 3.17). The 4R/3R ratio average for the FTDP-17 brains was 4.0 (S.D. 2.7) compared to a 4R/3R ratio average of 1.1 (S.D. 0.42) in controls.

ADTDP- brains in the amygdala had a 4R/3R ratio average of 1.5 (S.D. 0.58) compared to control average of 1.1 (S.D. 0.42), 4R tau isoforms were significantly increased in the ADTDP- group compared to controls ($p = 0.033$). The ADTDP+

brains also had a 4R/3R ratio average of 1.5 (S.D. 0.51), and this was borderline significant ($p = 0.054$). There were no differences between AD groups. The DM1 brain showed a decrease in 4R containing PCR products (ratio = 0.86; control average = 1.1).

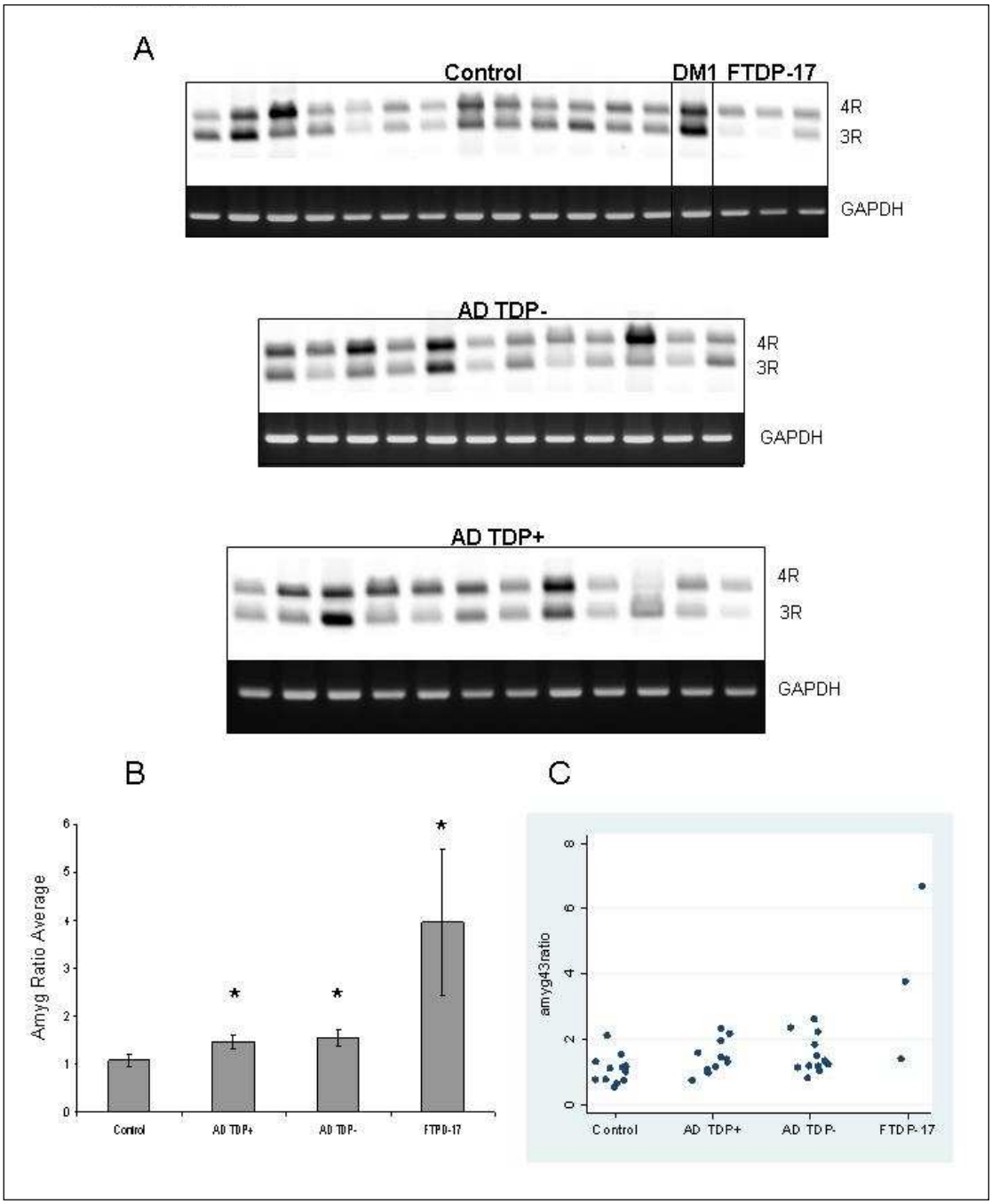

Figure 3.4. Tau exon 10 splicing in the amygdala of control, DM1, FTDP-17 and Alzheimer's disease brain.
(A) Exon 10 inclusion was assayed by RT-PCR with IR-labelled forward primer pair.
(B) Mean 4R/3R ratios were calculated for each group ± SEM. Significance was set at $p \leq 0.05$. Significant differences shown in this graph are all case vs control.
(C) Scatter plots showing 4R/3R ratios for each brain sampled

3.6. Tau exon 10 expression in the hippocampus

The entorhinal cortex has major projections to the hippocampus called the perforant pathway and these structures are heavily affected in AD. TDP-43 inclusions are also prevalent in the hippocampus of TDP-positive AD cases. In our sample set all but one case had cytoplasmic TDP-positive inclusions in the hippocampus.

The FTDP-17 samples had a 4R/3R ratio average of 4.2 (S.D. 0.39) compared to controls 4R/3R average of 0.9 (S.D. 0.24) and the increase in 4R transcript expression was highly significant ($p \leq 0.001$). The ADTDP- brains had a 4R/3R ratio average of 1.3 (S.D. 0.35) compared to control 0.9 and was significantly different compared to controls ($p = 0.01$). The ADTDP+ brains had a 4R/3R ratio of 1.4 (S.D. 0.55) and 4R transcripts were significantly higher in ADTDP+ brains compared to control ($p = 0.01$). There were no differences in 4R/3R ratios between ADTDP- and ADTDP+ brains. The DM1 brain actually showed an increase in 4R containing PCR products (ratio = 1.4; control average = 0.9).

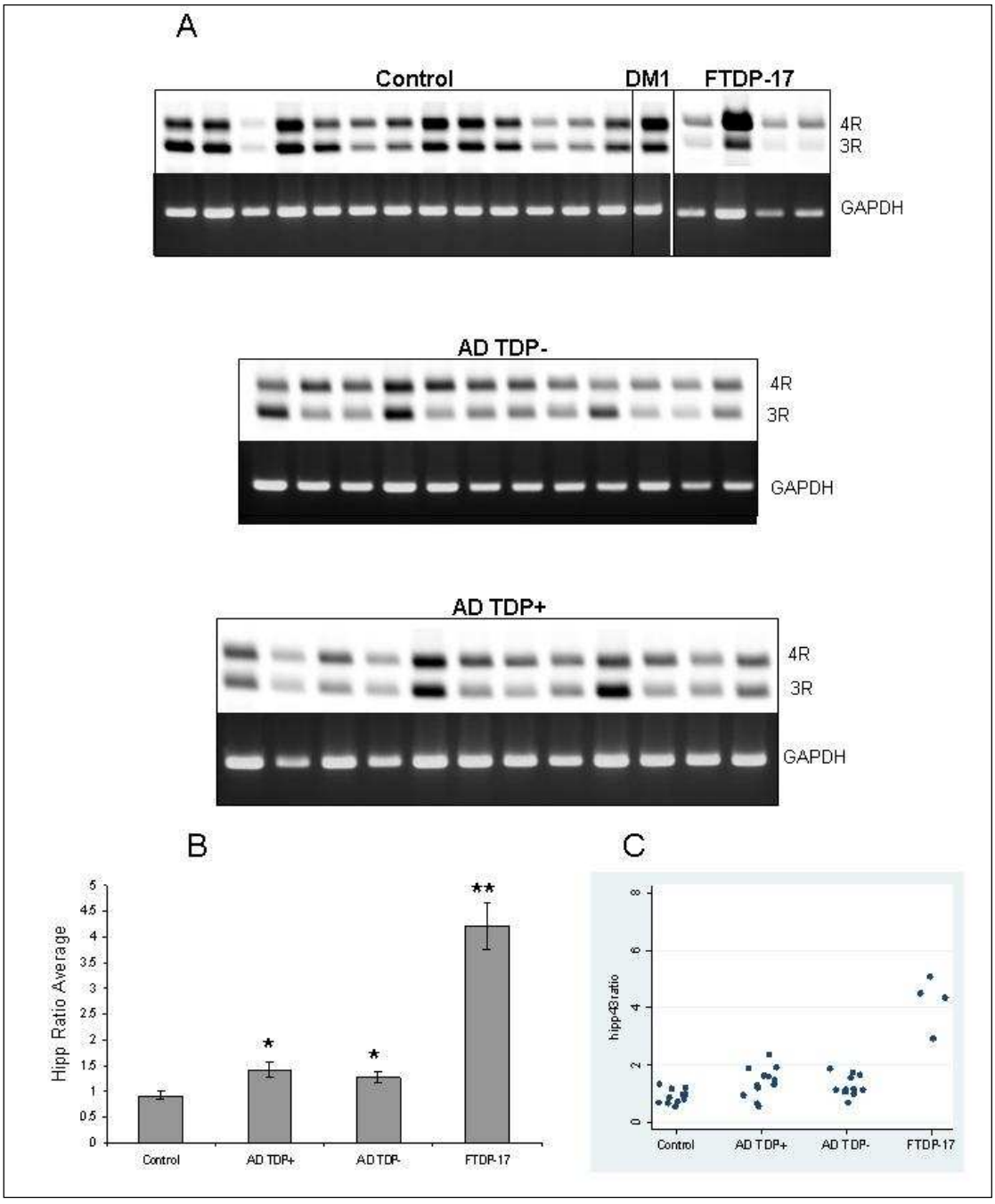

Figure 3.5. Tau exon 10 splicing in the hippocampus of control, DM1, FTDP-17 and Alzheimer's disease brain..

(A) Exon 10 inclusion was assayed by RT-PCR with IR-labelled primer pair.
(B) Mean 4R/3R ratios were calculated for each group ± SEM. Significance was set at $p \leq 0.05$, ** = $p \leq 0.005$. Significant differences shown are all case vs control.
(C) Scatter plots showing 4R/3R ratios for each brain sampled

3.7. Tau exon 10 expression in the cerebellum

In the cerebellum of AD brains, diffuse Aβ plaques are very common but there is no accompanying dystrophic neurites, no cell loss and no reactive astrocytes or microglia associated with the diffuse plaques and no tau inclusions (Joachim et al., 1989). TDP-43 inclusions are rarely found in the cerebellum of FTLD brains (King et al., 2011) and p62-positive, TDP-43-negative inclusions are associated with the *C9ORF72* repeat expansion (Troakes et al., 2012). Because the cerebellum has comparatively low levels of neurodegeneration in AD brains this brain region was included as a non-affected control.

Two of the FTDP-17 cases have very high 4R/3R ratios and one sample has a ratio within the control range (Figure 3.6C). The sample (A171/02) is the same as in the amygdala that also showed a normal 4R/3R ratio. The FTDP-17 4R/3R ratio average was 3.9 (S.D. 1.8) compared to the control 4R/3R ratio average of 1.2 (S.D. 0.38).

The ADTDP- group had a 4R/3R ratio average of 1.8 (S.D. 0.59) compared to the control 4R/3R ratio average of 1.2 and 4R containing transcripts were significantly increased in the ADTDP- brains compared to control ($p = 0.009$). The 4R/3R ratio average in ADTDP+ brains was 1.8 (S.D. 0.57) and a t-test comparing ADTDP+ and control 4R/3R ratios showed a significant difference ($p = 0.008$) and indicated that 4R containing transcripts were significantly increased in ADTDP+ brains compared to control. There were no differences in 4R/3R ratio between the AD groups. The DM1 brain showed an increase in transcripts containing exon 10 (DM1 ratio = 1.9 control average ratio = 1.2).

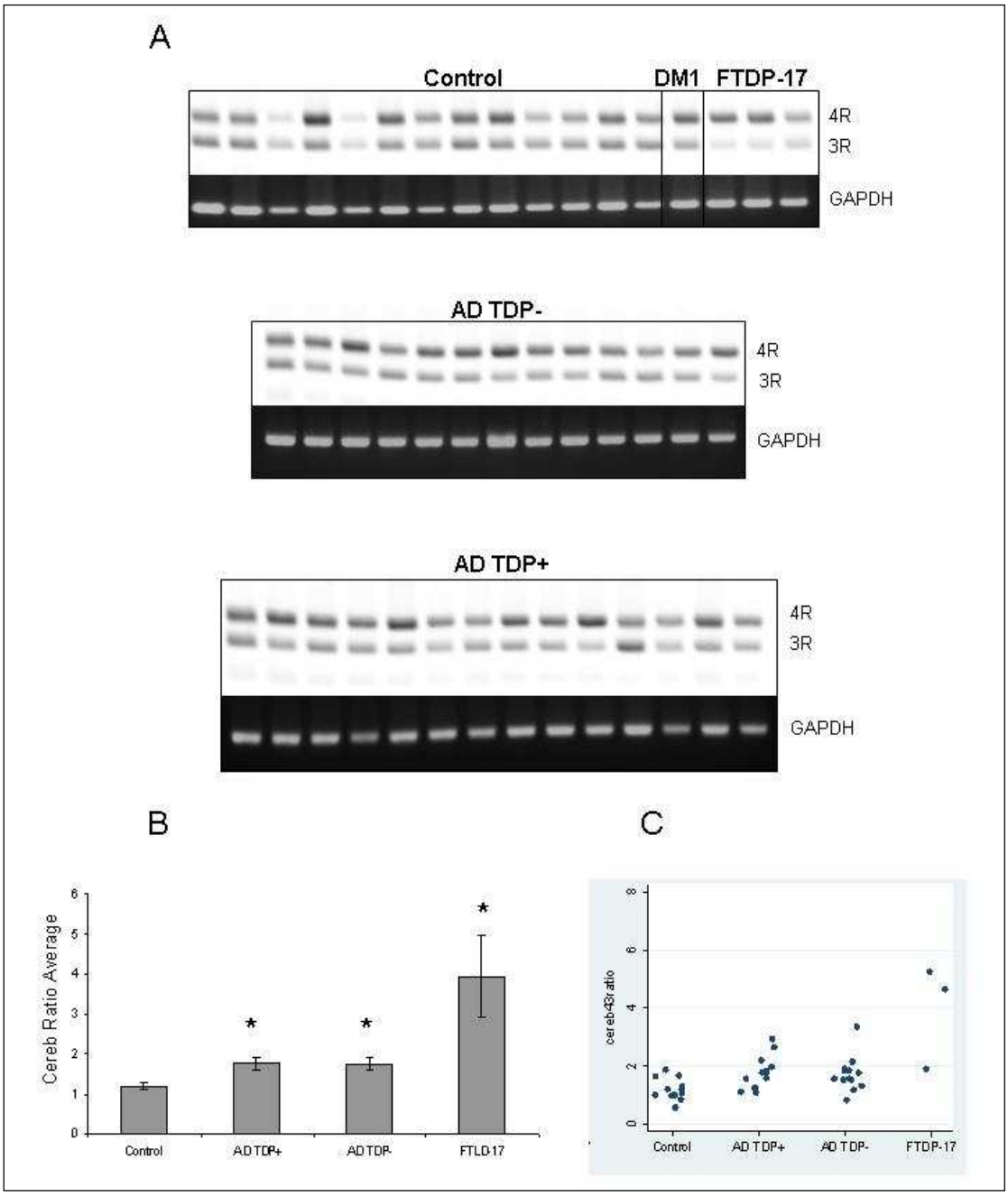

Figure 3.6. Tau exon 10 splicing in the cerebellum of control, DM1, FTDP-17 and Alzheimer's disease brain.
(A) Exon 10 inclusion was assayed by RT-PCR with IR-labelled primer pair.
(B) Mean 4R/3R ratios were calculated for each group ± SEM. Significance was set at $p \leq 0.05$. Significant differences shown are all case vs control.
(C) Scatter plots showing 4R/3R ratios for each brain sampled

3.8. Tau 4R/3R tau ratio correlation across brain regions

The analysis of tau 4R/3R ratios in AD and control brains found significant increases in 4R transcript expression in the frontal cortex, amygdala, hippocampus and cerebellum of AD brains.

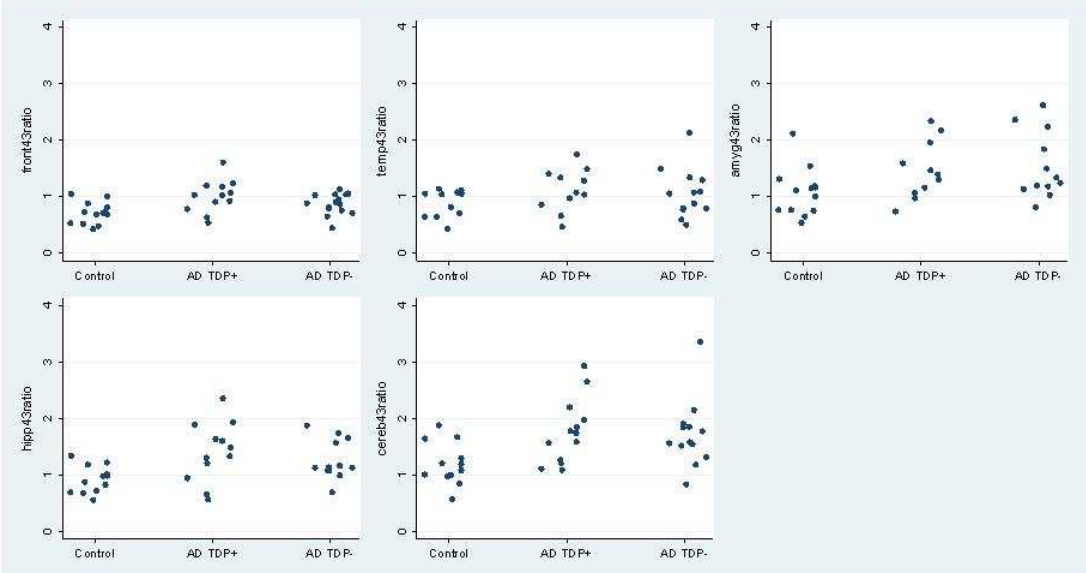

Figure 3.7. 4R/3R ratios in control and AD brains for five brain regions (FTDP-17 data excluded).

In both AD groups there was a noticeable group of brains that show high 4R transcript expression (Figure 3.7). To analyse this data further, individual 4R/3R ratios were ranked highest to lowest, for each brain region. Since there were no significant differences in 4R/3R ratios between the ADTDP- and ADTDP+ brains, the AD data was grouped together. The consistency of 4R/3R ratio for each individual in the AD group across each brain region was very apparent in this analysis. Those ranked high for tau 4R/3R ratio in one brain region remained so throughout all five brain regions measured. The consistency of 4R transcript

expression across brain regions was also found for those low 4R/3R ranking individuals.

To test the observation that tau RNA 4R/3R ratios were consistent across brain regions, a correlation analysis was performed on individual 4R/3R ratio data from one brain region with the 4R/3R ratio from all of the other brain regions. Correlation analysis was performed with 4R/3R ratios from control and a separate analysis with 4R/3R ratios from the combined AD brains.

In the combined AD group there were highly significant 4R/3R ratio correlation coefficients between frontal, temporal, amygdala and hippocampus brain regions (Table 3.1). In these brain areas, high 4R transcript expression in the frontal cortex also showed high 4R transcript expression in all other brain regions tested and these results suggest that high 4R expressors comprise a subgroup of AD patients within our sample set. This high 4R expressor group contribute the significant increases found in all brain regions in our sample set

The cerebellum, in general, showed much lower tau 4R/3R correlation coefficients with the frontal, amygdala and hippocampus and a non-significant result with the temporal cortex (Figure 3.8 and Table 3.1).

Although the control sample set was smaller than the combined AD group, control brains also had high correlation coefficients in tau 4R/3R ratio that were significant for frontal, temporal, amygdala and hippocampus brain regions. The tau 4R/3R ratio between the frontal cortex and amygdala were not significantly correlated (Table

3.2). There was a wide variability in the magnitude of correlation between the cerebellum and the other brain regions with the amygdala and cerebellum having very high correlation coefficients and the other regions showing borderline or not significant correlation with the cerebellum (Figure 3.9 and Table 3.2).

Correlation analysis carried out on the control 4R/3R data shown in the graphs in Figure 3.9, were to the same scale as the combined AD graphs in Figure 3.8. Consistent with the significant increases in 4R/3R tau ratios seen in most brain regions in AD brains, the AD scatter graphs show a wider distribution of 4R/3R ratio data points indicating higher tau 4R expression compared to controls (compare Figure 3.8 with Figure 3.9).

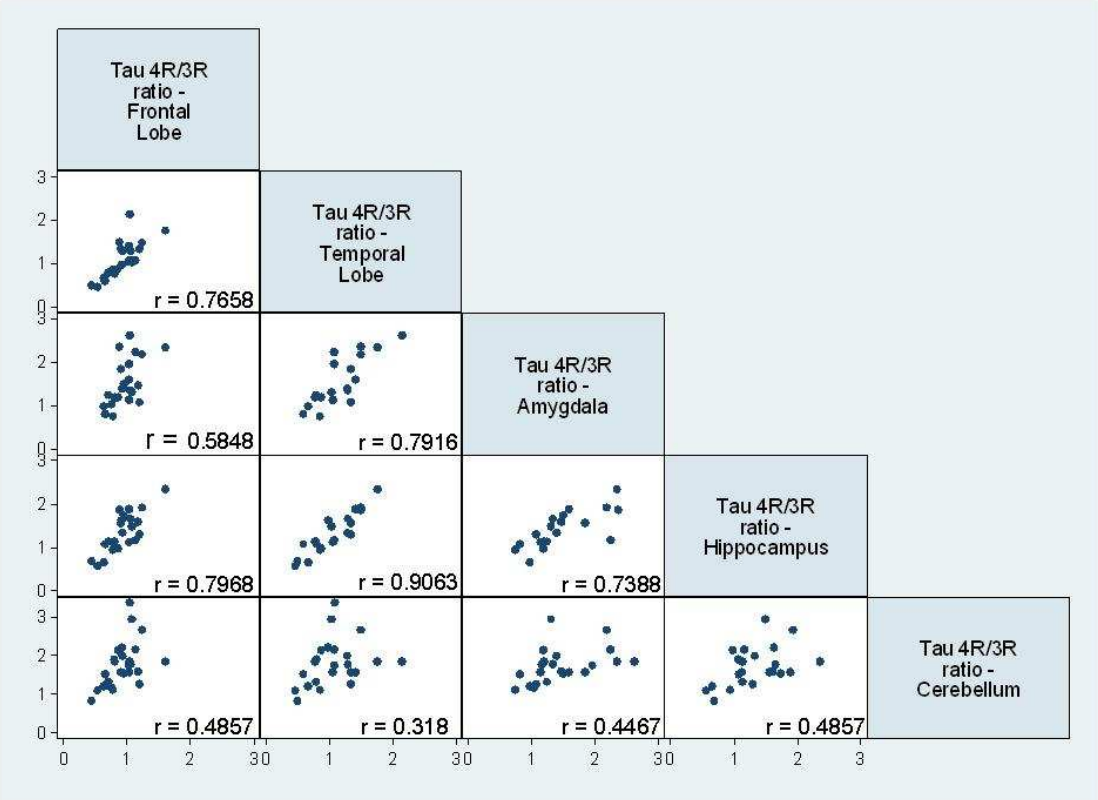

Figure 3.8. Scatter graphs of 4R/3R RNA expression ratios across the brain regions in combined AD group.

FRONTAL				
r = 0.7658 p < 0.0001 n = 24	TEMPORAL			
r = 0.5848 p = 0.0043 n = 22	r = 0.7916 p = 0.0001 n = 19	AMYGDALA		
r = 0.7968 p < 0.0001 n = 23	r = 0.9063 p < 0.0001 n = 21	r = 0.7388 p = 0.0003 n = 19	HIPPOCAMPUS	
r = 0.4857 p = 0.0119 n = 26	r = 0.318 p = 0.1392 n = 23	r = 0.4467 p = 0.0371 n = 22	r = 0.4857 p = 0.0219 n = 22	CEREBELLUM

Table 3.1. Correlation coefficients of 4R/3R expression across brain regions in AD brains.

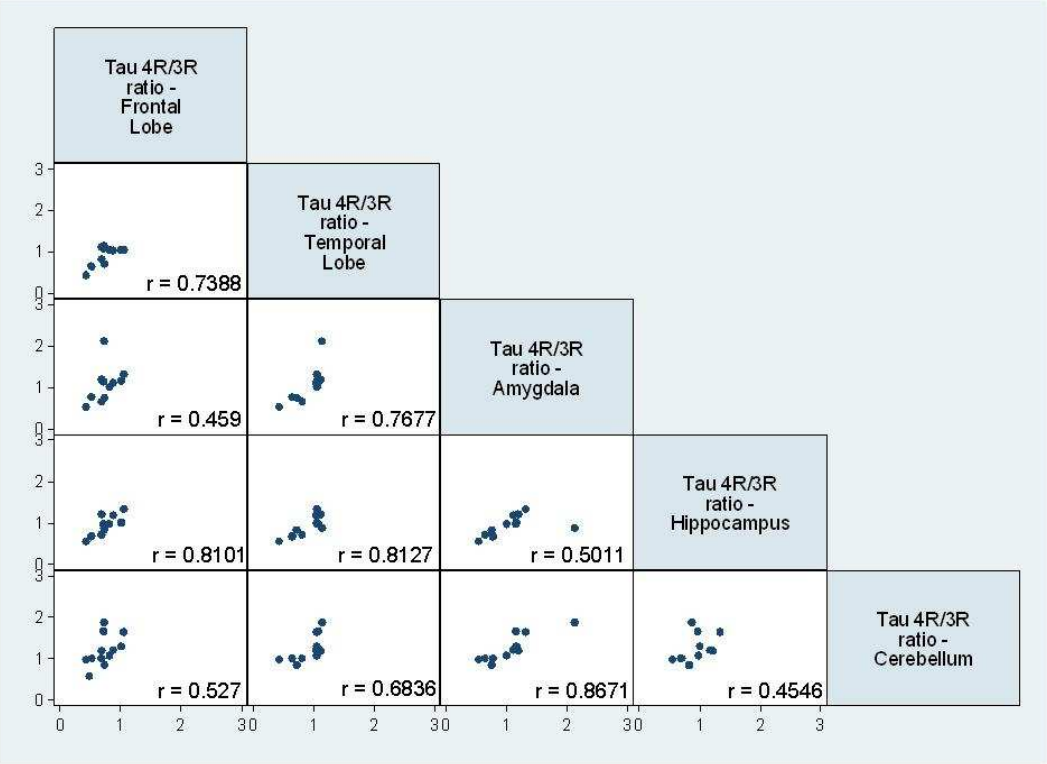

Figure 3.9. Scatter graphs of 4R/3R RNA expression ratios across the brain regions in control brains.

FRONTAL				
r = 0.7388 p = 0.0061 n = 12	TEMPORAL			
r = 0.459 p = 0.1333 n = 12	r = 0.7677 p = 0.0036 n = 12	AMYGDALA		
r = 0.8101 p = 0.0014 n = 12	r = 0.8127 p = 0.0013 n = 12	r = 0.5011 p = 0.097 n = 12	HIPPOCAMPUS	
r = 0.527 p = 0.0783 n = 12	r = 0.6836 p = 0.0204 n = 11	r = 0.8671 p = 0.0005 n = 11	r = 0.4546 p = 0.1601 n = 11	CEREBELLUM

Table 3.2. Correlation coefficients of 4R/3R expression acorss brain regions in control brains.

3.9. Tau exons 2 and 3 expression

N-terminal inserts of tau may determine the spacing between microtubules (Chen et al., 1992; Frappier et al., 1994). They also play a role in modulating aggregation properties of tau (Zhong et al., 2012), and may be involved in signalling through src mediated interaction with the cell membrane (Butner and Kirschner, 1991; Lee et al., 1998). The H2 haplotype is associated with higher expression of tau exon 3 (Caffrey et al., 2008; Trabzuni et al., 2012) which is interesting because H2 haplotype has a negative association with PSP and CBD and therefore suggests a protective role.

In this section the research question is does TDP-43 dysfunction in disease alter tau exon 2 and 3 splicing in AD brain? The expression levels of tau exons 2 and 3 were measured in control, ADTDP- and ADTDP+ human brains in five brain regions.

3.10. Determination of PCR conditions for tau exon 2 and 3

A primer pair for detection of tau exon 2 and 3 were chosen from previously published work (Leroy et al., 2006). The forward primer was modified by adding a DY682 tag onto the 5' end. For the tau N-terminal primer pair we initially found three PCR products corresponding to 0N, 1N and 2N tau isoforms (Figure 3.10A). Three PCR products of 284, 197 and 110 bp were found and sequenced. The 284 bp product includes tau exons 2 and 3 (2N), the 197 bp product has only exon 2 present (1N) and the 110 bp product has no N-terminal inserts (0N). cDNA was analysed with the DY682 labelled forward primer tau N-terminal pair for a different number cycles. Arbitrary fluorescent units for quadruplicate samples of the three N-terminal PCR products were measured by Odyssey software. Fluorescent units were plotted against differing cycle numbers and the linear range of the PCR amplification curve

was determined (Figure 3.10B). The number of cycles used in the final analysis was 30.

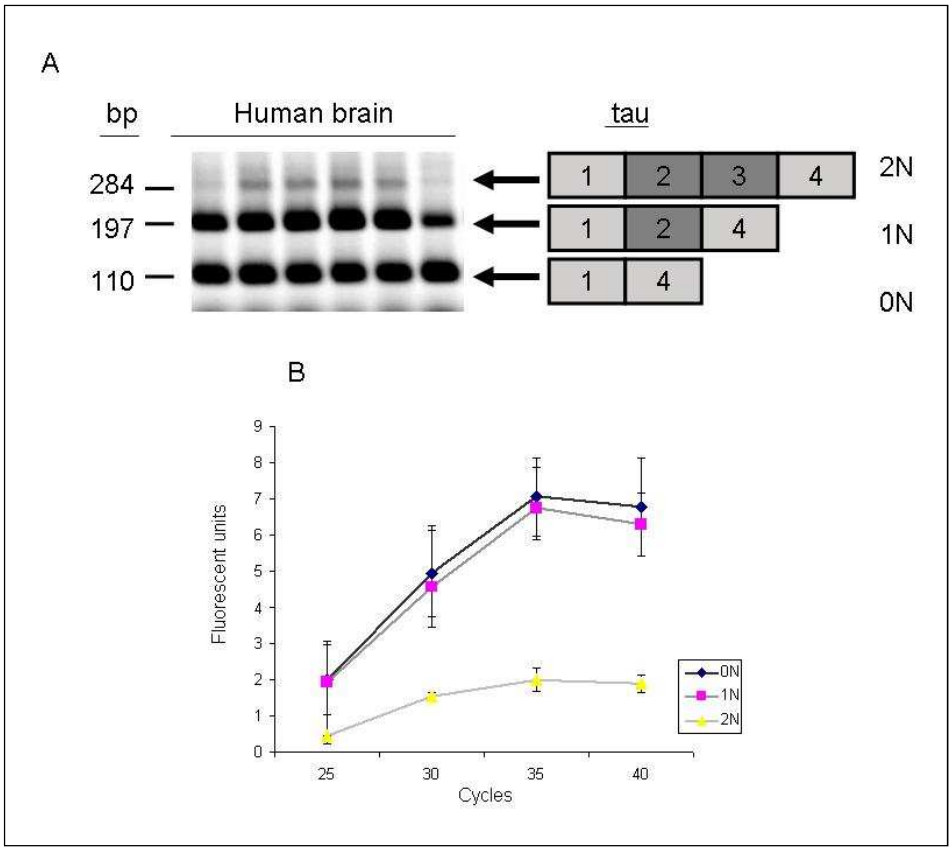

Figure 3.10. Determination of tau exons 2 and 3 primer amplification.
(A) The IR labelled forward primer N-terminal pair were tested with cDNA from frontal cortex human brain. PCR products of 284bp correspond to tau transcripts with two N-terminal exons (2N tau), products of 197bp correspond to transcripts with only exon 2 (1N tau) and PCR products of 110bp correspond to transcripts with no N-terminal exons (0N tau). (B) cDNA from quadruplicate samples were PCR amplified at different number of cycles (25, 30, 35, 40). PCR products were quantified and the values plotted to determine linear and plateau stages.

3.11. Tau exon 2 and 3 alternative splicing

cDNA from human brain samples from five brain regions (frontal, temporal, amygdala, hippocampus and cerebellum) were analysed by PCR with the DY682 labelled forward tau N terminal primers to measure alternative splicing of tau exons 2 and 3. In this analysis, a doublet in the bands corresponding to 2N and 1N tau consistently appeared in all brain regions (Fig 3.11 arrows on left).

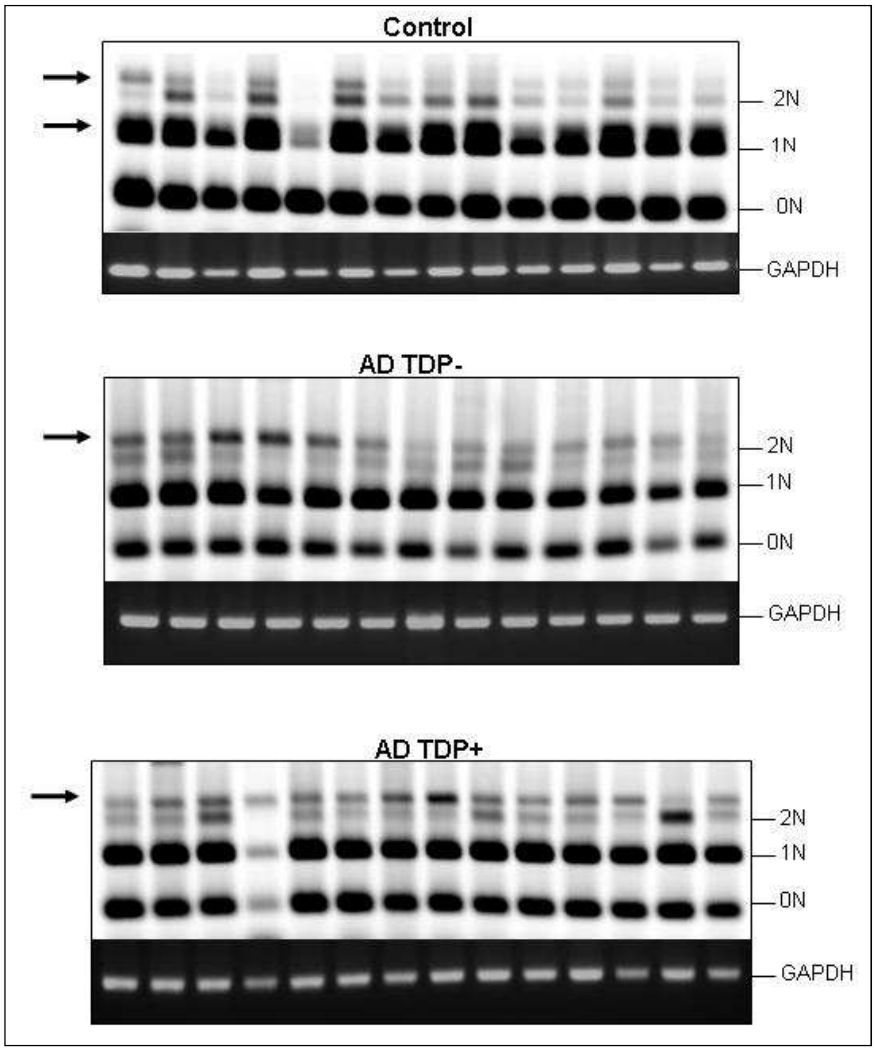

Figure 3.11. Tau exon 2 and 3 expression in the human cerebellum.
cDNA from the cerebellum was amplified by RT-PCR with IR labelled forward primer N-term pair to visualise tau exon 2 and 3 expression. PCR products were separated by agarose gel electrophoresis and scanned with an IR reader (Odyssey). A clear doublet was seen at the 2N band as well as the 1N band.

Five PCR products were not expected from this primer pair and in order to confirm their identity all five bands (2N larger, 2N, 1N larger, 1N and 0N) were cut from an agarose gel and the PCR products were sub-cloned and sequenced. The sub-cloned PCR products were run on an agarose gel to check their length before sequencing (Figure3.12A), however we were not able to isolate the lager 1N band for sequencing at this time. Sequencing results showed that the larger 2N band was tau with 1 N-terminal repeat (1N) but with an intronic sequence spliced in (Figure 3.12C). The intronic sequence was 135 base pairs long and is found in intron 1 of *MAPT*. In order to rule out any PCR artefacts, a new forward PCR primer was designed that spanned tau exon 1 and the putative exon found in intron 1. cDNA from the human cerebellum was analysed by PCR with the new primer pair. Two PCR products were found (Fig 3.12B), these were sequenced and, consistent with previous sequencing results, the larger band (263bp) corresponded to tau 1N with the intron 1 exon. The shorter band (176bp) corresponded to tau 0N and also contained the intron 1 exon (Figure 3.12B).

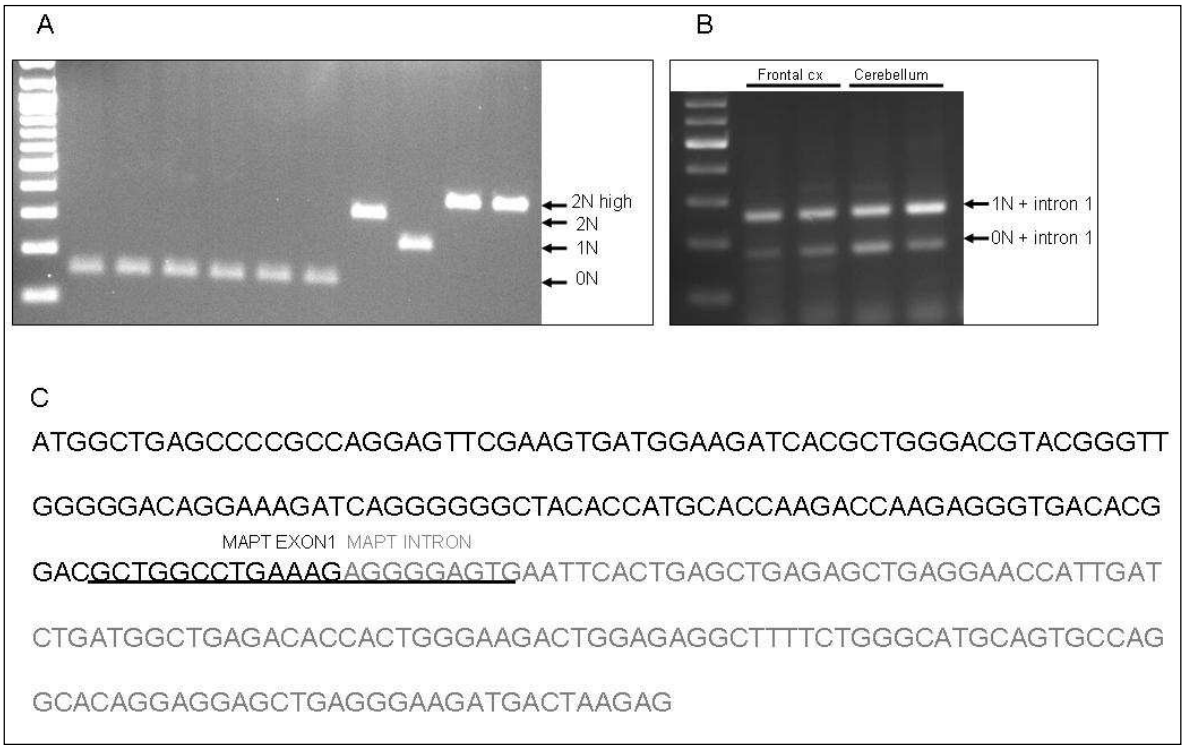

Figure 3.12. Sequence of PCR products containing a cryptic tau exon.
PCR products were excised from agarose gels and sub-cloned for sequencing (A). (B) PCR products from tau exon1 intron1 spanning primer show two PCR products containing a cryptic exon from intron 1 of *MAPT*. The sequence in black is *MAPT* exon 1, the sequence in grey is a cryptic exon spliced in from intron 1. The underlined sequence is the PCR primer that spans tau exon 1 and the cryptic exon in intron 1.

The presence of the intron 1 containing tau transcripts meant that all of the analysis of tau exon 2 and 3 could not be quantified because in the tau 1N bands there were also 0N tau (that include intron1) transcripts. Similarly for the 2N bands there were 1N tau containing intron 1 transcripts (although more distinguishable). In order to quantify these PCR products, greater separation of the bands by longer electrophoresis time would be necessary.

3.12. Total *MAPT* mRNA expression

Altered total mRNA levels of *MAPT* expression may also be a risk factor in AD and other tauopathies. TDP-43 could potentially regulate *MAPT* expression levels by

binding to pyrimidine-rich sequences on the *MAPT* gene and potentially repress transcription. Previously TDP-43 has been shown to inhibit HIV1 gene expression possibly by preventing the assembly of a functional transcription initiation complex (Ou et al., 1995). The promoter region of *MAPT* has multiple pryrimidine transcription factor binding sites (Andreadis et al., 1996; Maloney and Lahiri, 2012) and therefore altered nuclear TDP-43 levels may impact on *MAPT* transcriptional regulation. In addition, TDP-43 may regulate *MAPT* transcript levels through the role TDP-43 plays in stabilising mRNA (Ayala et al., 2011; Strong et al., 2007).

qRT-PCR was used to measure total levels of tau mRNA in five brain regions (frontal and temporal cortex, amygdala hippocampus and cerebellum). cDNA from the splicing analysis of tau was also used for this analysis. qRTPCR is a very sensitive technique and relies on measuring the increase in a fluorescent signal which is proportional to the amount of cDNA produced during each PCR cycle. Cycles continue until the fluorescent signal reaches a cycling threshold (CT). To determine relative expression of the gene of interest, the CT value is normalised to a reference gene. Reference gene expression should ideally be constant across the samples being compared. However expression of traditionally used reference genes can be variable and altered by disease state. Reference gene expression stability therefore needs to be checked for the specific sample set and normalisation should be performed using more than one reference gene (Vandesompele et al., 2002). The two most stable reference genes for each brain region were identified with primers and software (qbase^{PLUS}) from Primerdesign (UK). For the total tau RNA analysis, tau primers were used with a forward primer spanning exons 11 and 12 and a reverse primer spanning exons 12 and 13. This primer pair had been previously tested and

shown to produce a single qRT-PCR product and the identity of the PCR product was confirmed by sequencing. All samples were run in duplicate with SYBR green. The average cycle threshold (CT) was calculated for target and reference genes. The average CT for target samples was divided by the geometric mean of the two reference genes and each point plotted giving a target gene expression relative to reference gene expression for each sample (Fig 3.13).

The analysis showed that tau expression was the same across control and disease conditions and there were no significant differences found in tau expression in disease groups compared to controls in any brain region, by one way ANOVA. There were also no differences in ADTDP+ compared to ADTDP- groups in any brain region by t-test. This suggests that TDP-43 misregulation in AD brain does not play a role in altering tau transcription. The CT values plotted are relative to different sets of reference genes in each brain region and therefore levels of tau expression across brain regions are not comparable (Fig 3.13)

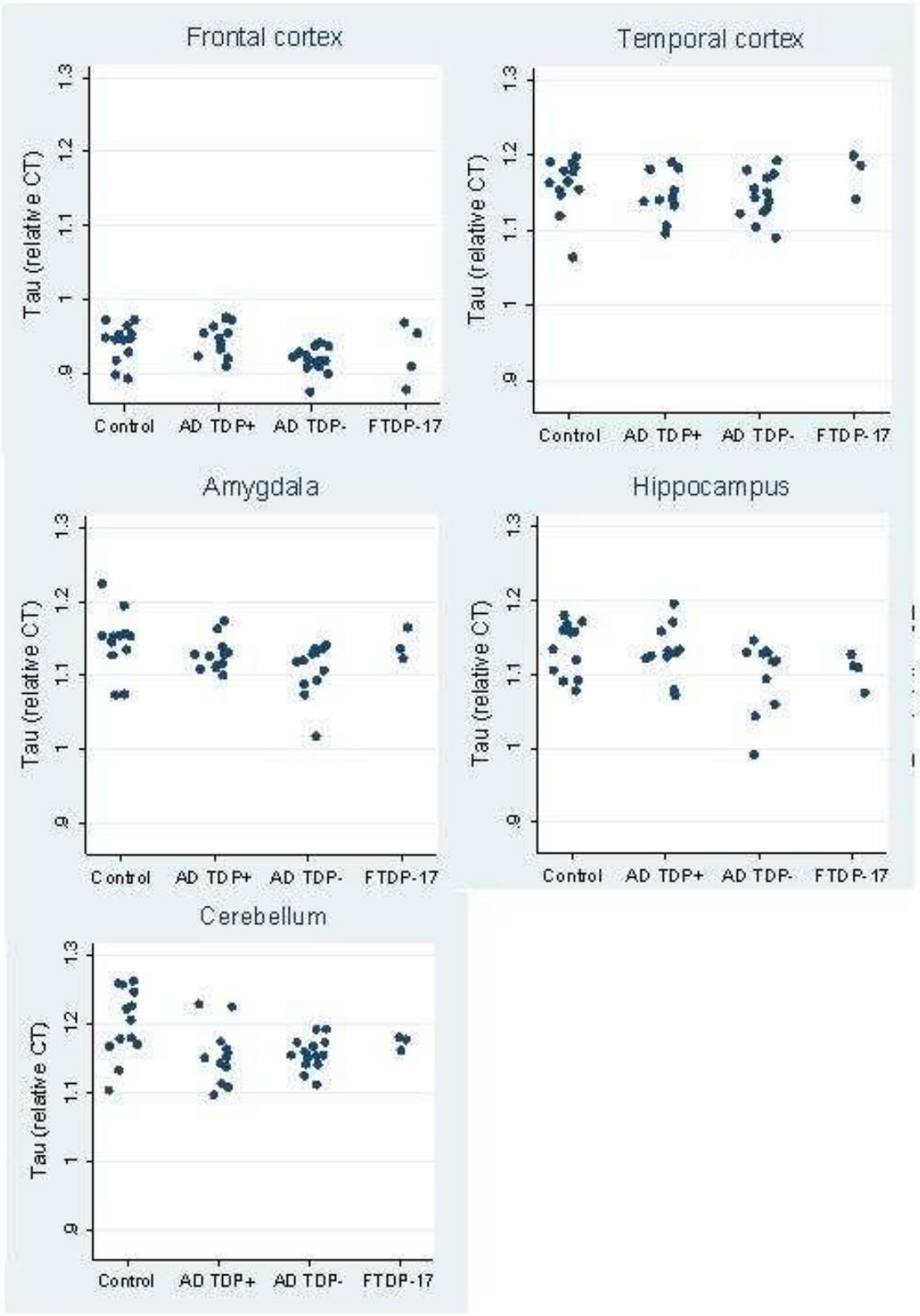

Figure 3.13. Total tau expression in AD and control brain.
RNA was isolated from post-mortem brain tissue and reverse transcribed. 20ng/µl of cDNA was used for qRTPCR analysis in duplicate. Each data point represents one sample, relative CT was calculated by dividing target CT by the geometric mean of the two reference genes.

3.13. *MAPT* haplotypes

The H1 haplotype of *MAPT* is associated with increased risk of developing PSP (Baker et al., 1999; Hoglinger et al., 2011), CBD (Houlden et al., 2001), PD (Golbe et al., 2001; Lill et al., 2012) and AD (Gerrish et al., 2012). The mechanism of pathogenesis for the association with disease is not known, however studies in post-mortem brain samples have shown that tau exon 10 containing RNA is increased in homozygous H1 haplotypes (Caffrey et al., 2006). Allele-specific PCR quantification in post mortem brain samples show that H1 haplotype expresses higher total tau than controls and higher 4R containing transcripts than controls (Myers et al., 2007). Another intriguing result has been the association of H2, which is negatively associated with PSP and CBD, with increases in tau exon 3 (Caffrey et al., 2008; Trabzuni et al., 2012). These findings demonstrate that genetic variability, most likely within the *MAPT* locus, alters tau splicing and/or expression and is a significant contributor to the risk of developing tauopathy.

We determined the *MAPT* H1, H2 haplotype in all our samples. Genomic DNA was extracted from cerebellar samples from control and AD cases (n = 42). The H2 haplotype can be identified by a 238 bp deletion within intron 9 not present in the H1 haplotype (Baker et al., 1999). H1 and H2 haplotypes were determined by visualising a PCR product on agarose gel (Figure 3.14 and Table 3.3). Further sub-haplotyping of our H1 samples would have been desirable but with such a small sample size a sub-haplotype analysis would be underpowered to get meaningful results.

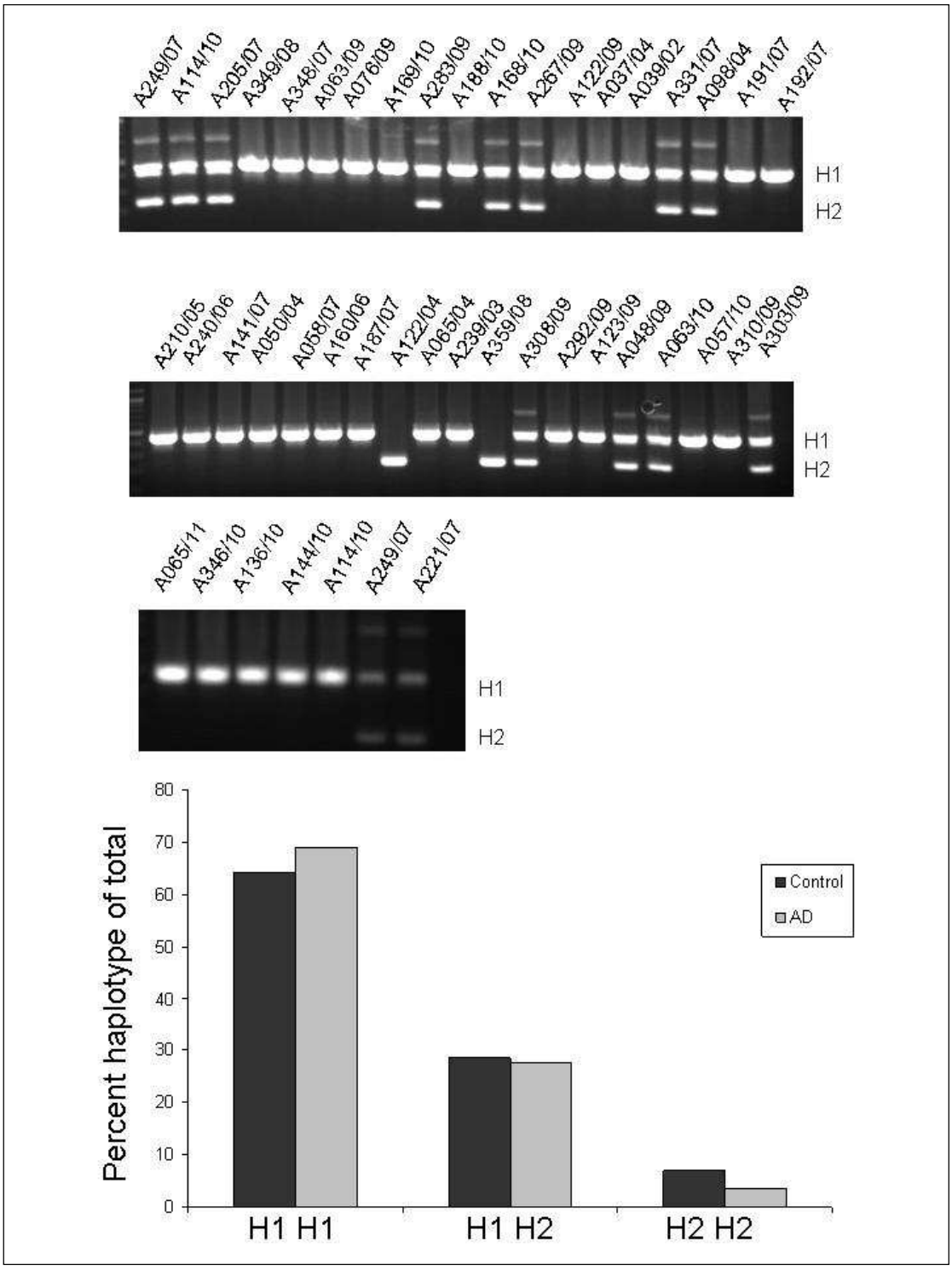

Figure 3.14. Haplotype analysis of samples.
DNA was extracted from the cerebellum of all brain samples. Primers spanning the 238bp deletion were used to distinguish H2 alleles from H1. The H2 haplotype with the deletion show as a lower band.

SAMPLE	HAPLOTYPE	CATEGORY	SAMPLE	HAPLOTYPE	CATEGORY
A239/03	H1/H1	CONTROL	A283/09	H1/H2	AD TDP+
A359/08	H2/H2	CONTROL	A188/10	H1/H1	AD TDP+
A308/09	H1/H2	CONTROL	A168/10	H1/H2	AD TDP+
A292/09	H1/H1	CONTROL	A267/09	H1/H2	AD TDP+
A123/09	H1/H1	CONTROL	A308/07	H1/H1	AD TDP+
A048/09	H1/H2	CONTROL	A122/09	H1/H1	AD TDP+
A063/10	H1/H2	CONTROL	A037/04	H1/H1	AD TDP-
A057/10	H1/H1	CONTROL	A039/02	H1/H1	AD TDP-
A310/09	H1/H1	CONTROL	A331/07	H1/H2	AD TDP-
A303/09	H1/H2	CONTROL	A098/04	H1/H2	AD TDP-
A065/11	H1/H1	CONTROL	A191/07	H1/H1	AD TDP-
A346/10	H1/H1	CONTROL	A192/07	H1/H1	AD TDP-
A136/10	H1/H1	CONTROL	A210/05	H1/H1	AD TDP-
A249/07	H1/H2	AD TDP+	A240/06	H1/H1	AD TDP-
A205/07	H1/H2	AD TDP+	A141/07	H1/H1	AD TDP-
A349/08	H1/H1	AD TDP+	A050/04	H1/H1	AD TDP-
A348/07	H1/H1	AD TDP+	A058/07	H1/H1	AD TDP-
A063/09	H1/H1	AD TDP+	A160/06	H1/H1	AD TDP-
A076/09	H1/H1	AD TDP+	A187/07	H1/H1	AD TDP-
A169/10	H1/H1	AD TDP+	A122/04	H2/H2	AD TDP-
A114/10	H1/H1	AD TDP+	A065/04	H1/H1	AD TDP-

Table 3.3. Haplotype analysis of AD and control samples.

Homozygosity for the tau H1haplotype has been shown to be associated with the increased risk of developing PSP and CBD. We tested tau haplotype for association with AD, by chi-square. No significant association was found for AD and presence of H1 alleles in this analysis.

CONDITION	%H1H1	%H1H2	%H2H2
Control	64.3	28.6	7.1
AD	69	27.6	3.4

Table 3.4. Proportion of *MAPT* haplotype alleles.

3.14. Correlation tau RNA expression with haplotype

Previous studies have suggested that the tau H1 haplotype expresses higher levels of *MAPT* mRNA transcripts than the H2 haplotype in brain and it was suggested that this increase in tau expression could explain the risk association between tauopathies and the H1 haplotype (Myers et al., 2007).

A test for an association between *MAPT* haplotype and *MAPT* mRNA expression was performed with the qRT-PCR data used before from the total tau expression levels by disease category (Fig. 3.13). Relative CT values for AD and control groups were analysed, the FTDP-17 samples were excluded for this analysis. Because our sample size is small and the H2/H2 haplotype is quite rare, there were very few cases for this haplotype and therefore the H2/H2 homozygotes were combined with the H2/H1 homozygotes for the statistical analysis. A t-test was performed on relative CT values from the two haplotype groups for each brain region. No significant differences between tau haplotype and total tau expression were found for any brain region (Fig. 3.15). This analysis shows that no particular tau haplotype was associated with an increase in total tau expression, H1 homozygotes and heterozygotes were not significantly different compared to H2 homozygotes in all brain regions tested.

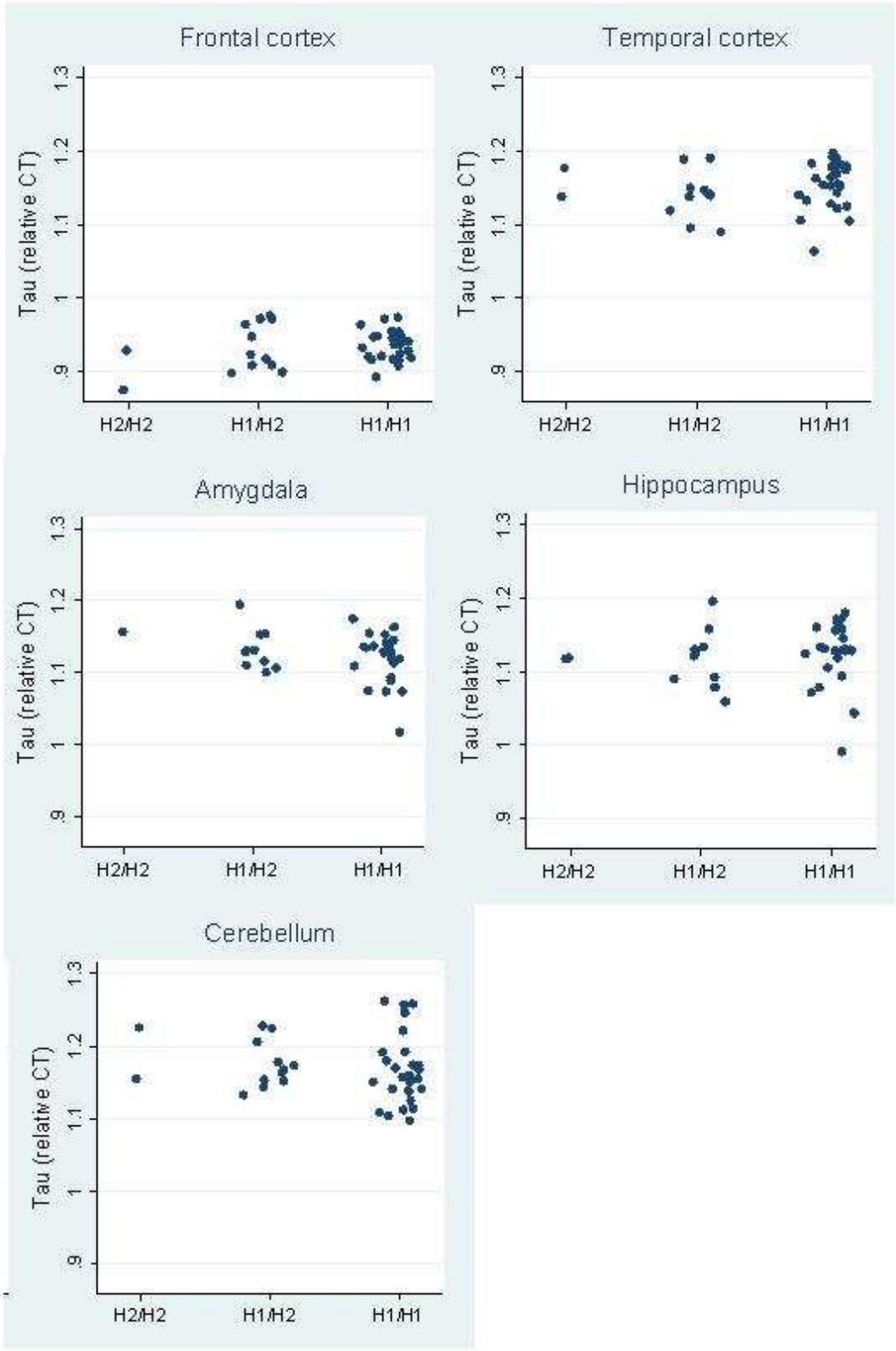

Figure 3.15. Association of *MAPT* expression with *MAPT* haplotype.
Control and AD groups were combined and relative CT tau expression from the qRT-PCR experiment (Figure 3.13) was used for the association with tau haplotype.

Homozygosity of the H1allele may also be associated with increases tau 4R expression in brain (Caffrey et al., 2006). A test for association between *MAPT* haplotype and 4R/3R tau ratio in all five brain regions was performed using data from the *MAPT* splicing assays in five brain regions (Fig. 3.2 – 3.6). Both AD and control groups were analysed and FTDP-17 and DM1 cases were excluded. As done previously, H2/H2 homozygotes were combined with H2/H1 heterozygotes for the statistical analysis. A t-test was performed on the data for each brain region, Fig 3.16 shows a representative scatter graph of results from the hippocampus. No significant differences were found between H1 homozygotes vs combined H2 homozygotes and H2/H1heterozygotes in any of the five brain regions.

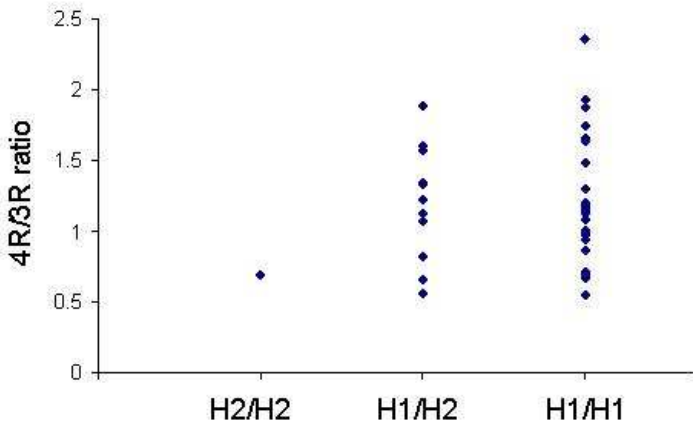

Figure 3.16. Tau 4R/3R ratio by tau haplotype from the hippocampus.
Control and AD 4R/3R ratio tau data were combined and tested for association with tau haplotype

3.15. Analysis of tau protein in Alzheimer's disease affected brain

TDP-43 plays a role in post-transcriptional processing of particular transcripts such as *NEFL* which is stabilised by TDP-43 binding to its 3'UTR (Strong et al., 2007). In addition, TDP-43 plays a role in the microRNA synthesis pathway and regulates expression of a number of miRNA species (Buratti et al., 2010). These finding suggest that TDP-43 mislocation into cytoplasmic aggregates may alter target transcript levels. In this section the first research question is does TDP-43 regulate post-transcriptional processing of tau transcripts? Quantification of *MAPT* exon 10 expression at the RNA level showed a sub-group of AD cases with consistently high 4R expression across all of the brain regions measured. The second question is: is there a the relationship between tau RNA expression and tau protein levels in control and AD brain?

The same set of brain tissue samples that were used for RNA extraction and tau 4R/3R analysis were used for protein analysis. The amygdala and hippocampus have previously been shown to be predominantly affected by TDP-43 pathology and contain the most severe aberrant TDP-43 immunoreactivity in AD brain (Arai et al., 2009; Hu et al., 2008). All of our samples had abnormal TDP-43 immunoreactivity in the amygdala and therefore this region was chosen for the analysis of tau protein.

The same set of AD, control and FTDP-17 samples that were used for RNA extraction and tau 4R/3R analysis were used for protein analysis. Samples were homogenised and subjected to a low speed centrifugation (12000 ×g) and the supernatant containing both soluble and insoluble tau (Greenberg and Davies, 1990) was collected. For the extraction of insoluble tau, 1% sarkosyl was added to

supernatant from the low speed centrifugation and then the samples were centrifuged at 100,000 ×g. The resulting pellet contains detergent insoluble tau and was solubilised with 8M guanidine.

Isoforms of tau in brain exist in multiple phosphorylation states. Insoluble tau deposited in AD was found to differ from soluble tau by increased phosphorylation resulting in a reduction of the electrophoretic mobility of tau on western blots (Hanger et al., 1991). Lambda protein phosphatase is widely used for tau dephosphorylation in brain and releases phosphate groups from phosphorylated serine, tyrosine and threonine residues in protein. The low speed centrifugation fraction and guanidine solubilised tau were dephosphorylated with lambda phosphatase (Material and Methods).

To test if the subgroup of high 4R tau expressors found at the RNA level were also found at the protein level, low speed centrifugation fraction from the amygdala were analysed by western blotting using a C-terminal antibody that recognises all isoforms of tau (DAKO). ADTDP-, ADTDP+, FTDP-17 and control brains were analysed. Membranes were also incubated in GAPDH antibody and this was used for a loading control.

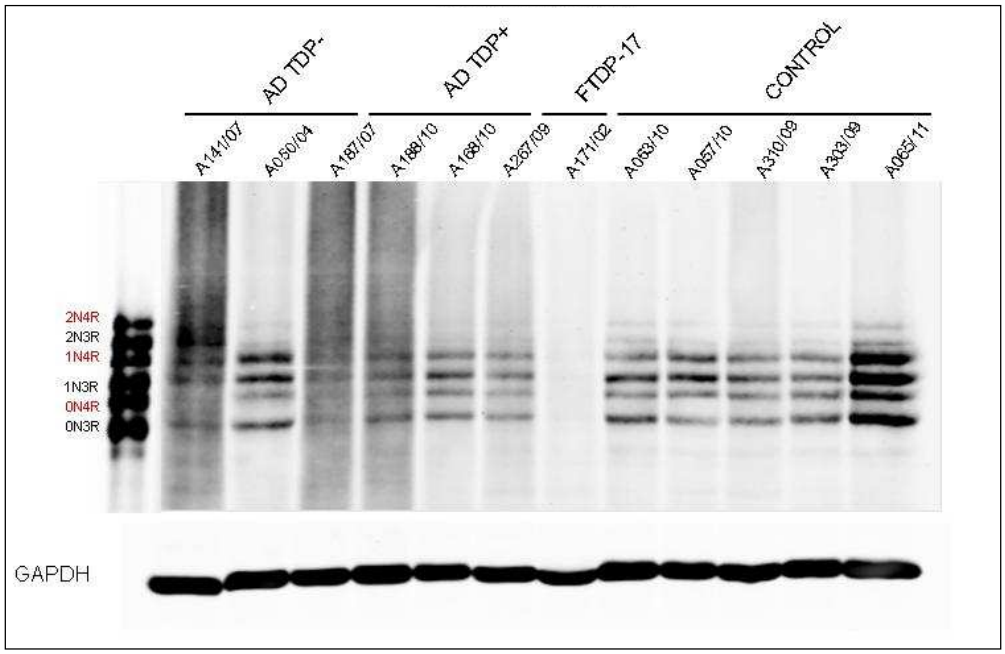

Figure 3.17. (and Figures 3.18 and 3.19) Tau protein isoform expression in the amygdala.
0.2g of brain from the amygdala from each brain was homogenised. Samples were subjected to a low speed centrifugation and dephosphorylated with lambda phosphatase. 15µg of protein were separated on 10% (w/v) SDS-PAGE gels. Proteins were transferred to nitrocellulose membranes and incubated in C-terminal, isoform independent antibody (DAKO). The membrane was also incubated with GAPDH antibody for normalisation.

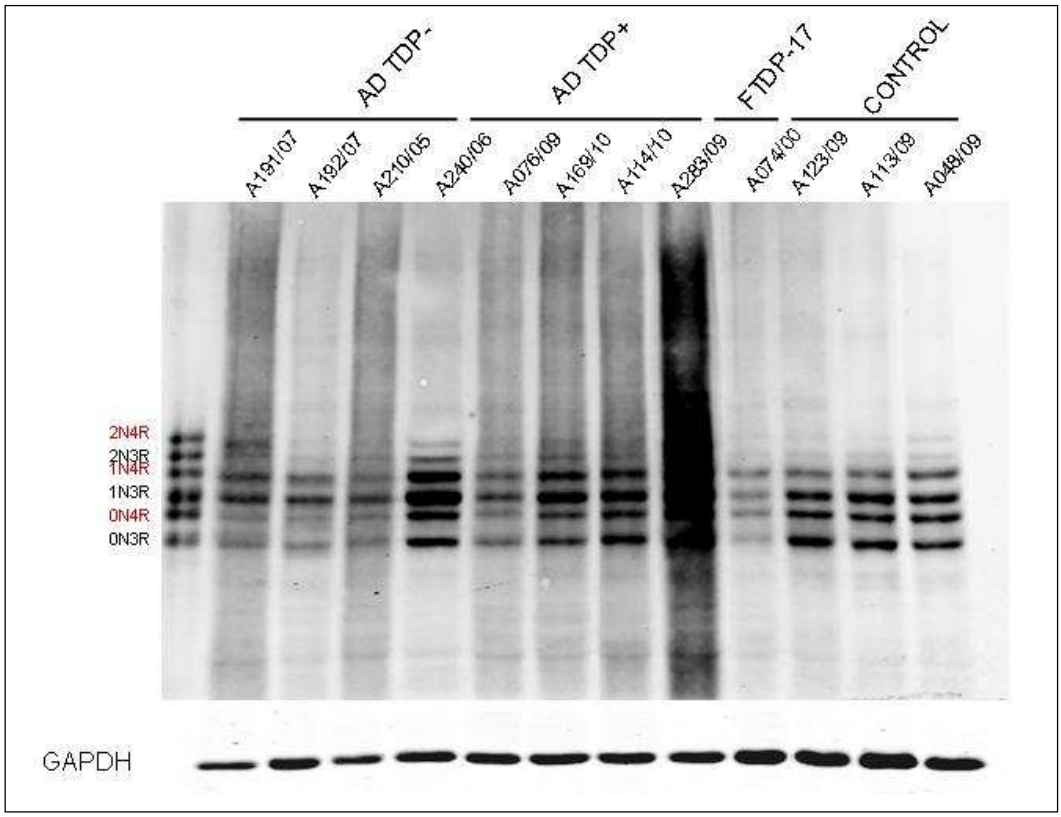

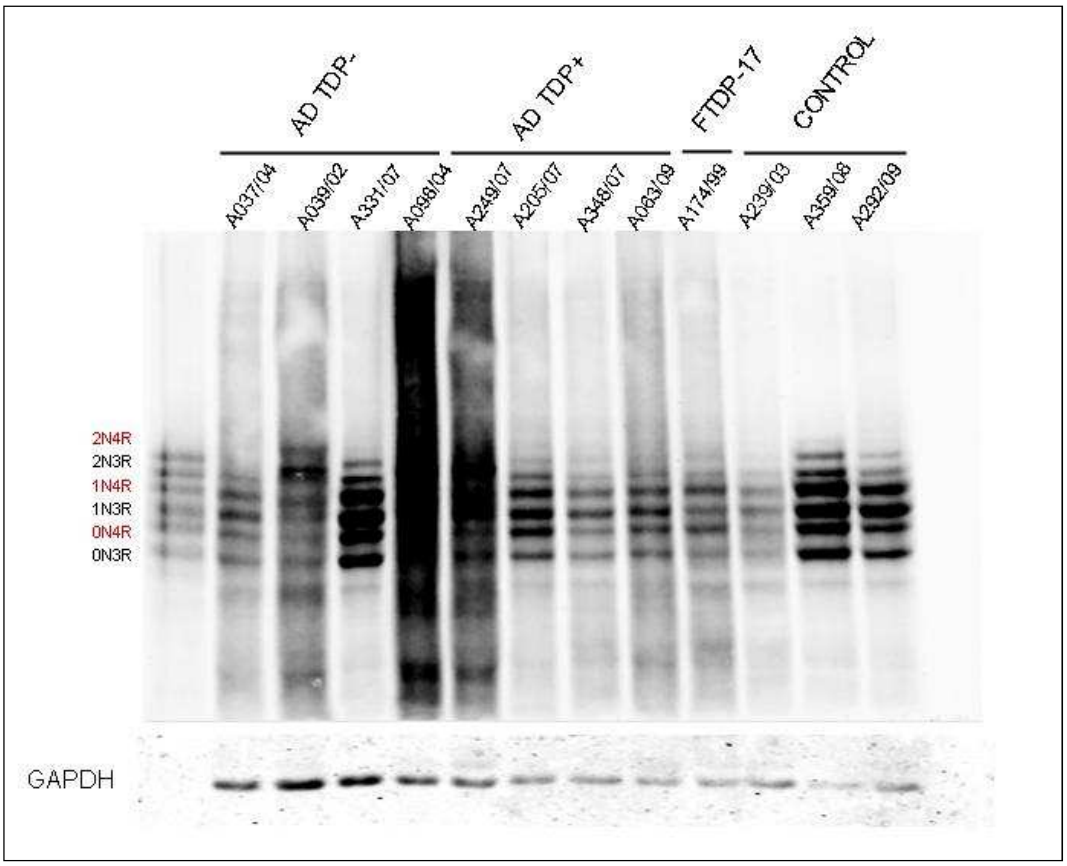

Figures 3.18. and 3.19. See legend for Fig. 3.17 above.

Tau immunoreactivity was detected and quantified by using the Odyssey Infrared Imaging System and the Odyssey software. Each tau isoform was quantified, a 4R/3R ratio was calculated and each data point was plotted against group (Fig. 3.20). A one-way ANOVA comparing 4R/3R ratio between control ADTDP-, ADTDP+ and FTDP-17 was performed on the data and was highly significant ($p \leq 0.0001$). Group comparisons were analysed by t-tests.

Similar to the results seen at the RNA level in the amygdala, two of the FTDP-17 data points clearly show increased tau protein 4R/3R ratios, but a FTDP-17 case with a 4R/3R RNA ratio (sample A171/02) within the control range also has a control range protein 4R/3R ratio. The FTDP-17 brains had an average total tau protein 4R/3R ratio of 1.3 (when all three 4R/3R ratios were included) compared to control 4R/3R ratio average of 0.7. The ADTDP- group had a 4R/3R ratio average for total tau protein of 0.62 and the ADTDP+ 4R/3R ratio average was 0.66. A t-test analysis showed that the 4R/3R tau protein ratio from control samples and both AD groups were not significantly different. There were no differences in total tau protein 4R/3R ratios between ADTDP- and ADTDP+ groups.

These results show that control and AD group brains do not show differences in 4R/3R tau protein ratios. This suggests that altered TDP-43 post-transcriptional processing in ADTDP- samples does not alter tau protein levels in the amygdala.

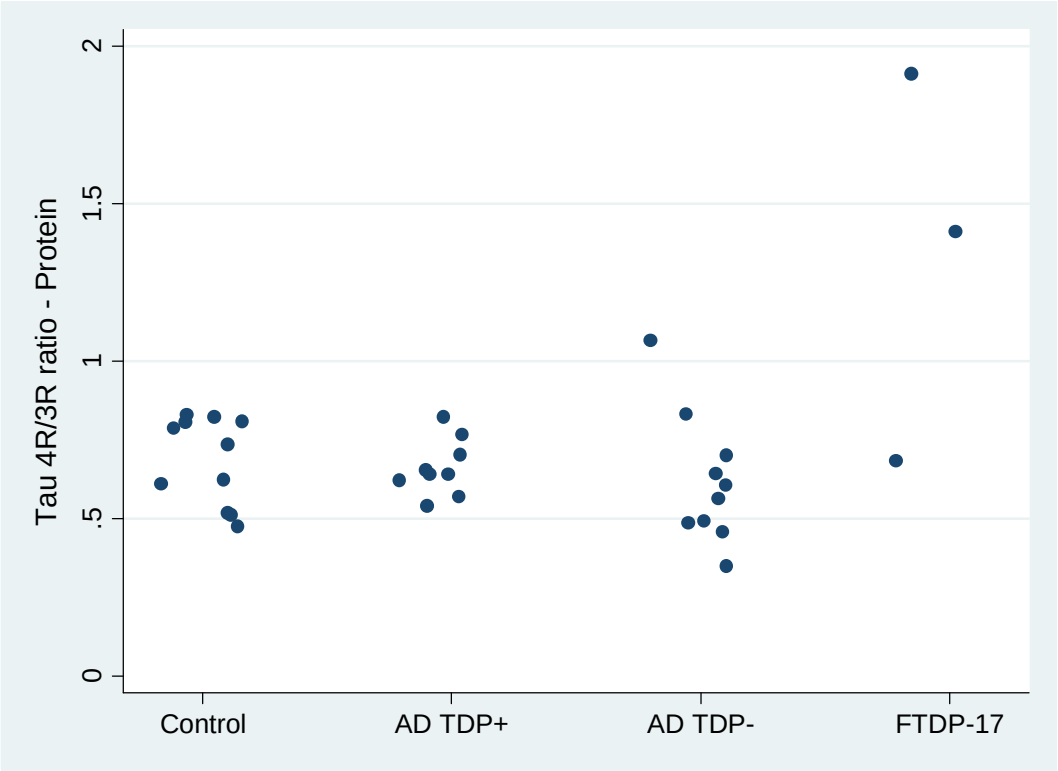

Figure 3.20. Tau 4R/3R ratio in low speed centrifugation fraction from the amygdala.
Tau 4R and 3R bands were quantified and normalised to GAPDH from western blots (Figures 3.16, 3.17 and 3.18). A 4R/3R tau protein ratio was calculated and plotted against group.

3.16. Tau protein and RNA 4R/3R correlation

A sub-group of AD cases showed increases of 4R tau transcripts compared to control, there were however, no differences found in tau 4R/3R ratios in the AD group compared to control at the protein level.

Altered tau 4R/3R ratios have been shown at the protein level in various tauopathies (for reviews and references therein see (Ballatore et al., 2007; Hernández and Avila, 2007)) but few studies have correlated *MAPT* RNA and protein levels in disease (Luk et al., 2010). In order to determine the relationship between *MAPT* RNA and protein isoform ratio in control and AD brains, a correlation analysis was performed

on 4R/3R ratio data from RNA and protein measures from the amygdala. The correlation analysis was performed for control samples and a separate analysis for the combined AD groups. No significant correlation between tau protein from the low speed centrifugation and tau RNA was found in the combined AD groups or controls in our samples from the amygdala. A trend line in the combined AD groups shows that there is a broad relationship between increasing gene expression and increasing protein levels, whereas the trendline in controls suggests a decreasing or flat trend (Fig. 3.21).

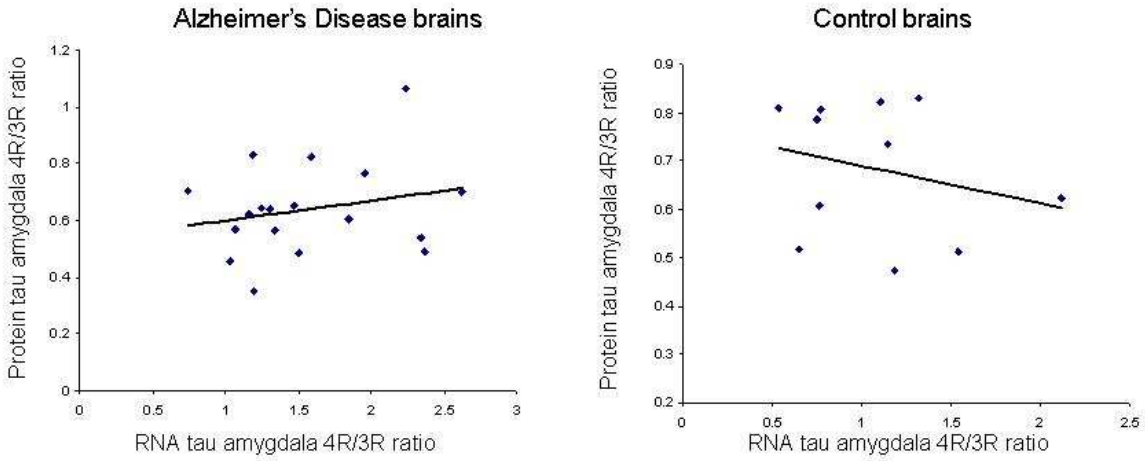

Figure 3.21. Tau protein RNA 4R/3R ratio correlation in AD and control brain. Tau RNA 4R/3R data for the amygdala was correlated with low speed fraction tau protein 4R/3R ratio data in control brains (n = 12) and combined AD brains (n = 18). No significant correlation was found.

3.17. Insoluble tau in control, AD and FTDP-17 brain

PHFs found in NFTs and neuritic plaques are composed of detergent-insoluble highly phosphorylated tau. Insoluble tau extracted and dephosphorylated from tauopathy brains show distinctive patterns characteristic of each tauopathy. For

example dephosphorylated insoluble tau from AD brains show all six tau isoforms (Hanger et al., 2002; Umeda et al., 2004) and CBD and PSP brains show a predominance of 4R over 3R (de Silva et al., 2003; Hanger et al., 2002; Liu et al., 2001; Takahashi et al., 2002).

In the previous section, 4R/3R protein ratios from the low speed fraction were not increased in AD brains compared to control and the total tau protein 4R/3R ratio did not correlate with RNA 4R/3R ratio in control or AD brains in the amygdala. The research question is firstly does TDP-43 misregulation alter tau insoluble tau ratios and secondly what is the relationship between tau 4R/3R insoluble protein and 4R/3R RNA ratios in ADTDP- and ADTDP+ brain.

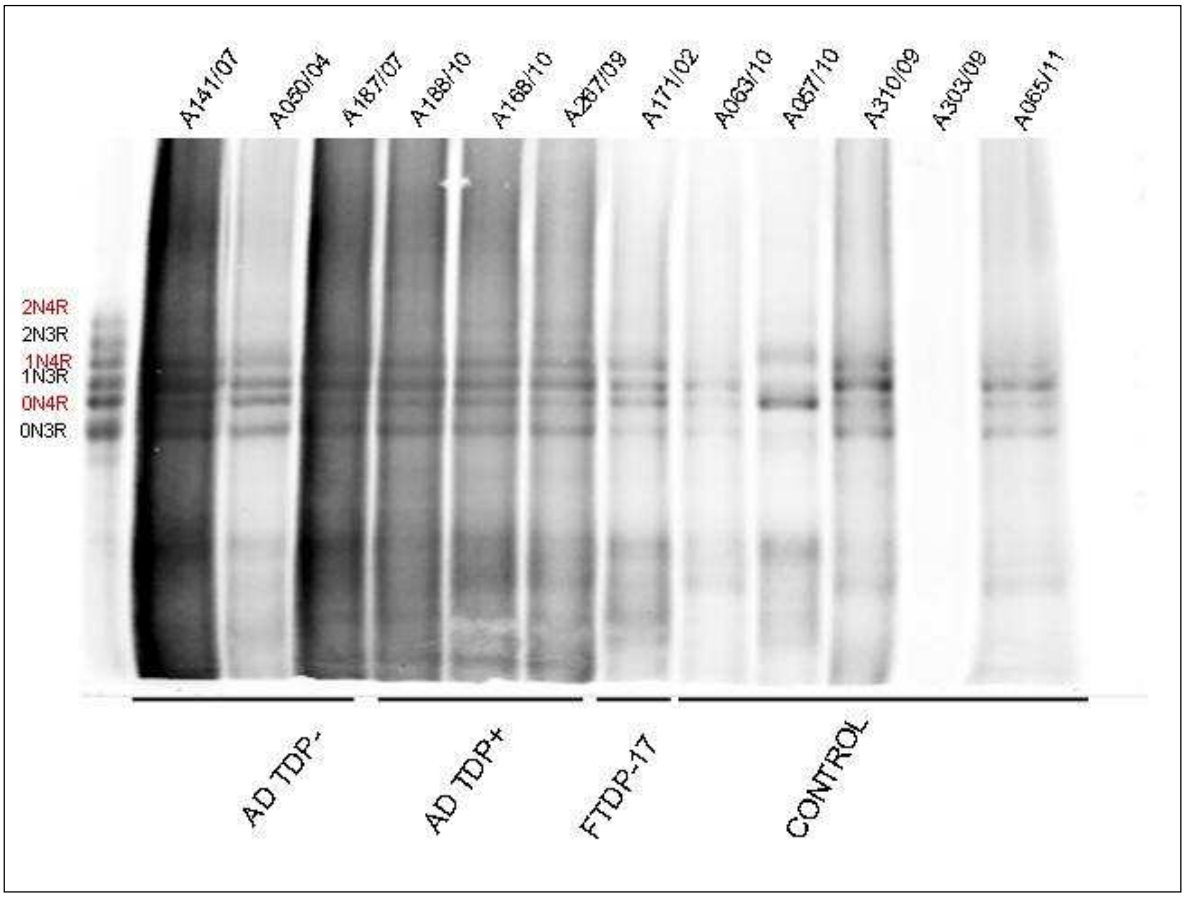

Figure 3.22. (and Figures 3.23 and 3.24) Isoform composition of insoluble tau extracted the amygdala.
To enrich the PHF content, supernatants from the low speed centrifugation were treated with 1% (v/v) sarkosyl and subjected to high speed centrifugation. The resulting pellet was washed with 1% (v/v) sarkosyl and denatured with 8M guanidine. Insoluble tau in guanidine was dialysed and dephsphorylated with lambda phosphatase. Proteins were separated on 10% (w/v) SDS PAGE and transferred to membranes. Membranes were probed with C-terminal antibody (DAKO).

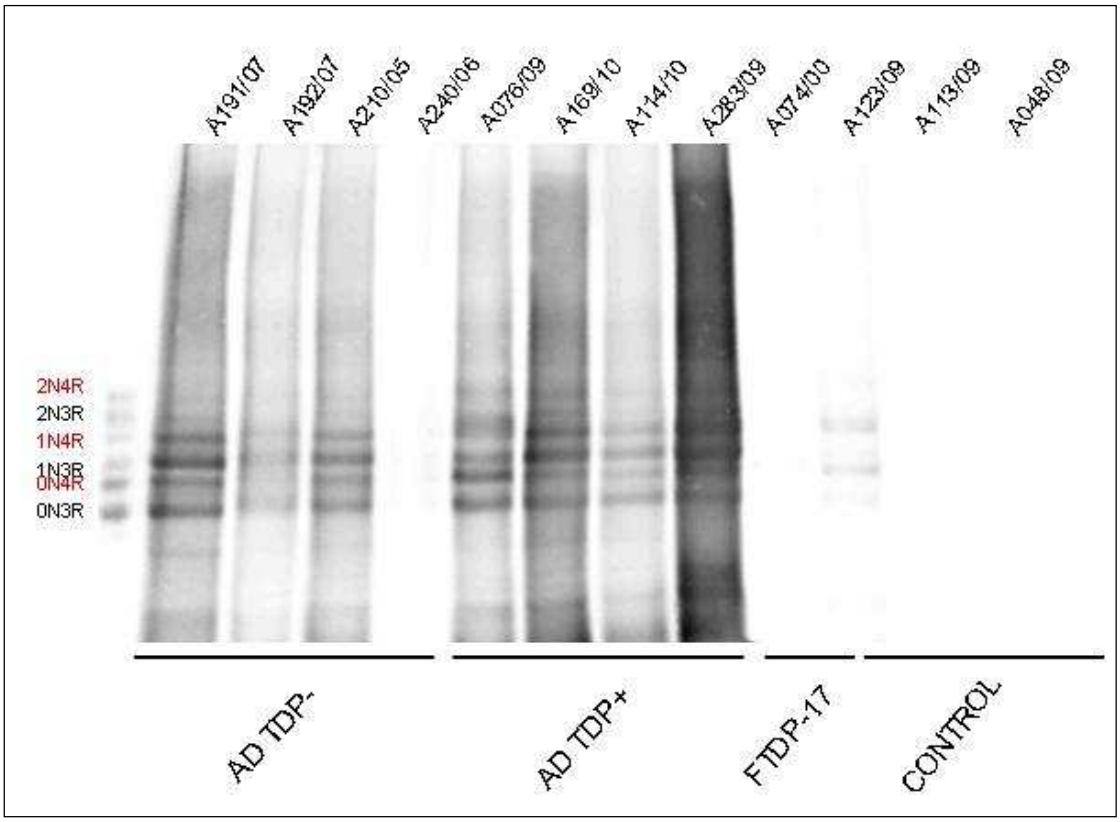

Figure 3.23. See the legend for Fig. 3.22

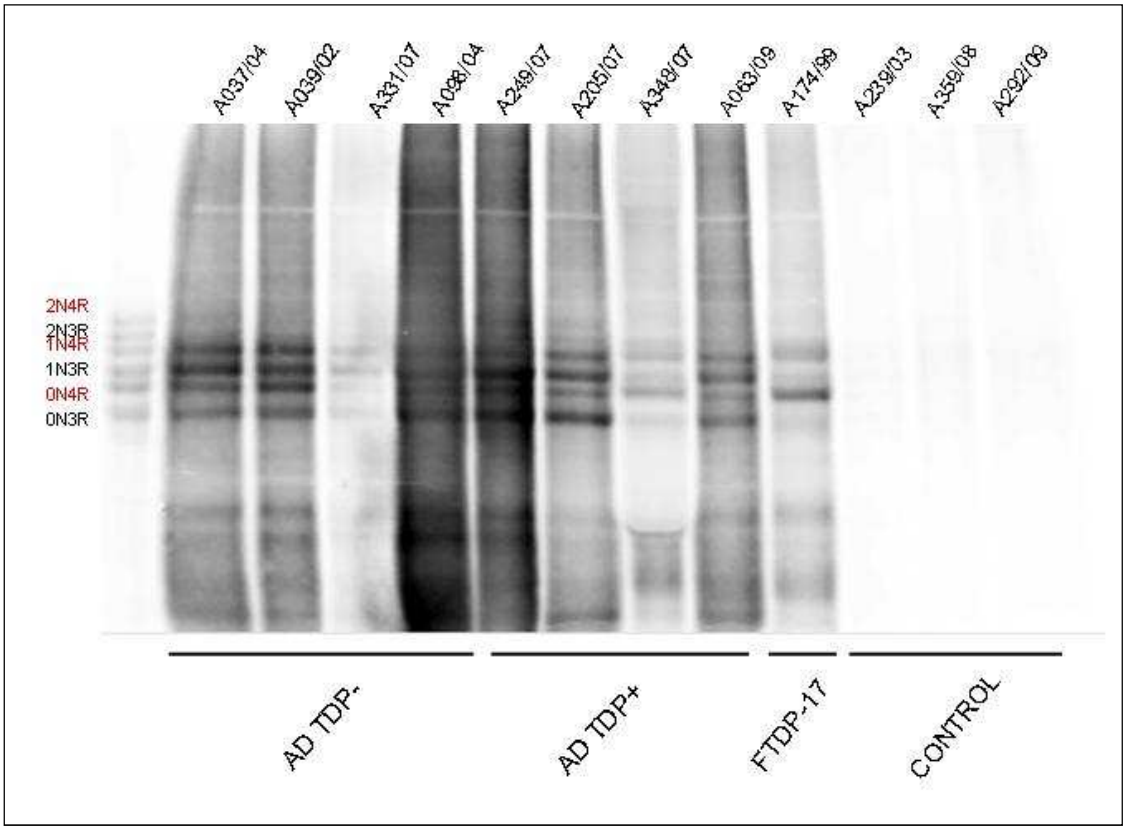

Figure 3.24. See the legend for Fig. 3.22.

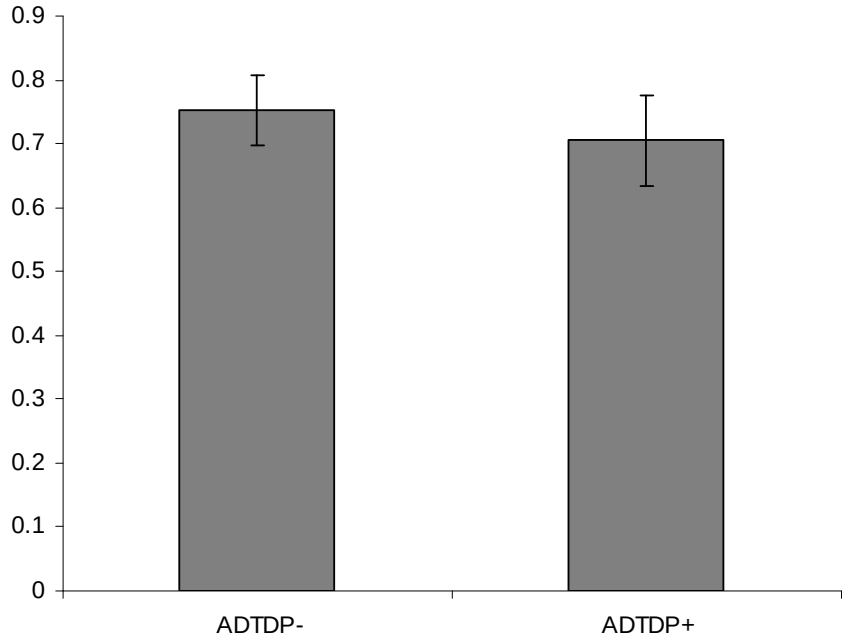

Figure 3.25. Tau 4R/3R ratio from sarkosyl insoluble fraction in the amygdala. Insoluble tau 4R/3R ratios from AD TDP- (n = 11) and AD TDP+ (n = 9) were calculated from western blots (figures 3.22, 3.23 and 3.24) and plotted. A t-test preformed on the data showed there were no significant differences between the groups.

Insoluble tau was isolated from control and AD brains from the amygdala using a previously published protocol with some modifications (Liu et al., 2001), as detailed in Materials and Methods. 4R and 3R tau isoforms were quantified in control, FTDP-17, ADTDP- and ADTDP+ brain samples and 4R/3R tau ratios were calculated.

Normally a 4R/3R ratio of case versus control is reported, however in this analysis control insoluble tau 4R/3R ratio is not a meaningful comparator because insoluble tau in control brain is extremely variable with none in some cases and very high 4R/3R ratios in others. The control samples that had sarkosyl insoluble tau staining (A063/10, A057/10, A310/09, A065/11 in Figure 3.22 and A123/09 in Figure 3.23) shows that these brains had NFT pathology in the amygdala and this was confirmed neuropathologically. Neuropathological reports state that these control cases had tau

pathology present in the amygdala and hippocampus corresponding to normal aging Braak stage 2.

The sarkosyl insoluble 4R/3R average for ADTDP- brains was 0.75 and the ADTDP+ average was 0.71. A t-test performed on the data showed there were no differences in 4R/3R sarkosyl insoluble tau ratios between the AD brains measured (Figure 3.23).

Two FTDP-17 samples had measurable sarkosyl insoluble tau 4R/3R ratios samples A171/02, (Figure 3.22) and A174/99 (Figure 3.24), sample A074/00 had tau protein concentration too low to detect (Figure 3.23). Sample A171/02 was the FTLD-17 brain that had a control range 4R/3R ratio at the RNA level and in the low speed centrifugation protein sample. This sample had a tau sarkosyl insoluble 4R/3R ratio of 1.17. The other FTDP-17 sample, A174/99, had a tau sarkosyl insoluble tau 4R/3R ratio of 16.9.

In section 3.19, a semi-quantitative immunohistological analysis of tau pathology from these brains is presented. The control brains that show the presence of sarkosyl insoluble tau in the amygdala by western blotting, also show tau pathology positive scores in the immunohistology analysis and the correlation between these two methods give a good indication of the validity of the semi-quantitative scoring method.

3.18. Sarkosyl insoluble tau and RNA 4R/3R correlation

Tau RNA 4R/3R ratios from the amygdala were correlated with sarkosyl insoluble tau protein 4R/3R from the amygdala to test if expression of 4R tau RNA isoforms in AD brains have a relationship with deposition of 4R tau protein into pathological inclusions. Since no differences were found in sarkosyl insoluble tau 4R/3R ratios between ADTDP- and ADTDP+ brains, these groups were combined. A significant positive correlation was found between 4R/3R insoluble tau ratio and 4R/3R RNA tau ratio ($p = 0.003$; $n = 20$) showing that increases in 4R/3R RNA ratio are associated with increases in insoluble tau 4R/3R ratio (Figure 3.26). These results suggest that the subgroup of high 4R RNA expressors also show high insoluble tau suggesting that in a subset of AD brains, increases in 4R RNA translate into increases of 4R tau protein sequestered into insoluble tau deposits in the amygdala.

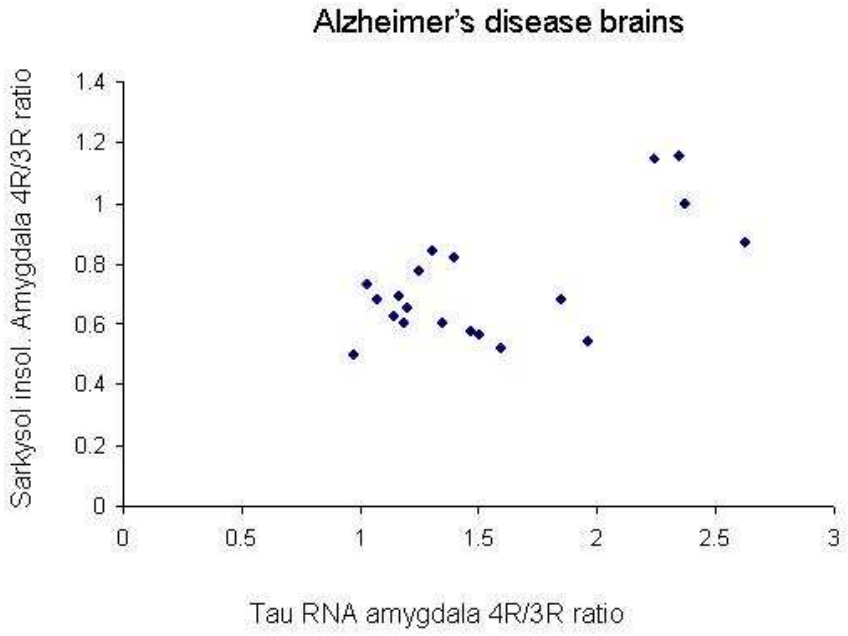

Figure 3.26. Tau RNA 4R/3R ratios correlate with sarkosyl insoluble tau 4R/3R ratios.

3.19. Immunohistochemical analysis of tau pathology in AD brains

The hippocampus and entorhinal cortex are brain regions that are vulnerable to tau pathology in AD brain and usually show very high TDP inclusion counts in TDP-43 positive AD brains (Hu et al., 2008). This is a different TDP-43 inclusion distribution to that generally seen in FTLD and ALS (Arai et al., 2009; Higashi et al., 2007; Hu et al., 2008; King et al., 2010; Lippa et al., 2009). The distribution of TDP-43 pathology in FTLD is predominantly in the frontal and temporal cortices while ALS shows TDP-43 inclusions predominantly in lower motor neuron nuclei and spinal cord (Geser et al., 2009b). It has been suggested that TDP-43 pathology in AD progresses from limbic regions into the temporal and frontal cortex at later stages of the disease (Higashi et al., 2007; Hu et al., 2008; King et al., 2010), although some cases have very severe frontal and little limbic TDP pathology (Kadokura et al., 2009).

At present the relationship between tau and TDP-43 pathologies is not clear. Since tau pathology appears to start in the entorhinal cortex and progresses to the hippocampus via synaptic connections, it may be that these neurons which are selectively vulnerable to tau pathology trigger TDP-43 pathology in a sub-group of TDP positive AD brains. This raises the question: do a sub-group of TDP positive AD brains have a pattern of tau pathology that is different to that in ADTDP negative brains?

The cases we had previously analysed for tau splicing and protein 4R/3R ratios were assessed for severity of tau pathology by examining brain sections on slides that had previously been prepared for routine diagnostic examination. The presence and

extent of tau AT8 immunoreactivity was semi-quantitiatively measured on all brain sections that were available. AT8 recognises a phospho-epitope at serine 202 and threonine 205 which are specifically phosphorylated in late stage NFTs (Augustinack et al., 2002). AT8 immunoreactivity in control and AD cases was measured in frontal, temporal, amygdala and hippocampus with a semi-quantitative scale of 0-3 with 0 = no pathology, 1 = rare or mild, 2 = moderate, 3 = severe (Table 3.5). Tau pathology types included tangles, threads, neurites, neuritic plaques and glial inclusions and a global AT8 immunoreactivity score (overall tau). A scoring of the amount of neuronal loss by hematoxylin and eosin stain (H&E) occurring predominantly in cortical layers 3 and 5 was also assessed. On the same set of slides, TDP-43 pathology status was confirmed. For this purpose, brain sections were stained with a phospho-TDP-43 serines 409/410 antibody that specifically detects ubiquitin-positive TDP-43 in inclusions and does not detect non-aggregated nuclear TDP-43.

FRONTAL	NEURON LOSS	OVERALL TAU	TANGLES	THREADS	NEURITES	NEURITIC PLAQUES	GLIAL INCLUSION
Control 0	10	13	13	13	13	13	13
Control 1	2	0	0	0	0	0	0
Control 2	1	0	0	0	0	0	0
Control 3	0	0	0	0	0	0	0
Totals	13	13	13	13	13	13	13
AD+ 0	0	0	0	0	0	0	2
AD+ 1	3	0	0	0	0	0	8
AD+ 2	6	0	1	1	7	4	0
AD+ 3	2	11	10	10	4	7	0
Totals	11	11	11	11	11	11	10
AD- 0	2	0	0	0	0	1	5
AD- 1	7	3	3	4	4	7	8
AD- 2	5	7	4	6	8	3	0
AD- 3	0	4	7	3	1	3	0
Totals	14	14	14	13	13	14	13

Table 3.5. Frequencies of semi-quantitative scores of tau AT8 immunoreactivity in ADTDP+, ADTDP- and control brains.

TEMPORAL	NEURON LOSS	OVERALL TAU	TANGLES	THREADS	NEURITES	NEURITIC PLAQUES	GLIAL INCLUSION
Control 0	11	12	13	13	13	13	13
Control 1	1	1	0	0	0	0	0
Control 2	1	0	0	0	0	0	0
Control 3	0	0	0	0	0	0	0
Totals	13	13	13	13	13	13	13
AD+ 0	0	0	0	0	0	0	0
AD+ 1	1	0	0	0	0	0	11
AD+ 2	5	0	2	0	2	1	0
AD+ 3	5	11	9	11	9	10	0
Totals	11	11	11	11	11	11	11
AD- 0	0	0	0	0	0	0	2
AD- 1	4	1	0	1	0	2	12
AD- 2	4	6	4	5	8	5	0
AD- 3	6	7	10	8	6	7	0
Totals	14	14	14	14	14	14	14

Table 3.5. Frequencies of semi-quantitative scores of tau AT8 immunoreactivity in ADTDP+, ADTDP- and control brains.

AMYGDALA	NEURON LOSS	OVERALL TAU	TANGLES	THREADS	NEURITES	NEURITIC PLAQUES	GLIAL INCLUSION
Control 0	5	4	3	3	4	10	12
Control 1	6	4	6	4	8	2	0
Control 2	1	4	3	5	0	0	0
Control 3	0	0	0	0	0	0	0
Totals	12	12	12	12	12	12	12
AD+ 0	0	0	0	0	0	0	2
AD+ 1	0	0	0	0	1	2	7
AD+ 2	7	0	1	0	3	4	1
AD+ 3	4	11	10	11	7	5	0
Totals	11	11	11	11	11	11	10
AD- 0	0	0	0	0	0	0	2
AD- 1	3	0	1	0	2	4	5
AD- 2	1	3	2	1	2	0	1
AD- 3	4	5	5	7	4	4	0
Totals	8	8	8	8	8	8	8

Table 3.5. Frequencies of semi-quantitative scores of tau AT8 immunoreactivity in ADTDP+, ADTDP- and control brains.

HIPPOCAMP	NEURON LOSS	OVERALL TAU	TANGLES	THREADS	NEURITES	NEURITIC PLAQUES	GLIAL INCLUSION
Control 0	5	3	3	4	4	12	12
Control 1	5	4	4	3	5	1	1
Control 2	3	3	1	2	4	0	0
Control 3	0	3	5	4	0	0	0
Totals	13	13	13	13	13	13	13
AD+ 0	0	0	0	0	0	0	0
AD+ 1	0	0	0	0	0	1	10
AD+ 2	1	0	0	0	1	4	0
AD+ 3	10	11	11	11	10	6	0
Totals	11	11	11	11	11	11	10
AD- 0	0	0	0	0	0	2	2
AD- 1	0	0	0	1	0	6	12
AD- 2	1	2	0	5	6	4	0
AD- 3	13	12	14	8	8	2	0
Totals	14	14	14	14	14	14	14

Table 3.5. Frequencies of semi-quantitative scores of tau AT8 immunoreactivity in ADTDP+, ADTDP- and control brains.

Differences in the severity of tau pathology between the ADTDP+ and ADTDP- groups were tested with Mann Whitney-U non- parametric tests. In this analysis (summarised in Table 3.5), ADTDP+ brains had significantly higher tau AT8 immunoreactivity in overall tau, threads, neurites and neuritic plaques compared to ADTDP- brains in the frontal cortex. ADTDP+ brains also had significantly higher neuronal loss compared to ADTDP- brains in the frontal cortex. In the temporal cortex, ADTDP+ brains had higher tau immunoreactivity in overall tau compared to ADTDP- brains, with only borderline differences in threads and plaques. ADTDP+ brains had significantly higher neuritic plaque immunoreactivity compared to ADTDP- brains in the hippocampus and only borderline differences in threads. This analysis suggests that the severity of tau pathology, at least in the frontal and temoparl cortices of ADTDP+ brains, is significantly higher than that in ADTDP- brains. Because the tau count data is semi-quantitative, this analysis probably has significant ceiling effects and may well underestimate the comparative levels of tau immunoreactivity seen in some brains and hence the differences between the two AD groups may actually be higher in some of the brain regions. Since the prevalence of TDP-43 pathology may be associated with increased age, a t-test for age and AD group was performed and was not significant. This sample set is fairly small and may be underpowered to detect any differences (for information regarding age, post-mortem delay etc see Material and Methods.

AD+ AD-	FRONTAL	TEMPORAL	AMYGDALA	HIPPOCAMPUS
Neuronal loss	0.044*	0.609	0.717	0.936
Overall tau	0.002*	0.033*	0.177	0.574
Tangles	0.244	0.687	0.31	0.999
Threads	0.002*	0.075	0.657	0.075
Neurites	0.047*	0.107	0.545	0.166
Plaques	0.006*	0.075	0.657	0.011*
Glial	0.483	0.572	0.965	0.585

Table 3.6. Table of p values for semi-quantitative scoring of ADTDP+ and ADTDP-brain sections.

Tested with Mann Whitney-U. p values with * are significant.

3.20. Regression analysis of tau sarkosyl insoluble 4R/3R ratio and semi-quantitative tau pathology

Previously a correlation between sarkosyl-insoluble tau 4R/3R ratios and tau RNA 4R/3R ratio was demonstrated (Figure 3.26). Linear regression was used to test if the tau sarkosyl insoluble 4R/3R ratio was an accurate predictor of tau immunoreactivity score for all of the semi-quantitative tau measurements in the amygdala. For this analysis the lowest score category was considered as the baseline (where there were low frequencies in a category, it was combined with an adjacent category). None of the 4R/3R ratios in sarkosyl insoluble predicted tau immunoreactivity count material for any tau parameter. Linear regression was used to test if the 4R/3R ratios from low speed total tau protein were predictors of tau immunoreactivity score and we found no evidence that tau scores were associated with total tau protein levels.

3.21.Summary

In this section we found altered splicing levels of exon 10 in a subset of AD cases.

- Tau 4R/3R RNA ratios in the frontal cortex, amygdala, hippocampus and cerebellum were significantly increased in AD brains compared to control. A subset of ~5 AD cases showed consistently high tau 4R transcript expression across all brain regions tested.
- Tau 4R/3R RNA expression was significantly associated with 4R/3R tau ratio from insoluble material in the amygdala. This shows that the subgroup of high 4R transcript expressors also have high levels of 4R tau in insoluble deposits.
- The increases in 4R transcript expression in the subgroup of AD cases were not due to misregulation by TDP-43 or tau haplotype. The subset of high 4R transcript expressors were from both ADTDP- and ADTDP+ groups and no significant differences were found between the AD groups for tau 4R/3R ratios. H1 homozygotes showed tau 4R/3R ratios not significantly different from a combined group of H2 homogygotes and H1/H2 heterozygotes.
- There were no significant differences in total tau RNA expression between ADTDP-, ADTDP+ and control groups in any brain region. In addition, H1 homozygotes showed no significant differences in total tau expression compared to a combined group of H2 homogygotes and H1/H2 heterozygotes.
- In AD brains with aberrant TDP-43 immunoreactivity there was greater severity of tau pathology compared to AD brains without TDP-43 inclusions.

4R/3R RATIO	CONTROL	ADTDP-	ADTDP+	FTDP-17	DM1
Frontal	0.71 (0.19)	0.87* (0.18)	1.0* (0.29)	2.8* (0.28)	0.73
Temporal	0.9 (0.24)	1.1 (0.44)	1.1 (0.38)	3.2* (0.38)	0.69
Amygdala	1.1 (0.42)	1.5* (0.58)	1.5* (0.51)	4.0* (2.7)	0.86
Hippocampus	0.9 (0.24)	1.3* (0.35)	1.4* (0.55)	4.2* (0.39)	1.4
Cerebellum	1.2 (0.38)	1.8* (0.59)	1.8* (0.57)	3.9* (1.8)	1.9

Table 3.7. 4R/3R ratio in disease groups and control.
Values with * indicate significant increases in 4R tau compared to control. Numbers in brackets are standard deviation.

Chapter 4: APP expression and splicing in affected brain regions in Alzheimer's disease.

There are three main isoforms of APP expressed in the CNS derived from the alternative splicing of exons 7 and 8. APP770 contains both exons 7 and 8, APP751 contains exon 7 and APP695 contains neither exon 7 nor 8. The APP695 isoform is the major neuronal species. The APP770 and APP751 isoforms contain a Kunitz family of protease inhibitors domain (KPI) domain in exon 7 and increased levels of KPI containing APP RNA isoforms have been found in AD brains and suggest that mis-regulation of alternative splicing of APP may contribute to AD.

Mis-regulation of TDP-43 in TDP-proteinopathies may alter levels and/or splicing either directly for specific TDP-43 targets or indirectly by altering levels and/or splicing of multiple RBP and transcription factors. RT-PCR was performed in control, ADTDP- and ADTDP+ human brain samples from five brain regions with primers spanning APP exons 7 and 8 in order to test an association between misregulation of TDP-43 and altered splicing of APP. An IR-labelled forward primer was used in this analysis to improve the accuracy of quantification.

Trisomy of the chromosome 21 where APP is located results in DS and AD pathology and suggests that increased levels of APP expression are associated with AD pathology. Levels of total APP RNA expression in five brain regions were quantified by qRT-PCR.

In order to determine if changes in alternative splicing in tau correlate with alternative splicing in APP a correlation between APP exons 7 and 8 and tau exon 10 expression in AD and control brains was performed.

4.1. Determination of PCR cycling parameters for APP primers in human brain

For the detection of APP isoforms arising from alternative splicing of exons 7 and 8, a APP primer pair from previously published work was used (Golde et al., 1990). The forward primer binds a sequence on exon 6 and the reverse primer binds to a sequence on exon 9. cDNA from human frontal cortex and HeLa cells were amplified with the APP 6-9 primer pair. PCR products were run on 1.5% agarose gels and three PCR products were detected and sequenced. The 313 bp product contains exons 7 and 8 and corresponds to APP770, the 256bp product has only exon 7 and corresponds to APP751 and the 88bp product has neither exons 7 or 8 and corresponds to APP695 (Figure 4.1). A DY 682 tag was added to the 5' end of the forward primer to improve the accuracy of quantification. The linear range of the APP 6-9 primer pair was determined as for tau and the final number of cycles used was 30.

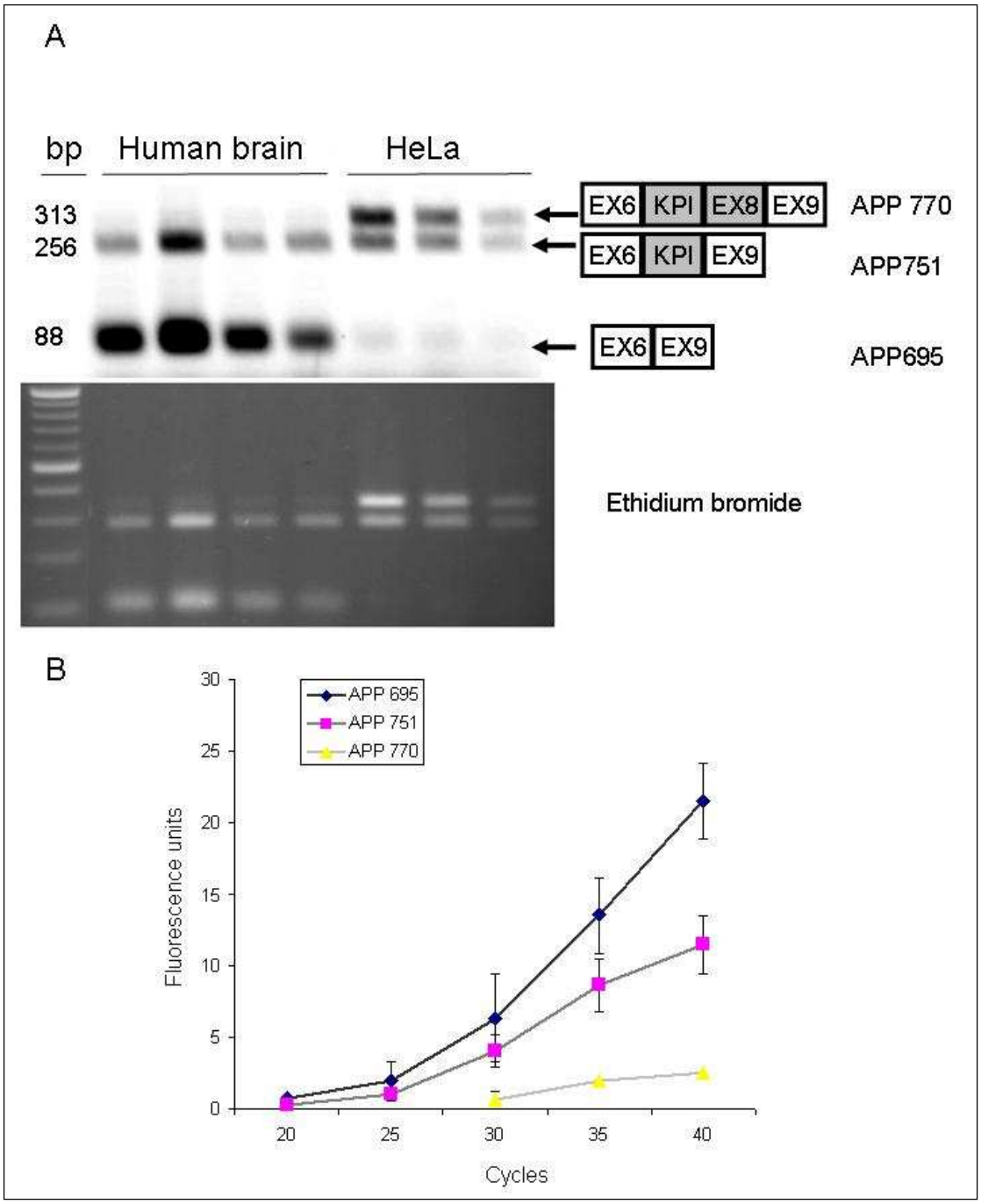

Figure 4.1. Determination of APP primer linear phase. A. IR- labelled APP primers were tested with cDNA from human brain and HeLa cells. PCR products of 88bp correspond to APP695, products of 256bp correspond to APP751 and products of 313 bp correspond to APP770. B. cDNA from quadruplicate samples were analysed by PCR at different number of cycles (25, 30, 35, 40) and PCR products were quantified and plotted to determine linear and plateau stages.

4.2. APP isoform expression in frontal cortex

cDNA from control, ADTDP- and ADTDP+ brain samples from the five brain regions (frontal and temporal cortex, amygdala, hippocampus and cerebellum) used for the tau splicing analysis were also used for APP splicing analysis. RNA extracted from all brain samples had previously been tested for a RIN above 3.6. cDNA from frontal cortex was amplified with the IR-labelled forward APP 6-9 primers and PCR products were run on 1.5% agarose gels. Three APP PCR products corresponding to APP695, APP751 and APP770 were quantified and percentage of each isoform was calculated (Figure 4.2).

In the frontal cortex the proportion of APP695 was around 60% for all conditions (Table 4.1). APP751 accounted for around 30% of total APP expression and APP770 was around 10% in all conditions. Statistical analysis was carried out by t-test comparing the percentage of each APP isoform by disease condition (control, ADTDP- and ADTDP+). No significant differences in expression for any of the APP isoforms was found in the frontal cortex.

FRONTAL AVE%	695	751	770
Control	56.2	33.4	10.4
ADTDP-	60.5	28.9	10.6
ADTDP+	56.3	30.8	12.9

Table 4.1. Percent average of APP isoforms in the frontal cortex

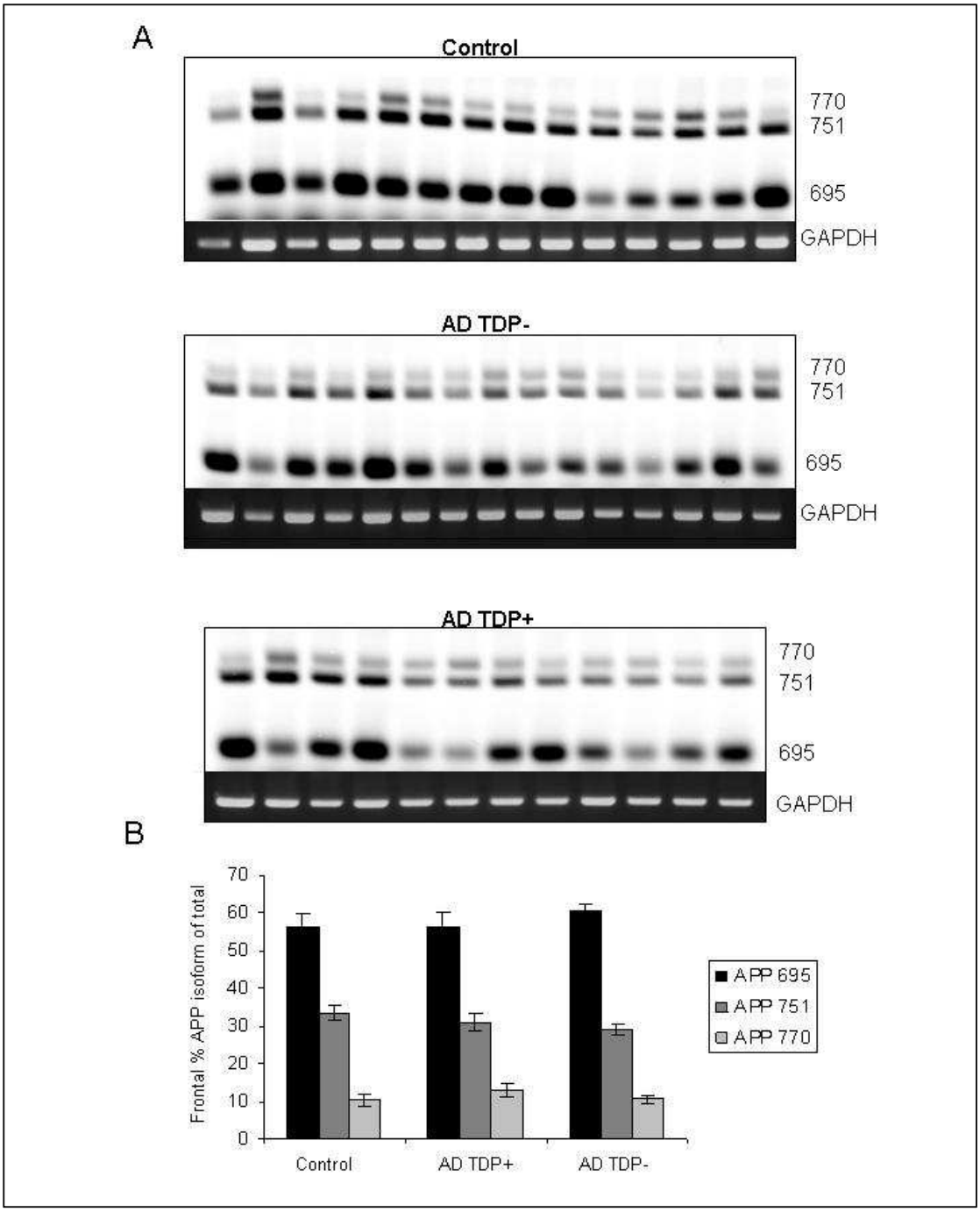

Figure 4.2. APP isoform expression in frontal cortex.
A.APP isoform ratios were assayed by RT-PCR with IR-labelled forward primer pair. B. Mean percentages for each APP isoform was calculated for each group ± SEM. Significance was set at p = 0.05. Significant differences shown in this graph are all case vs control.

4.3. APP isoform expression in the temporal cortex

In the temporal cortex, cDNA was analysed with the IR labelled forward APP 6-9 primers and PCR products were run on 1.5% agarose gels. Each APP isoform was quantified and a percent expression calculated (Figure 4.3 and Table 4.2). The proportions of APP isoform expression in the control temporal cortex were slightly different from that in the frontal cortex with the average percent APP 751 remaining at around 30% however there was an increase in APP770 to around 14% and a decrease in APP 695 to around 55% (Table 4.2).

In the ADTDP+ brains the APP695 percent proportion was reduced significantly compared to controls and there was a corresponding significant increase in APP751 compared to control ($p = 0.012$ and $p = 0.001$, respectively). In the ADTDP- brains there was a significant increase in APP751 isoforms compared to control ($p = 0.015$), and there was a trend for a decrease in APP695 however this was not significant. There were no differences between the two AD groups for any of the APP isoforms.

TEMPORAL AVE%	695	751	770
Control	54.7	31	14.3
ADTDP-	46.7	38.3*	15
ADTDP+	41.4*	42.4*	16.2

Table 4.2. Percent average APP isoforms in the temporal cortex.
Values with * were significantly different from control

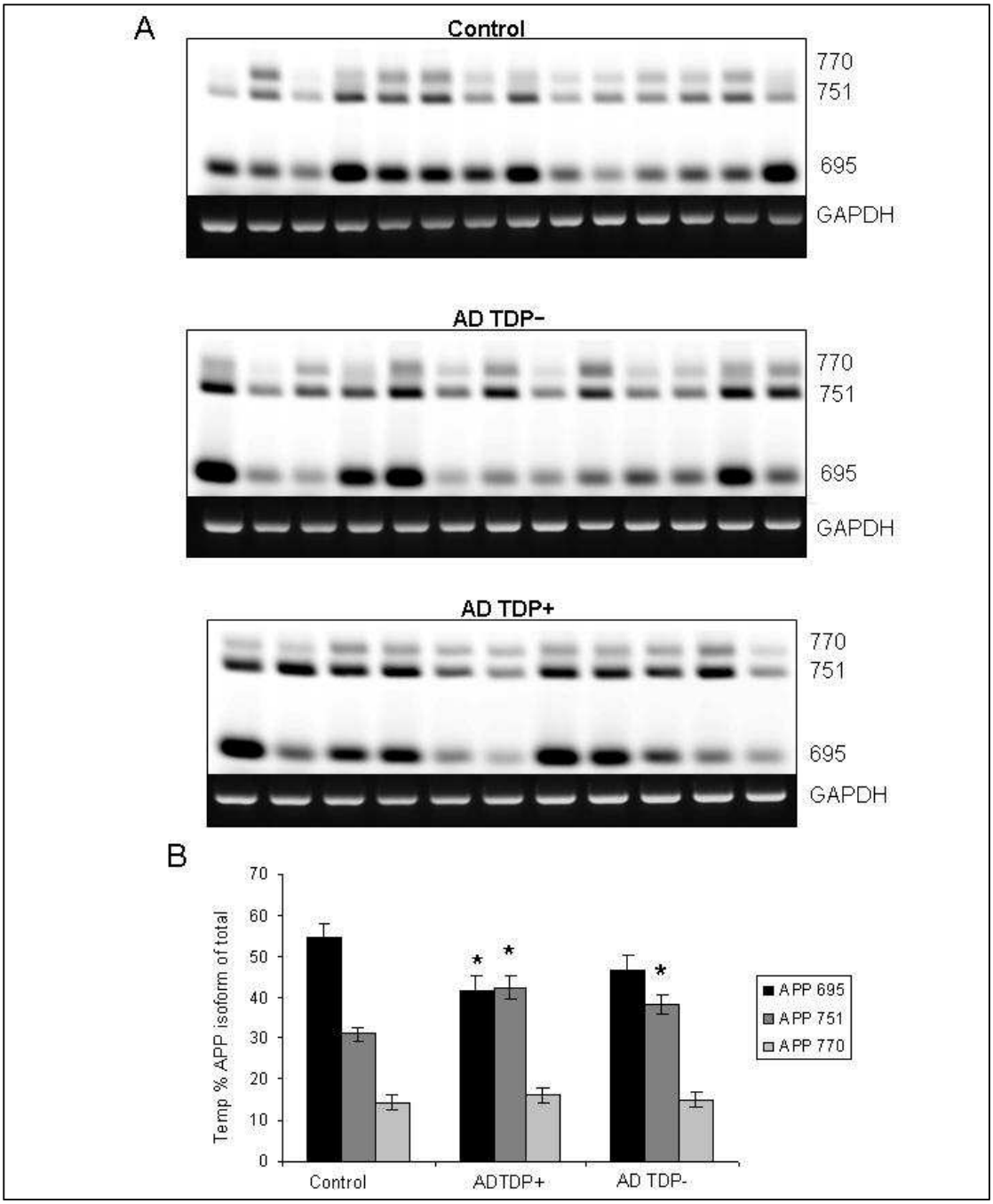

Figure 4.3. APP isoform expression in human temporal cortex.
A.APP isoform ratios were assayed by RT-PCR with IR-labelled forward primer pair. B. Mean percentages for each APP isoform was calculated for each group ± SEM. Significance was set at p = 0.05. Significant differences shown in this graph are all case vs control.

4.4. APP isoform expression in the amygdala

In the amygdala control brains show expression of the APP770 isoform at a much higher proportion compared to frontal cortex (15% in the amygdala compared to 10% in the frontal cortex). In addition APP695 only contributes around 41% as a proportion of total while the APP751 isoform is around 43% (Table 4.3).

In the ADTDP- brains there was a significant decrease in APP695 ($p = 0.044$) and a significant increase in APP751 in the ($p = 0.05$) compared to control. Even though there was an increase in the APP770 isoform expression in both ADTDP- and ADTDP+ brains this trend was not significant. For the ADTDP+ samples there was a trend for a decrease in APP695 and a trend for an increase in KPI containing APP isoforms however these differences were all not significant compared to control. There was also a borderline significant difference in APP751 expression between the ADTDP+ and ADTDP- brains ($p = 0.038$).

AMYGDALA AVE%	695	751	770
Control	41.4	43.6	15
ADTDP-	33.5*	49.4*	17.1
ADTDP+	39	43.1	17.9

Table 4.3. Percent average APP isoforms in the amygdala.
Values with * were significantly different from control

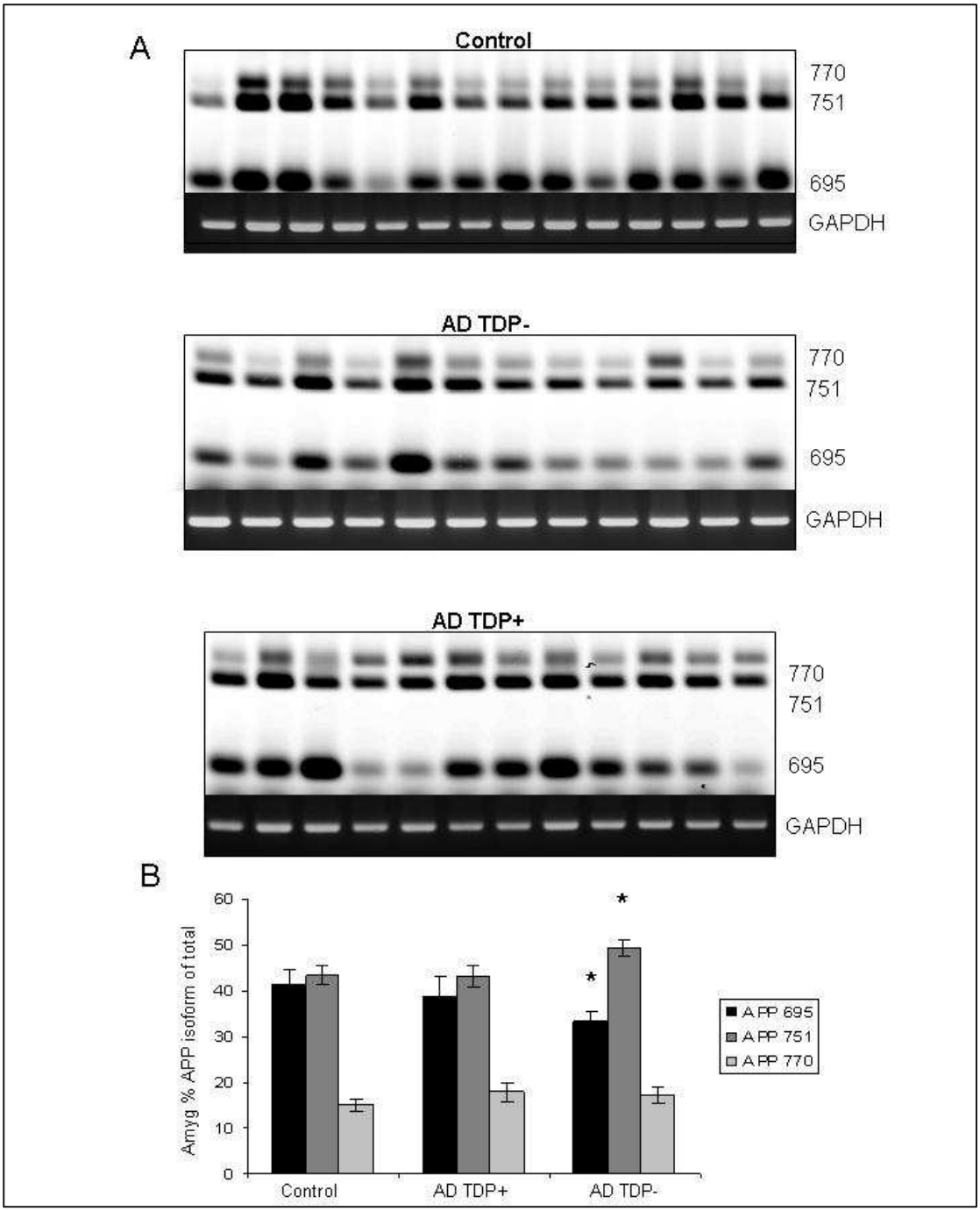

Figure 4.4. APP isoform expression in the human amygdala.
A.APP isoform ratios were assayed by RT-PCR with IR-labelled forward primer pair. B. Mean percentages for each APP isoform was calculated for each group ± SEM. Significance was set at p = 0.05. Significant differences shown in this graph are all case vs control.

4.5. APP isoform expression in the hippocampus

In control brains the proportions of APP695 isoform expression was around 50% while APP751 was around 37 percent and APP770 13% (Table 4.4).

Both ADTDP+ and ADTDP- brains showed significant decreases in APP 695 compared to controls ($p = 0.035$ and $p = 0.005$ respectively) and significant increases in APP751 compared to controls ($p = 0.024$ and $p = 0.021$ respectively) in the hippocampus. The decrease in APP695 isoform expression is clearly visible in the AD group brains (Figure 4.5) compared to control brains. APP770 was also significantly increased in ADTDP- brains compared to control ($p = 0.016$) and there was a trend for increased APP770 expression in ADTDP+ brains that was not significant. There were no differences between AD groups in any APP isoform expression.

HIPPOCAMPUS AVE%	695	751	770
Control	49.2	37.6	13.2
ADTDP-	35.8*	46*	18.2*
ADTDP+	38*	46.5*	15*

Table 4.4. Percent average APP isoforms in the hippocampus.
Values with * were significantly different from control

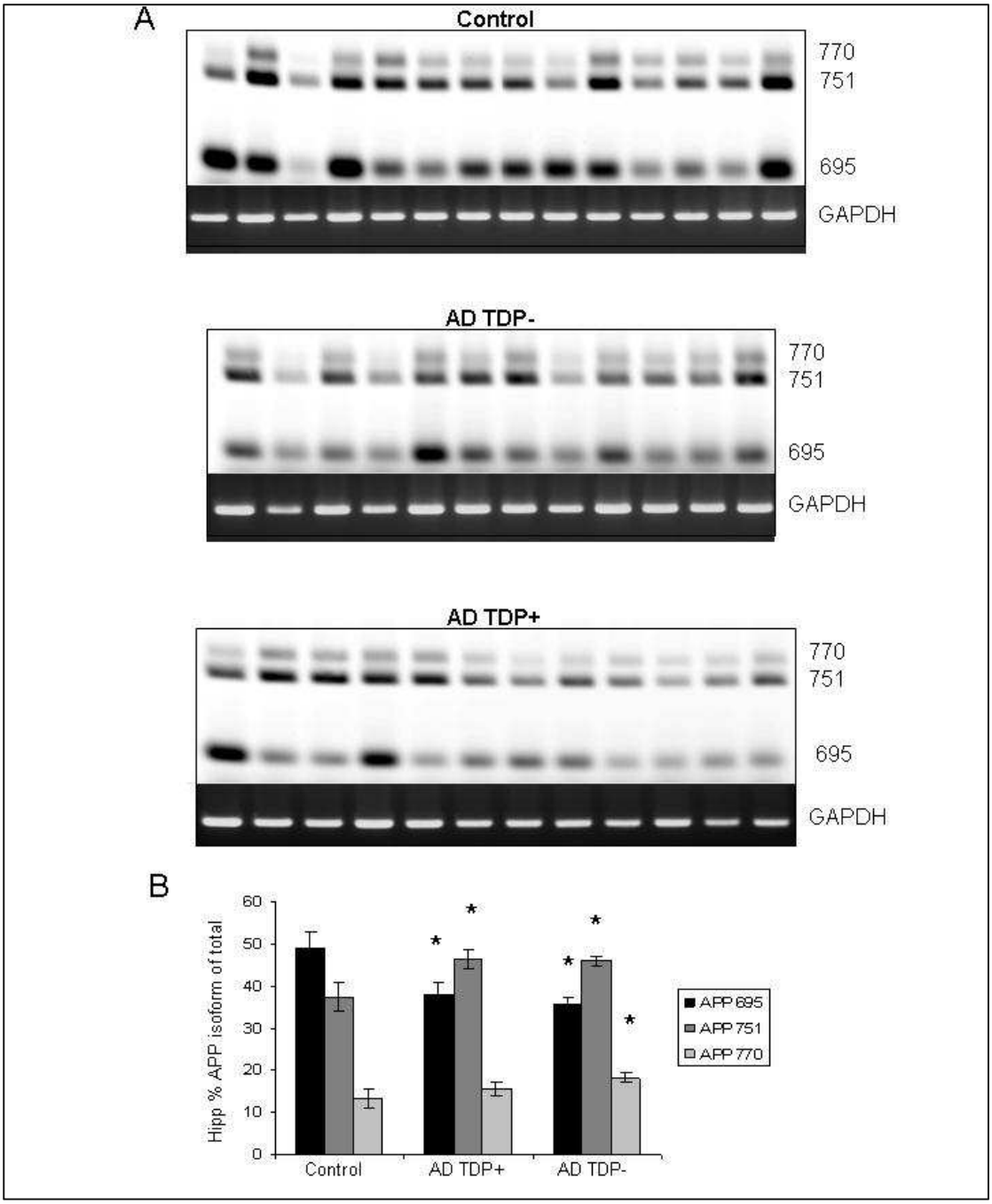

Figure 4.5. APP isoform expression in the human hippocampus.
A.APP isoform ratios were assayed by RT-PCR with IR-labelled forward primer pair. B. Mean percentages for each APP isoform was calculated for each group ± SEM. Significance was set at p = 0.05. Significant differences shown in this graph are all case vs control.

4.6. APP isoform expression in the cerebellum

cDNA from the cerebellum was amplified with the IR labelled forward APP 6-9 primers and PCR products were run on 1.5% agarose gels. A very different APP isoform expression proportion is found in the control cerebellum. APP695 comprises around 81% of the total APP751 around 12% and APP770 only 6.5% (Table 4.4). No significant differences were found in the cerebellum for any APP isoform.

CEREBELLUM AVE%	695	751	770
Control	81.2	12.3	6.5
ADTDP-	80.4	13.6	6
ADTDP+	80.8	14.9	4.3

Table 4.5. Percent average APP isoforms in the cerebellum.
Values with * were significantly different from control

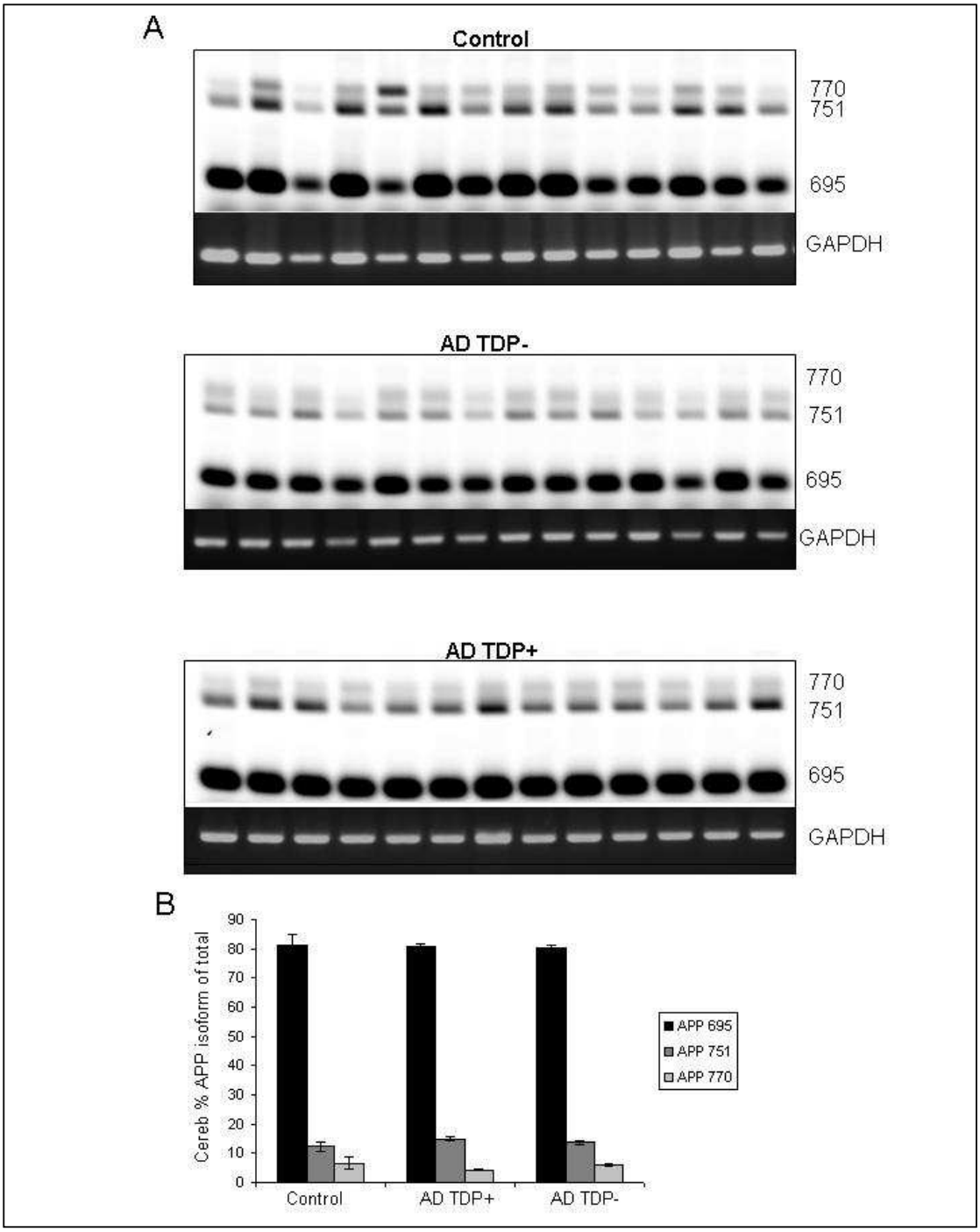

Figure 4.6. APP isoform expression in the human cerebellum.
A.APP isoform ratios were assayed by RT-PCR with IR-labelled forward primer pair. B. Mean percentages for each APP isoform was calculated for each group ± SEM. Significance was set at p = 0.05. Significant differences shown in this graph are all case vs control.

4.7. APP and tau splicing correlation

A correlation analysis was performed to examine the relationship between tau 4R/3R RNA ratio and APP RNA isoform expression. Separate correlation analyses of control and AD brain were carried out between percent expression of each of the APP isoforms with percent expression of tau exon 10 in five brain regions.

Differences in APP751 isoform between ADTDP- and ADTDP+ in the amygdala were only marginally significant and were no significant differences in tau 4R transcript expression in any brain region and therefore the two AD groups (ADTDP- and ADTDP+) were combined for the correlation analysis. Correlation analysis was carried out in all brain regions for control brains and there were no significant correlation found in any brain region (Figure 4.7 and 4.8). For the AD samples, significant correlations were found in the amygdala and hippocampus. In the combined AD group, percent APP751 expression showed a significant positive correlation with percent tau 4R expression in the amygdala (Figure 4.7 and Table 4.1) and hippocampus (Figure 4.8 and Table 4.1). APP770 showed a significant positive correlation with percent tau 4R expression in the amygdala and a trend for a positive association that was not significant in the hippocampus. APP695 expression showed a highly significant negative association with tau exon 10 expression in the amygdala and hippocampus.

In AD samples from the temporal cortex, APP751 and APP770 isoforms showed a trend toward positive association with tau exon 10 and APP695 showed a trend toward negative association with tau exon 10 in line with results from the amygdala and hippocampus however these result were not significant (Table 4.1).

The analysis shows that in the amygdala and hippocampus of AD brains, high 4R tau expression is related to high APP751 and APP770 expression and low APP695 expression and this relationship is specific to AD brains because no significant correlation was found in control brains.

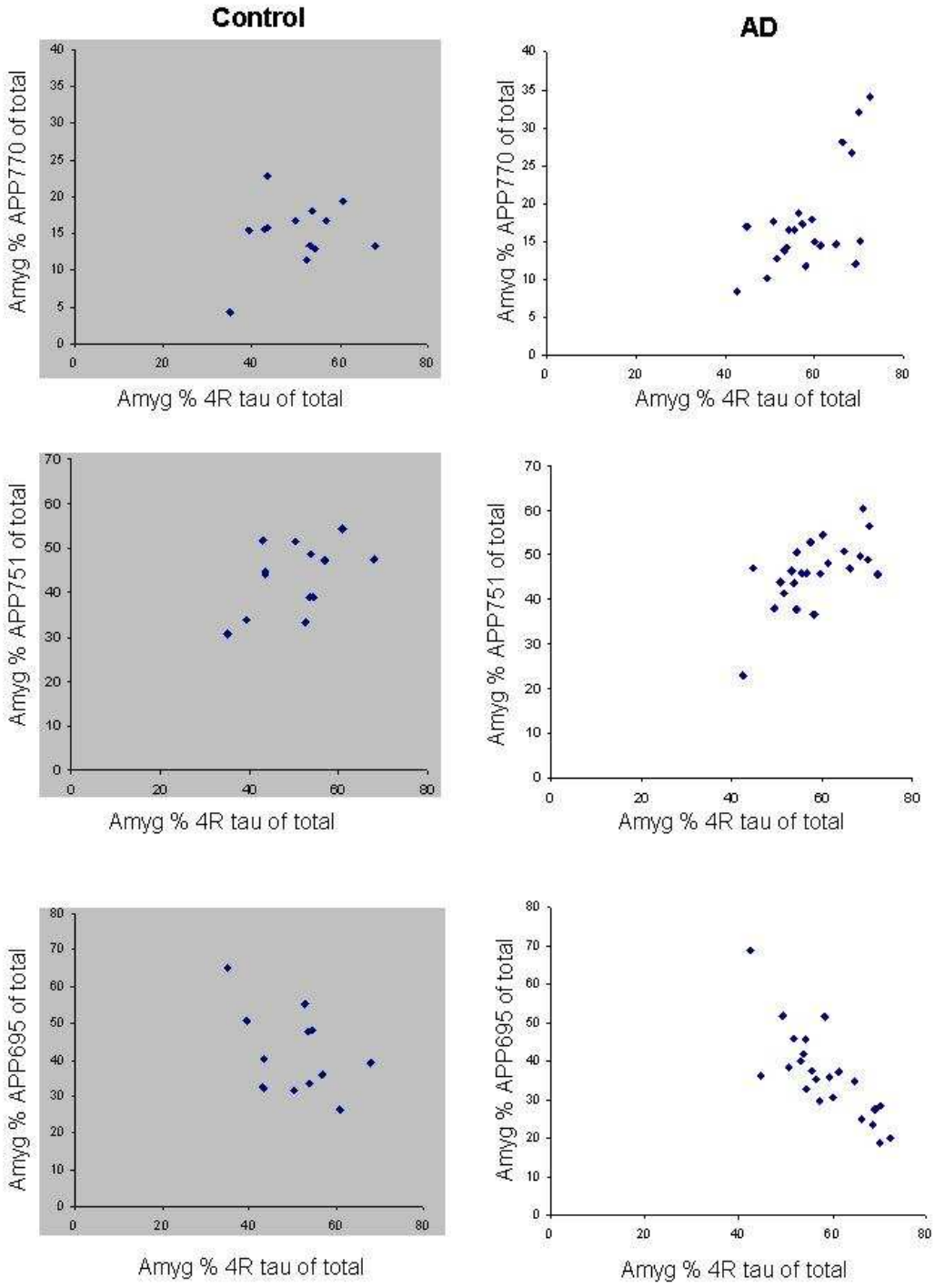

Figure 4.7. APP 770, 751 and 695 are highly correlated with tau 4R expression in the amygdala in the AD brain but not in control brains.

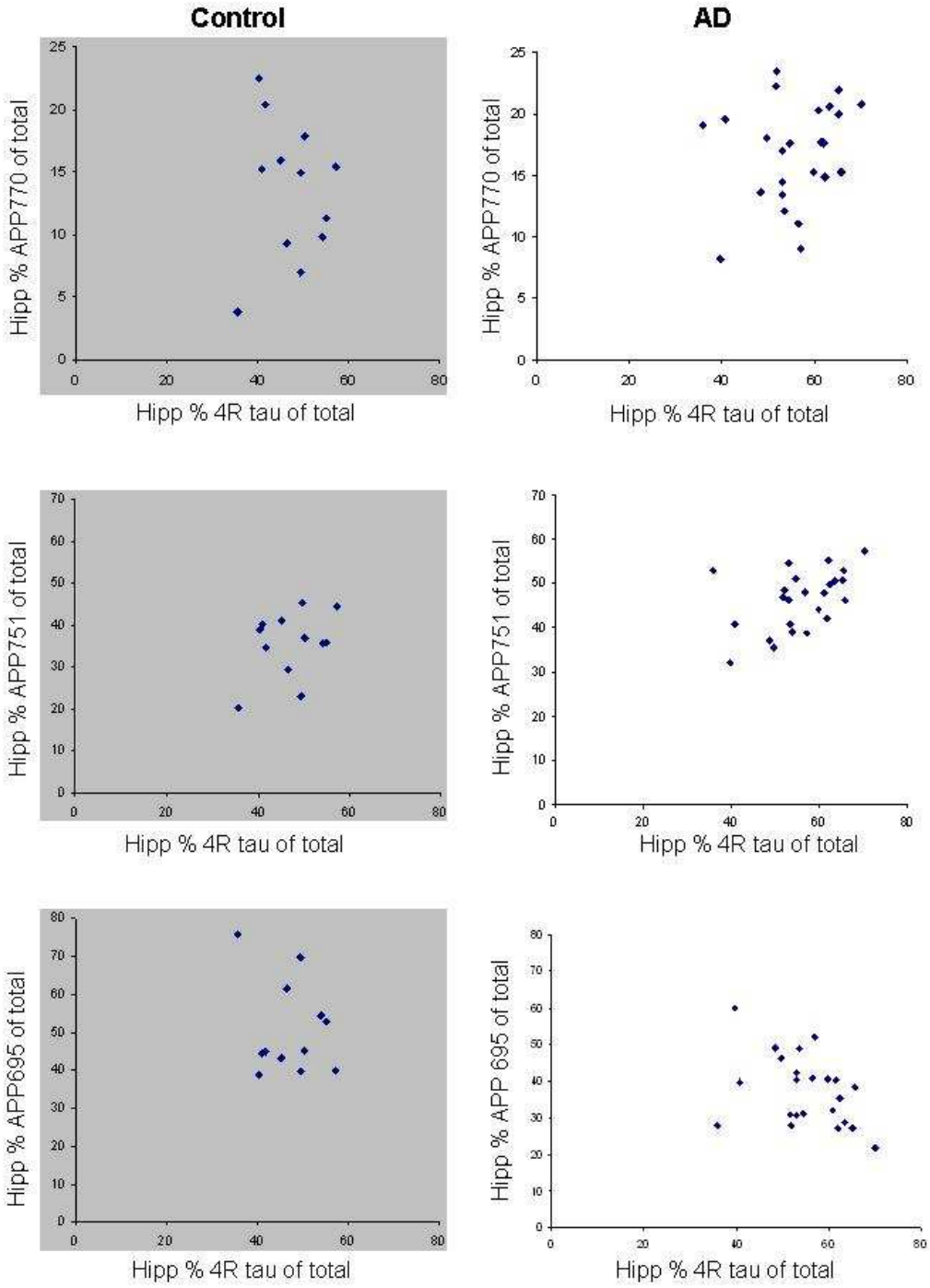

Figure 4.8. APP 751 and APP 695 expression are correlated with 4R tau expression in the hippocampus in AD brain but not in control brain.

REGION	AD CASES	CORRELATION COEFFICIENTS
Amygdala	Percent APP770	r = 0.622 p = 0.0015** n = 23
	Percent APP751	r = 0.6413 p = 0.001** n = 23
	Percent APP695	r = -0.7954 p < 0.00001*** n = 23
Hippocampus	Percent APP770	r = 0.2297 p = 0.2802 n = 24
	Percent APP751	r = 0.4791 p = 0.0179* n = 24
	Percent APP695	r = -0.437 p = 0.0327* n = 24
Temporal	Percent APP770	r = 0.3622 p = 0.082 n = 24
	Percent APP751	r = 0.3084 p = 0.1426 n = 24
	Percent APP695	r = -0.3732 p = 0.0725 n = 24

Table 4.1. Correlation coefficients and P values for correlation of percentage APP isoforms and percentage tau 4R in the amygdala, hippocampus and temporal cortex in AD brains.

4.8. Total APP mRNA expression

Total RNA levels of APP were measured by qRT-PCR. Samples were run in duplicate and the average cycle threshold (CT) was calculated for target and two reference genes. The average CT for target samples was divided by the geometric mean of the two reference genes and each point plotted giving a target gene expression relative to reference gene expression (Figure 4.9). There were no significant differences in APP expression by one way ANOVA in disease groups compared to controls in any brain

region. There were also no differences in ADTDP+ compared to ADTDP- groups by t-test in any brain region.

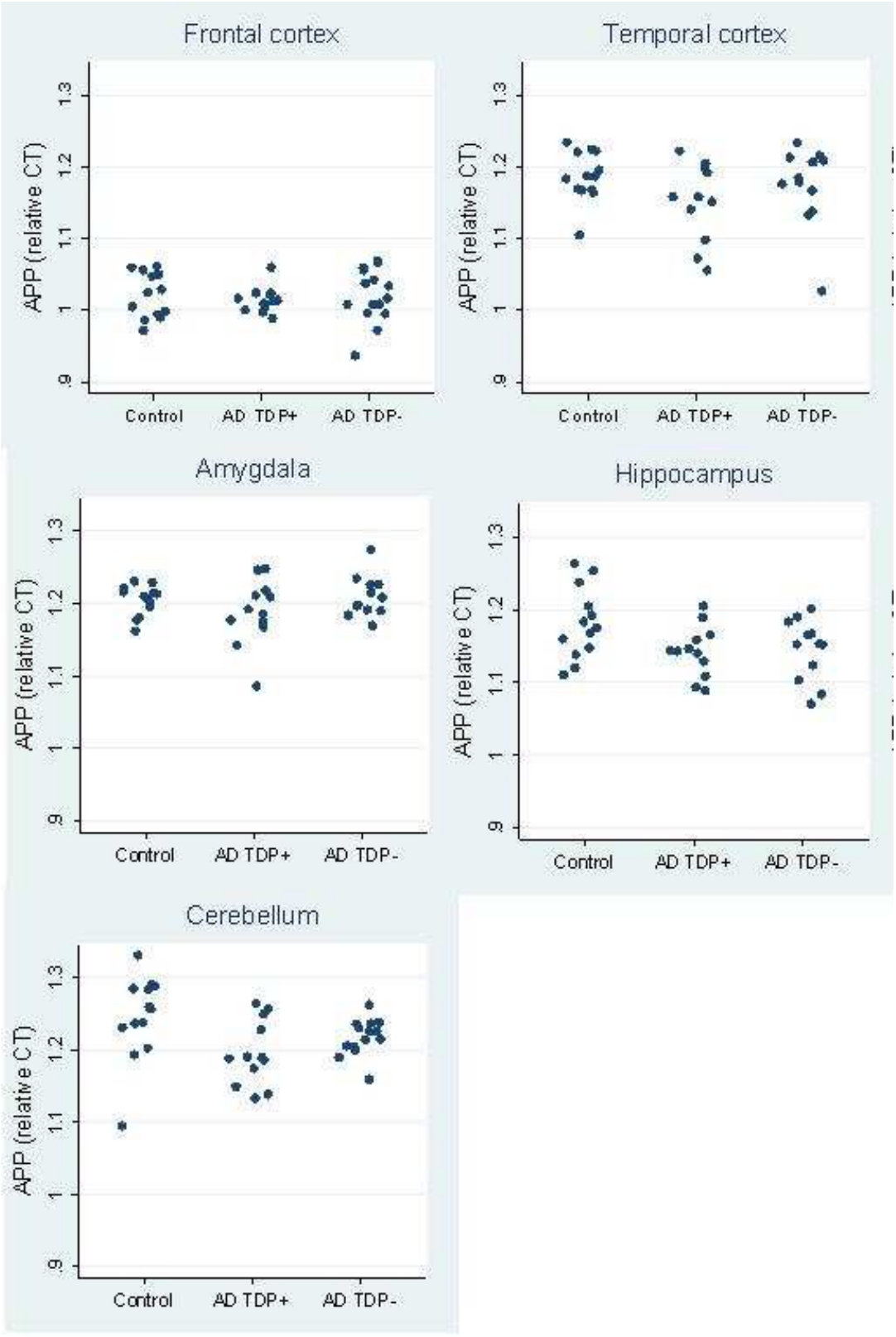

Figure 4.9. Total APP mRNA expression in AD and control brain.
RNA was isolated from post-mortem brain tissue and reverse transcribed. 20ng/µl of cDNA was used for qRTPCR analysis in duplicate. Each data point represents one sample, relative CT was calculated by dividing target CT by the geometric mean of the two reference genes.

4.9. Summary

The overall consistent finding in the splicing analysis is that APP751 was significantly increased in the temporal cortex, amygdala and hippocampus in ADTDP- and ADTDP+ brains compared to control (with only a trend in the amygdala of ADTDP+ brains). APP695 was significantly reduced or showed a trend for being reduced in the temporal cortex, amygdala and hippocampus in ADTDP- and ADTDP+ brains compared to control. In the hippocampus APP770 was significantly increased compared to control. This analysis showed no trend in APP splicing changes due to the presence or absence of TDP-43 inclusions. Other studies have shown APPKPI containing transcripts are increased in AD and the results from our splicing analysis of APP isoforms in AD and control samples were consistent with these previous findings.

Correlation of tau exon 10 expression with each APP isoform expression was carried out in control brains and combined AD group brains in five brain regions. For the AD brains, the amygdala and hippocampus showed highly significant positive correlations between APP751 and APP770 and 4R tau RNA expression (in the hippocampus APP770 showed a trend with tau 4R RNA expression). Both the amygdala and hippocampus showed highly significant negative correlation between APP695 and 4R tau RNA expression. In control brains no significant correlation between tau isoform expression and APP isoform expression was found in any brain region.

There were no differences in total APP RNA expression between control and AD brains. No differences in total APP expression was found between ADTDP- and

ADTDP+ brains and suggests that TDP-43 mis-regulation is has no effect on APP expression or RNA stability.

Chapter Five: 3'UTR splicing of TDP-43 in brain regions affected in Alzheimer's disease

Examination of the human genomic *TARDBP* sequence shows that there are four potential polyadenylation sites (PAS), defined by a (A)AATAAA(A) sequence in the 3'UTR of TDP-43. In HEK 293 cells, two major isoforms of TDP-43 are detected by northern blotting, V1pA1 which utilises the first PAS (pA1) and V1pA4 which utilises the fourth PAS (pA4) (Ayala et al., 2011). The pA1 isoform is three times more abundant in HEK 293 cells compared to the pA4 isoform (Ayala et al., 2011). Nothing has been demonstrated regarding utilisation of PAS three (pA3) however there is 100% homology of PAS one, two and four with the mouse TDP-43 genomic sequence and in mice, pA3 is not present.

Autoregulation by coupling nonsense mediated decay (NMD) with alternative splicing (AS) has been demonstrated for many RNA binding proteins (RBP) and is a ubiquitous mechanism for maintaining constant levels of RBP inside cells. In HEK 293 cells, TDP-43 autoregulates through two different mechanisms and both involve TDP-43 protein binding to a TDP-43 binding region (TDPBR) in the 3'UTR of the TDP-43 transcript. The first mechanism involves the splicing of two cryptic introns, one in TDP-43 exon 6 (intron 6 is spliced out in this transcript), and one in the 3'UTR (intron 7 is spliced out), result in NMD of these transcripts. This TDP-43 isoform is called V2 and is expressed at a low level, at least in HEK 293 cells (Introduction and Figure 1.3).

A novel second mechanism for TDP-43 autoregulation has been demonstrated, also in HEK 293 cells, where TDP-43 transcripts that have only intron 7 spliced out are

retained in the nucleus and thus are not available for translation (Avendaño-Vázquez et al., 2012). Splicing of intron 7 in the 3'UTR removes pA1 and therefore these transcripts utilise the non-optimal second PAS (pA2) and are called isoform pA2. (Avendaño-Vázquez et al., 2012). To our knowledge no study has yet determined if the same autoregulatory splicing demonstrated in HEK 293 cells also occurs in human brain. Human *TARDBP* EST in the Ensembl data base show a sequence that corresponds to the V2 isoform. There are three other transcripts are described as being subject to NMD however no EST exists for the pA2 isoform. This may be due to incomplete transcript sequences of all TDP-43 transcripts that occur in brain tissue.

Misregulation of TDP-43 by sequestration into cytoplasmic inclusions may alter auto-regulatory RNA processing of TDP-43 transcripts. In support of this, Mishra et al. (2007) quantify RNA levels in FTLD-TDP-43 and MND human brain samples with microarrays and found TDP-43 RNA levels are 1.5 fold increased compared to control. The question this section answers, is TDP-43 3'UTR splicing altered in TDP-43 proteinopathies?

5.1. Determination of the PCR cycling conditions for the TDP-43 pA2 splice isoform

PCR primers were designed to amplify a region of cDNA spanning the second splice site (intron 7) in the 3'UTR of TDP-43. For accurate quantification of molar ratios of PCR product the forward primer had a DY682 label attached to the 5' end. cDNA from human brain was analysed with the IR labelled forward primer and the resulting PCR products were sequenced (Figure 5.1). PCR products of 1176 bp (3'UTR) corresponds to a full length TDP 3'UTR utilising the fourth polyadenylation site (pA4). The database sequence (NCBI and Ensembl) predicts a PCR product of 1206

bp however our sequenced PCR product did not include a 30 bp sequence found within the published sequence. There may be sequence discrepancy between the published sequenced and what occurs in neuronal transcripts. Alternatively, secondary DNA structure may result in the polymerase skipping over this sequence. The 472bp product (TDP pA2) is the intron 7 spliced 3'UTR of TDP-43. A smaller product (**) is a mis-primed product where the forward primer binds to a sequence present within intron 7. These primers specifically exclude detection of the V2 isoform because the forward primer binds to a 3'UTR sequence that is spliced in the V2 isoform. cDNA was amplified with the TDP3'UTR with a labelled forward primer with a different number cycles. TDP-43 3'UTR and pA2 arbitrary fluorescent units for quadruplicate samples were measured by Odyssey software. Fluorescent units were plotted against cycle number and the linear range of the PCR amplification curve was determined for the TDP 3'UTR primer pair (Figure 5.1). The number of cycles used in the final analysis was 31.

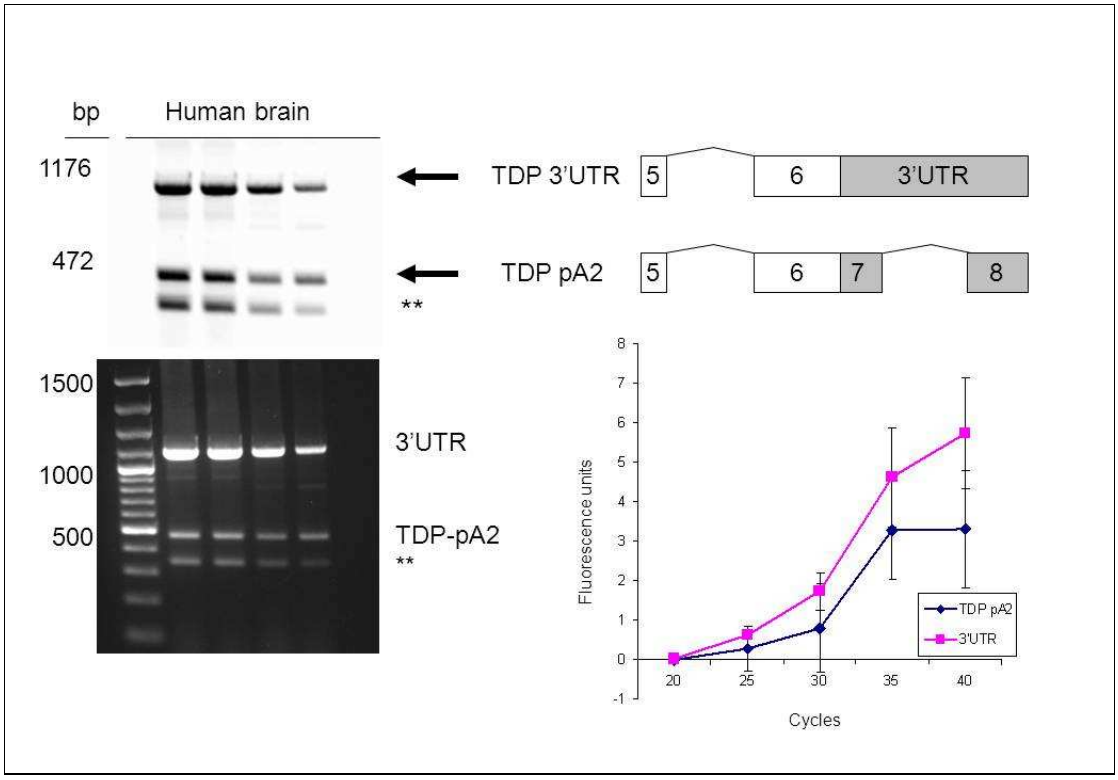

Figure 5.1. Determination of TDP-43 3'UTR primer linear phase. IR- labelled TDP-43 3'UTR primers were tested with cDNA from human brain. cDNA from quadruplicate samples were analysed by PCR at different cycles (25, 30, 35, 40) and PCR products were quantified and plotted to determine linear and plateau stages. The number of cycles finally used for quantification was 31 cycles.

5.2. The TDP pA2 transcript is not degraded by NMD in SH-SY5Y cells.

Autoregulation of RBP commonly occurs through coupling alternative splicing with NMD (AS-NMD). In HEK 293 cells the TDP-pA2 transcript was found not to be degraded by NMD. NMD can be demonstrated in a particular transcript by treating cells with a translation inhibitor such as cycloheximide (CHX), extracting RNA, and quantifying any putative NMD transcript(s) by RT-PCR. Since NMD is a translation dependent process, when translation is inhibited by CHX, transcripts that would normally be degraded by NMD will show an increased signal compared to no CHX treated (control) condition. In SH-SY5Y cells the pA2 transcript was only slightly increased when treated with CHX (Figure 5.2) and there was no significant difference

between pA2/3'UTR ratio in control and CHX treated cells. This demonstrates that the TDP-pA2 transcript was not degraded by the NMD pathway. This result is in line with results in HEK 293 cells where it has been demonstrated that only the V2 transcript is degraded by NMD (Ayala et al., 2011). Autoregulation of the intron 7 spliced isoform (TDP-pA2) in HEK 293 cells is achieved by nuclear retention of TDP-pA2 transcripts.

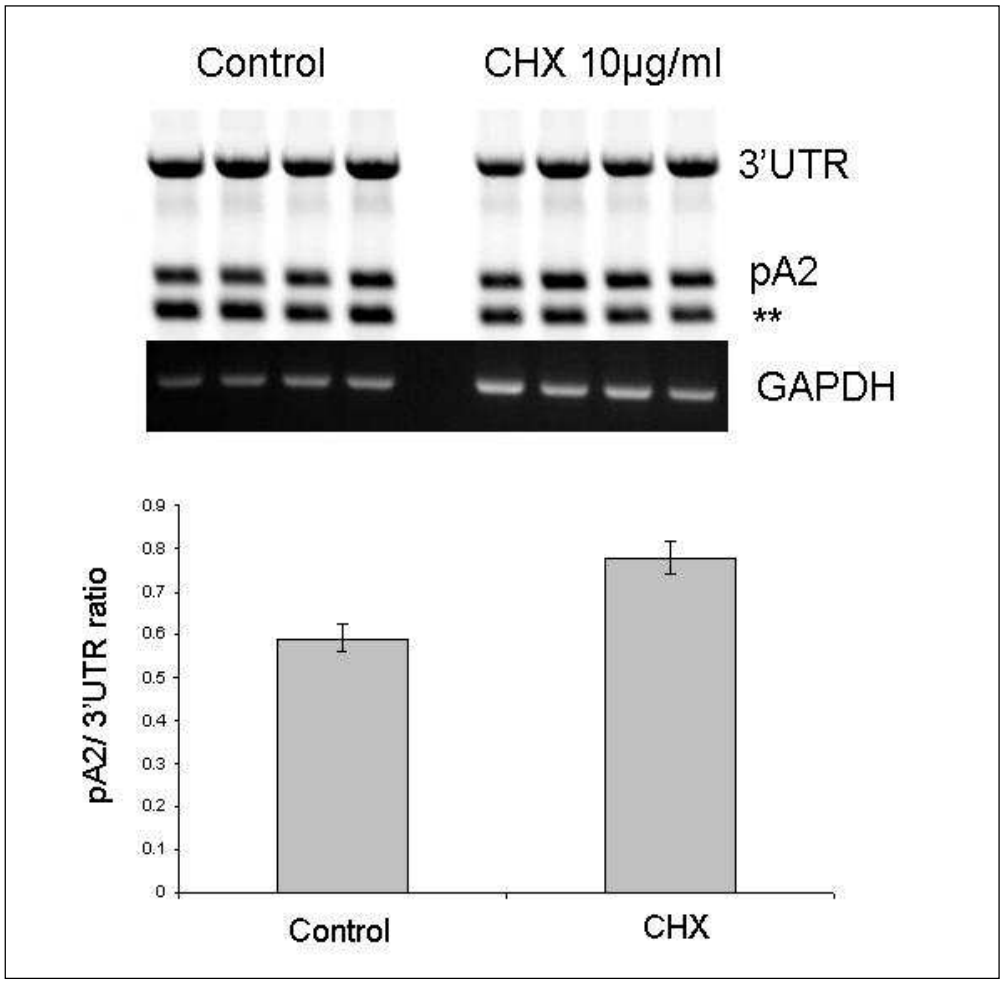

Figure 5.2. Cycloheximide treatment in SHSY5Y cells.
SH-SY5Y cells were treated with 10µg/ml of CHX for 12 hours. RNA was extracted for the cells and reverse transcribed. PCR with IR-labelled primers spanning the intron 7 splice site in the 3'UTR of TDP-43. Quantification of PCR products show no differences in pA2/3'UTR isoform ratio in control and CHX. ** is a mis-primed PCR product

5.3. TDP-pA2 RNA expression in frontal cortex

Nuclear clearance of TDP-43 in TDP-43 proteinopathies may result in impaired TDP-43 autoregulatory 3'UTR splicing. TDP-43 3'UTR splicing is a direct target for TDP-43 protein regulation and the question this section asks is does cytoplasmic mislocalisation of TDP-43 protein have an effect on downstream splicing events on a known TDP-43 splicing target? cDNA from five brain areas was used for this analysis. All samples had a RIN of 3.6 or higher.

TDP-43 3'UTR splicing was quantified by amplifying cDNA from control, ADTDP- and ADTDP+ brains with primers that span intron 7. A DY-682 labelled forward primer was used for accurate quantification. A pA2/3'UTR ratio was calculated for all samples in five brain regions frontal and temporal cortex, amygdala, hippocampus and cerebellum.

For all the brain regions tested there were no significantly different isoform ratios between control, ADTDP- and ADTDP+ brains by one way ANOVA. Of note is that there was a consistent trend for a decrease in TDP-pA2/3'UTR ratio in the AD group with TDP-43 inclusions for all brain regions except for the frontal cortex where control, ADTDP- and ADTDP+ samples have essentially equal TDP-pA2/3'UTR ratios. The decrease in TDP-pA2/3'UTR ratio in the ADTDP+ was not significant in any brain region.

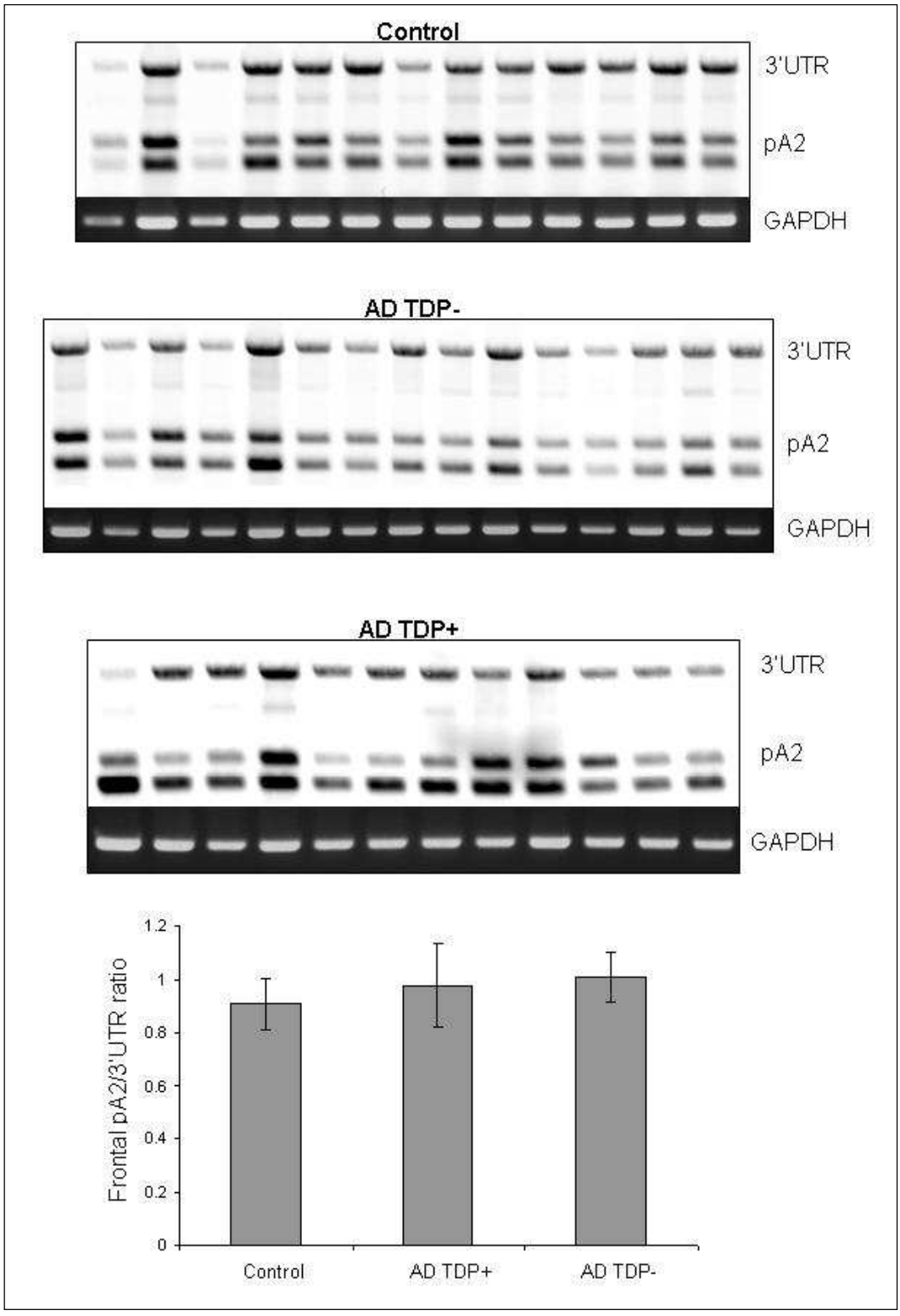

Figure 5.3. TDP-43 isoform expression in the frontal cortex.
pA2/3'UTR isoform ratios were assayed by RT-PCR.
Mean percentages for each APP isoform was calculated for each group ± SEM.
Significance was set at p = 0.05.

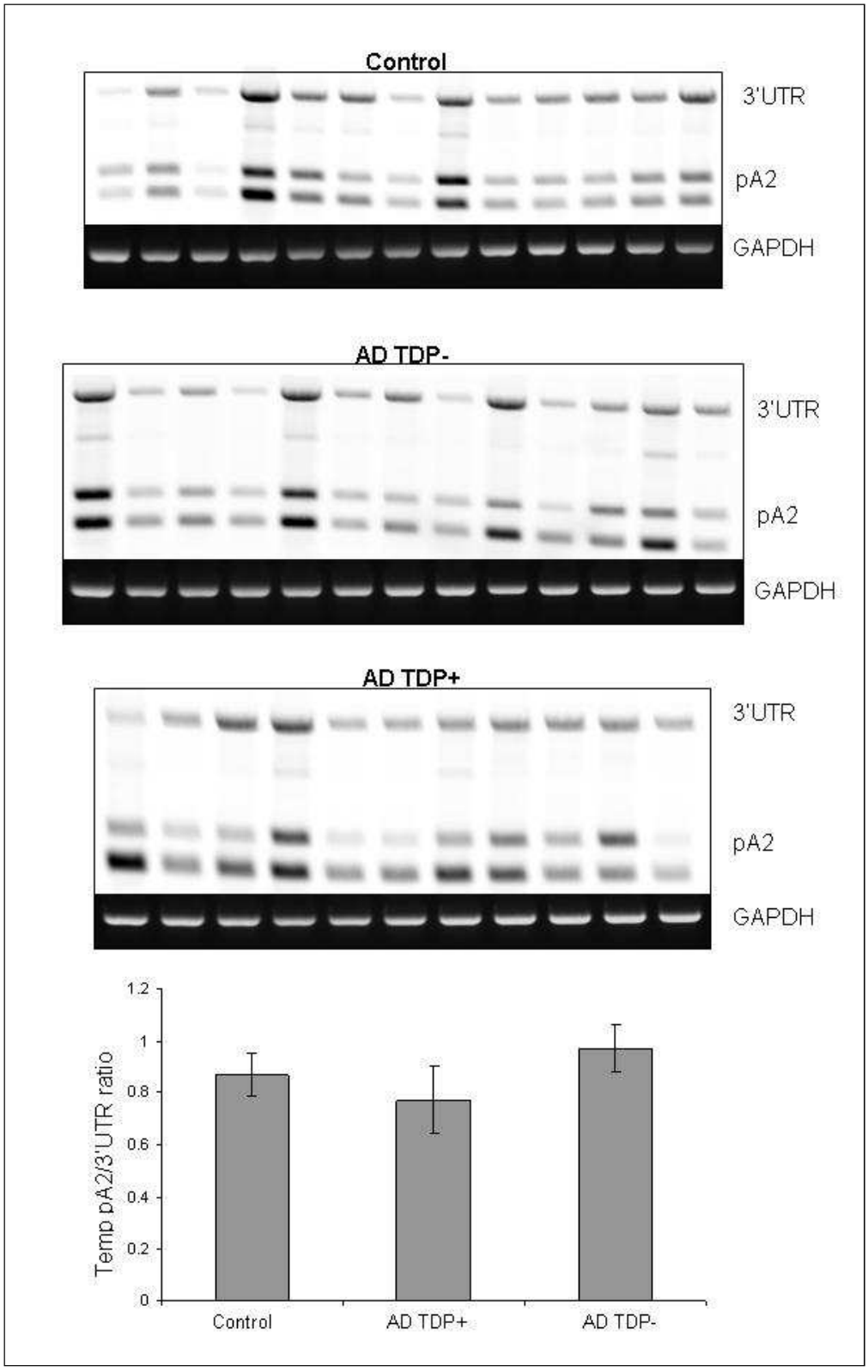

Figure 5.4. TDP-43 isoform expression in the temporal cortex.
pA2/3'UTR isoform ratios were assayed by RT-PCR.
Mean percentages for each APP isoform was calculated for each group ± SEM.
Significance was set at p = 0.05.

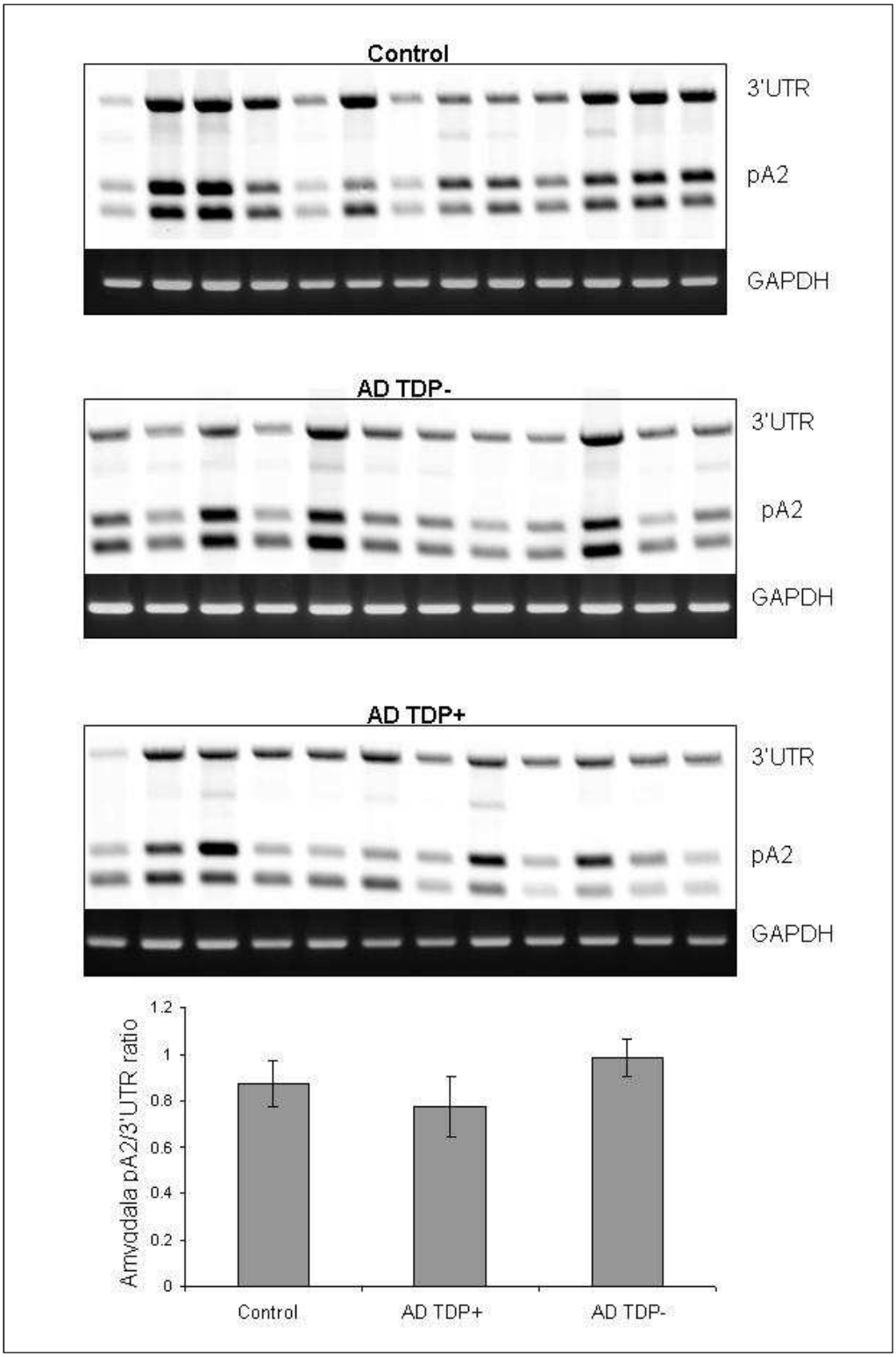

Figure 5.5. TDP-43 isoform expression in the amygdala.
pA2/3'UTR isoform ratios were assayed by RT-PCR.
Mean percentages for each APP isoform was calculated for each group ± SEM.
Significance was set at p = 0.05.

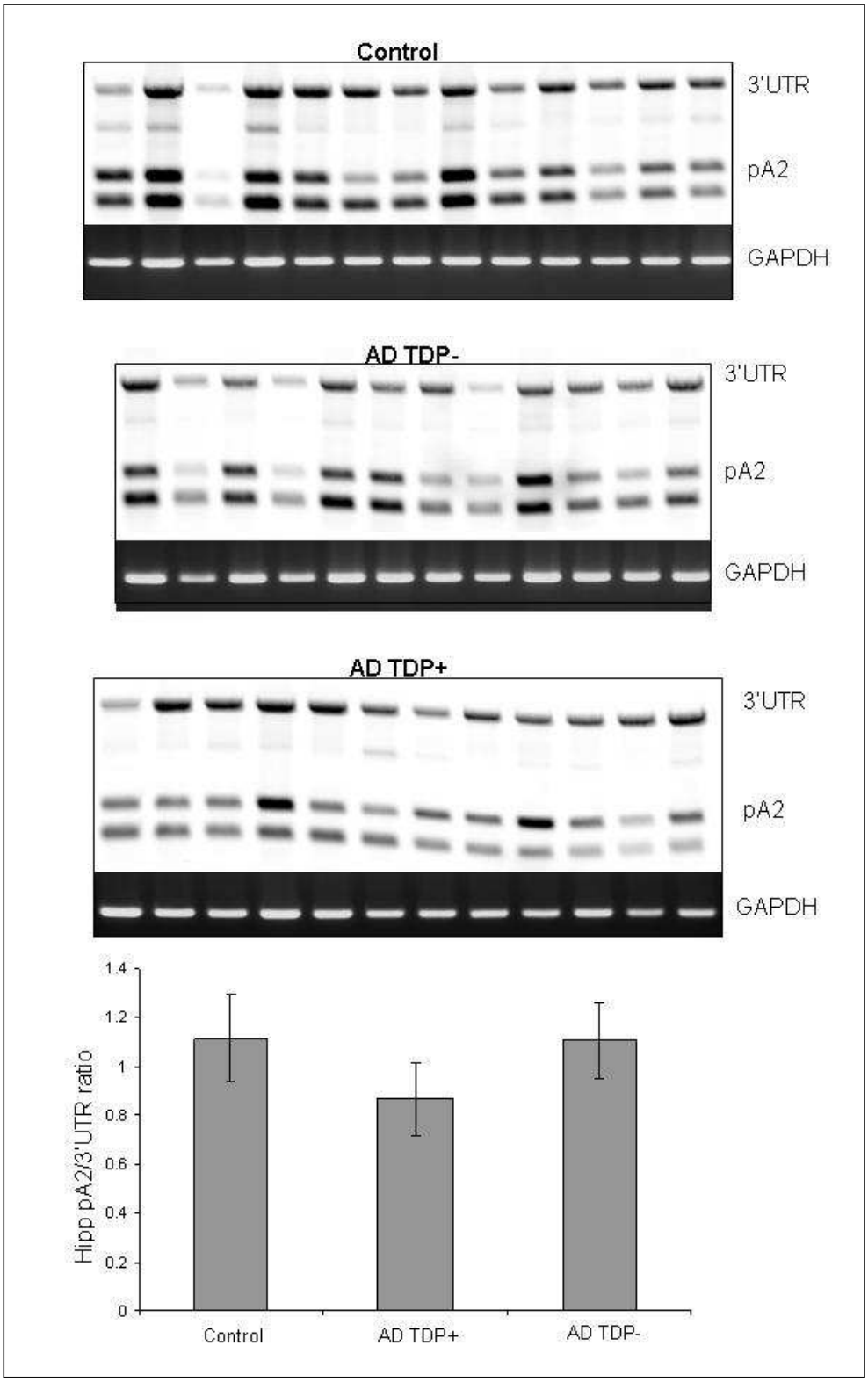

Figure 5.6. TDP-43 isoform expression in the hippocampus.
pA2/3'UTR isoform ratios were assayed by RT-PCR.
Mean percentages for each APP isoform was calculated for each group ± SEM.
Significance was set at p = 0.05.

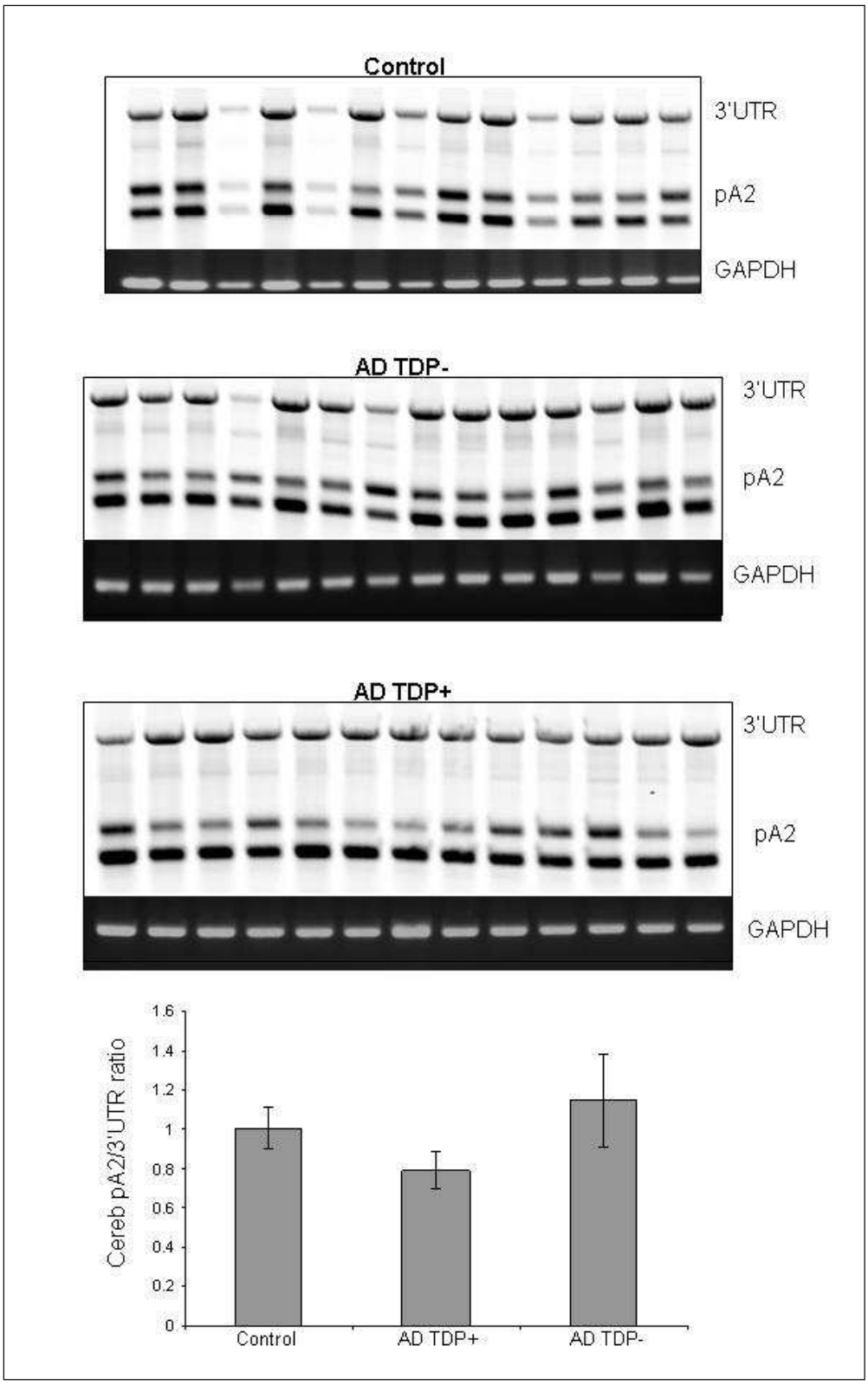

Figure 5.7. TDP-43 isoform expression in the cerebellum.
pA2/3'UTR isoform ratios were assayed by RT-PCR.
Mean percentages for each APP isoform was calculated for each group ± SEM.
Significance was set at p = 0.05.

5.4. pA2/3'UTR analysis in FTLD

AD brains with TDP-43 inclusions show a consistent reduction in the pA2/3'UTR ratio compared to control and ADTDP- brains however this result was not significant. This result suggests that TDP-43 pA2 isoforms are lower in brains with TDP-43 inclusions and is indicative of misregulation of TDP-43 autoregulation in brain harbouring TDP-43 inclusions. The small magnitude of effect may be due to a variable amount of TDP-43 inclusions in AD brains. In addition, in the AD brains we tested, TDP-43 pathology was predominantly confined to limbic structures. On the other hand, FTLD-TDP brain have widespread TDP-43 pathology and samples from the IOP brain bank were used to quantify TDP-43 pA2/3'UTR ratios. The question we ask in this section is TDP-43 autoregulatory splicing regulation altered in FTLD-TDP cases?

Only four FTLD-TDP brains had an RIN of 3.6 or greater for the analysis and RNA was extracted from different regions of same four brains. The four brain regions included were frontal and temporal cortex, amygdala and hippocampus, regions with extensive TDP-43 pathology in FTLD-TDP. Brain sample F2 has a PRGN mutation. All the other FTLD-TDP-43 cases, at that time, had no other known mutations. Referring to the FTLD-TDP samples in Figure 5.8, from left to right F2, F3, and F5 are from the frontal cortex, the next F2, F4 and F5 are from the temporal cortex, the next F5 is from the amygdala and F2 and F5 are from the hippocampus. Control brains were matched by brain area accordingly. Because the four FTLD brains contributed 3'UTR/pA2 splicing ratios to the analysis more than once and therefore were not independent, a hierarchical analysis was used to analyse differences between

the two groups and found an overall significant decrease of TDP pA2/3'UTR ratio in the FTLD group compared to controls ($p = 0.058$ log transformed data). There was a ~9% decrease in pA2 transcripts in the FTLD-TDP-43 brains compared to control. The hierarchical analysis showed a significant decrease in the temporal lobe TDP pA2/3'UTR ratio compared to control ($p = 0.037$ log transformed data) and this was due mainly to a single data point (F4) which has subsequently identified as having the C9ORF72 mutation. Sample F4 showed a ~25% decrease in pA2 transcripts in the temporal cortex.

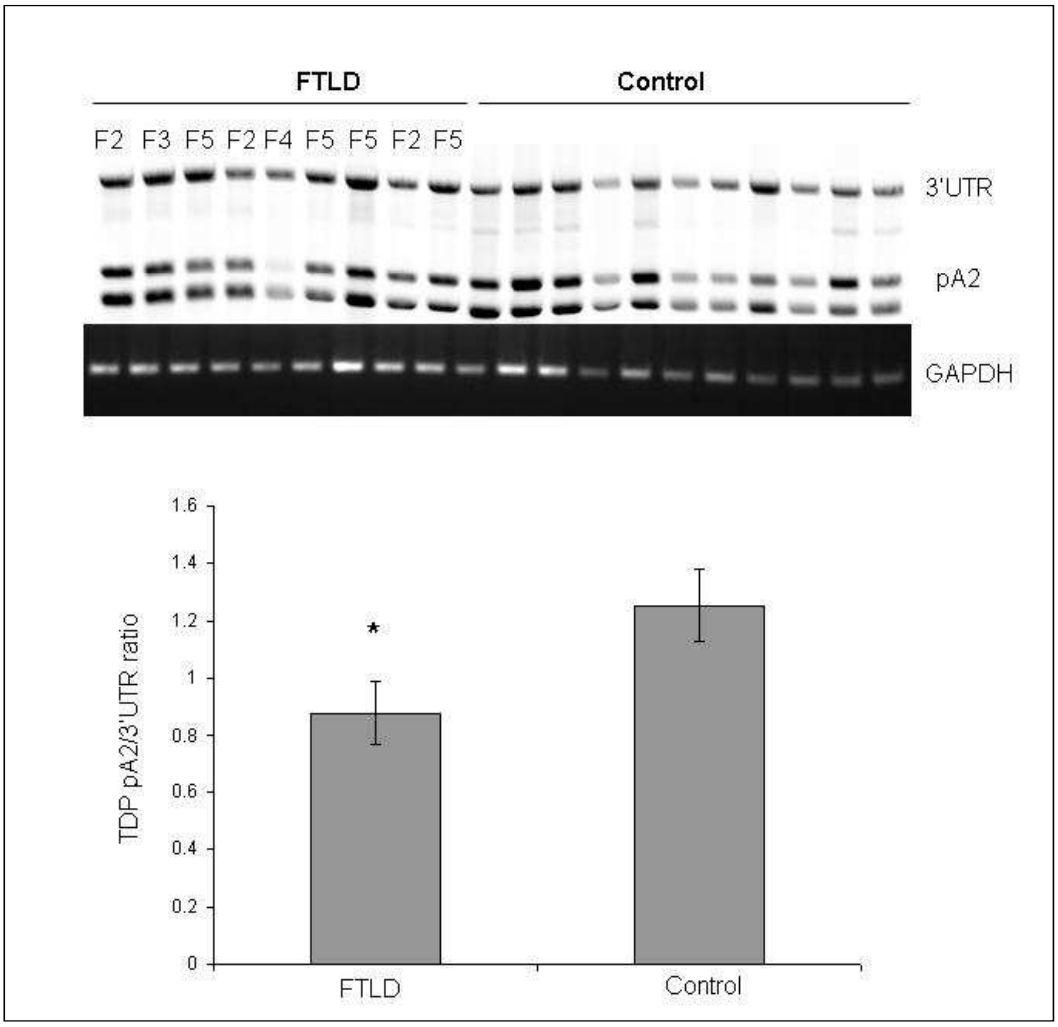

Figure 5.8. TDP-43 isoform expression in FTLD human brain samples.
pA2/3'UTR isoform ratios were assayed by RT-PCR.
Mean percentages for each APP isoform was calculated for each group ± SEM.
Significance was set at p = 0.05.

5.5. Summary

TDP-43 3'UTR splicing has been demonstrated in HEK cells to be a key regulator of TDP-43 transcript stability. The existence of TDP-43 3'UTR splicing has not yet been demonstrated in human brain tissue. PCR amplification of human brain cDNA with primers spanning the intron 7 3'UTR splice site (pA2) confirm that this splicing event occurs in all regions tested in the human brain. In HEK 293 cells pA2 transcripts are

not subject to NMD and we show that the pA2 transcript is not subject to NMD in SHSY-5Y cells.

TDP-43 3'UTR splicing ratios were quantified in control, ADTDP- and ADTDP+ human brain samples from five brain regions. No significant differences in pA2/3'UTR ratios were found between control, ADTDP- and ADTDP+ brains. A consistent non-significant decrease in the pA2 transcript was found in ADTDP+ brains.

TDP-43 pA2/3'UTR ratios were quantified in FTLD-TDP-43 samples from the frontal and temporal cortex, amygdala and hippocampus. A hierarchical analysis found a significant ~9% decrease of pA2 transcripts when pA2/3'UTR ratios from all brain regions were included. Hierarchical analysis showed a significant decrease in pA2 transcripts specific to the temporal cortex. This decrease may be due to one sample with the *C9ORF72* mutation however it has only been demonstrated in one sample and requires further investigation.

Chapter six: Limitations of the use of post-mortem tissue for gene expression studies

6.1 Variables affecting post-mortem tissue

Gene expression analysis of post-mortem brain tissue is widely used to validate data from cellular and animal models as well as to inform *in vitro* functional studies.

Comparison of expression profiles between disease and control brain tissue presents specific difficulties due to a number of different variables, both pre- and post-mortem, that potentially impact on the measurement of parameters such as RNA levels and/or splicing patterns. These variables can be divided into three categories:

1) Variables affecting brain tissue after death such as post mortem interval that potentially alter transcript stability in both disease and control samples.

2) Variables affecting brain tissue before death such as agonal state that potentially alter transcript expression in both disease and control samples.

3) Variables affecting brain tissue before death that predominantly alter transcript levels in disease brain, especially in neurodegenerative conditions such as AD, and include gliosis, oxidative stress and inflammatory signalling.

6.1.1 Post Mortem interval

Post mortem interval (PMI) refers to the time elapsed between death and the time when the tissue is frozen or fixed. Long PMIs could result in degradation of specific transcripts or alter the integrity of all transcripts. The consequences of RNA integrity on PCR-based quantification of gene expression has been clearly demonstrated where poor RNA integrity requires a larger number of cycles to reach threshold values in qRT-PCR analyses (Fleige and Pfaffl, 2006). Therefore variable PMI has the potential to contribute to variability in total levels of RNA transcripts as well as the level of specific transcripts.

Many early studies on human cerebral cortex using a variety of quantification methods including *in situ* hybridisation (Harrison et al., 1995), RT-PCR (Johnson et al., 1986) and microarrays (Popova et al., 2008; Tomita et al., 2004) showed no correlation between levels of mRNA and PMI. RNA integrity in many studies was also found not to be affected by PMI (Barton et al., 1993; Durrenberger et al., 2010; Popova et al., 2008; Ross et al., 1992). These data suggest that pronounced degradation of RNA does not take place in the initial post-mortem period, however the above studies used different methods to measure RNA levels and often had small sample sizes. By contrast, other studies do show an effect of long PMIs on levels of RNA with generally decreasing levels of specific transcripts and RNA integrity with increasing PMIs (Birdsill et al., 2011; Ferrer et al., 2008). In the case of specific transcripts, an effect of PMI length on APP transcripts has been reported; Burke et al. (1991) demonstrated a negative correlation between PMI length and stability of APP751 transcripts, however the sample size used in this study was small and

APP695 and APP770 transcripts were not decreased with increasing PMI. Clark et al. (1989) showed that total levels of APP transcripts were not degraded after PMIs of up to 22 hours in parietal cortex tissue.

The PMIs of the samples used in our study ranged from 3 hours to 120 hours; control tissue had and average PMI of 33.9 hours while AD cases had an average of 37 hours. Thus, the average PMI for disease and control samples used in this study are comparable. We found very stable levels of tau expression in control and AD brain in all the brain regions tested (Figure 3.13). This is in agreement with an earlier study showing that *MAPT* RNA levels were not altered for PMIs averaging around 50 hours in a large set of human brain samples (Trabzuni et al., 2011). Of note is a study conducted by BrainNet Europe analysing frontal gyrus, corpus callosum, thalamus and cerebellum from 193 brain samples from nine Brain Banks (Durrenberger et al., 2010). This study found no effect of PMI length on levels of commonly used housekeeping genes analysed by qRT-PCR, at least for PMIs of less than 2 days, and no effect of PMI length on RNA integrity. A possible reason for this is RNA is remarkably stable after death and this may be because degradation of RNA is energy-dependent and ceases rapidly after death. Alternatively, RNase inhibitors may persist longer than RNases after death in brain tissue or that once RNA stops being translated it is less susceptible to RNases (Barton et al., 1993).

Taken together this suggests that PMI does not contribute in a major way to differences found in total transcript levels for PMIs within the range of our study.

6.1.2 Agonal state and tissue pH

Agonal factors are the specific combination of conditions such as prolonged terminal phase, seizures, hypoxia and pyrexia leading up to death. The number of agonal factors the patient has experienced in the terminal phase has been found to be negatively correlated with RNA expression, RNA integrity or both (Bahn et al., 2001; Durrenberger et al., 2010; Harrison et al., 1995; Johnston et al., 1997; Kingsbury et al., 1995; Tomita et al., 2004).

Using a 4-point scale, Hardy et al. (1985) showed that a quick death (either violent or by natural causes) was associated with higher brain tissue pH than slow death. A longer terminal phase was associated with increased concentration of lactic acid causing acidosis. Hypoxia-inducible factor 1α (HIF-1α) levels have been found to be significantly increased in tissue from patients that have had agonal events such as coma, respiratory illness or long ventilation (Durrenberger et al., 2010). HIF-1α is usually rapidly degraded by the proteasome in normal aerobic conditions, however, in hypoxic conditions, HIF-1α is stabilised and activates genes essential to the cellular adaptation to low oxygen conditions (Dery et al., 2005). These results show that the increase in acidity in brain tissue is correlated with hypoxic conditions (Durrenberger et al., 2010) and that the increase in brain acidity is associated with decreased RNA integrity which may explain why decreased RNA levels are found in tissue from individuals with a complex agonal phase. However not all studies have found a correlation between RNA integrity and brain tissue pH (Sherwood et al., 2011) and these authors highlight the difficulty of quantifying agonal factors. For example,

hypoxia or dehydration are often scored using clinical notes however these notes may not give details of severity or length of particular agonal factors.

RNA integrity is profoundly affected by high brain acidity resulting in RNA degradation whereas less acidic conditions (pH values above a threshold of around 5.9) causes negligible RNA degradation (Trabzuni et al., 2011).

We measured the pH of the samples used in this study (Table 2.3) and found that only one sample had a pH lower than 5.9, the threshold below which acidity profoundly affects RNA integrity. We also measured RNA integrity number (RIN) for RNA from all brain regions and only used samples with a RIN of 3.6 or above. We found that samples with a RIN lower than 3.6 had decreased levels of tau RNA and quantification was unreliable and therefore a RIN of 3.6 was chosen as a cut-off for all samples.

We quantified total levels of tau and APP by qRT-PCR analysis relative to two house-keeping genes that were determined to have the most stable expression for each brain region analysed. Normalisation to stable housekeeping genes eliminates effects of variable RNA integrity in qRT-PCR-based analyses (Durrenberger et al., 2010; Fleige and Pfaffl, 2006). For splicing analysis we quantified tau, APP and TDP-43 isoform ratios. Measuring ratios mitigates the effects of variable RNA integrity in RNA analyses because transcripts for all isoforms will be affected approximately equally.

Sample selection on the basis of RIN and pH as well as calculation of isoform ratios mitigated the contribution of variable RNA integrity to the parameters measured and

therefore our results are unlikely to have been confounded by pre-mortem RNA degradation due to the agonal state.

Post mortem interval and agonal state affect both control and disease brain and can be controlled for by using selected samples and more than one methodology for measuring transcript levels or alternative splicing. It should be mentioned that other variables such as the number of freeze-thaw cycles that tissue samples have undergone or the effect of medication prior to death may also impact on RNA levels and these variables are not included in our analyses.

6.1.3 Changes in cell population in Alzheimer's disease

Neurodegeneration by definition is a reduction in the neuronal population. Neuronal loss has been found in the hippocampus, subiculum, dentate gyrus and entorhinal cortex of AD cases compared to controls (Braak and Braak, 1991; Gomez-Isla et al., 1997; Simic et al., 1997; West et al., 1994). Using stereology Gomez-isla et al., (1997) showed a decrease of 53% of neurons in the superior temporal sulcus of AD brain compared to control. There is also a consistent finding of reduced immunostaining for synaptophysin, a synaptic marker in AD brain compared to control (Brun et al., 1995; Gomez-Isla et al., 1997). The reduction in synaptic connections and reduction in branching is considered to be the predominant cause of memory loss in AD (Walsh and Selkoe, 2004). These findings show that populations of neurons and glia are altered in AD brain and differences in transcript or isoform expression found in post-mortem tissue from AD brain could reflect differences in cell populations. To some extent, neuronal loss takes place in normal aging however it

is generally considered to be rather small (Pakkenberg and Gundersen, 1997; Pakkenberg et al., 2003; Pannese, 2011; Tang et al., 1997) and in AD, the loss of neurons appears to be accelerated.

Astrocytes are specialised glial cells that perform many essential functions in the CNS (for review see Sofroniew and Vinters (2010)). They respond to insults through a process of reactive astrogliosis which, in AD brain, involves hypertrophy of the astrocyte cell body and processes, proliferation. Aβ plaques are surrounded by dense layers of processes from astrocytes. Inflammatory signalling by both microglia and astrocytes also recruit more astrocytes to sites of damage.

In our study no differences in levels were found in AD cases compared to control cases for either tau or APP by qRT-PCR which is consistent with other studies (Hyman et al., 2005; Ingelsson et al., 2006; Ingelsson et al., 2007; Matsui et al., 2007). For splicing, we found modest increases in 4R/3R tau ratios in AD cases compared to control. However we found no differences in total levels of tau. We also found increases in KPI-containing APP isoforms in AD cases compared to control. RNA from the same set of brain samples was used for analysis of total levels of APP and tau expression and splicing analysis. The change in APP splicing could be interpreted as reflecting the loss of neurons and increase in glial cells in AD brain, since neurons predominantly express APP695 whereas the APP751 and APP770 isoforms are expressed in many other cell types (de Silva et al., 1997; Matsui et al., 2007).

6.1.4 Inflammation in AD

Evidence for an inflammatory response in AD has been demonstrated by increased levels of chemokines and cytokines and the presence of proinflammatory markers on microglia such as interleukin-1 (IL-1), interleukin-6 (IL-6), Tumour Necrosis Factor-α (TNF-α) and toll-like receptors (Wyss-Coray and Rogers, 2012). Microglia are the main phagocytic cells of the CNS. Like macrophages from other tissues, microglia are very plastic and are able to dramatically alter their phenotype and exhibit a range of behaviours and morphologies in response to environmental stimuli (Cameron and Landreth, 2010). In the normal brain, microglia carry out tissue maintenance and immune surveillance and are found with a ramified morphology associated with the resting state. Tissue damage elicits a rapid redirection of processes to the area of damage and, if sustained, promotes the migration of cells to the affected area (Davalos et al., 2005). Engagement of the host defence mechanism converts the resting microglia into an activated phenotype and involves the production and secretion of cytokines and chemokines to mobilise the immune response.

Amyloid plaques in AD brain are surrounded by activated microglia (for reviews Cameron and Landreth (2010), Boche et al. (2013), Khandelwal et al. (2011)). Increases in proinflammatory factors are found in AD including elevated levels of TNF-α in the serum (Fillit et al., 1991) as well as IL-6 in brain tissue (Bauer et al., 1992; Bauer et al., 1991). In addition, Aβ induces the expression of toll-like receptors in AD and in mouse models of AD (Fassbender et al., 2004; Letiembre et al., 2009; Liu et al., 2005; Walter et al., 2007).

The promoter region of the APP gene contains regulatory elements responsive to cytokines and treatment of cells with TGFβ1, TNF-α (Ge and Lahiri, 2002) and IL-1 (Goldgaber et al., 1989) increases APP expression *in vitro.* In addition, the NF-κB transcription factor binding site, which is present in the *MAPT* promoter region (Maloney and Lahiri, 2012), is involved in neuroinflammatory signalling pathways (Bales et al., 2000) suggesting that inflammatory signalling in AD brain has the potential to regulate levels of and/or splicing of tau, APP or other transcripts. For example, induction of acute inflammation in mouse brain increased expression of KPI-containing APP isoforms in the cerebellum however total levels of APP were unchanged (Brugg et al., 1995). Furthermore cytokines induce increases in APP protein levels in primary human astrocytes (Rogers et al., 1999). These results show that cytokines are likely to impact on the levels of APP isoforms and may account for the increases in APP751 and APP770 that we observed in AD brain although we did not find changes in KPI-containing APP isoforms in the cerebellum in the AD cases we analysed.

Paracrine neuroinflammatory signalling between neurons and microglia linked to p38 MAPK signalling increases tau phosphorylation in mouse brain (Bhaskar et al., 2010) however no changes in tau isoform expression due to inflammatory signalling has been reported (Bhaskar et al., 2010; Kitazawa et al., 2005) suggesting that glial-derived cytokines do not alter splicing or total levels of tau.

Using microarrays, Cribbs et al. (2012) found that components of the inflammation and complement pathways were increased significantly in brain from AD patients and from aged individuals compared to brains from young normal individuals. In addition,

significant increases in glial activation, complement factors, inflammatory mediators and brain atrophy were found in non-demented aged individuals (Lu et al., 2004; Lucin and Wyss-Coray, 2009; Streit et al., 2008) suggesting that expression of inflammation-related genes undergo extensive changes in the course of normal aging and in AD and that general activation of inflammation signalling may not be significantly different between age-matched disease and control brain (Cribbs et al., 2012).

6.1.5 Conclusions

Findings from genome-wide association studies show that complex neurological diseases involve DNA sequence variants whose products act through complex pathways. Inherited genetic variability in gene expression or splicing, or both, contributes to disease risk. However measuring disease-specific changes at the RNA level in post mortem-human brain presents specific challenges. Human brain tissue can only be utilised at the end stage of a disease process and the disease course and RNA degradation arising after death affect measures of RNA levels. Nonetheless, meaningful data have been derived from expression analysis in post-mortem brain including in a recent study that confirmed the microglial/complement pathway and the role of TREM2 as strongly associated with the pathophysiology of late onset AD (Zhang et al., 2013). Bioinformatic tools have been developed to differentiate between pathologically relevant changes and secondary changes due, for example, to differences in cell population in neurodegenerative disease. Analysis of publically available transcriptome-wide gene expression data of AD and control post-mortem brain tissue has found regulatory genes predicted to mediate the transcriptional

changes observed in APOE4 carriers and LOAD patients including ITM2B, FYN and RNF219 (Rhinn et al., 2013). Thus, the effect of variables affecting gene expression in post-mortem disease brain can be mitigated through experimental design, the use of multiple controls and appropriate data analysis methods.

6.2 Experimental follow-up of expression studies in post-mortem material.

It is not possible to manipulate or perturb the human brain and measure a response to probe molecular mechanisms and test hypotheses and therefore results arising from studies in post-mortem material have to be followed up using cellular or animal models.

Here, we have shown that the potential loss of TDP-43 nuclear function that may result from cytoplasmic aggregation of TDP-43 does not alter total tau levels or exon 10 splicing and taken together these results suggest that TDP-43 does not have a direct effect on tau expression or splicing. This is consistent with a previous study that showed that knockdown of TDP-43 using antisense oligonucleotides does not alter transcription levels of tau in mice (Polymenidou et al., 2011). However, unlike mouse tau, TDP-43 could potentially play a role in the regulation of the splicing of human tau. TDP-43 binds predominantly to intronic regions (Tollervey et al., 2011a), regions that are not very highly conserved between human and mouse. Tau splicing is partly regulated by elements within the intronic region, thus TDP-43 could have a differential effect on tau splicing between human and mouse. Consequently, analysis of tau expression and splicing relevant to human disease, and how it may be regulated by TDP-43, requires cellular or animal model expressing human tau.

6.2.1 Experimental models of human tau expression and splicing

Several human neuroblastoma cell lines exist, most notably SH-SY5Y cells. While these cells are suitable to analyse regulation of expression levels of the *MAPT* genes, they are not ideal to study tau splicing as they express mainly tau 3R (Smith et al., 1995). Induced pluripotent stem cells (iPS cells) derived from normal individuals or AD patients could be an ideal alternative, but no data has been published to date on tau expression in these cells. Tau expression can be analysed in non-neuronal cells transfected with constructs comprising a minimal *MAPT* promoter upstream of a reporter gene such as luciferase. Tau splicing can be analysed in non-neuronal cells transfected with *MAPT* mini-genes containing exon 10 or exons 2 and 3 with flanking intronic sequences in non-neuronal cells. Minigenes are widely used to measure the activity of splicing factors on specific exons, including tau exon 10 (Chapple et al., 2007; Wang et al., 2005).

Many transgenic mouse lines expressing human tau have been generated, but most express tau cDNAs under a heterologous promoter and are therefore not suitable to study regulation of transcription or splicing. On the other hand, htau mice express the entire human *MAPT* gene, with 14 exons and 7kb of promoter sequence in a mouse *Mapt* null background (Andorfer et al., 2003). Adult htau mice express all tau isoforms and are a good mouse model to analyse and manipulate tau splicing (Avale et al., 2013).

Another popular vertebrate animal model is the zebrafish, *Danio rerio*, due to the ease of its experimental manipulation. However, the zebrafish only has one mapt isoform

listed in the Ensembl database. Secondly, as mentioned above, splicing is partly regulated by elements within intronic regions and these regions are not very highly conserved between human, mouse and zebrafish. Thus, this suggests that mapt expression in the zebrafish is unlikely to mimic human *MAPT* regulation.

6.2.2 Experimental analysis of the potential role of TDP-43 in the regulation of tau expression and splicing

TDP-43 expression can be manipulated in the cellular and animal models described above by different methods; expression of *MAPT* and splicing patterns of tau exons 2, 3 and 10 can be analysed by quantitative and semi-quantitative RT-PCR, as described in this thesis and by reporter gene assays, as appropriate.

In human neuronal cells, such as differentiated SH-SY5Y cells or iPS cells, TDP-43 levels can be increased by transfection of a TDP-43 cDNA or decreased by RNA interference following delivery of siRNAs or shRNA directed against TDP-43 mRNA. The same procedures can be applied to non-neuronal cells co-transfected with tau minigenes or tau reporter genes. Although these experiments are very informative about a possible role of a specific splicing factor on a particular exon, overexpression is artificial and may not reflect actual expression patterns in neurons. In addition, overexpression or down-regulation of a protein can result in cellular stress that can, in turn, affect splicing (Maracchioni et al., 2007). Therefore some caution needs to be taken in the interpretation of results from this type of experiment.

As indicated above, htau mice represent a good animal model of human *MAPT* expression. TDP-43 can be overexpressed or down-regulated in these animals by crossing them with TDP-43 overexpressing mice or TDP-43 knock-out mice. However, TDP-43 overexpression results in a pathological phenotype and heterozygous *Tdp-43* knock-out mice show widespread expression of TDP-43 and therefore cannot be used as a TDP-43 knockdown mouse model (Sephton et al., 2010); homozygous *Tdp-43* knock-out mice are not viable. An alternative would be down-regulation of TDP-43 by direct injection of antisense oligonucleotides as reported (Polymenidou et al., 2011).

Due to the differences in human *MAPT* and zebrafish *mapt* gene, the zebrafish might not be the most suitable model to analyse the potential role of TDP-43 in tau RNA processing. However TDP-43 can be easily manipulated in the zebrafish. The zebrafish genome has two orthologs of the human TDP-43 gene (*tardbp* and *tardbpl*), when both are knocked out, the embryos die at 8 days post fertilisation (Schmid et al., 2013). Knockdown of *tardbp* in zebrafish embryos using morpholinos result in a motor phenotype and shortened motor axons however the levels of mapt in these models was not reported (Kabashi et al., 2010; Schmid et al., 2013).

To conclude, carefully controlled analysis of post-mortem material combined with mechanistic analysis in animal and cellular models can provide robust results that could be ultimately translated into diagnostic tools and, hopefully, therapeutic strategies.

Chapter seven: Discussion

7.1. Summary

We quantified *MAPT* and APP splicing isoform ratios and total RNA levels in AD and control brain. In frontal, amygdala, hippocampus and cerebellum of AD brains tau 4R/3R ratios were significantly increased compared to controls and tau 4R/3R ratios were highly correlated across five brain regions in AD brains. A subgroup of AD brains showing consistently high 4R transcript expression in all brain regions measured were the major contributors to the increases in 4R transcripts found in the AD group however altered tau splicing ratios were not associated with TDP-43 inclusions in this subgroup.

APP751 isoform expression was significantly increased and APP695 significantly decreased compared to control in the temporal cortex, amygdala and hippocampus. APP770 was significantly increased in the hippocampus in AD brain compared to control.

The percentage of tau 4R also positively correlated with percentage APP751 and percentage APP770, and negatively correlated with percentage APP695 in the amygdala and hippocampus.

AD brains with TDP-43 inclusions were associated with increased severity of tau pathology in the frontal and temporal cortex however the severity of tau patholgy did not associate with either 4R tau expression or insoluble 4R tau in AD brain.

These results show that a subgroup of AD cases have increased 4R tau expression which correlated with increased expression of APPKPI isoforms. 4R/3R RNA tau ratios correlated with 4R/3R tau ratios from insoluble material in AD brains from the amygdala showing that imbalances in 4R/3R ratios at the RNA are reflected in imbalances in 4R/3R ratios at the insoluble protein level.

We found reduced TDP-43 3'UTR splicing ratios in FTLD brains compared to control brains and a consistent trend for reduced TDP-43 3'UTR splicing ratios in AD cases with TDP-43 inclusions compared to AD cases without TDP-43 inclusions and control showing that sequestration of TDP-43 into cytoplasmic inclusions alters TDP-43 3'UTR splicing. TDP-43 protein regulates its own expression by 3'UTR splicing of TDP-43 transcripts which targets particular mRNAs for nuclear retention or to a NMD pathway. These findings suggest that TDP-43 autoregulation in FTLD and AD brain are altered and that transcript and protein levels of TDP-43 may be altered in FTLD and AD brains with TDP-43 inclusions however we did not directly measure TDP-43 RNA or protein levels.

7.2. Lack of association between TDP-43 pathology and Tau and APP Splicing in Alzheimer's disease

7.2.1. Tau exon 10 and TDP-43 pathology

4R expression was significantly higher in AD brain compared to control and 4R expression was highly correlated between brain regions. We show that within our samples, a subset of ~5 AD cases have increased tau 4R expression and two mechanisms may account for this:

1) Genetic variation on *MAPT* locus and we tested for an association with exon 10 expression and total tau levels associated with a particular tau haplotype.
2) Misregulation of TDP-43 may alter splicing and/or transcription of multiple genes directly and indirectly. We determine if an association exists between misregulation of TDP-43 in AD and altered tau splicing ratios.

7.2.2. Influence of *MAPT* haplotype on tau splicing

In the combined control and AD group brains no association was found between relative tau expression and *MAPT* haplotype in any brain region by qRT-PCR. We also found expression of tau 4R/3R ratios were not associated with a particular tau haplotype in any brain region tested by RT-PCR. A caveat to the interpretation of these results is that we had a small sample size which may not be representative of a wider population.

Other studies using allele specific assays have shown that the H1 allele results in a 1.29 fold increase in 4R tau expression compared to the H2 allele in the frontal cortex of PSP brains (Caffrey et al., 2006). In addition, 25% increases in 4R expression and 11-13% increases in total *MAPT* expression have been found in H1c haplotype (Myers et al., 2005).

However other studies using allele specific expression in PSP brain samples found no differences in *MAPT* expression ratios between H1c and H2 alleles in H1c/H2 heterozygotes (Hayesmoore et al., 2009). More recently, using exon arrays, Trabzuni et al. (2012) found no differences in either H1 or H2 haplotype on total *MAPT* expression in human brain. Instead, they found increased expression of tau exon 3

was associated with H2 haplotype. The association between splicing of different tau exons and tau haplotype may be explained by co-regulation of tau exons 2,3 and 10 by shared splicing factors.

Different promoter regions have been shown to regulate alternative splicing through two different mechanisms (Kornblihtt, 2005). Firstly, transcription factors at a particular promoter region may directly bind different splicing factors and certain transcription factors may also be involved in the mechanics of alternative splicing events. Secondly, the rate of transcription elongation may determine alternative exon usage with fast elongation associated with exon skipping and slow/pausing elongation associated with exon inclusion (Kornblihtt, 2005). An additional mechanism may be that transcripts from alternative promoters have alternative 5'UTR start sites or 3'UTR end sites and these play a role in recruiting splicing factors that determine subsequent alternative exon usage (Pal et al., 2011).

Tau exon 2 and 10 are regulated by several splicing factors mainly by inhibition (Andreadis et al., 1995). Tau exon 2 expression may be correlated with exon 10 expression because both exons share splicing factors SRp30c, SRp55 and tra2β1 although these factors exert differing effects on each exon (Wang et al., 2005). SRp30c and SRp55 both inhibit the inclusion of exons 10 and 2 by binding to silencer elements (ESS), one within exon 2 and another within exon 10. Tra2β1 inhibits exon 2 inclusion by forming a complex with SRp30c and SRp55 at the exonic silencer while tra2β1acts as a exon 10 activator, increasing exon 10 inclusion by blocking the binding of the two inhibitors SRp30c and SRp55 at the ESS within exon 10 (Wang et al., 2005). Tau exon 3 is also regulated by SRp30c, SRp55 however for exon 3 both

SRp30c and SRp55 increase inclusion of exon 3 (Arikan et al., 2002). Coordinated splicing of exons 2,3 and 10 could be achieved by recruitment of particular transcription factors and splicing factors to the promoter region of *MAPT*.

The promoter sequence of *MAPT* spans ~4868bp and contains multiple putative transcription factor binding sites some of which differ according to tau haplotype (Maloney and Lahiri, 2012). SNPs or insertions/deletions (indels) in the *MAPT* promoter region associated with H1 or H2 haplotype may alter the recruitment of transcription and splicing factors that coordinate *MAPT* splicing.

The mechanism of risk association for H1 tau haplotype could be related to genetic variation in the promoter region in H1 and H2 and/or variation around exon 10 that potentially alter tau splicing or expression. In our AD and control samples we found that the H1 haplotype was not associated with altered ratios of tau exon 10 or increased expression compared to H2 homozygotes and heterozygotes.

7.2.3. Possible direct effect of TDP-43 on tau splicing

The increases in 4R transcripts found in the frontal cortex, amygdala, hippocampus and cerebellum were found in AD cases from both ADTDP- and ADTDP+ cases. In the AD brains, a very high 4R/3R ratio correlation was found between frontal, temporal, amygdala and hippocampus. The cerebellum showed significant increases in 4R transcripts in AD brain compared to control however the cerebellum showed less significant 4R/3R correlations with the other brain regions and this may be because this region has no tau pathology. This analysis shows that tau 4R expression was very consistent across brain regions and that the significant increases in 4R

transcripts were the contributed by the high 4R expressor group in all brain regions tested.

TDP-43 has RNA binding specificity to UG repeats (Buratti et al., 2001) and *MAPT* contains at least two UG repeat regions, one in an intronic 5'UTR region and another in intron 9. The sequence in intron 9 -CGUGUGUGUGUGUGUGUGUGUGUGUGUGGGCGCAC- suggests a TDP-43 binding site that has potential to regulate exon 10 splicing. However the *MAPT* intron 9 UG repeats in the human sequence are around 7000 base pairs from exon 10. We found no evidence that misregulation of TDP-43 alters splicing of tau exon 10 and therefore the putative TDP-43 binding site in intron 9 has no direct effect in tau exon 10 splicing regulation.

Cytoplasmic TDP-43 inclusions result in nuclear clearance of TDP-43 protein from the nucleus (Neumann et al., 2006) however it is not known what effect this has on the role of TDP-43 in RNA processing. Global changes in altered splice isoforms have been found in AD and FTLD brain by microarray (Tollervey et al., 2011b) however splicing changes specific for FTLD-TDP were not found when compared to AD brain, even in genes known to be targets for TDP-43 alternative splicing regulation. Altered splicing of specific exons were associated with altered levels of splicing factors such as a 1.6 fold increase in polypyrimidine tract binding protein 1 (PTBP1/PTB/hnRNPI), and decreases in PTBP 2 transcripts (Tollervey et al., 2011b). These results suggest that multiple trans-acting splicing factors, that include TDP-43, are altered in AD and FTLD.

7.2.4. Definition of an Alzheimer's disease subgroup with high exon 10 inclusion

Although we found no association between misregulation of TDP-43 and level of exon 10 inclusions in AD brain, we do find increased levels of tau exon 10 containing transcripts in a subgroup of AD cases. Intronic and exonic mutations within the *MAPT* gene also cause imbalances in tau isoform expression and are associated with tau pathology. It is not known how splicing imbalances result in tau pathology however overexpression of a particular isoform may promote seeding of tau aggregation. It is not clear if splicing imbalances are found in AD and tau pathology in AD may result from Aβ production and cause a different mechanism of tau pathology. Our results show that splicing imbalances found in a subset of AD cases may also contribute to tau pathology.

Three AD subtypes have previously been identified based on a ratio of hippocampal to cortical tau pathology and severity of lesions for each case has been found in post-mortem brain (Murray et al., 2011b). Another study which associated cognitive symptoms with MRI volumetric analysis in autopsied brain confirmed the three AD subtypes (Whitwell et al., 2012). AD cases can show unusual clinical symptoms that include PPA and others more typical of FTLD (Bigio et al., 2010; van der Zee et al., 2008a) although the majority of AD cases have an amnestic presentation. The three subtypes; limbic-predominant, hippocampal sparing and typical AD show consistent correlation with the clinical heterogeneity found in AD. Almost all of the limbic predominant AD had an amnestic presentation while hippocampal sparing (cortical predominant) showed significantly more association with focal cortical syndromes such as PPA, semantic dementia and Parkinson's disease dementia (Murray et al., 2011b). In limbic predominant AD, TDP-43 pathology was significantly more

common compared to hippocampal sparing AD, although no different to typical AD. We cannot comment if the high 4R expressor AD group we found has any particular clinical phenotype or pattern of pathology because this was not included in this study. The high 4R expressor group needs to be validated in another independent sample set.

7.2.5. Possible direct effect of TDP-43 misregulation on APP splicing ratios

We showed significant increases in APP751 and significant decreases in APP695 in the temporal cortex, amygdala and hippocampus in AD brains compared to control. In addition, a significant increase in APP770 isoform was found in the hippocampus of AD brains compared to control however no pattern emerged that clearly showed that any of these splicing changes were associated with TDP-43 misregulation. The increases in KPI containing APP transcripts in AD brain are in line with previous studies, Tharp et al. (2012) showed decreases in APP695 and increases in APP770 in the frontal cortex of AD brains compared to control by qRT-PCR. Increases in APP770 and APP751 transcripts have also been found in the temporal cortex of AD brains compared to control also by qRT-PCR (Matsui et al., 2007). Taken together these studies show consistent increases in APPKPI transcripts and particularly APP770 transcripts in AD brain compared to control.

The APP gene has canonical TDP-43 binding sites in intron 1, two in intron 4 and two in intron 13, however no association between TDP-43 misrgulation and altered APP splicing was found in our samples and show that these putative TDP-43 binding sites on the APP gene are not involved in APP exons 7 and 8 splicing regulation.

7.2.6. Correlation between tau and APP splicing

In our study, for the combined AD brain cases we found a significant positive correlation between percentage tau 4R expression and percentage APP751 isoform expression and a significant negative correlation between percentage tau 4R expression and percentage APP695 in the amygdala and hippocampus. A significant positive correlation between percentage tau 4R expression and percentage APP770 isoform expression was found in the amygdala. These correlations were not found in control brains and show that the subgroup of high tau 4R expressors also show correlated splicing changes in APP isoform expression.

The molecular basis for the correlated changes in splicing of tau and APP may be due to altered levels of *trans*-splicing factors that have a role in splicing of both transcripts. Only a few studies have looked at RBP that play a role in alternative splicing of the APP exon 7, SC35, hnRNPA1 and CELF 1 have all been shown to alter splicing of exon 7 or 8 using minigenes (Donev et al., 2007; Poleev et al., 2000). SC35 is regulated by glycogen synthase kinase-3β (GSK-3β) and has been found to have differential effects on tau exon 10 either inclusion (Hernández et al., 2004) or weak inhibition of exon 10 (Andreadis, 2005). hnRNPA1 and CELF 1 have no effect on tau exon 10 *in vitro* (Gao et al., 2000; Hernández et al., 2004; Kondo et al., 2004) suggesting that altered levels of these splicing factors in disease would not affect tau exon 10 splicing and would not result in correlated splicing changes in tau and APP.

More recent work on alternative splicing of APP shows that exons 7 and 8 may be regulated by miRNA *in vivo* (Smith et al., 2011a). Dicer knock-out mice have reduced levels of microRNA and these mice display increased APP transcripts containing

exons 7 and 8 compared to wild type mice (Smith et al., 2011a). When miR-124 was over-expressed in Neuro2A cells, APP transcripts containing exons 7 and 8 were increased suggesting that splicing of exons 7 and 8 may be regulated by particular microRNA possibly by regulating the levels of polypyrimidine tract binding protein 1 (PTBP1/PTB/hnRNPI), a splicing factor which has previously been identified as a target of miR-124 (Makeyev et al., 2007). These authors also found levels of miR-124 was reduced in AD brain compared to control quantified by qRTPCR, suggesting that decreases of miR-124 cause altered PTBP1 levels which target APP exon 7 and 8 and alter alternative splicing of these exons in AD.

microRNA may also play a role in tau exon 10 regulation. Fetal mouse expression of tau is exclusively 3R and changes to exclusive 4R expression during post natal development. Smith et al. (2011b) found that during the post natal switch, miR-132 increased ~16 fold and correlated with expression of 4R tau transcription expression. These authors found that miR-132 specifically targets polypyrimidine tract binding protein 2 (PTBP2/brPTB/nPTB), and that miR-132 is significantly reduced in PSP brain. These findings suggest that altered microRNA expression may also be responsible for altered exon 10 expression in disease.

Taken together these results show that tau exon 10 and APP exon 7 are at least partially regulated by PTBP2 and PTBP1 respectively. Levels of PTBP1 and PTBP2 expression may be regulated through a miRNA pathway and particular miRNAs were shown to be reduced in disease. Regulation of RBPs is complex involving both transcriptional and post-transcriptional processes, both PTBP1 and PTBP2 have been shown to autoregulate levels of its own transcript as well as cross regulate each other

(Boutz et al., 2007; Spellman et al., 2007; Spellman et al., 2005; Wollerton et al., 2004) through an AS-NMD mechanism (see Introduction). Tollervey et al., (2011b) found increases in PTBP1 and reduced PTBP2 transcript expression in AD and FTLD brains. Regulation of tau exon 10 and APP exon 7 KPI domain may be due to splicing factors whose levels are closely related through cross-regulation and suggest that in the subset of high 4R expressor brains we found, perturbations in a splicing factor pathway involving microRNA and PTBP1 and 2 may be involved. TDP-43 may play a role in altering miRNA levels in disease. TDP-43 associates with the Drosha complex (see Introduction), involved in production pre-miRNA in the nucleus suggesting that misregulation of TDP-43 could alter production of miRNA.

7.2.7. Regulation of APP splicing

Autosomal dominant mutations in the APP gene lead to early onset dementia (Goate et al., 1991). These mutations alter processing of APP resulting in increases in Aβ production (Haass et al., 1994; Nilsberth et al., 2001). However linkage to a locus in the APP gene associated with an increased risk for late onset AD has not been found (Butler et al., 2009). Common SNPs on the APP gene also did not show any significant association with AD (Gerrish et al., 2012; Nowotny et al., 2007).

No studies to our knowledge have shown an association between genetic variation on the APP gene and altered splicing. Sequencing of the entire APP locus has revealed a number of SNPs in the promoter region of APP that may increase APP expression and are associated with AD (Brouwers et al., 2006; Guyant-Maréchal et al., 2007; Lv et al., 2008) however the SNPs differ in each of these studies and suggest that these SNPs are weakly associated with an increase in disease risk.

Taken together these results show that genetic variation in both APP and tau may be only weakly associated with increased risk for AD. Sequencing of multiple genomes has revealed that novel SNPs occur regularly in individuals (Bras et al., 2012). These results suggest that disease related genetic mechanisms may be conferred by both common and rare SNPs that co-occur at particular loci and the combined effect of these SNPs will modulate association with risk (Singleton and Hardy, 2011). In our subset of AD cases that show correlated altered splicing ratios, common SNPs as well as rare SNPs/indels on both APP and *MAPT* could contribute to alter splicing and it would be interesting to sequence these cases to see if they have SNPs in common.

7.2.8. Alternative splicing of tau exons 2 and 3 in Alzheimer's disease

Quantification of exons 2 and 3 could not be done reliably because of the presence of an intron 1 containing transcript. A transcript with the exact tau intron 1 exon was found in the BLAST EST data base accession number DA117257.1. In a paper that accompanies this EST, the authors suggest that this transcript is produced using an alternative promoter site in the *MAPT* gene (Kimura et al., 2006). The DA117257.1 EST was produced using the oligo capping method where 5'cap on the RNA transcript is removed by enzymes and replaced with an oligo-cap (Maruyama and Sugano, 1994). The published DA117257.1 EST sequence in the BLAST database contains a *MAPT* 5'UTR sequence, exon 1, intron 1 (where it remains in frame) exon 2, does not include exon 3 and ends at exon 4. It is unknown if this transcript is translated, and its function, possibly as a long non-coding RNA, is at present unknown.

Our results suggest that the use of different promoters produce novel alternatively spliced isoforms of *MAPT*. Ratios of alternative spliced transcripts containing tau exons 2,3 and/or 10 could also be modulated by the use of different *MAPT* promoters. And therefore genetic variation in the promoter region of *MAPT* could potentially alter not only transcription levels but also splicing isoform ratios of *MAPT*.

7.2.9. Tau exon 10 splicing in FTDP-17

We found a range of 2.8-4.2 4R/3R average ratios in the brain region tested however some individual brains had 4R/3R ratios of 6.6 in the amygdala and 5.1 in the hippocampus which is above a theoretical maximum 4R/3R ratio of 3. These results may be due to inaccuracies of the technique however Hutton et al. (1998) also found 4R/3R ratios of ~6 in 10+14 FTDP-17 brains in the frontal cortex by RT-PCR. It is possible that expression of the mutant allele decreases stability of 3R transcripts or increases 4R expression in the normal allele however no mechanism has been described for this.

In our study it was apparent that one of the FTDP-17 cases had tau RNA and protein 4R/3R ratios within the control range. We have not directly tested each of the FTPD-17 sample for the presence of the 10+16 mutation however sequencing of intron 10 to determine if all our FTDP-17 samples have the 10+16 mutation needs to be done to confirm this case.

7.2.10. Tau exon 10 splicing in Myotonic Dystrophy, type 1

The single DM1 sample in our study showed decreased exon 10 containing transcripts in the temporal cortex and amygdala and increases in the hippocampus and cerebellum. In DM1 temporal cortex decreased levels of tau exons 2 and 10 and APP exon 7 have been found (Jiang et al., 2004). However Dhaenens et al. (2008) found only 2 brains in 5 had reduced expression of transcripts containing tau exon 10 while reductions in transcripts containing tau exon 2 were reliably reduced in five brain regions suggesting that reduction in E10 containing transcripts occur only in a subset of DM1 brains. Our results are consistent with Dhaenens et al., (2008) and show no consistent decrease in 4R containing transcripts across the different brain regions in our DM1 brain. Myotonic dystrophy type 1 (DM1) is primarily a muscle wasting disease but also involves CNS pathology. NFT are found in the hippocampus and cortical regions (Maurage et al., 2005; Sergeant et al., 2001; Vermersch et al., 1996). DM1 is caused by an expansion mutation of CTG repeats in the 3'UTR of dystrophia myotonica protein kinase (*DMPK*) mRNA (Brook et al., 1992) which alters the levels of available muscleblind-like family splicing factors and phosphorylation of CUG binding protein 1 (CUGBP1; also known as CELF1).

7.3. Lack of correlation between tau and APP transcript levels and TDP-43 pathology

7.3.1 Lack of correlation between Tau transcription and TDP-43 pathology

Levels of total *MAPT* expression were measured by qRT-PCR and no differences in *MAPT* expression were found between control and ADTDP+ and ADTDP- samples in any brain region. This suggests that TDP-43 misregulation in AD does not play a role in altering levels of transcription of *MAPT*.

In frontal or temporal cortex other studies have also shown no differences normalised total *MAPT* RNA levels in AD brain compared to control by qRT-PCR (Hyman et al., 2005; Ingelsson et al., 2006; Ingelsson et al., 2007) however in these studies found no increases in 4R tau transcripts in AD brains. The difference between these results and our results may be due to the fact that these studies have looked at changes in 3R and 4R transcript expression in the frontal and temporal cortex. We found small increases in 4R transcript expression in the frontal cortex but not in the temporal cortex and these areas may be highly variable in 4R/3R tau expression particularly in disease. Ingelsson et al. (2006) also measure 4R and 3R transcript expression in single NFT bearing neurons in the hippocampus by laser capturing microscopy coupled with qRT-PCR from six AD brains. This analysis showed no differences in 4R or 3R tau transcript expression compared to controls however our analysis demonstrates that 4R/3R tau ratio expression is very stable across brain regions and only a subset of AD brains have increased 4R/3R ratios and a sample size of six AD brains may not be enough to demonstrate a difference.

7.3.2. Lack of correlation between APP transcription and TDP-43 pathology

We found no differences in total APP expression were found between control, ADTDP+ and ADTDP- and control samples in any brain region. In DS patients over 50 years of age, plaques are similar in form, number and regional distribution to AD (Mann and Esiri, 1989).Triplications of chromosome 21 cause DS and show that increases in APP expression may increase risk to develop AD (Singleton et al., 2004). however either no differences (Matsui et al., 2007) or decreases (Tharp et al., 2012) in

total APP RNA expression in AD brain compared to control have previously been found by qRT-PCR.

7.4. The role of TDP-43 in splicing misregulation in post-translational processing of MAPT

4R/3R ratios of tau protein from low speed centrifuge and 4R/3R ratios from insoluble material were quantified from human brain in the amygdala. No differences in 4R/3R ratios were found in insoluble tau protein or from low speed centrifuge tau protein between ADTDP- and ADTDP+ brains in the amygdala. 4R/3R RNA ratio correlated with 4R/3R insoluble tau protein ratio in the amygdala and suggests that the stoichiometry of tau protein aggregates relates to the stoichiometry at the RNA level. Total levels of tau RNA were not different between control, ADTDP- and ADTDP+ brains showing that in the subgroup of AD cases with increases in 4R expression the 4R to 3R tau ratio were altered and not levels of total *MAPT*. Soluble tau ratios in AD brains were no different to control and did not correlate with RNA expression and this may be due to various post-transcriptional influences. These influences include RNA concentration and factors that influence the velocity of ribosomal translation including RNA secondary structure (Brockmann et al., 2007). In human post-mortem brain samples heterogeneity of cell type may also contribute to the lack of association between RNA and protein levels (Chen-Plotkin et al., 2010; Okaty et al., 2011).

Luk et al. (2010) correlated relative 4R and 3R RNA levels with combined soluble and insoluble protein 4R and 3R levels from PSP brains and found only a very broad non-significant trend for increases in both 3R and 4R tau RNA isoforms to associate

with increases of 3R and 4R protein. In this study the authors did not correlate tau RNA ratios with insoluble protein ratios.

A relationship between altered splicing ratios at the RNA level and increases in 4R protein isoforms has been demonstrated in FTDP-17 cases with splicing mutations (Connell et al., 2005; Umeda et al., 2004). These mutations cause neurodegeneration and therefore suggest that an excess in either 3R or 4R tau isoforms are associated with neurodegeneration. Our study shows that a sub-group of AD cases also show increased expression of 4R transcripts which are translated in insoluble tau deposits suggesting a common mechanism of neurodegeneration in tauopathies.

7.4.1. 3R and 4R isoforms at the protein level

The correlation between high 4R RNA expression and 4R found in insoluble material suggests that the imbalanced expression of one tau isoform may seed formation of aggregates. The majority of FTDP-17 mutations promote tau exon 10 inclusion and therefore an excess of 4R tau, however there are a few mutations such as L266V, G272V E10+19 and E10+29 which promote exon 10 exclusion resulting in an excess of 3R isoforms (Bronner et al., 2005; Hogg et al., 2003; Stanford et al., 2003).

4R and 3R isoforms have different aggregation properties that may also be dependent on exons 2 and 3 (Adams et al., 2010; Zhong et al., 2012). Propagation of tau aggregates has been shown in vitro and in vivo (de Calignon et al., 2012; Dinkel et al., 2011; Liu et al., 2012) and suggest that tau aggregation seeded in the entorhinal cortex could spread via synaptic connections to limbic, temporal and frontal regions.

On the other hand, functional differences of the two isoforms may provide clues into the disease process. For example, 4R isoforms display different MT stabilising and mitochondrial transport properties compared to 3R isoforms. (Drechsel et al., 1992; Stoothoff et al., 2009).

Our results suggest that imbalances in tau exon 10 expression in a subset of AD cases may share the same pathogenic mechanism as FTLD cases.

7.5. The role of TDP-43 modulating tau pathology

We found tau AT8 immunoreactivity scores were higher in the frontal and temporal cortices, in particular, threads and neuritic plaques were found to be significantly higher in ADTDP+ brains compared to ADTDP- brains. Higher AT8 staining relates to severity of tau inclusions and therefore the ADTDP+ brains had significantly greater severity of tau pathology compared to ADTDP- brains in the frontal and temporal cortex.

We found no differences in severity of tau pathology in the amygdala or hippocampus, however there were significant ceiling effects in the semi-quantitative scoring of tau severity in the amygdala and hippocampus and therefore our results may underestimate the severity of tau pathology in these regions.

Arai et al. (2009) found that in the amygdala, hippocampus, and temporal cortex of AD brains, Braak NFT stage was higher in cases with pTDP-43 pathology compared to those without however these authors note that the ADTDP+ group were on average

older than the ADTDP- group and therefore aging may account for the increases in Braak stage found in ADTDP+ cases. There were no differences in age between ADTDP- and ADTDP+ cases in our analysis however disease duration and other co-pathologies such as Lewy bodies that may contribute to tau pathology were not measured in our study (Popescu et al., 2004).

In AD brains with TDP-43 inclusions, the amygdala and hippocampus are consistently affected with TDP-43 pathology (Amador-Ortiz et al., 2007; Arai et al., 2009; Hu et al., 2008). TDP-43 inclusions in AD cases are also consistently associated with HS and it has been proposed that tau and TDP-43 pathologies combine and may cause greater neuronal loss in the hippocampus (Probst et al., 2007). HS in AD is regarded as neuronal loss in the hippocampus disproportionate to the amount of NFT present in the hippocampus (Amador-Ortiz et al., 2007; Pao et al., 2011).

These findings have remarkable parallels with Lewy body (LB) and tau co-existent pathology within the amygdala of AD and PiD brains (Popescu et al., 2004) and suggest that limbic regions have a propensity for co-pathologies. Around 50% of AD cases also have LBs (Jellinger, 2004) and LBs colocalise with NFT in many cases (Galpern and Lang, 2006; Popescu et al., 2004). Lewy bodies are composed predominantely of α-synuclein and are the pathological hallmark of a group of diseases collectively known as synucleinopathies which include Parkinson's Disease (PD), Dementia with Lewy bodies (DLB) and multiple system atrophy.

The association between tau and α-synuclein suggests that tau inclusions could directly or indirectly promote the fibrillation of α-synuclein to form LBs in regions

with abundant NFT, and suggest that tau and may also promote TDP-43 inclusion formation. Tau and α-synuclein aggregation is dependent on altered conformation of proteins into β-sheet aggregates. The prion domain of TDP-43 is also capable of altered conformation into β-sheets (Fuentealba et al., 2010; Soto, 2012; Udan and Baloh, 2011) and suggests that tau may cross-seed TDP-43 aggregation.

Cross-seeding of aggregated proteins has been demonstrated between Aβ and α-synuclein (Tsigelny et al., 2008). These authors demonstrated that Aβ and α-synuclein directly interact in the brains of patients with Lewy body disease and in APP/ α-synuclein double knock-in mice and form ring-like structures (Tsigelny et al., 2008).

Convincing evidence has been accumulating that Aβ and tau aggregation are propagated by mechanisms that are similar to the infectivity of prions (for recent reviews see (Soto, 2012; Walker and LeVine, 2012)) suggesting that once aggregation is initiated at one foci, it spreads to other brain regions via synaptic connections (de Calignon et al., 2012; Liu et al., 2012).

At present it is not clear why co-pathologies occur in some AD brains and not others. TDP-43 inclusions in AD may be due to a propensity for aggregation that has no interaction with tau. The association we found between TDP-43 pathology and increased tau severity suggests that there is an interaction, however if TDP-43 exacerbates tau pathology or high concentration of β-sheet containing tau aggregates causes cross-seeding of TDP-43 pathology is not known. Another possibility is altered levels of a co-factor in disease that results in aggregation in both TDP-43 and tau.

We found no relationship between severity of tau pathology and tau protein 4R/3R ratios from insoluble or from low speed centrifuge material. These results suggest that high levels of 4R tau protein were not associated with the level of AT8 immunoreactivity however total levels of insoluble tau protein may be a better correlate with the severity of tau pathologybecause in AD both 3R and 4R isoforms are found in insoluble NFTs. TDP-43 misregulation does not alter tau protein or RNA isoform levels through altered transcription or post-transcriptional processing and therefore the association between increased severity of tau pathology and presence of TDP-43 inclusions may not be dependent on altered tau splicing ratios or transcript expression however immunohistology with antibodies that recognise 4R or 3R tau could be carried out. Our results are in line with Ingelsson et al. (2006) where they correlated 4R and 3R levels of RNA expression with stereologically measured tau NFT density in the temporal cortex and found no association.

7.6. Autoregulation of TDP-43 in Alzheimer's disease

The 3'UTR of TDP-43 is a confirmed autoregulatory splicing target of TDP-43 in HEK 293 cells (Avendaño-Vázquez et al., 2012; Ayala et al., 2011; Polymenidou et al., 2011; Tollervey et al., 2011a) and we show that a 3'UTR spliced TDP-43 isoform pA2 is produced in human brain. We found a consistent decrease in the pA2 transcript in AD brains with TDP-43 inclusions compared to control and AD brains without TDP-43 inclusions however these results did not reach significance. A significant reduction in pA2 transcripts was found in FTLD-TDP samples from the frontal and temporal cortices, hippocampus and amygdala. The significant finding in the temporal cortex was predominantly due to a single sample which has the *C9ORF72*

hexanucleotide repeat. These results show that a detectable altered splicing ratio was found for a confirmed TDP-43 target and suggests that there is a loss of TDP-43 function in TDP-proteinopathies. The reduction in the pA2 TDP-43 isoform may be due to a reduction of TDP-43 splicing activity because of nuclear clearance of TDP-43 protein into inclusions. The significance of the reduction in pA2 isoforms in the *C9ORF72* sample needs to be validated in more samples.

Mishra et al. (2007) has found TDP-43 transcripts were increased 1.5 fold in FTLD-TDP brains compared to controls measured by microarray. Our results demonstrate altered autoregulation of TDP-43 and suggest that TDP-43 RNA and possibly protein levels are altered in TDP-43 proteinopathies.

7.7. Future directions

We have shown a sub-grouping of AD cases however our sample size is small and therefore these findings should be replicated in a larger sample of AD and control cases. Altered splicing found in the AD subgroup may be due to cis- acting elements or trans- acting factors. We were not able to show differences in splicing or transcription for the tau H1 haplotype compared to the H2 haplotype however a larger sample is needed for this analysis. Other common or rare SNPs or indels may alter splicing in the AD subgroup and sequencing of the promoter region of tau and APP as well as intronic and exonic regions around exon 10 of tau and exons 7 and 8 of APP may show if genetic variation in these genes contribute to altered splicing ratios found these cases. Levels of splicing factors have been shown to be altered in neurodegenerative disease. Global changes in RNA levels of splicing factors could be

measured by microarray in our AD subgroup compared to AD and control groups. Specific splicing factors that were found to be reduced could be further tested by qRT-PCR and protein levels measured by western blotting.

We show that TDP-43 3'UTR splicing was significantly reduced in FTLD cases compared to controls and in AD brains with TDP-43 inclusions there was a consistent trend for reduced TDP-43 3'UTR splice isoforms compared to controls and AD cases without TDP-43 inclusions however this finding was not significant. TDP-43 3'UTR splicing is the key event in autoregulation of TDP-43 and in HEK cells two routes have been reported, nuclear retention being the predominant mechanism and only minor involvement of NMD. We found 3'UTR splicing occurs in human brain and may be altered in disease and further investigation of the role of TDP-43 autoregulation in disease is warranted.

7.8. Conclusions

This study aimed to analyse tau and APP splicing in relation with the presence of TDP-43 pathology and the molecular pathology in AD.

Altered tau splicing causes neurodegeneration in FTDP-17 and splicing imbalances are associated with other tauopathies however it was not clear if altered tau splicing plays a role in AD. We found that a subset of AD cases can be defined by imbalances in tau 4R expression. We also found that increased expression of tau 4R isoforms at the RNA level correlated with increased insoluble tau 4R and show that the stoichiometry of tau protein aggregates reflects the stoichiometry at the RNA level.

Imbalances in tau isoform ratios at the RNA level are also found at the insoluble tau protein level in FTDP-17 brains. Our results show that the pathway toward tau pathology associated with tau splicing imbalances also contributes to AD pathology in a subset of AD cases.

Increased severity of tau pathology was associated with the presence of TDP-43 inclusions and this association suggests an interaction between the two pathologies.

No association was found between TDP-43 inclusions and altered tau and APP splicing or transcription however we found correlated increases in 4R and APP exon 7 isoforms in a subset of AD cases.

Autoregulatory splicing in AD brain with TDP-43 inclusions was not significantly altered compared to control and AD brain without TDP-43 inclusions however there was a consistent trend for a reduction in TDP-43 isoforms associated with autoregulation. There was significantly reduced expression of the pA2 isoform in FTLD brain compared to control showing that FTLD-TDP brains have altered TDP-43 autoregulation. Whether this is due to a reduction of TDP-43 splicing activity because of nuclear clearance of TDP-43 protein into inclusions is not known. This analysis suggests that TDP-43 autoregulation is altered in TDP-43 proteinopathies and possibly more severely in brains harbouring the *C9ORF72* expansion and is worth further investigation.

Bibliography

Adams, S.J., DeTure, M.A., McBride, M., Dickson, D.W., and Petrucelli, L. (2010). Three repeat isoforms of tau inhibit assembly of four repeat tau filaments. PLoS One 5, e10810.

Aguzzi, A. (2009). Cell biology: Beyond the prion principle. Nature 459, 924-925.

Aguzzi, A., and Rajendran, L. (2009). The transcellular spread of cytosolic amyloids, prions, and prionoids. Neuron 64, 783-790.

Al-Sarraj, S., King, A., Troakes, C., Smith, B., Maekawa, S., Bodi, I., Rogelj, B., Al-Chalabi, A., Hortobágyi, T., and Shaw, C.E. (2011). p62 positive, TDP-43 negative, neuronal cytoplasmic and intranuclear inclusions in the cerebellum and hippocampus define the pathology of *C9orf72*-linked FTLD and MND/ALS. Acta Neuropathol (Berl) 122, 691-702.

Alafuzoff, I., Thal, D., Arzberger, T., Bogdanovic, N., Al-Sarraj, S., Bodi, I., Boluda, S., Bugiani, O., Duyckaerts, C., Gelpi, E., *et al.* (2009). Assessment of β-amyloid deposits in human brain: a study of the BrainNet Europe Consortium. Acta Neuropathol (Berl) 117, 309-320.

Alberti, S., Halfmann, R., King, O., Kapila, A., and Lindquist, S. (2009). A systematic survey identifies prions and illuminates sequence features of prionogenic proteins. Cell 137, 146-158.

Amador-Ortiz, C., Lin, W.L., Ahmed, Z., Personett, D., Davies, P., Duara, R., Graff-Radford, N.R., Hutton, M.L., and Dickson, D.W. (2007). TDP-43 immunoreactivity in hippocampal sclerosis and Alzheimer's disease. Ann Neurol 61, 435-445.

Andersen, P.M., and Al-Chalabi, A. (2011). Clinical genetics of amyotrophic lateral sclerosis: what do we really know? Nat Rev Neurol 7, 603-615.

Anderson, P., and Kedersha, N. (2002). Stressful initiations. J Cell Sci 115, 3227-3234.

Anderson, P., and Kedersha, N. (2008). Stress granules: the Tao of RNA triage. Trends Biochem Sci 33, 141-150.

Andorfer, C., Kress, Y., Espinoza, M., De Silva, R., Tucker, K.L., Barde, Y.-A., Duff, K., and Davies, P. (2003). Hyperphosphorylation and aggregation of tau in mice expressing normal human tau isoforms. J Neurochem 86, 582-590.

Andreadis, A. (2005). Tau gene alternative splicing: expression patterns, regulation and modulation of function in normal brain and neurodegenerative diseases. Biochim Biophys Acta 1739, 91-103.

Andreadis, A. (2006). Misregulation of tau alternative splicing in neurodegeneration and dementia. Prog Mol Subcell Biol 44, 89-107.

Andreadis, A., Broderick, J.A., and Kosik, K.S. (1995). Relative exon affinities and suboptimal splice site signals lead to non-equivalence of two cassette exons. Nucleic Acids Res 23, 3585-3593.

Andreadis, A., Brown, W.M., and Kosik, K.S. (1992). Structure and novel exons of the human tau gene. Biochemistry 31, 10626-10633.

Andreadis, A., Wagner, B.K., Broderick, J.A., and Kosik, K.S. (1996). A τ promoter region without neuronal specificity. J Neurochem 66, 2257-2263.

Anthony, K., and Gallo, J.-M. (2010). Aberrant RNA processing events in neurological disorders. Brain Res 1338, 67-77.

Arai, T., Ikeda, K., Akiyama, H., Shikamoto, Y., Tsuchiya, K., Yagishita, S., Beach, T., Rogers, J., Schwab, C., and McGeer, P.L. (2001). Distinct isoforms of tau aggregated in neurons and glial cells in brains of patients with Pick's disease, corticobasal degeneration and progressive supranuclear palsy. Acta Neuropathol (Berl) 101, 167-173.

Arai, T., Mackenzie, I.R., Hasegawa, M., Nonoka, T., Niizato, K., Tsuchiya, K., Iritani, S., Onaya, M., and Akiyama, H. (2009). Phosphorylated TDP-43 in Alzheimer's disease and dementia with Lewy bodies. Acta Neuropathol 117, 125-136.

Arikan, M.C., Memmott, J., Broderick, J.A., Lafyatis, R., Screaton, G., Stamm, S., and Andreadis, A. (2002). Modulation of the membrane-binding projection domain of tau protein: splicing regulation of exon 3. Mol Brain Res 101, 109-121.

Augustinack, J., Schneider, A., Mandelkow, E.-M., and Hyman, B. (2002). Specific tau phosphorylation sites correlate with severity of neuronal cytopathology in Alzheimer's disease. Acta Neuropathol (Berl) 103, 26-35.

Avale, M.E., Rodriguez-Martin, T., and Gallo, J.M. (2013). Trans-splicing correction of tau isoform imbalance in a mouse model of tau mis-splicing. Hum Mol Genet 22, 2603-2611.

Avendaño-Vázquez, S.E., Dhir, A., Bembich, S., Buratti, E., Proudfoot, N., and Baralle, F.E. (2012). Autoregulation of TDP-43 mRNA levels involves interplay between transcription, splicing, and alternative polyA site selection. Genes Dev 26, 1679-1684.

Ayala, Y.M., De Conti, L., Avendano-Vazquez, S.E., Dhir, A., Romano, M., D'Ambrogio, A., Tollervey, J., Ule, J., Baralle, M., Buratti, E., and Baralle, F.E. (2011). TDP-43 regulates its mRNA levels through a negative feedback loop. EMBO J 30, 277-288.

Ayala, Y.M., Misteli, T., and Baralle, F.E. (2008). TDP-43 regulates retinoblastoma protein phosphorylation through the repression of cyclin-dependent kinase 6 expression. Proc Natl Acad Sci USA 105, 3785-3789.

Babu, M.M., van der Lee, R., de Groot, N.S., and Gsponer, J. (2011). Intrinsically disordered proteins: regulation and disease. Curr Opin Struct Biol 21, 432-440.

Bahn, S., Augood, S.J., Ryan, M., Standaert, D.G., Starkey, M., and Emson, P.C. (2001). Gene expression profiling in the post-mortem human brain--no cause for dismay. J Chem Neuroanat 22, 79-94.

Baker, M., Litvan, I., Houlden, H., Adamson, J., Dickson, D., Perez-Tur, J., Hardy, J., Lynch, T., Bigio, E., and Hutton, M. (1999). Association of an extended haplotype in the tau gene with progressive supranuclear palsy. Hum Mol Genet 8, 711-715.

Baker, M., Mackenzie, I.R., Pickering-Brown, S.M., Gass, J., Rademakers, R., Lindholm, C., Snowden, J., Adamson, J., Sadovnick, A.D., Rollinson, S., *et al.* (2006). Mutations in progranulin cause tau-negative frontotemporal dementia linked to chromosome 17. Nature 442, 916-919.

Bales, K.R., Du, Y., Holtzman, D., Cordell, B., and Paul, S.M. (2000). Neuroinflammation and Alzheimer's disease: critical roles for cytokine/Aβ-induced glial activation, NF-κB, and apolipoprotein E. Neurobiol Aging 21, 427-432.

Ballatore, C., Lee, V.M.Y., and Trojanowski, J.Q. (2007). Tau-mediated neurodegeneration in Alzheimer's disease and related disorders. Nat Rev Neurosci 8, 663-672.

Bancher, C., Brunner, C., Lassmann, H., Budka, H., Jellinger, K., Wiche, G., Seitelberger, F., Grundke-Iqbal, I., Iqbal, K., and Wisniewski, H.M. (1989). Accumulation of abnormally phosphorylated τau precedes the formation of neurofibrillary tangles in Alzheimer's disease. Brain Res 477, 90-99.

Barghorn, S., and Mandelkow, E. (2002). Toward a unified scheme for the aggregation of tau into Alzheimer paired helical filaments. Biochemistry 41, 14885-14896.

Barton, A.J., Pearson, R.C., Najlerahim, A., and Harrison, P.J. (1993). Pre- and postmortem influences on brain RNA. J Neurochem 61, 1-11.

Bauer, J., Ganter, U., Strauss, S., Stadtmüller, G., Frommberger, U., Bauer, H., Volk, B., and Berger, M. (1992). The participation of interleukin-6 in the pathogenesis of alzheimer's disease. Res Immunol 143, 650-657.

Bauer, J., Strauss, S., Schreiter-Gasser, U., Ganter, U., Schlegel, P., Witt, I., Yolk, B., and Berger, M. (1991). Interleukin-6 and α-2-macroglobulin indicate an acute-phase state in Alzheimer's disease cortices. FEBS Lett 285, 111-114.

Bertram, L., McQueen, M.B., Mullin, K., Blacker, D., and Tanzi, R.E. (2007). Systematic meta-analyses of Alzheimer disease genetic association studies: the AlzGene database. Nat Genet 39, 17-23.

Bhaskar, K., Konerth, M., Kokiko-Cochran, O.N., Cardona, A., Ransohoff, R.M., and Lamb, B.T. (2010). Regulation of tau pathology by the microglial fractalkine receptor. Neuron 68, 19-31.

Bhuvanagiri, M., Schlitter, A.M., Hentze, M.W., and Kulozik, A.E. (2010). NMD: RNA biology meets human genetic medicine. Biochem J 430, 365-377.

Biedler, J.L., Helson, L., and Spengler, B.A. (1973). Morphology and growth, tumorigenicity, and cytogenetics of human neuroblastoma cells in continuous culture. Cancer Res 33, 2643-2652.

Bigio, E.H., Mishra, M., Hatanpaa, K.J., White, C.L., 3rd, Johnson, N., Rademaker, A., Weitner, B.B., Deng, H.X., Dubner, S.D., Weintraub, S., and Mesulam, M. (2010). TDP-43 pathology in primary progressive aphasia and frontotemporal dementia with pathologic Alzheimer disease. Acta Neuropathol (Berl) 120, 43-54.

Birdsill, A.C., Walker, D.G., Lue, L., Sue, L.I., and Beach, T.G. (2011). Postmortem interval effect on RNA and gene expression in human brain tissue. Cell Tissue Bank 12, 311-318.

Blass, D.M., Hatanpaa, K.J., Brandt, J., Rao, V., Steinberg, M., Troncoso, J.C., and Rabins, P.V. (2004). Dementia in hippocampal sclerosis resembles frontotemporal dementia more than Alzheimer disease. Neurol 63, 492-497.

Boche, D., Perry, V.H., and Nicoll, J.A. (2013). Review: activation patterns of microglia and their identification in the human brain. Neuropathol Applied Neurobiol 39, 3-18.

Boeve, B.F., Lang, A.E., and Litvan, I. (2003). Corticobasal degeneration and its relationship to progressive supranuclear palsy and frontotemporal dementia. Ann Neurol 54, S15-S19.

Boutajangout, A., Boom, A., Leroy, K., and Brion, J.P. (2004). Expression of tau mRNA and soluble tau isoforms in affected and non-affected brain areas in Alzheimer's disease. FEBS Lett 576, 183-189.

Boutz, P.L., Stoilov, P., Li, Q., Lin, C.-H., Chawla, G., Ostrow, K., Shiue, L., Ares, M., and Black, D.L. (2007). A post-transcriptional regulatory switch in polypyrimidine tract-binding proteins reprograms alternative splicing in developing neurons. Genes Dev 21, 1636-1652.

Braak, E., Braak, H., and Mandelkow, E.M. (1994). A sequence of cytoskeleton changes related to the formation of neurofibrillary tangles and neuropil threads. Acta Neuropathol (Berl) 87, 554-567.

Braak, H., and Braak, E. (1991). Neuropathological stageing of Alzheimer-related changes. Acta Neuropathol (Berl) 82, 239-259.

Braak, H., Thal, D.R., Ghebremedhin, E., and Del Tredici, K. (2011). Stages of the pathologic process in Alzheimer disease: age categories from 1 to 100 years. J Neuropathol Exp Neurol 70, 960-969.

Bramblett, G.T., Goedert, M., Jakes, R., Merrick, S.E., Trojanowski, J.Q., and Lee, V.M.Y. (1993). Abnormal tau phosphorylation at Ser396 in alzheimer's disease recapitulates development and contributes to reduced microtubule binding. Neuron 10, 1089-1099.

Brandt, R., Leger, J., and Lee, G. (1995). Interaction of tau with the neural plasma membrane mediated by tau's amino-terminal projection domain. J Cell Biol 131, 1327-1340.

Bras, J., Guerreiro, R., and Hardy, J. (2012). Use of next-generation sequencing and other whole-genome strategies to dissect neurological disease. Nat Rev Neurosci 13, 453-464.

Brockmann, R., Beyer, A., Heinisch, J.J., and Wilhelm, T. (2007). Posttranscriptional expression regulation: what determines translation rates? PLoS Comput Biol 3, e57.

Brogna, S., and Wen, J. (2009). Nonsense-mediated mRNA decay (NMD) mechanisms. Nat Struct Mol Biol 16, 107-113.

Bronner, I.F., ter Meulen, B.C., Azmani, A., Severijnen, L.A., Willemsen, R., Kamphorst, W., Ravid, R., Heutink, P., and van Swieten, J.C. (2005). Hereditary Pick's disease with the G272V tau mutation shows predominant three-repeat tau pathology. Brain 128, 2645-2653.

Brook, J.D., McCurrach, M.E., Harley, H.G., Buckler, A.J., Church, D., Aburatani, H., Hunter, K., Stanton, V.P., Thirion, J.P., and Hudson, T. (1992). Molecular basis of myotonic dystrophy: expansion of a trinucleotide (CTG) repeat at the 3' end of a transcript encoding a protein kinase family member. Cell 68, 799-808.

Brouwers, N., Sleegers, K., Engelborghs, S., Bogaerts, V., Serneels, S., Kamali, K., Corsmit, E., Leenheir, E.D., Martin, J.-J., De Deyn, P.P., *et al.* (2006). Genetic risk and transcriptional variability of amyloid precursor protein in Alzheimer's disease. Brain 129, 2984-2991.

Brugg, B., Dubreuil, Y.L., Huber, G., Wollman, E.E., Delhaye-Bouchaud, N., and Mariani, J. (1995). Inflammatory processes induce beta-amyloid precursor protein changes in mouse brain. Proc Natl Acad Sci USA 92, 3032-3035.

Brun, A., Liu, X., and Erikson, C. (1995). Synapse loss and gliosis in the molecular layer of the cerebral cortex in Alzheimer's disease and in frontal lobe degeneration. Neurodegeneration 4, 171-177.

Budini, M., Buratti, E., Stuani, C., Guarnaccia, C., Romano, V., De Conti, L., and Baralle, F.E. (2012). Cellular model of TAR DNA-binding protein 43 (TDP-43) aggregation based on its C-terminal Gln/Asn-rich region. J Biol Chem 287, 7512-7525.

Buée, L., and Delacourte, A. (1999). Comparative biochemistry of tau in Progressive Supranuclear Palsy, Corticobasal Degeneration, FTDP-17 and Pick's Disease. Brain Pathol 9, 681-693.

Buratti, E., and Baralle, F.E. (2001). Characterization and functional implications of the RNA binding properties of nuclear factor TDP-43, a novel splicing regulator of CFTR exon 9. J Biol Chem 276, 36337-36343.

Buratti, E., and Baralle, F.E. (2008). Multiple roles of TDP-43 in gene expression, splicing regulation, and human disease. Front Biosci 13, 867-878.

Buratti, E., De Conti, L., Stuani, C., Romano, M., Baralle, M., and Baralle, F. (2010). Nuclear factor TDP-43 can affect selected microRNA levels. FEBS J 277, 2268-2281.

Buratti, E., Dork, T., Zuccato, E., Pagani, F., Romano, M., and Baralle, F.E. (2001). Nuclear factor TDP-43 and SR proteins promote in vitro and in vivo CFTR exon 9 skipping. EMBO J 20, 1774-1784.

Burke, W.J., O'Malley, K.L., Chung, H.D., Harmon, S.K., Philip Miller, J., and Berg, L. (1991). Effect of pre- and postmortem variables on specific mRNA levels in human brain. Mol Brain Res 11, 37-41.

Butler, A.W., Ng, M.Y., Hamshere, M.L., Forabosco, P., Wroe, R., Al-Chalabi, A., Lewis, C.M., and Powell, J.F. (2009). Meta-analysis of linkage studies for Alzheimer's disease--a web resource. Neurobiol Aging 30, 1037-1047.

Butner, K.A., and Kirschner, M.W. (1991). Tau protein binds to microtubules through a flexible array of distributed weak sites. J Cell Biol 115, 717-730.

Caffrey, T.M., Joachim, C., Paracchini, S., Esiri, M.M., and Wade-Martins, R. (2006). Haplotype-specific expression of exon 10 at the human MAPT locus. Hum Mol Genet 15, 3529-3537.

Caffrey, T.M., Joachim, C., and Wade-Martins, R. (2008). Haplotype-specific expression of the N-terminal exons 2 and 3 at the human MAPT locus. Neurobiol Aging 29, 1923-1929.

Caffrey, T.M., and Wade-Martins, R. (2007). Functional MAPT haplotypes: bridging the gap between genotype and neuropathology. Neurobiol Dis 27, 1-10.

Cameron, B., and Landreth, G.E. (2010). Inflammation, microglia, and Alzheimer's disease. Neurobiol Dis 37, 503-509.

Cannon, A., Yang, B., Knight, J., Farnham, I., Zhang, Y., Wuertzer, C., D'Alton, S., Lin, W.-l., Castanedes-Casey, M., Rousseau, L., *et al.* (2012). Neuronal sensitivity to TDP-43 overexpression is dependent on timing of induction. Acta Neuropathol (Berl) 123, 807-823.

Chambers, C.B., Lee, J.M., Troncoso, J.C., Reich, S., and Muma, N.A. (1999). Overexpression of four-repeat tau mRNA isoforms in progressive supranuclear palsy but not in Alzheimer's disease. Ann Neurol 46, 325-332.

Chapple, J.P., Anthony, K., Martin, T.R., Dev, A., Cooper, T.A., and Gallo, J.M. (2007). Expression, localization and tau exon 10 splicing activity of the brain RNA-binding protein TNRC4. Hum Mol Genet 16, 2760-2769.

Chauvet, N., Apert, C., Dumoulin, A., Epelbaum, J., and Alonso, G. (1997). Mab22C11 antibody to amyloid precursor protein recognizes a protein associated with specific astroglial cells of the rat central nervous system characterized by their capacity to support axonal outgrowth. J Comp Neurol 377, 550-564.

Chen-Plotkin, A., Xiao, J., Geser, F., Martinez-Lage, M., Grossman, M., Unger, T., Wood, E., Van Deerlin, V., Trojanowski, J., and Lee, V. (2010). Brain progranulin expression in GRN -associated frontotemporal lobar degeneration. Acta Neuropathol (Berl) 119, 111-122.

Chen, J., Kanai, Y., Cowan, N.J., and Hirokawa, N. (1992). Projection domains of MAP2 and tau determine spacings between microtubules in dendrites and axons. Nature 360, 674-677.

Chien, P., Weissman, J.S., and DePace, A.H. (2004). Emerging principles of confrmation-based prion inheritance. Annu Rev Biochem 73, 617-656.

Clark, A.W., Krekoski, C.A., Parhad, I.M., Liston, D., Julien, J.-P., and Hoar, D.I. (1989). Altered expression of genes for amyloid and cytoskeletal proteins in Alzheimer cortex. Ann Neurol 25, 331-339.

Colombrita, C., Zennaro, E., Fallini, C., Weber, M., Sommacal, A., Buratti, E., Silani, V., and Ratti, A. (2009). TDP-43 is recruited to stress granules in conditions of oxidative insult. J Neurochem 111, 1051-1061.

Connell, J.W., Rodriguez-Martin, T., Gibb, G.M., Kahn, N.M., Grierson, A.J., Hanger, D.P., Revesz, T., Lantos, P.L., Anderton, B.H., and Gallo, J.M. (2005). Quantitative analysis of tau isoform transcripts in sporadic tauopathies. Mol Brain Res 137, 104-109.

Conrad, C., Zhu, J., Schoenfeld, D., Fang, Z., Ingelsson, M., Stamm, S., Church, G., and Hyman, B.T. (2007). Single molecule profiling of tau gene expression in Alzheimer's disease. J Neurochem 103, 1228-1236.

Corder, E.H., Saunders, A.M., Risch, N.J., Strittmatter, W.J., Schmechel, D.E., Gaskell, P.C., Jr., Rimmler, J.B., Locke, P.A., Conneally, P.M., Schmader, K.E., and et al. (1994). Protective effect of apolipoprotein E type 2 allele for late onset Alzheimer disease. Nat Genet 7, 180-184.

Corder, E.H., Saunders, A.M., Strittmatter, W.J., Schmechel, D.E., Gaskell, P.C., Small, G.W., Roses, A.D., Haines, J.L., and Pericak-Vance, M.A. (1993). Gene dose of apolipoprotein E type 4 allele and the risk of Alzheimer's disease in late onset families. Science 261, 921-923.

Cribbs, D.H., Berchtold, N.C., Perreau, V., Coleman, P.D., Rogers, J., Tenner, A.J., and Cotman, C.W. (2012). Extensive innate immune gene activation accompanies brain aging, increasing vulnerability to cognitive decline and neurodegeneration: a microarray study. J Neuroinflammation 9, 179.

Crowther, R.A., and Goedert, M. (2000). Abnormal tau-containing filaments in neurodegenerative diseases. J Struc Biol 130, 271-279.

D'Souza, I., Poorkaj, P., Hong, M., Nochlin, D., Lee, V.M.Y., Bird, T.D., and Schellenberg, G.D. (1999). Missense and silent tau gene mutations cause frontotemporal dementia with parkinsonism-chromosome 17 type, by affecting multiple alternative RNA splicing regulatory elements. Proc Natl Acad Sci USA 96, 5598-5603.

D'Souza, I., and Schellenberg, G.D. (2000). Determinants of 4-Repeat Tau Expression: Coordination between enhancing and inhibitory splicing sequences for exon 10 inclusion. J Biol Chem 275, 17700-17709.

Davalos, D., Grutzendler, J., Yang, G., Kim, J.V., Zuo, Y., Jung, S., Littman, D.R., Dustin, M.L., and Gan, W.B. (2005). ATP mediates rapid microglial response to local brain injury in vivo. Nat Neurosci 8, 752-758.

Davidson, Y., Raby, S., Foulds, P., Robinson, A., Thompson, J., Sikkink, S., Yusuf, I., Amin, H., DuPlessis, D., Troakes, C., *et al.* (2011). TDP-43 pathological changes in early onset familial and sporadic Alzheimer's disease, late onset Alzheimer's disease and Down's Syndrome: association with age, hippocampal sclerosis and clinical phenotype. Acta Neuropathol (Berl) 122, 703-713.

De Conti, L., Baralle, M., and Buratti, E. (2012). Exon and intron definition in pre-mRNA splicing. RNA.

de Silva, R., Jen, A., Wickenden, C., Jen, L.-S., Wilkinson, S.L., and Patel, A.J. (1997). Cell-specific expression of β-amyloid precursor protein isoform mRNAs and proteins in neurons and astrocytes. Mol Brain Res 47, 147-156.

de Silva, R., Lashley, T., Gibb, G., Hanger, D., Hope, A., Reid, A., Bandopadhyay, R., Utton, M., Strand, C., Jowett, T., *et al.* (2003). Pathological inclusion bodies in tauopathies contain distinct complements of tau with three or four microtubule-binding repeat domains as demonstrated by new specific monoclonal antibodies. Neuropathol Applied Neurobiol 29, 288-302.

de Silva, R., Lashley, T., Strand, C., Shiarli, A.-M., Shi, J., Tian, J., Bailey, K., Davies, P., Bigio, E., Arima, K., *et al.* (2006). An immunohistochemical study of cases of sporadic and inherited frontotemporal lobar degeneration using 3R- and 4R-specific tau monoclonal antibodies. Acta Neuropathol (Berl) 111, 329-340.

de Calignon, A., Polydoro, M., Suárez-Calvet, M., William, C., Adamowicz, David H., Kopeikina, Kathy J., Pitstick, R., Sahara, N., Ashe, Karen H., Carlson, George A., *et al.* (2012). Propagation of tau pathology in a model of early Alzheimer's disease. Neuron 73, 685-697.

DeJesus-Hernandez, M., Mackenzie, I.R., Boeve, B.F., Boxer, A.L., Baker, M., Rutherford, N.J., Nicholson, A.M., Finch, N.A., Flynn, H., Adamson, J., *et al.* (2011). Expanded GGGGCC hexanucleotide repeat in noncoding region of C9ORF72 causes chromosome 9p-linked FTD and ALS. Neuron 72, 245-256.

Delacourte, A., Robitaille, Y., Sergeant, N., Buée, L., Hof, P.R., Wattez, A., Laroche-Cholette, A., Mathieu, J., Chagnon, P., and Gauvreau, D. (1996). Specific Pathological Tau Protein Variants Characterize Pick's Disease. Journal of Neuropathology & Experimental Neurology 55, 159-168.

Dery, M.A., Michaud, M.D., and Richard, D.E. (2005). Hypoxia-inducible factor 1: regulation by hypoxic and non-hypoxic activators. Int J Biochem Cell Biol 37, 535-540.

Dewey, C.M., Cenik, B., Sephton, C.F., Dries, D.R., Mayer, P., Good, S.K., Johnson, B.A., Herz, J., and Yu, G. (2011). TDP-43 is directed to stress granules by sorbitol, a novel physiological osmotic and oxidative stressor. Mol Cell Biol 31, 1098-1108.

Dewey, C.M., Cenik, B., Sephton, C.F., Johnson, B.A., Herz, J., and Yu, G. (2012). TDP-43 aggregation in neurodegeneration: Are stress granules the key? Brain Res 1462, 16-25.

Dhaenens, C.M., Schraen-Maschke, S., Tran, H., Vingtdeux, V., Ghanem, D., Leroy, O., Delplanque, J., Vanbrussel, E., Delacourte, A., Vermersch, P., *et al.* (2008). Overexpression of MBNL1 fetal isoforms and modified splicing of Tau in the DM1 brain: Two individual consequences of CUG trinucleotide repeats. Exp Neurol 210, 467-478.

Dickson, D.W. (1999). Neuropathologic differentiation of progressive supranuclear palsy and corticobasal degeneration. J Neurol 246, II6-II15.

Dickson, D.W., Baker, M., and Rademakers, R. (2010). Common variant in GRN is a genetic risk factor for hippocampal sclerosis in the elderly. Neurodegen Dis 7, 170-174.

Dinkel, P.D., Siddiqua, A., Huynh, H., Shah, M., and Margittai, M. (2011). Variations in filament conformation dictate seeding barrier between three- and four- repeat tau. Biochemistry 50, 4330-4336.

Dixit, R., Ross, J.L., Goldman, Y.E., and Holzbaur, E.L.F. (2008). Differential regulation of dynein and kinesin motor proteins by tau. Science 319, 1086-1089.

Doi, H., Koyano, S., Suzuki, Y., Nukina, N., and Kuroiwa, Y. (2010). The RNA-binding protein FUS/TLS is a common aggregate-interacting protein in polyglutamine diseases. Neurosci Res 66, 131-133.

Donev, R., Newall, A., Thome, J., and Sheer, D. (2007). A role for SC35 and hnRNPA1 in the determination of amyloid precursor protein isoforms. Mol Psychiatry 12, 681-690.

Drechsel, D.N., Hyman, A.A., Cobb, M.H., and Kirschner, M.W. (1992). Modulation of the dynamic instability of tubulin assembly by the microtubule-associated protein tau. Mol Biol Cell 3, 1141-1154.

Dreyfuss, G., Kim, V.N., and Kataoka, N. (2002). Messenger-RNA-binding proteins and the messages they carry. Nat Rev Mol Cell Biol 3, 195-205.

Durrenberger, P.F., Fernando, S., Kashefi, S.N., Ferrer, I., Hauw, J.J., Seilhean, D., Smith, C., Walker, R., Al-Sarraj, S., Troakes, C., *et al.* (2010). Effects of antemortem and postmortem variables on human brain mRNA quality: a BrainNet Europe study. J Neuropathol Exp Neurol 69, 70-81.

Fabian, M.R., Sonenberg, N., and Filipowicz, W. (2010). Regulation of mRNA translation and stability by microRNAs. Annu Rev Biochem 79, 351-379.

Fassbender, K., Walter, S., Kuhl, S., Landmann, R., Ishii, K., Bertsch, T., Stalder, A.K., Muehlhauser, F., Liu, Y., Ulmer, A.J., *et al.* (2004). The LPS receptor (CD14) links innate immunity with Alzheimer's disease. The FASEB Journal 18, 203-205.

Ferrer, I., Martinez, A., Boluda, S., Parchi, P., and Barrachina, M. (2008). Brain banks: benefits, limitations and cautions concerning the use of post-mortem brain tissue for molecular studies. Cell Tissue Bank 9, 181-194.

Filipowicz, W., Bhattacharyya, S.N., and Sonenberg, N. (2008). Mechanisms of post-transcriptional regulation by microRNAs: are the answers in sight? Nat Rev Genet 9, 102-114.

Fillit, H., Ding, W., Buee, L., Kalman, J., Altstiel, L., Lawlor, B., and Wolf-Klein, G. (1991). Elevated circulating tumor necrosis factor levels in Alzheimer's disease. Neurosci Lett 129, 318-320.

Fleige, S., and Pfaffl, M.W. (2006). RNA integrity and the effect on the real-time qRT-PCR performance. Mol Aspects Med 27, 126-139.

Frappier, T.F., Georgieff, I.S., Brown, K., and Shelanski, M.L. (1994). τ regulation of microtubule-microtubule spacing and bundling. J Neurochem 63, 2288-2294.

Friedhoff, P., von Bergen, M., Mandelkow, E.M., Davies, P., and Mandelkow, E. (1998). A nucleated assembly mechanism of Alzheimer paired helical filaments. Proc Natl Acad Sci USA 95, 15712-15717.

Fu, Y.H., Friedman, D.L., Richards, S., Pearlman, J.A., Gibbs, R.A., Pizzuti, A., Ashizawa, T., Perryman, M.B., Scarlato, G., and Fenwick, R.G. (1993). Decreased expression of myotonin-protein kinase messenger RNA and protein in adult form of myotonic dystrophy. Science 260, 235-238.

Fuentealba, R.A., Udan, M., Bell, S., Wegorzewska, I., Shao, J., Diamond, M.I., Weihl, C.C., and Baloh, R.H. (2010). Interaction with polyglutamine aggregates reveals a Q/N-rich domain in TDP-43. J Biol Chem 285, 26304-26314.

Furukawa, Y., Kaneko, K., Watanabe, S., Yamanaka, K., and Nukina, N. (2011). A seeding reaction recapitulates intracellular formation of sarkosyl-insoluble transactivation response element (TAR) DNA-binding protein-43 inclusions. J Biol Chem 286, 18664-18672.

Galpern, W.R., and Lang, A.E. (2006). Interface between tauopathies and synucleinopathies: A tale of two proteins. Ann Neurol 59, 449-458.

Galton, C.J., Patterson, K., Xuereb, J.H., and Hodges, J.R. (2000). Atypical and typical presentations of Alzheimer's disease: a clinical, neuropsychological, neuroimaging and pathological study of 13 cases. Brain 123, 484-498.

Gao, Q.S., Memmott, J., Lafyatis, R., Stamm, S., Screaton, G., and Andreadis, A. (2000). Complex regulation of tau exon 10, whose missplicing causes frontotemporal dementia. J Neurochem 74, 490-500.

Ge, Y.W., and Lahiri, D.K. (2002). Regulation of promoter activity of the APP gene by cytokines and growth factors. Ann N Y Acad Sci 973, 463-467.

Gendron, T.F., Rademakers, R., and Petrucelli, L. (2012). TARDBP mutation analysis in TDP-43 proteinopathies and deciphering the toxicity of mutant TDP-43. J Alzheimer's Dis.

Gerrish, A., Russo, G., Richards, A., Moskvina, V., Ivanov, D., Harold, D., Sims, R., Abraham, R., Hollingworth, P., Chapman, J., *et al.* (2012). The role of variation at AβPP, PSEN1, PSEN2, and MAPT in late onset Alzheimer's disease. J Alzheimer's Dis 28, 377-387.

Geser, F., Lee, V.M., and Trojanowski, J.Q. (2010). Amyotrophic lateral sclerosis and frontotemporal lobar degeneration: a spectrum of TDP-43 proteinopathies. Neuropathol 30, 103-112.

Geser, F., Martinez-Lage, M., Kwong, L.K., Lee, V.M., and Trojanowski, J.Q. (2009a). Amyotrophic lateral sclerosis, frontotemporal dementia and beyond: the TDP-43 diseases. J Neurol 256, 1205-1214.

Geser, F., Martinez-Lage, M., Robinson, J., Uryu, K., Neumann, M., Brandmeir, N.J., Xie, S.X., Kwong, L.K., Elman, L., McCluskey, L., *et al.* (2009b). Clinical and pathological continuum of multisystem TDP-43 proteinopathies. Arch Neurol 66, 180-189.

Ghiso, J., Rostagno, A., Gardella, J.E., Liem, L., Gorevic, P.D., and Frangione, B. (1992). A 109-amino-acid C-terminal fragment of Alzheimer's-disease amyloid precursor protein contains a sequence, -RHDS-, that promotes cell adhesion. Biochem J 288 (Pt 3), 1053-1059.

Giannakopoulos, P., Von Gunten, A., Kövari, E., Gold, G., Herrmann, F.R., Hof, P.R., and Bouras, C. (2007). Stereological analysis of neuropil threads in the hippocampal formation: relationships with Alzheimer's disease neuronal pathology and cognition. Neuropathol Applied Neurobiol 33, 334-343.

Gibb, G.M., de Silva, R., Revesz, T., Lees, A.J., Anderton, B.H., and Hanger, D.P. (2004). Differential involvement and heterogeneous phosphorylation of tau isoforms in progressive supranuclear palsy. Mol Brain Res 121, 95-101.

Gilks, N., Kedersha, N., Ayodele, M., Shen, L., Stoecklin, G., Dember, L.M., and Anderson, P. (2004). Stress Granule Assembly Is Mediated by Prion-like Aggregation of TIA-1. Mol Biol Cell 15, 5383-5398.

Ginsberg, S.D., Che, S., Counts, S.E., and Mufson, E.J. (2006). Shift in the ratio of three-repeat tau and four-repeat tau mRNAs in individual cholinergic basal forebrain neurons in mild cognitive impairment and Alzheimer's disease. J Neurochem 96, 1401-1408.

Giorgi, C., Yeo, G.W., Stone, M.E., Katz, D.B., Burge, C., Turrigiano, G., and Moore, M.J. (2007). The EJC factor eIF4AIII modulates synaptic strength and neuronal protein expression. Cell 130, 179-191.

Glatz, D.C., Rujescu, D., Tang, Y., Berendt, F.J., Hartmann, A.M., Faltraco, F., Rosenberg, C., Hulette, C., Jellinger, K., Hampel, H., *et al.* (2006). The alternative splicing of tau exon 10 and its regulatory proteins CLK2 and TRA2-BETA1 changes in sporadic Alzheimer's disease. J Neurochem 96, 635-644.

Goate, A., Chartier-Harlin, M.-C., Mullan, M., Brown, J., Crawford, F., Fidani, L., Giuffra, L., Haynes, A., Irving, N., James, L., *et al.* (1991). Segregation of a missense mutation in the amyloid precursor protein gene with familial Alzheimer's disease. Nature 349, 704-706.

Goedert, M. (2005). Tau gene mutations and their effects. Mov Disord 20, S45-S52.

Goedert, M., and Jakes, R. (2005). Mutations causing neurodegenerative tauopathies. Biochim Biophys Acta 1739, 240-250.

Goedert, M., Spillantini, M.G., Potier, M.C., Ulrich, J., and Crowther, R.A. (1989). Cloning and sequencing of the cDNA encoding an isoform of microtubule-associated protein tau containing four tandem repeats: differential expression of tau protein mRNAs in human brain. EMBO J 8, 393-399.

Golbe, L.I., Lazzarini, A.M., Spychala, J.R., Johnson, W.G., Stenroos, E.S., Mark, M.H., and Sage, J.I. (2001). The tau A0 allele in Parkinson's disease. Mov Disord 16, 442-447.

Golde, T.E., Estus, S., Usiak, M., Younkin, L.H., and Younkin, S.G. (1990). Expression of beta amyloid protein precursor mRNAs: recognition of a novel alternatively spliced form and quantitation in Alzheimer's disease using PCR. Neuron 4, 253-267.

Goldgaber, D., Harris, H.W., Hla, T., Maciag, T., Donnelly, R.J., Jacobsen, J.S., Vitek, M.P., and Gajdusek, D.C. (1989). Interleukin 1 regulates synthesis of amyloid beta-protein precursor mRNA in human endothelial cells. Proc Natl Acad Sci USA 86, 7606-7610.

Gomez-Isla, T., Hollister, R., West, H., Mui, S., Growdon, J.H., Petersen, R.C., Parisi, J.E., and Hyman, B.T. (1997). Neuronal loss correlates with but exceeds neurofibrillary tangles in Alzheimer's disease. Ann Neurol 41, 17-24.

Goode, B.L., Chau, M., Denis, P.E., and Feinstein, S.C. (2000). Structural and functional differences between 3-repeat and 4-repeat tau isoforms. Implications for normal tau function and the onset of neurodegenetative disease. J Biol Chem 275, 38182-38189.

Greenberg, S.G., and Davies, P. (1990). A preparation of Alzheimer paired helical filaments that displays distinct tau proteins by polyacrylamide gel electrophoresis. Proc Natl Acad Sci USA 87, 5827-5831.

Gsponer, J., and Babu, M.M. (2009). The rules of disorder or why disorder rules. Prog Biophys Mol Biol 99, 94-103.

Guo, J.L., and Lee, V.M.Y. (2011). Seeding of normal tau by pathological tau conformers drives pathogenesis of Alzheimer-like tangles. J Biol Chem 286, 15317-15331.

Guo, Q., Li, H., Gaddam, S.S.K., Justice, N.J., Robertson, C.S., and Zheng, H. (2012). Amyloid Precursor Protein revisited. J Biol Chem 287, 2437-2445.

Guyant-Maréchal, L., Rovelet-Lecrux, A., Goumidi, L., Cousin, E., Hannequin, D., Raux, G., Penet, C., Ricard, S., Macé, S., Amouyel, P., *et al.* (2007). Variations in the APP gene promoter region and risk of Alzheimer disease. Neurol 68, 684-687.

Haass, C., Hung, A.Y., Selkoe, D.J., and Teplow, D.B. (1994). Mutations associated with a locus for familial Alzheimer's disease result in alternative processing of amyloid beta-protein precursor. J Biol Chem 269, 17741-17748.

Haider, S., Ballester, B., Smedley, D., Zhang, J., Rice, P., and Kasprzyk, A. (2009). BioMart Central Portal—unified access to biological data. Nucleic Acids Res 37, W23-W27.

Hanger, D.P., Betts, J.C., Loviny, T.L.F., Blackstock, W.P., and Anderton, B.H. (1998). New phosphorylation sites identified in hyperphosphorylated tau (paired helical filament-tau) from Alzheimer's disease brain using nanoelectrospray mass spectrometry. J Neurochem 71, 2465-2476.

Hanger, D.P., Brion, J.P., Gallo, J.M., Cairns, N.J., Luthert, P.J., and Anderton, B.H. (1991). Tau in Alzheimer's disease and Down's syndrome is insoluble and abnormally phosphorylated. Biochem J 275 (Pt 1), 99-104.

Hanger, D.P., Gibb, G.M., de Silva, R., Boutajangout, A., Brion, J.P., Revesz, T., Lees, A.J., and Anderton, B.H. (2002). The complex relationship between soluble and insoluble tau in tauopathies revealed by efficient dephosphorylation and specific antibodies. FEBS Lett 531, 538-542.

Hardy, J. (2005). Expression of normal sequence pathogenic proteins for neurodegenerative disease contributes to disease risk: 'permissive templating' as a general mechanism underlying neurodegeneration. Biochem Soc Trans 33, 578-581.

Hardy, J.A., Wester, P., Winblad, B., Gezelius, C., Bring, G., and Eriksson, A. (1985). The patients dying after long terminal phase have acidotic brains; implications for biochemical measurements on autopsy tissue. J Neural Trans 61, 253-264.

Harold, D., Abraham, R., Hollingworth, P., Sims, R., Gerrish, A., Hamshere, M.L., Pahwa, J.S., Moskvina, V., Dowzell, K., Williams, A., *et al.* (2009). Genome-wide association study identifies variants at CLU and PICALM associated with Alzheimer's disease. Nat Genet 41, 1088-1093.

Harrison, P.J., Heath, P.R., Eastwood, S.L., Burnet, P.W., McDonald, B., and Pearson, R.C. (1995). The relative importance of premortem acidosis and postmortem interval for human brain gene expression studies: selective mRNA vulnerability and comparison with their encoded proteins. Neurosci Lett 200, 151-154.

Hasegawa, M., Smith, M.J., and Goedert, M. (1998). Tau proteins with FTDP-17 mutations have a reduced ability to promote microtubule assembly. FEBS Lett 437, 207-210.

Hayesmoore, J.B., Bray, N.J., Cross, W.C., Owen, M.J., O'Donovan, M.C., and Morris, H.R. (2009). The effect of age and the H1c MAPT haplotype on MAPT expression in human brain. Neurobiol Aging 30, 1652-1656.

He, Y., and Smith, R. (2009). Nuclear functions of heterogeneous nuclear ribonucleoproteins A/B. Cell Mol Life Sci 66, 1239-1256.

Hernández, F., and Avila, J. (2007). Tauopathies. Cell Mol Life Sci 64, 2219-2233.

Hernández, F., Pérez, M., Lucas, J.J., Mata, A.M., Bhat, R., and Avila, J. (2004). Glycogen synthase kinase-3 plays a crucial role in tau exon 10 splicing and intranuclear distribution of SC35: implications for Alzheimer's disease. J Biol Chem 279, 3801-3806.

Higashi, S., Iseki, E., Yamamoto, R., Minegishi, M., Hino, H., Fujisawa, K., Togo, T., Katsuse, O., Uchikado, H., Furukawa, Y., *et al.* (2007). Concurrence of TDP-43, tau and alpha-synuclein pathology in brains of Alzheimer's disease and dementia with Lewy bodies. Brain Res 1184, 284-294.

Ho, L., Fukuchi, K.-i., and Younkin, S.G. (1996). The alternatively spliced Kunitz Protease Inhibitor domain alters amyloid β precursor protein processing and amyloid β proteinpProduction in cultured cells. J Biol Chem 271, 30929-30934.

Hogg, M., Grujic, Z.M., Baker, M., Demirci, S., Guillozet, A.L., Sweet, A.P., Herzog, L.L., Weintraub, S., Mesulam, M.M., LaPointe, N.E., *et al.* (2003). The L266V tau mutation is associated with frontotemporal dementia and Pick-like 3R and 4R tauopathy. Acta Neuropathol (Berl) 106, 323-336.

Hoglinger, G.U., Melhem, N.M., Dickson, D.W., Sleiman, P.M.A., Wang, L.-S., Klei, L., Rademakers, R., de Silva, R., Litvan, I., Riley, D.E., *et al.* (2011). Identification of common variants influencing risk of the tauopathy progressive supranuclear palsy. Nat Genet 43, 699-705.

Hong, M., Zhukareva, V., Vogelsberg-Ragaglia, V., Wszolek, Z., Reed, L., Miller, B.I., Geschwind, D.H., Bird, T.D., McKeel, D., Goate, A., *et al.* (1998). Mutation-specific functional impairments in distinct tau isoforms of hereditary FTDP-17. Science 282, 1914-1917.

Houlden, H., Baker, M., Morris, H.R., MacDonald, N., Pickering-Brown, S., Adamson, J., Lees, A.J., Rossor, M.N., Quinn, N.P., Kertesz, A., *et al.* (2001). Corticobasal degeneration and progressive supranuclear palsy share a common tau haplotype. Neurol 56, 1702-1706.

Hu, W., Josephs, K., Knopman, D., Boeve, B., Dickson, D., Petersen, R., and Parisi, J. (2008). Temporal lobar predominance of TDP-43 neuronal cytoplasmic inclusions in Alzheimer disease. Acta Neuropathol (Berl) 116, 215-220.

Hutton, M., Lendon, C.L., Rizzu, P., Baker, M., Froelich, S., Houlden, H., Pickering-Brown, S., Chakraverty, S., Isaacs, A., Grover, A., *et al.* (1998). Association of missense and 5'-splice-site mutations in tau with the inherited dementia FTDP-17. Nature 393, 702-705.

Hyman, B.T., Augustinack, J.C., and Ingelsson, M. (2005). Transcriptional and conformational changes of the tau molecule in Alzheimer's disease. Biochim Biophys Acta 1739, 150-157.

Ingelsson, M., Ramasamy, K., Cantuti-Castelvetri, I., Skoglund, L., Matsui, T., Orne, J., Kowa, H., Raju, S., Vanderburg, C.R., Augustinack, J.C., *et al.* (2006). No alteration in tau exon 10 alternative splicing in tangle-bearing neurons of the Alzheimer's disease brain. Acta Neuropathol (Berl) 112, 439-449.

Ingelsson, M., Ramasamy, K., Russ, C., Freeman, S.H., Orne, J., Raju, S., Matsui, T., Growdon, J.H., Frosch, M.P., Ghetti, B., *et al.* (2007). Increase in the relative expression of tau with four microtubule binding repeat regions in frontotemporal lobar degeneration and progressive supranuclear palsy brains. Acta Neuropathol (Berl) 114, 471-479.

Isaacs, A.M., Johannsen, P., Holm, I., and Nielsen, J.E. (2011). Frontotemporal dementia caused by CHMP2B mutations. Curr Alzheimer's Res 8, 246-251.

Jacobsen, K.T., and Iverfeldt, K. (2009). Amyloid precursor protein and its homologues: a family of proteolysis-dependent receptors. Cell Mol Life Sci 66, 2299-2318.

Jansen, G., Groenen, P.J.T.A., Bachner, D., Jap, P.H.K., Coerwinkel, M., Oerlemans, F., van den Broek, W., Gohlsch, B., Pette, D., Plomp, J.J., *et al.* (1996). Abnormal myotonic dystrophy protein kinase levels produce only mild myopathy in mice. Nat Genet 13, 316-324.

Janssen, J.C., Warrington, E.K., Morris, H.R., Lantos, P., Brown, J., Revesz, T., Wood, N., Khan, M.N., Cipolotti, L., Fox, N.C., and Rossor, M.N. (2002). Clinical features of frontotemporal dementia due to the intronic tau 10+16 mutation. Neurol 58, 1161-1168.

Jellinger, K.A. (2004). Lewy body-related α-synucleinopathy in the aged human brain. J Neural Trans 111, 1219-1235.

Jiang, H., Mankodi, A., Swanson, M.S., Moxley, R.T., and Thornton, C.A. (2004). Myotonic dystrophy type 1 is associated with nuclear foci of mutant RNA, sequestration of muscleblind proteins and deregulated alternative splicing in neurons. Hum Mol Genet 13, 3079-3088.

Jiang, Z., Cote, J., Kwon, J.M., Goate, A.M., and Wu, J.Y. (2000). Aberrant Splicing of tau Pre-mRNA Caused by Intronic Mutations Associated with the Inherited Dementia Frontotemporal Dementia with Parkinsonism Linked to Chromosome 17. Mol Cell Biol 20, 4036-4048.

Joachim, C.L., Morris, J.H., and Selkoe, D.J. (1989). Diffuse senile plaques occur commonly in the cerebellum in Alzheimer's disease. Am J Pathol 135, 309-319.

Johnson, B.S., Snead, D., Lee, J.J., McCaffery, J.M., Shorter, J., and Gitler, A.D. (2009). TDP-43 is intrinsically aggregation-prone, and amyotrophic lateral sclerosis-linked mutations accelerate aggregation and increase toxicity. J Biol Chem 284, 20329-20339.

Johnson, S.A., Morgan, D.G., and Finch, C.E. (1986). Extensive postmortem stability of RNA from rat and human brain. J Neurosci Res 16, 267-280.

Johnston, N.L., Cervenak, J., Shore, A.D., Torrey, E.F., and Yolken, R.H. (1997). Multivariate analysis of RNA levels from postmortem human brains as measured by three different methods of RT-PCR. Stanley Neuropathology Consortium. J Neurosci Methods 77, 83-92.

Josephs, K.A., and Dickson, D.W. (2007). Hippocampal sclerosis in tau-negative frontotemporal lobar degeneration. Neurobiol Aging 28, 1718-1722.

Josephs, K.A., Whitwell, J.L., Knopman, D.S., Hu, W.T., Stroh, D.A., Baker, M., Rademakers, R., Boeve, B.F., Parisi, J.E., Smith, G.E., *et al.* (2008). Abnormal TDP-43 immunoreactivity in AD modifies clinicopathologic and radiologic phenotype. Neurol 70, 1850-1857.

Kabashi, E., Lin, L., Tradewell, M.L., Dion, P.A., Bercier, V., Bourgouin, P., Rochefort, D., Bel Hadj, S., Durham, H.D., Velde, C.V., *et al.* (2010). Gain and loss of function of ALS-related mutations of TARDBP (TDP-43) cause motor deficits in vivo. Hum Mol Genet 19, 671-683.

Kabashi, E., Valdmanis, P.N., Dion, P., Spiegelman, D., McConkey, B.J., Vande Velde, C., Bouchard, J.P., Lacomblez, L., Pochigaeva, K., Salachas, F., *et al.* (2008). TARDBP mutations in individuals with sporadic and familial amyotrophic lateral sclerosis. Nat Genet 40, 572-574.

Kadokura, A., Yamazaki, T., Lemere, C.A., Takatama, M., and Okamoto, K. (2009). Regional distribution of TDP-43 inclusions in Alzheimer disease (AD) brains: Their relation to AD common pathology. Neuropathol 29, 566-573.

Kang, J., Lemaire, H.G., Unterbeck, A., Salbaum, J.M., Masters, C.L., Grzeschik, K.H., Multhaup, G., Beyreuther, K., and Muller-Hill, B. (1987). The precursor of Alzheimer's disease amyloid A4 protein resembles a cell-surface receptor. Nature 325, 733-736.

Kedersha, N.L., Gupta, M., Li, W., Miller, I., and Anderson, P. (1999). RNA-binding proteins tia-1 and tiar link the phosphorylation of eif-2α to the assembly of mammalian stress granules. J Cell Biol 147, 1431-1442.

Kenan, D.J., Query, C.C., and Keene, J.D. (1991). RNA recognition: towards identifying determinants of specificity. Trends Biochem Sci 16, 214-220.

Kertesz, A., Martinez-Lage, P., Davidson, W., and Munoz, D.G. (2000). The corticobasal degeneration syndrome overlaps progressive aphasia and frontotemporal dementia. Neurol 55, 1368-1375.

Khandelwal, P.J., Herman, A.M., and Moussa, C.E. (2011). Inflammation in the early stages of neurodegenerative pathology. J Neuroimmunol 238, 1-11.

Kimura, K., Wakamatsu, A., Suzuki, Y., Ota, T., Nishikawa, T., Yamashita, R., Yamamoto, J., Sekine, M., Tsuritani, K., Wakaguri, H., *et al.* (2006). Diversification of transcriptional modulation: large-scale identification and characterization of putative alternative promoters of human genes. Genome Res 16, 55-65.

King, A., Maekawa, S., Bodi, I., Troakes, C., and Al-Sarraj, S. (2011). Ubiquitinated, p62 immunopositive cerebellar cortical neuronal inclusions are evident across the spectrum of TDP-43 proteinopathies but are only rarely additionally immunopositive for phosphorylation-dependent TDP-43. Neuropathol 31, 239-249.

King, A., Sweeney, F., Bodi, I., Troakes, C., Maekawa, S., and Al-Sarraj, S. (2010). Abnormal TDP-43 expression is identified in the neocortex in cases of dementia pugilistica, but is mainly confined to the limbic system when identified in high and moderate stages of Alzheimer's disease. Neuropathol 30, 408-419.

King, M.E., Ghoshal, N., Wall, J.S., Binder, L.I., and Ksiezak-Reding, H. (2001). Structural analysis of Pick’s disease-derived and in vitro-assembled tau filaments. Am J Pathol 158, 1481-1490.

King, O.D., Gitler, A.D., and Shorter, J. (2012). The tip of the iceberg: RNA-binding proteins with prion-like domains in neurodegenerative disease. Brain Res 1462, 61-80.

Kingsbury, A.E., Foster, O.J., Nisbet, A.P., Cairns, N., Bray, L., Eve, D.J., Lees, A.J., and Marsden, C.D. (1995). Tissue pH as an indicator of mRNA preservation in human post-mortem brain. Mol Brain Res 28, 311-318.

Kitazawa, M., Oddo, S., Yamasaki, T.R., Green, K.N., and LaFerla, F.M. (2005). Lipopolysaccharide-induced inflammation exacerbates tau pathology by a cyclin-dependent kinase 5-mediated pathway in a transgenic model of Alzheimer's disease. J Neurosci 25, 8843-8853.

Klauer, A.A., and van Hoof, A. (2012). Degradation of mRNAs that lack a stop codon: a decade of nonstop progress. RNA 3, 649-660.

Kondo, S., Yamamoto, N., Murakami, T., Okumura, M., Mayeda, A., and Imaizumi, K. (2004). Tra2β, SF2/ASF and SRp30c modulate the function of an exonic splicing enhancer in exon 10 of tau pre-mRNA. Genes to Cells 9, 121-130.

Kornblihtt, A.R. (2005). Promoter usage and alternative splicing. Curr Opin Cell Biol 17, 262-268.

Kuersten, S., and Goodwin, E.B. (2003). The power of the 3' UTR: translational control and development. Nat Rev Genet 4, 626-637.

Kuyumcu-Martinez, N.M., Wang, G.-S., and Cooper, T.A. (2007). Increased steady-state levels of CUGBP1 in Myotonic Dystrophy 1 are due to PKC-mediated hyperphosphorylation. Mol Cell 28, 68-78.

Lagier-Tourenne, C., and Cleveland, D.W. (2009). Rethinking ALS: the FUS about TDP-43. Cell 136, 1001-1004.

Lansbury Jr, P.T., and Caughey, B. (1995). The chemistry of scrapie infection: implications of the 'ice 9' metaphor. Chem Biol 2, 1-5.

Lantos, P.L., Cairns, N.J., Khan, M.N., King, A., Revesz, T., Janssen, J.C., Morris, H., and Rossor, M.N. (2002). Neuropathologic variation in frontotemporal dementia due to the intronic tau 10+16 mutation. Neurol 58, 1169-1175.

Lareau, L.F., Inada, M., Green, R.E., Wengrod, J.C., and Brenner, S.E. (2007). Unproductive splicing of SR genes associated with highly conserved and ultraconserved DNA elements. Nature 446, 926-929.

Le Hir, H., Gatfield, D., Izaurralde, E., and Moore, M.J. (2001). The exon-exon junction complex provides a binding platform for factors involved in mRNA export and nonsense-mediated mRNA decay. EMBO J 20, 4987-4997.

Le Hir, H., Moore, M.J., and Maquat, L.E. (2000). Pre-mRNA splicing alters mRNP composition: evidence for stable association of proteins at exon-exon junctions. Genes Dev 14, 1098-1108.

LeBlanc, A.C., Papadopoulos, M., Bélair, C., Chu, W., Crosato, M., Powell, J., and Goodyer, C.G. (1997). Processing of amyloid precursor protein in human primary neuron and astrocyte cultures. J Neurochem 68, 1183-1190.

Lee, G., Newman, S.T., Gard, D.L., Band, H., and Panchamoorthy, G. (1998). Tau interacts with src-family non-receptor tyrosine kinases. J Cell Sci 111, 3167-3177.

Lee, Y., Kim, M., Han, J., Yeom, K.-H., Lee, S., Baek, S.H., and Kim, V.N. (2004). MicroRNA genes are transcribed by RNA polymerase II. EMBO J 23, 4051-4060.

Leroy, O., Dhaenens, C.M., Schraen-Maschke, S., Belarbi, K., Delacourte, A., Andreadis, A., Sablonniere, B., Buee, L., Sergeant, N., and Caillet-Boudin, M.L. (2006). ETR-3 represses tau exons 2/3 inclusion, a splicing event abnormally enhanced in myotonic dystrophy type I. J Neurosci Res 84, 852-859.

Letiembre, M., Liu, Y., Walter, S., Hao, W., Pfander, T., Wrede, A., Schulz-Schaeffer, W., and Fassbender, K. (2009). Screening of innate immune receptors in neurodegenerative diseases: A similar pattern. Neurobiol Aging 30, 759-768.

Lill, C.M., Roehr, J.T., McQueen, M.B., Kavvoura, F.K., Bagade, S., Schjeide, B.-M.M., Schjeide, L.M., Meissner, E., Zauft, U., Allen, N.C., *et al.* (2012). Comprehensive research synopsis and systematic meta-analyses in Parkinson's disease genetics: The PDGene database. PLoS Genet 8, e1002548.

Lindwall, G., and Cole, R.D. (1984). Phosphorylation affects the ability of tau protein to promote microtubule assembly. J Biol Chem 259, 5301-5305.

Ling, S.C., Albuquerque, C.P., Han, J.S., Lagier-Tourenne, C., Tokunaga, S., Zhou, H., and Cleveland, D.W. (2010). ALS-associated mutations in TDP-43 increase its stability and promote TDP-43 complexes with FUS/TLS. Proc Natl Acad Sci USA 107, 13318-13323.

Lippa, C.F., and Dickson, D.W. (2004). Hippocampal sclerosis dementia. Neurol 63, 414-415.

Lippa, C.F., Rosso, A.L., Stutzbach, L.D., Neumann, M., Lee, V.M., and Trojanowski, J.Q. (2009). Transactive response DNA-binding protein 43 burden in familial Alzheimer disease and Down syndrome. Arch Neurol 66, 1483-1488.

Litvan, I., Mega, M.S., Cummings, J.L., and Fairbanks, L. (1996). Neuropsychiatric aspects of progressive supranuclear palsy. Neurol 47, 1184-1189.

Liu-Yesucevitz, L., Bilgutay, A., Zhang, Y.-J., Vanderwyde, T., Citro, A., Mehta, T., Zaarur, N., McKee, A., Bowser, R., Sherman, M., *et al.* (2010). Tar DNA binding protein-43 (TDP-43) associates with stress granules: analysis of cultured cells and pathological brain tissue. PLoS One 5, e13250.

Liu, L., Drouet, V., Wu, J.W., Witter, M.P., Small, S.A., Clelland, C., and Duff, K. (2012). Trans-synaptic spread of tau pathology *in vivo*. PLoS One 7, e31302.

Liu, W.-K., Le, T.V., Adamson, J., Baker, M., Cookson, N., Hardy, J., Hutton, M., Yen, S.-H., and Dickson, D.W. (2001). Relationship of the extended tau haplotype to tau biochemistry and neuropathology in progressive supranuclear palsy. Ann Neurol 50, 494-502.

Liu, Y., Walter, S., Stagi, M., Cherny, D., Letiembre, M., Schulz-Schaeffer, W., Heine, H., Penke, B., Neumann, H., and Fassbender, K. (2005). LPS receptor (CD14): a receptor for phagocytosis of Alzheimer's amyloid peptide. Brain 128, 1778-1789.

Lu, T., Pan, Y., Kao, S.-Y., Li, C., Kohane, I., Chan, J., and Yankner, B.A. (2004). Gene regulation and DNA damage in the ageing human brain. Nature 429, 883-891.

Lucin, K.M., and Wyss-Coray, T. (2009). Immune activation in brain aging and neurodegeneration: too much or too little? Neuron 64, 110-122.

Luk, C., Jana, V., Elke, M., Andrew, L., and de Rohan, S. (2010). Brain tau isoform mRNA and protein correlation in PSP brain. Trans Neurosci 1, 30-36.

Lv, H., Jia, L., and Jia, J. (2008). Promoter polymorphisms which modulate APP expression may increase susceptibility to Alzheimer's disease. Neurobiol Aging 29, 194-202.

Mackenzie, I., Baborie, A., Pickering-Brown, S., Plessis, D., Jaros, E., Perry, R., Neary, D., Snowden, J., and Mann, D. (2006). Heterogeneity of ubiquitin pathology in frontotemporal lobar degeneration: classification and relation to clinical phenotype. Acta Neuropathol (Berl) 112, 539-549.

Mackenzie, I., Neumann, M., Baborie, A., Sampathu, D., Du Plessis, D., Jaros, E., Perry, R., Trojanowski, J., Mann, D., and Lee, V. (2011). A harmonized classification system for FTLD-TDP pathology. Acta Neuropathol (Berl) 122, 111-113.

Mackenzie, I.R., Foti, D., Woulfe, J., and Hurwitz, T.A. (2008). Atypical frontotemporal lobar degeneration with ubiquitin-positive, TDP-43-negative neuronal inclusions. Brain 131, 1282-1293.

Mackenzie, I.R., Neumann, M., Bigio, E.H., Cairns, N.J., Alafuzoff, I., Kril, J., Kovacs, G.G., Ghetti, B., Halliday, G., Holm, I.E., *et al.* (2009). Nomenclature for neuropathologic subtypes of frontotemporal lobar degeneration: consensus recommendations. Acta Neuropathol (Berl) 117, 15-18.

Mackenzie, I.R., Neumann, M., Bigio, E.H., Cairns, N.J., Alafuzoff, I., Kril, J., Kovacs, G.G., Ghetti, B., Halliday, G., Holm, I.E., *et al.* (2010). Nomenclature and nosology for neuropathologic subtypes of frontotemporal lobar degeneration: an update. Acta Neuropathol 119, 1-4.

Maeda, S., Sahara, N., Saito, Y., Murayama, M., Yoshiike, Y., Kim, H., Miyasaka, T., Murayama, S., Ikai, A., and Takashima, A. (2007). Granular tau oligomers as intermediates of tau filaments. Biochemistry 46, 3856-3861.

Makeyev, E.V., Zhang, J., Carrasco, M.A., and Maniatis, T. (2007). The microRNA miR-124 promotes neuronal differentiation by triggering brain-specific alternative pre-mRNA splicing. Mol Cell 27, 435-448.

Maloney, B., and Lahiri, D.K. (2012). Structural and functional characterization of H2 haplotype MAPT promoter: Unique neurospecific domains and a hypoxia-inducible element would enhance rationally targeted tauopathy research for Alzheimer's disease. Gene 501, 63-78.

Mandelkow, E.-M., Thies, E., Trinczek, B., Biernat, J., and Mandelkow, E. (2004). MARK/PAR1 kinase is a regulator of microtubule-dependent transport in axons. J Cell Biol 167, 99-110.

Mann, D.M.A., and Esiri, M.M. (1989). The pattern of acquisition of plaques and tangles in the brains of patients under 50 years of age with Down's syndrome. J Neurol Sci 89, 169-179.

Maquat, L.E., and Gong, C. (2009). Gene expression networks: competing mRNA decay pathways in mammalian cells. Biochem Soc Trans 37, 1287-1292.

Maquat, L.E., Tarn, W.-Y., and Isken, O. (2010). The pioneer round of translation: features and functions. Cell 142, 368-374.

Maracchioni, A., Totaro, A., Angelini, D.F., Di Penta, A., Bernardi, G., Carrì, M.T., and Achsel, T. (2007). Mitochondrial damage modulates alternative splicing in neuronal cells: implications for neurodegeneration. J Neurochem 100, 142-153.

Maruyama, K., and Sugano, S. (1994). Oligo-capping: a simple method to replace the cap structure of eukaryotic mRNAs with oligoribonucleotides. Gene 138, 171-174.

Matsui, T., Ingelsson, M., Fukumoto, H., Ramasamy, K., Kowa, H., Frosch, M.P., Irizarry, M.C., and Hyman, B.T. (2007). Expression of APP pathway mRNAs and proteins in Alzheimer's disease. Brain Res 1161, 116-123.

Maurage, C.A., Udd, B., Ruchoux, M.M., Vermersch, P., Kalimo, H., Krahe, R., Delacourte, A., and Sergeant, N. (2005). Similar brain tau pathology in DM2/PROMM and DM1/Steinert disease. Neurol 65, 1636-1638.

McDonald, K.K., Aulas, A., Destroismaisons, L., Pickles, S., Beleac, E., Camu, W., Rouleau, G.A., and Vande Velde, C. (2011). TAR DNA-binding protein 43 (TDP-43) regulates stress granule dynamics via differential regulation of G3BP and TIA-1. Hum Mol Genet 20, 1400-1410.

McGlincy, N.J., and Smith, C.W. (2008). Alternative splicing resulting in nonsense-mediated mRNA decay: what is the meaning of nonsense? Trends Biochem Sci 33, 385-393.

Mesulam, M., Wicklund, A., Johnson, N., Rogalski, E., Léger, G.C., Rademaker, A., Weintraub, S., and Bigio, E.H. (2008). Alzheimer and frontotemporal pathology in subsets of primary progressive aphasia. Ann Neurol 63, 709-719.

Mishra, M., Paunesku, T., Woloschak, G., Siddique, T., Zhu, L., Lin, S., Greco, K., and Bigio, E. (2007). Gene expression analysis of frontotemporal lobar degeneration of the motor neuron disease type with ubiquitinated inclusions. Acta Neuropathol (Berl) 114, 81-94.

Mitchell, T.W., Nissanov, J., Han, L.-Y., Mufson, E.J., Schneider, J.A., Cochran, E.J., Bennett, D.A., Lee, V.M.-Y., Trojanowski, J.Q., and Arnold, S.E. (2000). Novel method to quantify neuropil threads in brains from elders with or without cognitive impairment. J Histochem Cytochem 48, 1627-1637.

Munoz, D., Woulfe, J., and Kertesz, A. (2007). Argyrophilic thorny astrocyte clusters in association with Alzheimer's disease pathology in possible primary progressive aphasia. Acta Neuropathol (Berl) 114, 347-357.

Munoz, D.G., Neumann, M., Kusaka, H., Yokota, O., Ishihara, K., Terada, S., Kuroda, S., and Mackenzie, I.R. (2009). FUS pathology in basophilic inclusion body disease. Acta Neuropathol 118, 617-627.

Murray, M., DeJesus-Hernandez, M., Rutherford, N., Baker, M., Duara, R., Graff-Radford, N., Wszolek, Z., Ferman, T., Josephs, K., Boylan, K., *et al.* (2011a). Clinical and neuropathologic heterogeneity of c9FTD/ALS associated with hexanucleotide repeat expansion in C9ORF72. Acta Neuropathol (Berl) 122, 673-690.

Murray, M.E., Graff-Radford, N.R., Ross, O.A., Petersen, R.C., Duara, R., and Dickson, D.W. (2011b). Neuropathologically defined subtypes of Alzheimer's disease with distinct clinical characteristics: a retrospective study. Lancet Neurol 10, 785-796.

Myers, A.J., Kaleem, M., Marlowe, L., Pittman, A.M., Lees, A.J., Fung, H.C., Duckworth, J., Leung, D., Gibson, A., Morris, C.M., *et al.* (2005). The H1c haplotype at the MAPT locus is associated with Alzheimer's disease. Hum Mol Genet 14, 2399-2404.

Myers, A.J., Pittman, A.M., Zhao, A.S., Rohrer, K., Kaleem, M., Marlowe, L., Lees, A., Leung, D., McKeith, I.G., Perry, R.H., *et al.* (2007). The MAPT H1c risk haplotype is associated with increased expression of tau and especially of 4 repeat containing transcripts. Neurobiol Dis 25, 561-570.

Nelson, P.T., Alafuzoff, I., Bigio, E.H., Bouras, C., Braak, H., Cairns, N.J., Castellani, R.J., Crain, B.J., Davies, P., Tredici, K.D., *et al.* (2012). Correlation of Alzheimer disease neuropathologic changes with cognitive status: a review of the literature. J Neuropathol Exp Neurol 71, 362-381.

Nelson, P.T., Braak, H., and Markesbery, W.R. (2009). Neuropathology and cognitive impairment in Alzheimer disease: a complex but coherent relationship. J Neuropathol Exp Neurol 68, 1-14.

Nelson, P.T., Schmitt, F.A., Lin, Y., Abner, E.L., Jicha, G.A., Patel, E., Thomason, P.C., Neltner, J.H., Smith, C.D., Santacruz, K.S., *et al.* (2011). Hippocampal sclerosis in advanced age: clinical and pathological features. Brain 134, 1506-1518.

Neumann, M., Igaz, L.M., Kwong, L.K., Nakashima-Yasuda, H., Kolb, S.J., Dreyfuss, G., Kretzschmar, H.A., Trojanowski, J.Q., and Lee, V.M. (2007a). Absence of heterogeneous nuclear ribonucleoproteins and survival motor neuron protein in TDP-43 positive inclusions in frontotemporal lobar degeneration. Acta Neuropathol (Berl) 113, 543-548.

Neumann, M., Mackenzie, I.R., Cairns, N.J., Boyer, P.J., Markesbery, W.R., Smith, C.D., Taylor, J.P., Kretzschmar, H.A., Kimonis, V.E., and Forman, M.S. (2007b). TDP-43 in the ubiquitin pathology of frontotemporal dementia with VCP gene mutations. J Neuropathol Exp Neurol 66, 152-157.

Neumann, M., Rademakers, R., Roeber, S., Baker, M., Kretzschmar, H.A., and Mackenzie, I.R. (2009a). A new subtype of frontotemporal lobar degeneration with FUS pathology. Brain 132, 2922-2931.

Neumann, M., Roeber, S., Kretzschmar, H.A., Rademakers, R., Baker, M., and Mackenzie, I.R. (2009b). Abundant FUS-immunoreactive pathology in neuronal intermediate filament inclusion disease. Acta Neuropathol (Berl) 118, 605-616.

Neumann, M., Sampathu, D.M., Kwong, L.K., Truax, A.C., Micsenyi, M.C., Chou, T.T., Bruce, J., Schuck, T., Grossman, M., Clark, C.M., *et al.* (2006). Ubiquitinated TDP-43 in frontotemporal lobar degeneration and amyotrophic lateral sclerosis. Science 314, 130-133.

Ni, J.Z., Grate, L., Donohue, J.P., Preston, C., Nobida, N., O'Brien, G., Shiue, L., Clark, T.A., Blume, J.E., and Ares, M. (2007). Ultraconserved elements are associated with homeostatic control of splicing regulators by alternative splicing and nonsense-mediated decay. Genes Dev 21, 708-718.

Nijholt, D.A.T., van Haastert, E.S., Rozemuller, A.J.M., Scheper, W., and Hoozemans, J.J.M. (2012). The unfolded protein response is associated with early tau pathology in the hippocampus of tauopathies. J Pathol 226, 693-702.

Nilsberth, C., Westlind-Danielsson, A., Eckman, C.B., Condron, M.M., Axelman, K., Forsell, C., Stenh, C., Luthman, J., Teplow, D.B., Younkin, S.G., *et al.* (2001). The 'Arctic' APP mutation (E693G) causes Alzheimer's disease by enhanced Abeta protofibril formation. Nat Neurosci 4, 887-893.

Nowotny, P., Simcock, X., Bertelsen, S., Hinrichs, A.L., Kauwe, J.S.K., Mayo, K., Smemo, S., Morris, J.C., and Goate, A. (2007). Association studies testing for risk for late-onset Alzheimer's disease with common variants in the β-amyloid precursor protein (APP). Am J Med Genet 144B, 469-474.

Okaty, B.W., Sugino, K., and Nelson, S.B. (2011). A quantitative comparison of cell-type-specific microarray gene expression profiling methods in the mouse brain. PLoS One 6, e16493.

Ou, S.H., Wu, F., Harrich, D., Garcia-Martinez, L.F., and Gaynor, R.B. (1995). Cloning and characterization of a novel cellular protein, TDP-43, that binds to human immunodeficiency virus type 1 TAR DNA sequence motifs. J Virol 69, 3584-3596.

Pakkenberg, B., and Gundersen, H.J. (1997). Neocortical neuron number in humans: effect of sex and age. J Comp Neurol 384, 312-320.

Pakkenberg, B., Pelvig, D., Marner, L., Bundgaard, M.J., Gundersen, H.J., Nyengaard, J.R., and Regeur, L. (2003). Aging and the human neocortex. Exp Gerontol 38, 95-99.

Pal, S., Gupta, R., Kim, H., Wickramasinghe, P., Baubet, V., Showe, L.C., Dahmane, N., and Davuluri, R.V. (2011). Alternative transcription exceeds alternative splicing in generating the transcriptome diversity of cerebellar development. Genome Res 21, 1260-1272.

Panegyres, P.K., Zafiris-Toufexis, K., and Kakulas, B.A. (2000). Amyloid precursor protein gene isoforms in Alzheimer's disease and other neurodegenerative disorders. J Neurol Sci 173, 81-92.

Pannese, E. (2011). Morphological changes in nerve cells during normal aging. Brain Struct Funct 216, 85-89.

Pao, W.C., Dickson, D.W., Crook, J.E., Finch, N.A., Rademakers, R., and Graff-Radford, N.R. (2011). Hippocampal sclerosis in the elderly: genetic and pathologic findings, some mimicking Alzheimer's disease clinically. Alzheimer's Dis Assoc Disord 25, 364-368.

Park, J.W., Parisky, K., Celotto, A.M., Reenan, R.A., and Graveley, B.R. (2004). Identification of alternative splicing regulators by RNA interference in Drosophila. Proc Natl Acad Sci USA 101, 15974-15979.

Pesiridis, G.S., Tripathy, K., Tanik, S., Trojanowski, J.Q., and Lee, V.M.Y. (2011). A “Two-hit” hypothesis for inclusion formation by carboxyl-terminal fragments of TDP-43 protein linked to RNA depletion and impaired microtubule-dependent transport. J Biol Chem 286, 18845-18855.

Piguet, O., Halliday, G.M., Reid, W.G.J., Casey, B., Carman, R., Huang, Y., Xuereb, J.H., Hodges, J.R., and Kril, J.J. (2011a). Clinical phenotypes in autopsy-confirmed Pick's disease. Neurol 76, 253-259.

Piguet, O., Hornberger, M., Mioshi, E., and Hodges, J.R. (2011b). Behavioural-variant frontotemporal dementia: diagnosis, clinical staging, and management. Lancet Neurol 10, 162-172.

Pikkarainen, M., Hartikainen, P., and Alafuzoff, I. (2008). Neuropathologic features of frontotemporal lobar degeneration with ubiquitin-positive inclusions visualized with ubiquitin-binding protein p62 immunohistochemistry. J Neuropathol Exp Neurol 67, 280-298.

Pittman, A.M., Myers, A.J., Abou-Sleiman, P., Fung, H.C., Kaleem, M., Marlowe, L., Duckworth, J., Leung, D., Williams, D., Kilford, L., *et al.* (2005). Linkage disequilibrium fine mapping and haplotype association analysis of the tau gene in progressive supranuclear palsy and corticobasal degeneration. J Med Genet 42, 837-846.

Pittman, A.M., Myers, A.J., Duckworth, J., Bryden, L., Hanson, M., Abou-Sleiman, P., Wood, N.W., Hardy, J., Lees, A., and de Silva, R. (2004). The structure of the tau haplotype in controls and in progressive supranuclear palsy. Hum Mol Genet 13, 1267-1274.

Poleev, A., Hartmann, A., and Stamm, S. (2000). A trans-acting factor, isolated by the three-hybrid system, that influences alternative splicing of the amyloid precursor protein minigene. Eur J Biochem 267, 4002-4010.

Polymenidou, M., and Cleveland, Don W. (2011). The seeds of neurodegeneration: prion-like spreading in ALS. Cell 147, 498-508.

Polymenidou, M., Lagier-Tourenne, C., Hutt, K.R., Huelga, S.C., Moran, J., Liang, T.Y., Ling, S.-C., Sun, E., Wancewicz, E., Mazur, C., *et al.* (2011). Long pre-mRNA depletion and RNA missplicing contribute to neuronal vulnerability from loss of TDP-43. Nat Neurosci 14, 459-468.

Popescu, A., Lippa, C.F., Lee, V.Y., and Trojanowski, J.Q. (2004). Lewy bodies in the amygdala: Increase of α-synuclein aggregates in neurodegenerative diseases with tau-based inclusions. Arch Neurol 61, 1915-1919.

Popova, T., Mennerich, D., Weith, A., and Quast, K. (2008). Effect of RNA quality on transcript intensity levels in microarray analysis of human post-mortem brain tissues. BMC Genomics 9, 91.

Prasanth, K.V., Prasanth, S.G., Xuan, Z., Hearn, S., Freier, S.M., Bennett, C.F., Zhang, M.Q., and Spector, D.L. (2005). Regulating gene expression through RNA nuclear retention. Cell 123, 249-263.

Preece, P., Virley, D.J., Costandi, M., Coombes, R., Moss, S.J., Mudge, A.W., Jazin, E., and Cairns, N.J. (2004). Amyloid precursor protein mRNA levels in Alzheimer's disease brain. Mol Brain Res 122, 1-9.

Probst, A., Taylor, K., and Tolnay, M. (2007). Hippocampal sclerosis dementia: a reappraisal. Acta Neuropathol (Berl) 114, 335-345.

Prusiner, S.B. (1982). Novel proteinaceous infectious particles cause scrapie. Science 216, 136-144.

Rademakers, R., Eriksen, J.L., Baker, M., Robinson, T., Ahmed, Z., Lincoln, S.J., Finch, N., Rutherford, N.J., Crook, R.J., Josephs, K.A., *et al.* (2008). Common variation in the miR-659 binding-site of GRN is a major risk factor for TDP43-positive frontotemporal dementia. Hum Mol Genet 17, 3631-3642.

Rademakers, R., Melquist, S., Cruts, M., Theuns, J., Del-Favero, J., Poorkaj, P., Baker, M., Sleegers, K., Crook, R., De Pooter, T., *et al.* (2005). High-density SNP haplotyping suggests altered regulation of tau gene expression in progressive supranuclear palsy. Hum Mol Genet 14, 3281-3292.

Rademakers, R., Neumann, M., and Mackenzie, I.R. (2012). Advances in understanding the molecular basis of frontotemporal dementia. Nat Rev Neurol 8, 423-434.

Renton, A.E., Majounie, E., Waite, A., Simon-Sanchez, J., Rollinson, S., Gibbs, J.R., Schymick, J.C., Laaksovirta, H., van Swieten, J.C., Myllykangas, L., *et al.* (2011). A hexanucleotide repeat expansion in C9ORF72 is the cause of chromosome 9p21-linked ALS-FTD. Neuron 72, 257-268.

Rhinn, H., Fujita, R., Qiang, L., Cheng, R., Lee, J.H., and Abeliovich, A. (2013). Integrative genomics identifies APOE ε4 effectors in Alzheimer's disease. Nature 500, 45-50.

Robinson, J.L., Geser, F., Corrada, M.M., Berlau, D.J., Arnold, S.E., Lee, V.M.Y., Kawas, C.H., and Trojanowski, J.Q. (2011). Neocortical and hippocampal amyloid-β and tau measures associate with dementia in the oldest-old. Brain 134, 3708-3715.

Roeber, S., Mackenzie, I.R., Kretzschmar, H.A., and Neumann, M. (2008). TDP-43-negative FTLD-U is a significant new clinico-pathological subtype of FTLD. Acta Neuropathol (Berl) 116, 147-157.

Rogelj, B. (2011). The functions of glycine-rich regions in TDP-43, FUS and related RNA-binding proteins RNA Binding Proteins (Lorkovic ZJ, ed.) Landes Bioscience and Springer Science+Business Media, Austin,TX., 1-17.

Rogers, J.T., Leiter, L.M., McPhee, J., Cahill, C.M., Zhan, S.-S., Potter, H., and Nilsson, L.N.G. (1999). Translation of the Alzheimer Amyloid Precursor Protein mRNA is up-regulated by Interleukin-1 through 5′-untranslated region sequences. J Biol Chem 274, 6421-6431.

Roses, M.D.A.D. (1996). Apolipoprotein E alleles as risk factors in Alzheimer's disease. Annu Rev Med 47, 387-400.

Ross, B.M., Knowler, J.T., and McCulloch, J. (1992). On the stability of messenger RNA and ribosomal RNA in the brains of control human subjects and patients with Alzheimer's disease. J Neurochem 58, 1810-1819.

Ross, R.A., Spengler, B.A., and Biedler, J.L. (1983). Coordinate morphological and biochemical interconversion of human neuroblastoma cells. J Natl Cancer Inst 71, 741-747.

Rutherford, N.J., Zhang, Y.-J., Baker, M., Gass, J.M., Finch, N.A., Xu, Y.-F., Stewart, H., Kelley, B.J., Kuntz, K., Crook, R.J.P., *et al.* (2008). Novel Mutations in *TARDBP* (TDP-43) in Patients with Familial Amyotrophic Lateral Sclerosis. Plos Genetics 4, e1000193.

Sahara, N., Maeda, S., and Takashima, A. (2008). Tau oligomerization: A role for tau aggregation intermediates linked to neurodegeneration. Curr Alzheimer's Res 5, 591-598.

Saltzman, A.L., Kim, Y.K., Pan, Q., Fagnani, M.M., Maquat, L.E., and Blencowe, B.J. (2008). Regulation of multiple core spliceosomal proteins by alternative splicing-coupled nonsense-mediated mRNA decay. Mol Cell Biol 28, 4320-4330.

Sampathu, D.M., Neumann, M., Kwong, L.K., Chou, T.T., Micsenyi, M., Truax, A., Bruce, J., Grossman, M., Trojanowski, J.Q., and Lee, V.M.Y. (2006). Pathological heterogeneity of frontotemporal lobar degeneration with ubiquitin-positive inclusions delineated by ubiquitin immunohistochemistry and novel monoclonal antibodies. Am J Pathol 169, 1343-1352.

Schmid, B., Hruscha, A., Hogl, S., Banzhaf-Strathmann, J., Strecker, K., van der Zee, J., Teucke, M., Eimer, S., Hegermann, J., Kittelmann, M., *et al.* (2013). Loss of ALS-associated TDP-43 in zebrafish causes muscle degeneration, vascular dysfunction, and reduced motor neuron axon outgrowth. Proc Natl Acad Sci USA.

Schoenberg, D.R., and Maquat, L.E. (2012). Regulation of cytoplasmic mRNA decay. Nat Rev Genet 13, 246-259.

Sephton, C.F., Cenik, C., Kucukural, A., Dammer, E.B., Cenik, B., Han, Y., Dewey, C.M., Roth, F.P., Herz, J., Peng, J., *et al.* (2011). Identification of neuronal RNA targets of TDP-43-containing ribonucleoprotein complexes. J Biol Chem 286, 1204-1215.

Sephton, C.F., Good, S.K., Atkin, S., Dewey, C.M., Mayer, P., Herz, J., and Yu, G. (2010). TDP-43 is a developmentally regulated protein essential for early embryonic development. J Biol Chem 285, 6826-6834.

Sergeant, N., Sablonnière, B., Schraen-Maschke, S., Ghestem, A., Maurage, C.-A., Wattez, A., Vermersch, P., and Delacourte, A. (2001). Dysregulation of human brain microtubule-associated tau mRNA maturation in myotonic dystrophy type 1. Hum Mol Genet 10, 2143-2155.

Sherwood, K.R., Head, M.W., Walker, R., Smith, C., Ironside, J.W., and Fazakerley, J.K. (2011). RNA integrity in post mortem human variant Creutzfeldt–Jakob disease (vCJD) and control brain tissue. Neuropathol Applied Neurobiol 37, 633-642.

Simic, G., Kostovic, I., Winblad, B., and Bogdanovic, N. (1997). Volume and number of neurons of the human hippocampal formation in normal aging and Alzheimer's disease. J Comp Neurol 379, 482-494.

Simón-Sánchez, J., Seelaar, H., Bochdanovits, Z., Deeg, D.J.H., van Swieten, J.C., and Heutink, P. (2009). Variation at *GRN* 3′-UTR rs5848 is not associated with a risk of frontotemporal lobar degeneration in Dutch population. PLoS One 4, e7494.

Singleton, A., and Hardy, J. (2011). A generalizable hypothesis for the genetic architecture of disease: pleomorphic risk loci. Hum Mol Genet 20, R158-R162.

Singleton, A., Myers, A., and Hardy, J. (2004). The law of mass action applied to neurodegenerative disease: a hypothesis concerning the etiology and pathogenesis of complex diseases. Hum Mol Genet 13, R123-R126.

Skibinski, G., Parkinson, N.J., Brown, J.M., Chakrabarti, L., Lloyd, S.L., Hummerich, H., Nielsen, J.E., Hodges, J.R., Spillantini, M.G., Thusgaard, T., *et al.* (2005). Mutations in the endosomal ESCRTIII-complex subunit CHMP2B in frontotemporal dementia. Nat Genet 37, 806-808.

Small, D.H., Clarris, H.L., Williamson, T.G., Reed, G., Key, B., Mok, S.S., Beyreuther, K., Masters, C.L., and Nurcombe, V. (1999). Neurite-outgrowth regulating functions of the amyloid protein precursor of Alzheimer's disease. J Alzheimer's Dis 1, 275-285.

Smith, C.J., Anderton, B.H., Davis, D.R., and Gallo, J.M. (1995). Tau isoform expression and phosphorylation state during differentiation of cultured neuronal cells. FEBS Lett 375, 243-248.

Smith, P., Al Hashimi, A., Girard, J., Delay, C., and Hébert, S.S. (2011a). In vivo regulation of amyloid precursor protein neuronal splicing by microRNAs. J Neurochem 116, 240-247.

Smith, P.Y., Delay, C., Girard, J., Papon, M.-A., Planel, E., Sergeant, N., Buée, L., and Hébert, S.S. (2011b). MicroRNA-132 loss is associated with tau exon 10 inclusion in progressive supranuclear palsy. Hum Mol Genet 20, 4016-4024.

Snowden, J., Neary, D., and Mann, D. (2007a). Frontotemporal lobar degeneration: clinical and pathological relationships. Acta Neuropathol (Berl) 114, 31-38.

Snowden, J.S., Stopford, C.L., Julien, C.L., Thompson, J.C., Davidson, Y., Gibbons, L., Pritchard, A., Lendon, C.L., Richardson, A.M., Varma, A., *et al.* (2007b). Cognitive phenotypes in Alzheimer's disease and genetic risk. Cortex 43, 835-845.

Sofroniew, M., and Vinters, H. (2010). Astrocytes: biology and pathology. Acta Neuropathol (Berl) 119, 7-35.

Soto, C. (2012). Transmissible proteins: expanding the prion heresy. Cell 149, 968-977.

Spellman, R., Llorian, M., and Smith, C.W. (2007). Crossregulation and functional redundancy between the splicing regulator PTB and its paralogs nPTB and ROD1. Mol Cell 27, 420-434.

Spellman, R., Rideau, A., Matlin, A., Gooding, C., Robinson, F., McGlincy, N., Grellscheid, S.N., Southby, J., Wollerton, M., and Smith, C.W. (2005). Regulation of alternative splicing by PTB and associated factors. Biochem Soc Trans 33, 457-460.

Spillantini, M.G., Crowther, R.A., Kamphorst, W., Heutink, P., and van Swieten, J.C. (1998a). Tau pathology in two Dutch families with mutations in the microtubule-binding region of tau. Am J Pathol 153, 1359-1363.

Spillantini, M.G., Murrell, J.R., Goedert, M., Farlow, M.R., Klug, A., and Ghetti, B. (1998b). Mutation in the tau gene in familial multiple system tauopathy with presenile dementia. Proc Natl Acad Sci USA 95, 7737-7741.

Sreedharan, J., Blair, I.P., Tripathi, V.B., Hu, X., Vance, C., Rogelj, B., Ackerley, S., Durnall, J.C., Williams, K.L., Buratti, E., *et al.* (2008). TDP-43 mutations in familial and sporadic amyotrophic lateral sclerosis. Science 319, 1668-1672.

Stanford, P.M., Shepherd, C.E., Halliday, G.M., Brooks, W.S., Schofield, P.W., Brodaty, H., Martins, R.N., Kwok, J.B.J., and Schofield, P.R. (2003). Mutations in the tau gene that cause an increase in three repeat tau and frontotemporal dementia. Brain 126, 814-826.

Stoothoff, W., Jones, P.B., Spires-Jones, T.L., Joyner, D., Chhabra, E., Bercury, K., Fan, Z., Xie, H., Bacskai, B., Edd, J., *et al.* (2009). Differential effect of three-repeat and four-repeat tau on mitochondrial axonal transport. J Neurochem 111, 417-427.

Stopford, C.L., Snowden, J.S., Thompson, J.C., and Neary, D. (2008). Variability in cognitive presentation of Alzheimer's disease. Cortex 44, 185-195.

Streit, W.J., Miller, K.R., Lopes, K.O., and Njie, E. (2008). Microglial degeneration in the aging brain--bad news for neurons? Front Biosci 13, 3423-3438.

Strong, M.J., Volkening, K., Hammond, R., Yang, W., Strong, W., Leystra-Lantz, C., and Shoesmith, C. (2007). TDP43 is a human low molecular weight neurofilament (hNFL) mRNA-binding protein. Mol Cell Neurosci 35, 320-327.

Sugnet, C.W., Srinivasan, K., Clark, T.A., O'Brien, G., Cline, M.S., Wang, H., Williams, A., Kulp, D., Blume, J.E., Haussler, D., and Ares, M., Jr. (2006). Unusual intron conservation near tissue-regulated exons found by splicing microarrays. PLoS Comput Biol 2, e4.

Takahashi, M., Weidenheim, K.M., Dickson, D.W., and and Ksiezak-Reding, H. (2002). Morphological and biochemical correlations of abnormal tau filaments in progressive supranuclear palsy. J Neuropathol Exp Neurol 61, 33-45.

Takanashi, M., Mori, H., Arima, K., Mizuno, Y., and Hattori, N. (2002). Expression patterns of tau mRNA isoforms correlate with susceptible lesions in progressive supranuclear palsy and corticobasal degeneration. Mol Brain Res 104, 210-219.

Takuma, H., Arawaka, S., and Mori, H. (2003). Isoforms changes of tau protein during development in various species. Dev Brain Res 142, 121-127.

Tang, Y., Nyengaard, J.R., Pakkenberg, B., and Gundersen, H.J.G. (1997). Age-induced white matter changes in the human brain: a stereological investigation. Neurobiol Aging 18, 609-615.

Taniguchi, S., McDonagh, A.M., Pickering-Brown, S.M., Umeda, Y., Iwatsubo, T., Hasegawa, M., and Mann, D.M.A. (2004). The neuropathology of frontotemporal lobar degeneration with respect to the cytological and biochemical characteristics of tau protein. Neuropathol Applied Neurobiol 30, 1-18.

Thal, D.R., Rub, U., Orantes, M., and Braak, H. (2002). Phases of A beta-deposition in the human brain and its relevance for the development of AD. Neurol 58, 1791-1800.

Thal, D.R., Rub, U., Schultz, C., Sassin, I., Ghebremedhin, E., Del Tredici, K., Braak, E., and Braak, H. (2000). Sequence of Abeta-protein deposition in the human medial temporal lobe. J Neuropathol Exp Neurol 59, 733-748.

Tharp, W.G., Lee, Y.-H., Greene, S.M., Vincellete, E., Beach, T.G., and Pratley, R.E. (2012). Measurement of altered AβPP isoform expression in frontal cortex of patients with Alzheimer's disease by absolute quantification real-time PCR. J Alzheimer's Dis 29, 449-457.

Thomas, M.G., Loschi, M., Desbats, M.A., and Boccaccio, G.L. (2011). RNA granules: The good, the bad and the ugly. Cell Signal 23, 324-334.

Tichopad, A., Didier, A., and Pfaffl, M.W. (2004). Inhibition of real-time RT–PCR quantification due to tissue-specific contaminants. Mol Cell Probes 18, 45-50.

Tichopad, A., Dzidic, A., and Pfaffl, M.W. (2002). Improving quantitative real-time RT-PCR reproducibility by boosting primer-linked amplification efficiency. Biotech Letters 24, 2053-2056.

Tollervey, J.R., Curk, T., Rogelj, B., Briese, M., Cereda, M., Kayikci, M., Konig, J., Hortobagyi, T., Nishimura, A.L., Zupunski, V., *et al.* (2011a). Characterizing the RNA targets and position-dependent splicing regulation by TDP-43. Nat Neurosci 14, 452-458.

Tollervey, J.R., Wang, Z., Hortobágyi, T., Witten, J.T., Zarnack, K., Kayikci, M., Clark, T.A., Schweitzer, A.C., Rot, G., Curk, T., *et al.* (2011b). Analysis of alternative splicing associated with aging and neurodegeneration in the human brain. Genome Res 21, 1572-1582.

Tomita, H., Vawter, M.P., Walsh, D.M., Evans, S.J., Choudary, P.V., Li, J., Overman, K.M., Atz, M.E., Myers, R.M., Jones, E.G., *et al.* (2004). Effect of agonal and postmortem factors on gene expression profile: quality control in microarray analyses of postmortem human brain. Biol Psychiatry 55, 346-352.

Toombs, J.A., McCarty, B.R., and Ross, E.D. (2010). Compositional determinants of prion formation in Yeast. Mol Cell Biol 30, 319-332.

Trabzuni, D., Ryten, M., Walker, R., Smith, C., Imran, S., Ramasamy, A., Weale, M.E., and Hardy, J. (2011). Quality control parameters on a large dataset of regionally dissected human control brains for whole genome expression studies. J Neurochem 119, 275-282.

Trabzuni, D., Wray, S., Vandrovcova, J., Ramasamy, A., Walker, R., Smith, C., Luk, C., Gibbs, J.R., Dillman, A., Hernandez, D.G., *et al.* (2012). MAPT expression and splicing is differentially regulated by brain region: relation to genotype and implication for tauopathies. Hum Mol Genet 21, 4094-4103.

Tran, M.D. (2011). P2 receptor stimulation induces amyloid precursor protein production and secretion in rat cortical astrocytes. Neurosci Lett 492, 155-159.

Trinczek, B., Biernat, J., Baumann, K., Mandelkow, E.M., and Mandelkow, E. (1995). Domains of tau protein, differential phosphorylation, and dynamic instability of microtubules. Mol Biol Cell 6, 1887-1902.

Troakes, C., Maekawa, S., Wijesekera, L., Rogelj, B., Siklós, L., Bell, C., Smith, B., Newhouse, S., Vance, C., Johnson, L., *et al.* (2012). An MND/ALS phenotype associated with C9orf72 repeat expansion: Abundant p62-positive, TDP-43-negative inclusions in cerebral cortex, hippocampus and cerebellum but without associated cognitive decline. Neuropathol 32, 505-514.

Tsigelny, I.F., Crews, L., Desplats, P., Shaked, G.M., Sharikov, Y., Mizuno, H., Spencer, B., Rockenstein, E., Trejo, M., Platoshyn, O., *et al.* (2008). Mechanisms of hybrid oligomer formation in the pathogenesis of combined Alzheimer's and Parkinson's diseases. PLoS One 3, e3135.

Twine, N.A., Janitz, K., Wilkins, M.R., and Janitz, M. (2011). Whole transcriptome sequencing reveals gene expression and splicing differences in brain regions affected by Alzheimer's disease. PLoS One 6, e16266.

Udan, M., and Baloh, R.H. (2011). Implications of the prion-related Q/N domains in TDP-43 and FUS. Prion 5, 1-5.

Ule, J., Jensen, K.B., Ruggiu, M., Mele, A., Ule, A., and Darnell, R.B. (2003). CLIP identifies Nova-regulated RNA networks in the brain. Science 302, 1212-1215.

Ule, J., Ule, A., Spencer, J., Williams, A., Hu, J.S., Cline, M., Wang, H., Clark, T., Fraser, C., Ruggiu, M., *et al.* (2005). Nova regulates brain-specific splicing to shape the synapse. Nat Genet 37, 844-852.

Umeda, Y., Taniguchi, S., Arima, K., Piao, Y.-S., Takahashi, H., Iwatsubo, T., Mann, D., and Hasegawa, M. (2004). Alterations in human tau transcripts correlate with those of neurofilament in sporadic tauopathies. Neurosci Lett 359, 151-154.

Urwin, H., Josephs, K.A., Rohrer, J.D., Mackenzie, I.R., Neumann, M., Authier, A., Seelaar, H., Van Swieten, J.C., Brown, J.M., Johannsen, P., *et al.* (2010). FUS pathology defines the majority of tau- and TDP-43-negative frontotemporal lobar degeneration. Acta Neuropathol (Berl) 120, 33-41.

Uryu, K., Nakashima-Yasuda, H., Forman, M.S., Kwong, L.K., Clark, C.M., Grossman, M., Miller, B.L., Kretzschmar, H.A., Lee, V.M., Trojanowski, J.Q., and Neumann, M. (2008). Concomitant TAR-DNA-binding protein 43 pathology is present in Alzheimer disease and corticobasal degeneration but not in other tauopathies. J Neuropathol Exp Neurol 67, 555-564.

van der Zee, J., Sleegers, K., and Broeckhoven, C.V. (2008a). Invited Article: The Alzheimer disease–frontotemporal lobar degeneration spectrum. Neurol 71, 1191-1197.

van der Zee, J., Urwin, H., Engelborghs, S., Bruyland, M., Vandenberghe, R., Dermaut, B., De Pooter, T., Peeters, K., Santens, P., De Deyn, P.P., *et al.* (2008b). CHMP2B C-truncating mutations in frontotemporal lobar degeneration are associated with an aberrant endosomal phenotype in vitro. Hum Mol Genet 17, 313-322.

van Hoesen, G.W., Hyman, B.T., and Damasio, A.R. (1991). Entorhinal cortex pathology in Alzheimer's disease. Hippocampus 1, 1-8.

Vandesompele, J., De Preter, K., Pattyn, F., Poppe, B., Van Roy, N., De Paepe, A., and Speleman, F. (2002). Accurate normalization of real-time quantitative RT-PCR data by geometric averaging of multiple internal control genes. Genome Biol 3, 1-12.

Varani, L., Hasegawa, M., Spillantini, M.G., Smith, M.J., Murrell, J.R., Ghetti, B., Klug, A., Goedert, M., and Varani, G. (1999). Structure of tau exon 10 splicing regulatory element RNA and destabilization by mutations of frontotemporal dementia and parkinsonism linked to chromosome 17. Proc Natl Acad Sci USA 96, 8229-8234.

Vermersch, P., Sergeant, N., Ruchoux, M.M., Hofmann-Radvanyi, H., Wattez, A., Petit, H., Dewailly, P., and Delacourte, A. (1996). Specific tau variants in the brains of patients with myotonic dystrophy. Neurol 47, 711-717.

Vogt, L.J.K., Hyman, B.T., Van Hoesen, G.W., and Damasio, A.R. (1990). Pathological alterations in the amygdala in Alzheimer's disease. Neurosci 37, 377-385.

Wahl, M.C., Will, C.L., and Luhrmann, R. (2009). The spliceosome: design principles of a dynamic RNP machine. Cell 136, 701-718.

Walker, L.C., and LeVine, H. (2012). The corruption and spread of pathogenic proteins in neurodegenerative diseases. J Biol Chem 287, 33109-33115.

Walsh, D.M., and Selkoe, D.J. (2004). Deciphering the molecular basis of memory failure in Alzheimer's disease. Neuron 44, 181-193.

Walter, S., Letiembre, M., Liu, Y., Heine, H., Penke, B., Hao, W., Bode, B., Manietta, N., Walter, J., Schulz-Schüffer, W., and Fassbender, K. (2007). Role of the Toll-like receptor 4 in neuroinflammation in Alzheimer’s disease. Cell Physiol Biochem 20, 947-956.

Wang, Y., Wang, J., Gao, L., Lafyatis, R., Stamm, S., and Andreadis, A. (2005). Tau exons 2 and 10, which are misregulated in neurodegenerative diseases, are partly regulated by silencers which bind a SRp30c.SRp55 complex that either recruits or antagonizes htra2beta1. J Biol Chem 280, 14230-14239.

West, M.J., Coleman, P.D., Flood, D.G., and Troncoso, J.C. (1994). Differences in the pattern of hippocampal neuronal loss in normal ageing and Alzheimer's disease. Lancet 344, 769-772.

Whitwell, J.L., Dickson, D.W., Murray, M.E., Weigand, S.D., Tosakulwong, N., Senjem, M.L., Knopman, D.S., Boeve, B.F., Parisi, J.E., Petersen, R.C., *et al.* (2012). Neuroimaging correlates of pathologically defined subtypes of Alzheimer's disease: a case-control study. Lancet Neurol 11, 868-877.

Whitwell, J.L., Jack, C.R., Boeve, B.F., Senjem, M.L., Baker, M., Ivnik, R.J., Knopman, D.S., Wszolek, Z.K., Petersen, R.C., Rademakers, R., and Josephs, K.A. (2009). Atrophy patterns in IVS10+16, IVS10+3, N279K, S305N, P301L, and V337M MAPT mutations. Neurol 73, 1058-1065.

Wils, H., Kleinberger, G., Janssens, J., Pereson, S., Joris, G., Cuijt, I., Smits, V., Ceuterick-de Groote, C., Van Broeckhoven, C., and Kumar-Singh, S. (2010). TDP-43 transgenic mice develop spastic paralysis and neuronal inclusions characteristic of ALS and frontotemporal lobar degeneration. Proc Natl Acad Sci USA 107, 3858-3863.

Wollerton, M.C., Gooding, C., Wagner, E.J., Garcia-Blanco, M.A., and Smith, C.W.J. (2004). Autoregulation of polypyrimidine tract binding protein by alternative splicing leading to nonsense-mediated decay. Mol Cell 13, 91-100.

Wu, L.-S., Cheng, W.-C., Hou, S.-C., Yan, Y.-T., Jiang, S.-T., and Shen, C.K.J. (2010). TDP-43, a neuro-pathosignature factor, is essential for early mouse embryogenesis. Genesis 48, 56-62.

Wyss-Coray, T., and Rogers, J. (2012). Inflammation in Alzheimer's disease— a brief review of the basic science and clinical literature. Cold Spring Harb Perspect Med 2.

Xiao, S., Sanelli, T., Dib, S., Sheps, D., Findlater, J., Bilbao, J., Keith, J., Zinman, L., Rogaeva, E., and Robertson, J. (2011). RNA targets of TDP-43 identified by UV-CLIP are deregulated in ALS. Mol Cell Neurosci 47, 167-180.

Xie, X., Lu, J., Kulbokas, E.J., Golub, T.R., Mootha, V., Lindblad-Toh, K., Lander, E.S., and Kellis, M. (2005). Systematic discovery of regulatory motifs in human promoters and 3' UTRs by comparison of several mammals. Nature 434, 338-345.

Yasojima, K., McGeer, E.G., and McGeer, P.L. (1999). Tangled areas of Alzheimer brain have upregulated levels of exon 10 containing tau mRNA. Brain Res 831, 301-305.

Yasuoka, K., Hirata, K., Kuraoka, A., He, J.-w., and Kawabuchi, M. (2004). Expression of amyloid precursor protein-like molecule in astroglial cells of the subventricular zone and rostral migratory stream of the adult rat forebrain. J Anatomy 205, 135-146.

Yeo, G.W., Nostrand, E.L.V., and Liang, T.Y. (2007). Discovery and Analysis of Evolutionarily Conserved Intronic Splicing Regulatory Elements. PLoS Genet 3, e85.

Yokota, O., Davidson, Y., Bigio, E.H., Ishizu, H., Terada, S., Arai, T., Hasegawa, M., Akiyama, H., Sikkink, S., Pickering-Brown, S., and Mann, D.M. (2010). Phosphorylated TDP-43 pathology and hippocampal sclerosis in progressive supranuclear palsy. Acta Neuropathol (Berl) 120, 55-66.

Yu, X., Luo, Y., Dinkel, P., Zheng, J., Wei, G., Margittai, M., Nussinov, R., and Ma, B. (2012). Cross-seeding and conformational selection between three- and four-repeat human tau proteins. J Biol Chem 287, 14950-14959.

Zarow, C., Sitzer, T., and Chui, H. (2008). Understanding hippocampal sclerosis in the elderly: Epidemiology, characterization, and diagnostic issues. Curr Neurol Neurosci Reports 8, 363-370.

Zarow, C., Weiner, M.W., Ellis, W.G., and Chui, H.C. (2012). Prevalence, laterality, and comorbidity of hippocampal sclerosis in an autopsy sample. Brain Behaviour 2, 435-442.

Zhang, B., Gaiteri, C., Bodea, L.-G., Wang, Z., McElwee, J., Podtelezhnikov, Alexei A., Zhang, C., Xie, T., Tran, L., Dobrin, R., *et al.* (2013). Integrated systems approach identifies genetic nodes and networks in late-onset Alzheimer's disease. Cell 153, 707-720.

Zhang, C., Zhang, Z., Castle, J., Sun, S., Johnson, J., Krainer, A.R., and Zhang, M.Q. (2008a). Defining the regulatory network of the tissue-specific splicing factors Fox-1 and Fox-2. Genes Dev 22, 2550-2563.

Zhang, Z., Lotti, F., Dittmar, K., Younis, I., Wan, L., Kasim, M., and Dreyfuss, G. (2008b). SMN deficiency causes tissue-specific perturbations in the repertoire of snRNAs and widespread defects in splicing. Cell 133, 585-600.

Zhong, Q., Congdon, E.E., Nagaraja, H.N., and Kuret, J. (2012). Tau isoform composition influences rate and extent of filament formation. J Biol Chem 287, 20711-20719.

Zhu, J., Shendure, J., Mitra, R.D., and Church, G.M. (2003). Single molecule profiling of alternative pre-mRNA splicing. Science 301, 836-838.

Zhukareva, V., Mann, D., Pickering-Brown, S., Uryu, K., Shuck, T., Shah, K., Grossman, M., Miller, B.L., Hulette, C.M., Feinstein, S.C., *et al.* (2002). Sporadic Pick's disease: A tauopathy characterized by a spectrum of pathological τ isoforms in gray and white matter. Ann Neurol 51, 730-739.